

**Phosphatidylserine exposure in red blood cells:
A suggestion for the active role of red blood cells in
blood clot formation**

Dissertation

zur Erlangung des Grades
des Doktors der Naturwissenschaften
der Naturwissenschaftlich-Technischen Fakultät III
Chemie, Pharmazie, Bio- und Werkstoffwissenschaften
der Universität des Saarlandes

von

Duc Bach Nguyen

Saarbrücken

2010

Tag des Kolloquiums:

Dekan:

Berichterstatter:

.....

.....

Vorsitz:

Akad. Mitarbeiter:

Table of content	i
Abbreviations	iv
1. Introduction	1
2. Theoretical background	3
2.1. Red blood cell membrane	3
2.1.1. Membrane lipids	3
2.1.2. Membrane proteins	5
2.1.3. Membrane transport	7
2.2. Movement of membrane phospholipids	12
2.2.1. Flippase, floppase, and scramblase	12
2.2.2. Maintenance of plasma membrane lipid asymmetry	15
2.2.3. Loss of phospholipid asymmetry and its consequences	15
2.3. Phosphatidylserine exposure and cell adhesion	16
2.3.1. Possible mechanisms for phosphatidylserine exposure	16
2.3.2. Cellular microvesicle formation	18
2.3.3. Adhesion of phosphatidylserine exposed red blood cells	19
2.3.4. Traditional and new concepts about red blood cells in thrombosis	19
2.4. Biological role of Ca²⁺ in human red blood cells	21
2.4.1. Ca ²⁺ homeostasis	21
2.4.2. Influence of intracellular Ca ²⁺ on phosphatidylserine exposure	21
2.4.3. Influence of intracellular Ca ²⁺ on protein kinase C	22
2.5. The ageing of red blood cells	23
2.5.1. Young and old red blood cells	23
2.5.2. Ca ²⁺ content in young and old red blood cells	24
2.5.3. Influence of ageing on membrane redox system in red blood cells	25
2.5.4. Relevance of ageing and apoptosis	27

3. Materials and Methods	28
3.1. Materials	28
3.1.1. Chemicals and reagents.....	28
3.1.2. Main equipments and softwares used	32
3.2. Methods	33
3.2.1. Cell biology methods based on fluorescence microscopy and flow cytometry	33
3.2.2. Biochemistry methods	39
3.2.3. Atomic force microscopy method.....	44
3.2.4. Informatics tools	46
3.2.5. Statistics	46
4. Results	47
4.1. Investigation of Ca²⁺ uptake in human red blood cells	47
4.1.1. Calibration of intracellular Ca ²⁺ content.....	47
4.1.2. Influence of lysophosphatidic acid on the uptake of Ca ²⁺	51
4.1.3. Influence of phorbol 12-myristate 13-acetate on the uptake of Ca ²⁺	53
4.1.4. Investigation of the Ca ²⁺ content in sickle red blood cells	57
4.1.5. Investigation of Ca ²⁺ uptake in sheep red blood cells.....	60
4.2. Investigation of phosphatidylserine exposure in red blood cells	63
4.2.1. Phosphatidylserine exposure in red blood cells under stimulated conditions...	63
4.2.2. Kinetics of phosphatidylserine exposure	67
4.2.3. Intracellular pH in phosphatidylserine exposed human red blood cells	70
4.2.4. Investigation of phosphatidylserine exposure under other conditions.....	71
4.2.5. Relevance of intracellular Ca ²⁺ for the phosphatidylserine exposure	79
4.2.6. Phosphatidylserine exposure in sheep red blood cells	82
4.3. Adhesion of phosphatidylserine exposed red blood cells	83
4.3.1. Determination of fibrinogen concentration in washed cell suspension	83
4.3.2. Adhesion of red blood cells	85
4.4. Detection of scramblase in red blood cells	88
4.4.1. Alignment of amino acid sequences of scramblases in human red blood cells	88
4.4.2. BLAST analysis of phospholipid scramblases	90
4.4.3. Detection of scramblases using Western blot analysis	94

4.5. Young and old red blood cells	98
4.5.1. Separation of red blood cells into young and old cell fractions.....	98
4.5.2. Determination of reticulocytes in fraction of different cell age.....	99
4.5.3. Investigation of the relative volume of young and old red blood cells.....	100
4.5.4. Determination of Ca ²⁺ content in young and old red blood cells.....	100
4.5.5. Phosphatidylserine exposure of young and old red blood cells	101
4.5.6. Phosphatidylserine exposure of stored red blood cells	103
4.5.7. Membrane redox activity of young and old red blood cells	105
4.5.8. Surface structure of young and old red blood cells.....	105
5. Discussion	107
5.1. Role of Ca²⁺ in red blood cells under physiological condition	107
5.2. Increase of intracellular Ca²⁺ and its consequences	108
5.3. Scramblases in red blood cells	109
5.4. Phosphatidylserine exposure in red blood cells	111
5.5. Adhesion of red blood cells	118
5.6. Red blood cells in the process of thrombosis	121
6. Summary / Zusammenfassung	125
7. References	127
Statement / Erklärung	143
Acknowledgment	144

Abbreviations

ABC transporter	ATP binding cassette transporter
a.u.	Arbitrary unit
aa	Amino acid
AChE	Acetylcholinesterase
ADP	Adenosin diphosphate
AFM	Atomic force microscope
AM	Acetoxymethyl
ANOVA	Analysis of variance
APLT	Amino phospholipid translocase
APS	Ammonium persulfate
ATP	Adenosine triphosphate
BCECF	2',7'-bis (2-carboxyethyl), 5 (and -6) carboxyfluorescein
BLAST	Basic local alignment search tool
BLASTp	Basic local alignment search tool for protein
CCD	Couple charge device
CD	Cluster of differentiation
cDNA	Complementary deoxyribonucleic acid
CFTR	Cystic fibrosis transmembrane conductance regulator
DMSO	Dimethyl sulfoxide
EC	Endothelial cell
ECL	Electrochemiluminescence
EDTA	Ethylenediaminetetraacetic acid
EGTA	Ethylene glycol tetraacetic acid
FACS	Fluorescence-activated cell sorter
FITC	Fluorescein isothiocyanate
FL	Fluorescence
FRAP	Reducing ability of plasma
FSC	Forward scatter
G3PD	Glyceraldehyde-3-phosphate dehydrogenase
G6PD	Glucose-6-phosphate dehydrogenase
GLUT1	Glucose transporter 1
GOT	Glutamate oxaloacetate transaminase
GP	Glycophorins
hPLSCR	Human phospholipids scramblase
HUVEC	Human umbilical vein endothelial cells
Hx	Hexokinase
IgG	Immunoglobulin G

IU	International unit
K _d	Dissociation constant
kDa	Atomic mass unit (1000 dalton)
LDH	Lactate dehydrogenase
LPA	Lysophosphatidic acid
LSCM	Laser scanning confocal microscope
NADH	Nicotinamide adenine dinucleotide
NADPH	Nicotinamide adenine dinucleotide phosphate
NBD	7-nitrobenz-2-oxa-1,3-diazol-4-yl
NHE	Sodium proton exchanger
NMR	Nuclear magnetic resonance
NSVDC	Non selective voltage dependent cation channel
PAS	Periodic acid Schiff
PBS-T	Phosphate buffer saline plus Tween 20
PC	Phosphatidylcholine
PE	Phosphatidylethanolamine
PGE ₂	Prostaglandin E ₂
pH _i	Intracellular pH
PI	Phosphatidylinositol
PKC	Protein kinase C
PLSCR	Phospholipid scramblase
PMA	Phorbol 12-myristate 13-acetate
PMRS	Plasma membrane redox system
PMSF	Phenylmethanesulphonylfluoride
PMT	Photomultiplier tube
PS	Phosphatidylserine
RBC	Red blood cell
RNA	Ribonucleic acid
RNA	Ribonucleic acid
S.D	Standard deviation
SDS	Sodium dodecylsulfate
SDS-PAGE	Sodium dodecyl sulfate polyacrylamide gel electrophoresis
SM	Sphingomyelin
SPM	Scanning probe microscope
SSC	Side scatter
t-BOOH	Tert-butyl hydroperoxide
TEMED	Tetramethylethylenediamine
TF	Tissue factor
TSP	Thrombospondin

1. Introduction

From stem cells in bone marrow, human erythroid cells are differentiated through a process named erythropoiesis to become mature erythrocytes or red blood cells (RBCs). The lifespan of the cells in circulation is about 100 – 120 days. RBCs are relative simple cells due to the lack of organelles and nucleus. The main duty of them is to transport oxygen and carbon dioxide. Although RBCs have been intensively studied for many years, many questions concerning these cells are still not fully answered. For example, what is the role of RBCs in blood clot formation, how do RBCs become old, what is the role of Ca^{2+} in the ageing process or is there an apoptosis of RBCs? Another open question is how are RBCs removed from blood circulation? The mechanisms of these processes are still unclear because it seems that they involve many factors, which are mostly located in the cell membrane.

With the development of microscopes and other techniques as well as newly developed fluorescent dyes for labelling, the answers for such questions have gradually become clearer at the molecular level. For instance, in blood clot formation, so far medical textbooks have mentioned that when an injury happens, RBCs are merely “trapped” into a fibrin network, and thus they prevent the blood from continuously bleeding. However, some recent findings suggest that together with platelets and other factors, RBCs play an active role in the process of blood clot formation.

Although the apoptosis of RBCs is still under consideration, it is gradually accepted that they undergo a type of determined cell death called eryptosis. The reason is that some common apoptotic signals have been observed such as the exposure of phosphatidylserine (PS) on the outer leaflet of the membrane, membrane blebbing, and vesicle formation. The PS exposure is an important signal not only for the recognition and phagocytosis by macrophages, but also for the adhesion of RBCs to endothelium in some diseases such as sickle cell anaemia, malaria, and diabetes. The increase of the intracellular Ca^{2+} level is one of the most important factors leading to PS exposure because it activates the phospholipid scramblase (PLSCR). Currently, the mechanisms involving PS exposure in RBCs still awaits a full understanding.

The difference between young and old RBCs is also a problem of concern because it relates to the process of ageing and removing of old RBCs out of the blood circulation. Regarding young and old RBCs, it has been speculated that the intracellular Ca^{2+} level in old RBCs is higher than in the young ones but so far there is not enough evidence to support this idea.

By means of fluorescent dyes, fluorescence microscopy, flow cytometry and other modern techniques, the main work of this thesis has been focused on the relation of intracellular Ca^{2+} and PS exposure in RBCs. Factors related to the PS exposure and the relations between the ageing of RBCs and eryptosis have been also examined. The experiments have been carried out for two main purposes. The first reason is to clarify the role of Ca^{2+} in the PS exposure process in RBCs to contribute to our understanding of the mechanisms of this process. The second reason is to give some support to the idea that RBCs play an active role in blood clot formation.

The presented work has been done in Saarland University in the laboratory of biophysics under the leadership of Prof. Ingolf Bernhardt.

2. Theoretical background

2.1. Red blood cell membrane

2.1.1. Membrane lipids

The human RBC (RBC) membrane consists of lipids (41%), proteins (52%), and carbohydrates (7%) [1, 2]. In average, there are about 5.2 mg membrane lipids per ml of packed RBCs or approximately 5.2×10^{-13} g/cell. Membrane lipids can be classified into three classes: neutral lipids (25.2%), phospholipids (62.7%) and glycosphingolipids (about 12%). Neutral lipids of human RBCs represent cholesterol almost exclusively [3, 4]. The ratio of cholesterol to phospholipid is about 0.8 [5]. Phospholipids consist of sphingomyelin (SM, 26%), and glycerophospholipids. Glycerophospholipids can be divided into 3 main fractions: phosphatidylcholine (PC, 30%), phosphatidylethanolamine (PE, 27%), and phosphatidylserine, (PS, 13%), and several minor fractions phosphatidic acid, lyso PC, phosphatidylinositol (PI), mono and disphosphates PI [3, 5, 6].

RBCs of various species differ in their fatty acid and phospholipid compositions. For example, RBCs from rat and mouse have a high content of PC (42 – 45%) and a low content of SM (12%) [3]. The low content of PC in ruminant RBCs results from an endogenous phospholipase A₂, which is present at the outside of the membrane and cleaves PC [7, 8].

The lipid composition of RBC membrane is rather stable and only alters with diet to a limited extent [9, 10]. This is due to the lack of de novo synthesis of phospholipids in the mature RBC. Limited alterations of the fatty acid composition by diet result from the exchange of phospholipids, primarily PC, between plasma lipoproteins and the cell membrane, as well as the exchange of fatty acids [11, 12].

The phospholipids in the plasma membrane of RBCs, platelets, lymphocytes and many other cells are asymmetrically distributed [13]. The two leaflets of the plasma membrane differ in their phospholipid composition. In RBCs, the best established cell system for lipid distribution investigation, SM and PC are found predominantly in the outer membrane leaflet of the bilayer while the amino phospholipids, PS and PE, are located predominantly in the inner bilayer leaflet [14]. Fig. 1 shows the distribution of the major phospholipids between the outer and inner membrane.

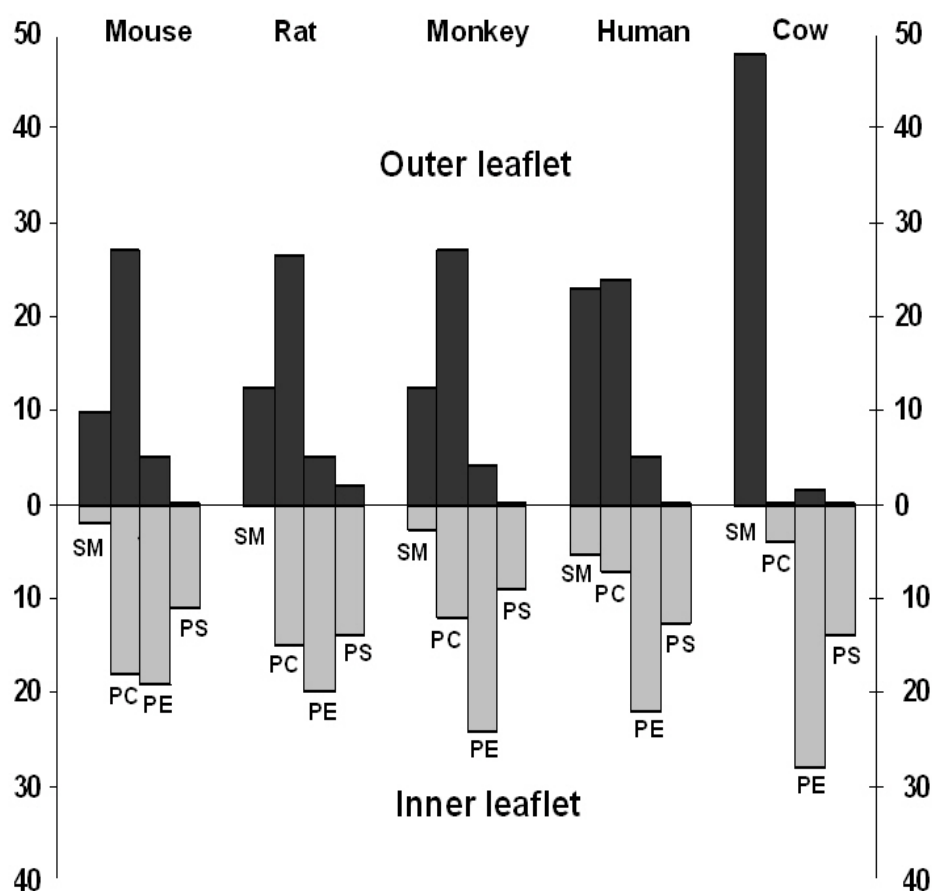


Fig. 1: Distribution of the major phospholipids between the outer and inner membrane leaflets (taken from [1]). The analysis data are from human [15], rat [16], mouse [17], monkey [18], and cow [8]). PS data for rat and cow include PI.

The transbilayer lipid distribution is under the control of three major players: (i) an inward-directed pump, a “flippase”, specific for PS and PE, also known as aminophospholipid translocase (APTL), (ii) an outward-directed pump referred to as “floppase”, and (iii) a lipid scramblase, promoting unspecific bidirectional redistribution across the bilayer [19]. A significant and sustained increase of cytosolic Ca^{2+} accompanying cell stimulation may lead to the collapse of the membrane lipid asymmetry by stimulating scramblase and floppase activities and concomitantly inhibiting the flippase. The most prominent change in lipid distribution is surface exposure of PS, followed by microvesicle release due to the cytoskeleton degradation by Ca^{2+} -dependent proteolysis [20].

2.1.2. Membrane proteins

The RBC membranes contain more than ten major proteins known, and probably hundreds of minor proteins. In almost all protocols, membrane proteins are isolated from cell ghosts. In general, the RBC ghosts are prepared by haemolysis of RBCs in hypotonic solution. The proteins from RBC ghosts are extracted by using mild detergents and analyzed by sodium dodecyl sulfate polyacrylamide gel electrophoresis (SDS-PAGE). However, with these procedures or other similar methods, there are still some peripheral proteins, which can be lost when the cell membrane fragments of the ghosts are washed [2, 21].

According to Fairbanks [22], the individual protein fractions are separated and named according to their electrophoresis mobility in the SDS-PAGE. The slowest migrating band is band 1 (on top); the next band is band 2 protein, and so on. Sub-bands are designated with decimals, that is, protein 4.1 and protein 4.2, which are two sub-bands constituting a region at the position of the fourth migrating band. The protein bands are named logically from 1 to 7 [22]. The major membrane proteins are summarized in Table 1 [21]. Although numerous membrane proteins are identified as protein bands based on SDS-PAGE, there are some proteins such as glycoporphins only can be detected by the staining method using Periodic acid Schiff (see Fig. 2) [21].

Based on the binding with lipids, membrane proteins are classified into two groups. Peripheral proteins locate only at one side, exterior or interior of the membrane, and are more loosely associated. These proteins can be easily removed by high or low salt or high pH extraction. Integral proteins are embedded tightly into or through the lipid bilayer by hydrophobic domains within their amino acid sequences. They can be extracted by harsh reagents (chaotropic solvents or detergents).

In the membrane ultra structure, based on the functional properties, membrane proteins of RBCs can be classified into three categories. Cytoskeletal proteins (α and β spectrins, protein 4.1, actin), these proteins located just beneath the lipid bilayer. Integral proteins (band 3 and glycoporphins) are strongly embedded into the lipid bilayer. Anchoring proteins (ankyrin and protein 4.2) connect with the cytoskeletal network as well as integral proteins. The functions of the membrane proteins are mostly regulated by the state of phosphorylation, methylation, glycosylation, or lipid modification (myristylation, palmitylation, or farnesylation) [21, 23]. Expression of membrane proteins is also under the control of genetic and epigenetic (gene phosphorylation, acetylation, methylation, and others) modification of membrane protein genes. Table 1 shows the molecular characteristic of major membrane proteins in human RBCs. Fig. 2 shows RBC ghost proteins analyzed by SDS-PAGE by the methods of Fairbanks and Steck, and Laemmli.

Table 1: Molecular characteristics of major membrane proteins in human RBCs (taken from [21]).

Band on SDS gel	Protein	Molecular mass (kDa)		Copy number ($\times 10^3/\text{cell}$)	Relative amount of total ghost proteins (%)	Localization on membrane
		On SDS gel	Calculated			
1	α -Spectrin	240	280	242 ± 20	14	SKL
2	β -Spectrin	220	246	242 ± 20	13	SKL
2.1	Ankyrin	210	206	124 ± 11	5	ANC
2.9	α -Adducin	103	81	30	1	SKL
	β -Adducin	97	80	30	1	SKL
3	Anion exchanger 1 (AE-1): band 3	90~100	102	1200	26	INT
4.1	Protein 4.1	80, 78	66	200	5	SKL
4.2	Protein 4.2	72	77	250	5	ANC
4.9	Dematin	48, 52	43, 46	140	1	SKL
	p55	55	53	80	1	SKL
5	β -Actin	43	42	500	6	SKL
	Tropomodulin	43	41	30		SKL
6	Glyceraldehyde-3-phosphate dehydrogenase(G3PD)	35	36	500	5	SKL
7	Stomatin	31	32		4	INT
	Tropomyosin	27, 29	28	70	1	SKL
8	Protein 8	23	22	200	1	SKL
Glycoproteins:						
PAS-1	Glycophorin A	36	14	1000	1.6	INT
PAS-2	Glycophorin C	32	14	150	0.1	INT
PAS-3	Glycophorin B	20	8	150	0.2	INT
	Glycophorin D	23	11	82	0.02	INT
	Glycophorin E	–	6	(not expressed)		

SDS-gel: sodium dodecylsulfate polyacrylamide gel electrophoresis, SKL: skeletal protein, ANC: anchor protein, INT: integral protein.

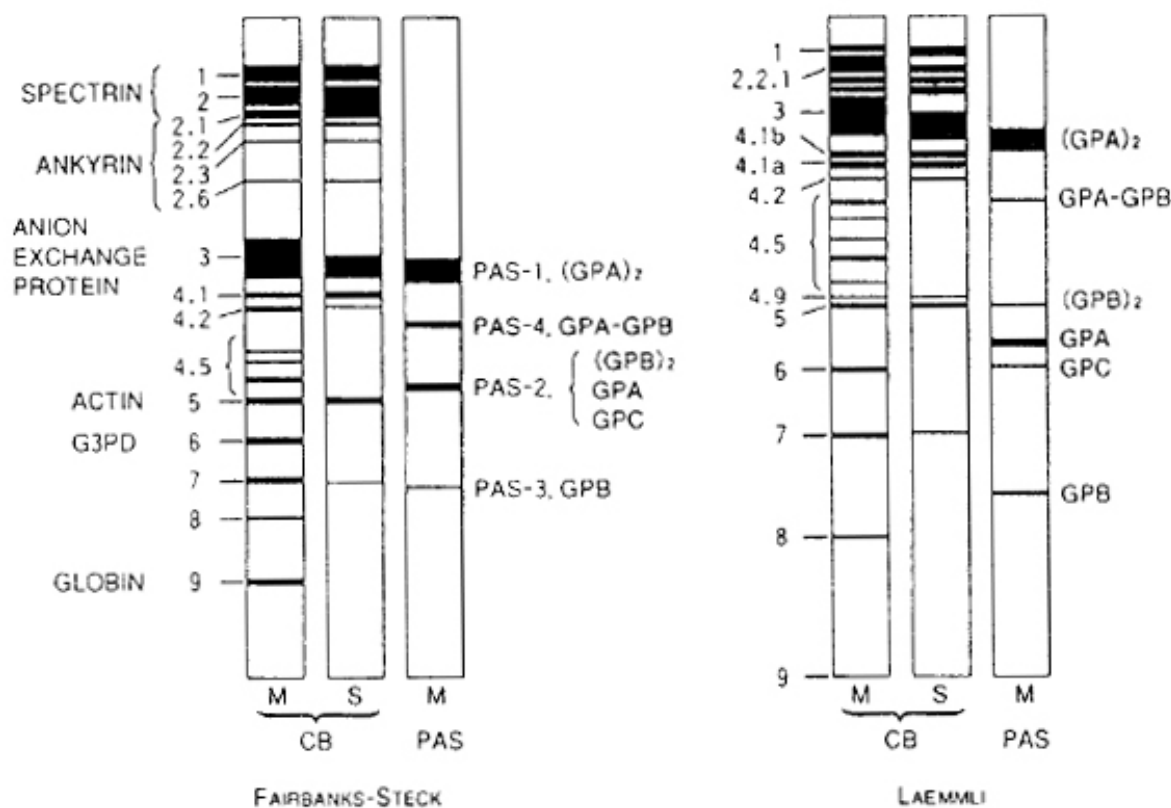


Fig. 2: A schematic demonstration of the findings of RBC ghost proteins analyzed by SDS-PAGE (taken from [21]). Left: methods of Fairbanks and Steck, right: method of Laemmli. CS: Coomsie blue staining, PAS: periodic acid Schiff staining, M: membrane fraction, S: soluble fraction, GP (A, B, C) glycophorins, G3PD: Glyceraldehyde-3-phosphate dedydrogenase.

2.1.3. Membrane transport

Ion transport through biological membranes can be divided into 4 principal mechanisms: pump, carrier, channel, and residual transport (also called “leak” transport). Various techniques are available to determine transport rates including radioactive tracers (flux measurements) and fluorescent dyes. Alternatively, electrophysiological methodology including the patch-clamp technique is applicable to electrogenic transport.

(1) Pumps (active transport)

Active transport is characterized by one or more ions moving against the electrochemical potential(s) through direct coupling to the consumption of ATP. ATPases, which hydrolyse ATP, often need co-substrates, e.g. Na^+ and K^+ for the Na^+, K^+ -ATPase (or Na^+/K^+ pump), Ca^{2+} and H^+ for the Ca^{2+} -ATPase (or Ca^{2+} pump). During transport, the energy released from ATP hydrolysis is used to change the

conformation of the pump protein. There are 4 different types of ATPases in biological membranes: P-type ATPases, V-type ATPases, F-type ATPases, and ABC transporters [24].

a) P-type ATPases (P stands for phosphorylation) have a phosphorylated aspartate residue as an intermediate product during the reaction cycle. The prototype ATPase first discovered was the Na^+/K^+ -ATPase by Skou J. C. et al. in 1957 [25]. This Na^+/K^+ pump is able to maintain a 10-fold gradient for Na^+ and K^+ across the biological membrane. For each molecule of ATP hydrolysed, three Na^+ are transported out of the cell and two K^+ inwards [26, 27]. Nearly all cells contain a Na^+/K^+ pump in their membrane, except RBCs of carnivores including cats and dogs [27, 28]. Ca^{2+} pumps also belong to P-type ATPase family, they are responsible for Ca^{2+} homeostasis in cells [29].

b) V-type ATPases (V stands for vacuole) transport exclusively H^+ and are therefore, termed H^+ -ATPases. V-type ATPases are membrane-bound multiprotein complexes that are localized in the endomembrane systems of eukaryotic cells and in the plasma membranes of some specialized cells. They couple ATP hydrolysis with the transport of protons across membranes. They also occur in vacuoles of fungi, yeast, and higher plants but are also found in the secretory vesicles of animal cells [30]. The V-type ATPase is much larger than the P-type ATPase and consists of many subunits. It is neither phosphorylated nor dephosphorylated. V-type ATPases contain an integral membrane domain (V0), which acts as an H^+ channel and a peripheral domain (V1) with the ATP binding site. The mechanism of the coupling of ATP hydrolysis and H^+ transport is still unknown. Through analysis of structure and transport function, it is apparent that the V-type ATPase is closely related to the F-type ATPase [30-32].

c) F-type ATPases (F stands for factors participating in energy coupling) like the V-type ATPases and F-type ATPases catalyze ATP hydrolysis and the transport of H^+ through the membrane against its electrochemical gradient. However, in contrast to the V-type ATPases, the F-type ATPases are able to synthesize ATP from ADP and inorganic phosphate by using dissipative H^+ movement down its electrochemical gradient (inverse reaction). In this mode, they are called ATP-synthases. F-type ATPases contain an integral membrane domain (F_0) acting as H^+ channel and a peripheral domain (F_1), which is of importance for both ATP-synthase and ATPase activity. This type of ATPases plays a central role in energy conserving reactions in mitochondria, bacteria, and chloroplasts [33, 34].

d) ABC transporters (ABC stands for **A**TP **b**inding **c**assette) represent for a large protein super family from prokaryotes to humans. They use energy from ATP hydrolysis to change their conformation to transport a large variety of substances actively across the cell membrane (both import and export). Typical functions of different ABC transporters include, for example, cholesterol and phospholipid transport out of eukaryotic cells, or the uptake of the substances such as amino acids, saccharides, peptides, and vitamins into prokaryotic cells. ABC transporters are also involved in multidrug resistance, which can cause many problems in clinical treatments. Some proteins functioning as ion channels are also belong to the ABC transporters. These channels are regulated by ATP but do not carry out an active transport [35].

(2) Carrier mediated transport

Proteins acting as carriers mediate the transport of ions or other substrates by making use of a periodic repeated conformational change of the protein. By this means, it becomes possible for the transported substrate to gain access to its binding site at both the inner or outer membrane surface. In general, a carrier mediated transport can be divided into two different mechanisms: uniport and cotransport. A uniport mediates the transport of a single ion or other substrate “downhill” the concentration or electrochemical gradient. Cotransporters can be divided in symporters and antiporters. A symporter binds the ions and/or substances (two or more substrates) and transports them together in one step in the same direction through the membrane. Movement of one substrate down its chemical or, in most cases, its electrochemical gradient is used to power the “uphill” transport of the cotransported substrate(s), i.e. against their chemical or electrochemical gradients. Examples are the glucose- Na^+ -symporter, present in the membrane of epithelial cells, and the lactose-permease, a lactose- H^+ -symporter, in the membrane of bacteria. The AE1 protein (band 3) which mediates the $\text{Cl}^-/\text{HCO}_3^-$ exchange, crucial gas transport by RBCs is an example for an antiporter. In cardiac muscle cells, Na^+ -linked antiporter exports Ca^{2+} out of these cells [24].

(3) Transport through channels

Ion channels are groups of proteins, which can form pore structures. The pore structures establish and monitor the ion going through the plasma membrane. In general, the ion channels allow the flow of ions down their electrochemical gradient [36, 37]. Ion

channels are relatively easy to investigate using the patch-clamp technique. They are closely packed by multi-subunits to form a specifically selective pore [37, 38]. All channels display two general features, they possess a mechanism for opening and closing, and they have a selectivity filter. The high-frequency switch between the open and closed state of the channel is termed gating, and the duration of opening is called open time. The selectivity filter is responsible for the more-or-less specific transport of one or several ion species. Gating can be divided into 4 categories by modality:

1. Change of the electrical membrane potential, i.e. change of the electrical field strength in the membrane,
2. Binding of a regulatory substance (including Ca^{2+}) or ligands,
3. Mechanical forces (membrane “stretch” or cell volume changes),
4. Light.

Recently, Agre et al. [39] discovered the aquaporin or so called “water channel”. Aquaporins are integral membrane proteins belonging to a larger family of major intrinsic proteins that form pores in the membrane of biological cells. The three-dimensional structure of aquaporin 1 and the pathway by which water is transported through the channel (but not other small solutes) were described by Agre.

(4) Residual (“leak”) transport

The residual or “leak” transport of an ion or a substance is a general term used to define a transport through a membrane which does not involve a specific transport pathway. Such residual transport would remain when all transporters including pumps, carriers, and channels are blocked [40]. There are several possible explanations for residual transport:

1. Diffusion through fluctuations in the lipid bilayer (existence of non-bilayer structures, kinks, interfaces of lipids in different states, and rafts),
2. Diffusion at the protein-lipid interface,
3. Diffusion through structures formed in the interior of protein aggregates or on protein subunits.

The mechanisms of ion transport pathways through biological membranes are summarized in Fig. 3. An overview of the principal transport pathways for Na^+ and K^+ in the human RBC membrane is shown in Fig. 4.

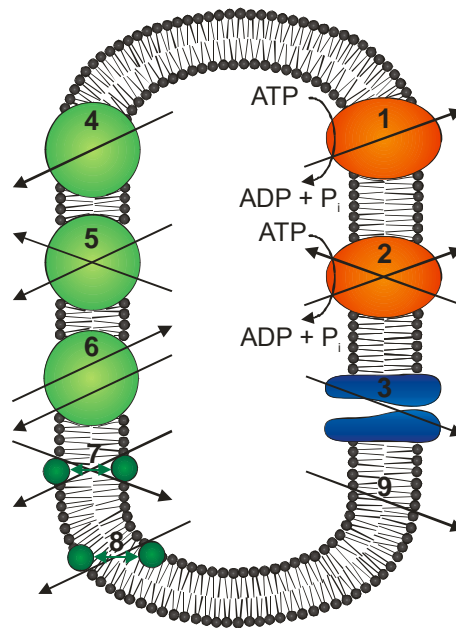


Fig. 3: Schematic illustration of the mechanisms of the ion transport through biological membranes (taken from [24]). 1, 2: active transport; 3: transport through channels; 4 – 8: carrier-mediated transport (4: uniport realized by an integral membrane protein, 5: symport realized by an integral membrane protein, 6: antiport realized by an integral membrane protein, 7: ionophore acting as antiporter, 8: ionophore-mediated uniport; 9: leak transport.

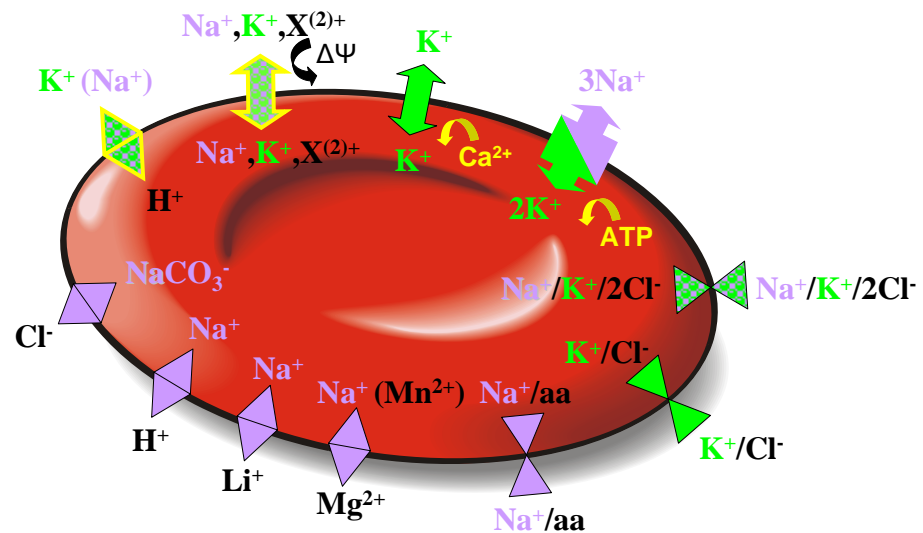


Fig. 4: Overview of the principal transport pathways for Na^+ and K^+ in human RBC membrane (taken from [40]). The following transport mechanisms are shown: Na^+/K^+ pump; $\text{Na}^+/\text{K}^+/\text{Cl}^-$ symporter; K^+/Cl^- symporter; Na^+ dependent amino acid (aa) transport (several discrete transporters); $\text{Na}^+(\text{Mn}^{2+})/\text{Mg}^{2+}$ antiporter; Na^+/Li^+ antiporter; Na^+/H^+ antiporter; $\text{NaCO}_3^-/\text{Cl}^-$ exchange (via the protein band 3); $\text{K}^+(\text{Na}^+)/\text{H}^+$ antiporter; non-selective voltage dependent cation (NSVDC) channel; Ca^{2+} -activated K^+ channel (Gardos channel).

2.2. Movement of membrane phospholipids

2.2.1. Flippase, floppase, and scramblase

In artificial liposomes, lipids form symmetrical and stable bilayers with a random spontaneous transbilayer lipid diffusion (or flip-flop) between both leaflets [41]. However, lipids in biological membranes are asymmetrically distributed across the bilayer. The choline-containing lipids, phosphatidylcholine (PC) and sphingomyelin (SM), are enriched primarily on the external leaflet of the plasma membrane. In contrast, the amine-containing

glycerophospholipids, phosphatidylethanolamine (PE) and phosphatidylserine (PS), are located preferentially on the cytoplasmic leaflet. The maintenance of transbilayer lipid asymmetry is essential for normal membrane function, and disruption of this asymmetry is associated with inducing or pathologic conditions. Lipid asymmetry is generated primarily by selective synthesis of lipids on one side of the membrane. Because passive lipid transbilayer diffusion is slow, a number of proteins are involved in either breakdown or maintain this lipid gradient. These proteins fall into three classes [41-43]:

- 1) Cytofacially-directed, ATP-dependent transporters (“flippases”);
- 2) Exofacially-directed, ATP-dependent transporters (“floppases”);
- 3) Bidirectional, ATP-independent transporters (“scramblases”).

Flippases

Flippase or aminophospholipid translocase (APTL) activity was first reported by Devaux and co-workers who measured the ATP-dependent uptake of spin-labelled lipid analogues in human RBCs [42, 44]. Phospholipids labelled with fluorescent fatty acids, particularly 7-nitrobenz-2-oxa-1,3-diazol-4-yl (NBD) derivatives, have also been used extensively to study this transporter [42, 45, 46]. The flippase is a 130 kDa integral membrane protein which is a member of the Mg^{2+} dependent P-glycoprotein ATPases [21]. It is responsible for translocation of phospholipids from one side of a membrane to the other against their gradients of concentration. Transport catalyzed by flippase is coupled with an ATPase; transport activity requires ATP and Mg^{2+} [46] and is inhibited by vanadate [44]. Flippase activity is also inhibited by Ca^{2+} [47, 48], indicating that the activity of this enzyme may be regulated in stimulated cells. The flippase is widely distributed and is present in most plasma membranes including RBCs, platelets,

lymphocytes, aortic endothelial cells, fibroblasts, pheochromocytoma cells, hepatocytes, and spermatozoa [49-53].

In principle, the transbilayer diffusion of phospholipids also occurs at a low speed, associated with very long residence time of lipids in each monolayer (several hours for long chain phospholipids) [54, 55]. Therefore, in the absence of flippase, gradually, the plasma membrane composition would eventually be randomized by the transbilayer lipid diffusion. Thereby flippases take part in maintenance of a transmembrane asymmetrical lipid distribution [41].

Flippase is responsible for localization of PS and PE in the inner leaflet by rapidly translocating them from the outer to the inner leaflet against the concentration gradient. The aminophospholipid flippase is perhaps the most selective of the lipid transporters. It prefers PS over other lipids [42, 44] and the specificity for PS is defined by each of the functional groups of the lipid in which the amine group is absolutely required [42]. When phosphatidyl hydroxypropionate, a PS analogue without an amino group has been used, it is not transported by flippase [56]. The enzyme can tolerate mono-methylation of PS and to a lesser extent, PE [57]. Recent data have shown that PC can be transported by an ATP-dependent flippase in mammalian cells and yeast [41, 58, 59]. However, progressive methylation of PE reduces transport significantly [57]. The carboxyl group is not essential (PE is also a transport substrate), but its absence lowers the rate of transport approximately 10-fold [60], and methyl esterification of the carboxyl group reduces transport activity significantly [57]. In contrast to other PS-specific proteins, such as protein kinase C [61] and the macrophage PS receptor [62, 63], the stereochemistry of the L-serine head group is unimportant for recognition by the flippase; both the D- and L-serine isomers are transported equally well [56, 57, 64]. So far, the best strategies to identify the function of flippases is using knock-out cells or natural mutants depleted of specific ATPases [42]. However, the mechanisms as well as the relation of flippase to Ca^{2+} , ATPase and protein kinase C is still under discussion. Nevertheless, the asymmetry of membrane lipids appears to depend on the activity of flippase, which actively translocates PS and PE to the inner leaflet [21, 65, 66].

Floppase

The second class of ATP-dependent lipid transporters are the exofacially-directed floppases. Early studies in RBCs revealed a nonspecific outward flux pathway for NBD- and spin-labelled lipids [21, 42, 67, 68]. It was recognized subsequently that not all but

some members of the ABC transporter super family are also capable of transporting lipids [42, 69, 70].

According to Borst et al. [69], ABC transporters are a diverse group of proteins that are responsible for the export of amphipathic compounds, a part of them is coupled with ATP consumption. Some of them are multidrug resistance proteins, which export cytotoxic xenobiotics. The most well characterized lipid floppase activities are those catalyzed by ABCA1, ABCB1, ABCB4, and ABCC1. The ABC transporter ABCA1 (ABC1) has been shown to transport cholesterol out of cells. This transporter may act as a floppase for both cholesterol and PS. Whether there exist a connection between cholesterol and PS transport is unclear, but this protein likely serves an efflux function, and is not involved in the maintenance of lipid asymmetry [69].

Scramblase

Daleke et al. [42] reported that rather than assist in the maintenance of lipid asymmetry, scramblases degrade the transbilayer phospholipid gradients by bidirectional transport without consuming ATP. Three scramblase activities have been reported; two are involved in dissipating lipid gradients in biogenic membranes and the third is activated by Ca^{2+} in the plasma membrane of induced cells. The scramblases are supposed to be ATP-independent transmembrane proteins, which are triggered by the presence of cytosolic Ca^{2+} in human RBCs [71-73]

The scramblases facilitate the flip-flop of lipids in a non-selective fashion. In the presence of Ca^{2+} , the scramblases behave like a channel for lipids allowing them to diffuse from one monolayer to the other according solely to the concentration gradient [41]. Recently, Wiedmer and colleague reported that phospholipid scramblase, a 35 kDa protein, mediates Ca^{2+} -induced bidirectional transbilayer movement of plasma membrane phospholipids in induced, injured, or apoptotic cells [74]. Furthermore, three additional novel cDNAs encoding proteins with high homology to HuPLSCR1 have been discovered. The fifth PLSCR was discovered by Strausberg et al [75]. PLSCR1, PLSCR2, and PLSCR4 are closely clustered on the short arm of chromosome 3 (3q23), PLSCR5 is located at 3q25 of chromosome 3, and PLSCR3 clustered on the long arm of chromosome 17 (17p13).

In 2008, Sahu et al. [76] reported that hPLSCR1 is activated when cytosolic Ca^{2+} levels rise by 1,000-fold and it scrambles phospholipids across the plasma membrane. Lopez-Montero et al. [77] reported that a Ca^{2+} dependent soluble sphingomyelinase (SMase) can

trigger scrambling of lipids by destabilizing the plasma membrane via conversion of the inner leaflet sphingomyelin to ceramide, a lipid with a very small polar head group. The change in the area occupied by this lipid in one leaflet can form temporary pores going along with lipid flip-flop would be facilitated.

2.2.2. Maintenance of plasma membrane lipid asymmetry

Once lipid asymmetry has been established, it is maintained by a combination of slow transbilayer diffusion, protein-lipid interactions, and protein-mediated transport [78]. Normal circulating RBCs exhibit an asymmetric distribution of phospholipids in the membrane where PS and PE reside in the inner leaflet and PC and SM are enriched on the outer leaflet [78]. Under physiological conditions, phospholipid asymmetry in the RBC membrane is relatively stable with slow exchange of phospholipids between the bilayer. Escape of PS or PE to the outer leaflet is quickly corrected by the action of an APTL that selectively transports aminophospholipids such as PS, and to a lesser extent PE, from the outer leaflet back to the inner leaflet [78, 79].

Experiments using several model membrane systems have given evidence supporting the direct interactions of the membrane skeleton and PS. Studies with liposomes and monolayer lipid films have demonstrated that the major cytoskeletal components, spectrin and band 4.1 specifically interact with PS. These data suggested that both spectrin and band 4.1 contribute to the maintenance of phospholipid asymmetry, by their capacity to “fix” PS to the inner leaflet. It becomes evident that considerable interaction between cytoskeletal proteins and aminophospholipids could occur in the cell [79].

2.2.3. Loss of phospholipid asymmetry and its consequences

The appearance of PS on the surface of the cell membrane can have major physiological consequences, including increased cell-cell interactions. The increased adherence of PS exposing RBCs to endothelial cells (ECs) may be pathologically important in haemoglobinopathies such as sickle cell disease and thalassaemia [80].

In several cases of RBC disorders, the passive and/or active phospholipid translocation processes have been found to be altered. In sickle cell anaemia and irreversibly sickled patients, active translocation of aminophospholipid is decreased even under aerobic conditions [81]. This causes a decrease of the asymmetric distribution of PS and the

microvesicles released from sickle cells while the PS level in the outer membrane leaflet of the remnant cells remains low [19]. A detailed analysis of sickle cells showed that PS exposure is limited to a subpopulation of the cells, varies widely among sickle cell patients, and takes place at several stages in the life of the sickle cell [82]. In RBCs of thalassaemic patients, the passive transbilayer mobility of phospholipids is enhanced while the active APTL mediated process is not altered. This enhanced passive transbilayer movement is probably responsible for the observed variable accumulation of PS in the outer leaflet of these cells [65, 83]. In patients with sickle cell anaemia and thalassaemia, exposure of PS to the outer membrane leaflet enhances adherence of cells to the endothelium [84], promotes phagocytosis of cells [85] and stimulates thrombotic events [72].

PS exposure on the surface of platelet membrane plays a central role in promoting blood coagulation, as this lipid serves as assembly site for coagulation factors, including the prothrombinase and tenase enzyme complexes [72, 86-88]. A defect in phospholipid scramblase has been found in Scott syndrome, in which activated platelets fail to expose PS on their surface sufficient for assembly of prothrombinase [89]. The exposure of PS is also a significant signal for a determined cell death called eryptosis and the remove of apoptotic cells by macrophages [89-95].

2.3. Phosphatidylserine exposure and cell adhesion

2.3.1. Possible mechanisms for phosphatidylserine exposure

The exposure of PS on the outer leaflet of the cell membrane is a complicated process because it involves many factors acting in combination ways. Although the pathways for PS exposure are not simply classified, some of them can be noted as following.

Ca²⁺ dependent pathway

It has been mentioned in over hundreds of publications that Ca²⁺ plays an important role in activating scramblases, thereby leading to the exposure of PS to outer leaflet of the cell membrane. The activation of Ca²⁺-activated K⁺ channel (Gardos channel) by an increase of intracellular Ca²⁺ content also leads to several effects such as cellular KCl loss, and

cell shrinkage due to loss of water. These effects could contribute to the PS exposure at a certain extent [96].

Osmotic shock is mediated by two distinct signalling pathways [97, 98]. First, it stimulates a cyclooxygenase leading to the formation of prostaglandin E₂ (PGE₂) and subsequent activation of Ca²⁺ permeable cation channels [99]. Second, it activates a phospholipase A₂ leading to the release of platelet activating factor, which in turn activates a SMase and thus stimulates the formation of ceramide [100]. The treatment of RBCs with some substances such as chlorpromazine, methyldopa, gold, and bismuth leads to an increase of intracellular Ca²⁺ and subsequently PS exposure [101-104].

Ca²⁺ independent pathway

The activity of APTL depends on the ATP level in the cells. In some reports, under glucose free or ATP depleted conditions or in the presence of orthovanadate, the exposure of PS was observed in RBCs. However, the number of cells showing PS exposure is very low even after long time treatment (24h - 48h) [101, 105-107]. Recently, Quan et al. [108] reported that under high concentration of glucose (0.8 M) RBCs showed PS exposure (80%). However, under this experimental conditions, caspase 3 and caspase 8 were not activated. PS exposure also was observed under stimulated conditions by Zn²⁺, Pb⁺ [109]. The PS exposure was also observed when RBCs have been induced by Pb⁺ (0.1 mM). This effect was paralleled by RBC shrinkage, which was apparent on the basis of the decrease in forward scatter of FACS analysis [110]. Caspases are a family of cysteine proteinases involved in the apoptotic process. Under normal conditions, they exist in zymogens. In initial stage, the caspase 8 or caspase 10 is activated and later they activate other caspases in a cascade. This cascade eventually leads to the activation of the effector caspases, such as caspase 3 and caspase 6. These caspases are responsible for the cleavage of the key cellular proteins, such as cytoskeletal proteins, that lead to the typical morphological changes observed in cells undergoing apoptosis such as membrane blebbing, and vesicle formation. Berg et al. [111] noted that *in vivo*, human mature RBCs express caspase 3 and caspase 8 but they a lack of mitochondrial regulators such as Apaf-1, cytochrome c, and caspases 2, 6, 7 and 9. Therefore, they can not undergo an apoptosis process. However, under oxidative stress conditions, e.g after adding 0.1 mM tert-butyl hydroperoxide, 100% of RBCs showed PS exposure. Mercury and some heavy metals also lead to activation of caspase 3 and in consequence to PS exposure [13, 112, 113].

2.3.2. Cellular microvesicle formation

Microvesicles (or microparticles) are small membrane bladder structures that are released from cells upon activation or during apoptosis. Cellular microvesicles constitute a heterogeneous population, differing in cellular origin, numbers, size, antigenic composition and functional properties. Microvesicles support coagulation by exposure of negatively charged phospholipids and sometimes tissue factor, the initiator of coagulation *in vivo*. Microvesicles may transfer bioactive molecules to other cells or other microvesicles, thereby stimulating cells to produce cytokines, cell-adhesion molecules, growth factors and tissue factors, and modulate endothelial functions. Microvesicles derived from various cells, most notably platelets but also leucocytes, lymphocytes, RBCs and endothelial cells, are present in the circulation of healthy subjects [114].

Microvesicles do not only carry accessible PS, but also membrane antigens including adhesion proteins, receptors and other procoagulant entities such as tissue factor. Membrane vesiculation in platelets may be seen as a method to increase the procoagulant surface for optimal spatially limited haemostasis, provided microvesicles are retained at the site of platelet adhesion and activation. Fig. 5 shows the multi-biological functions of microvesicles.

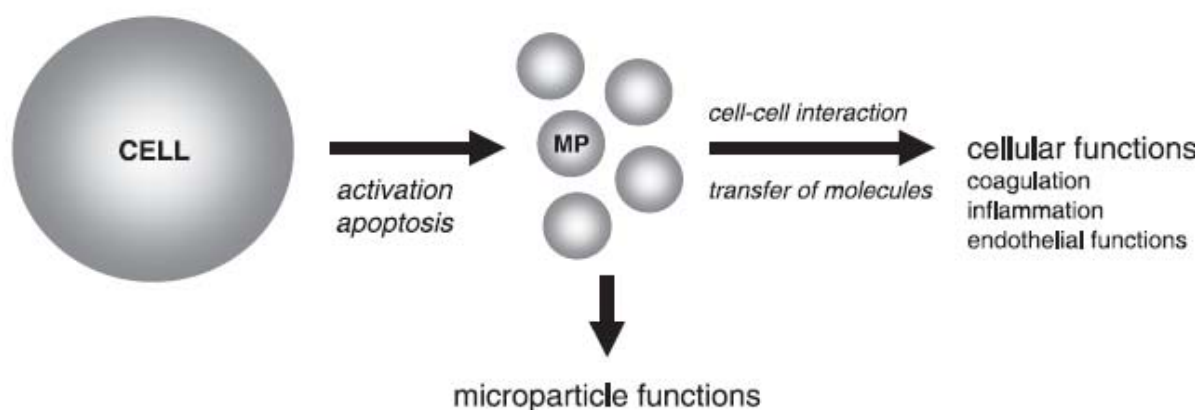


Fig. 5: Multi-biological functions of microvesicles (taken from [114]).

The mechanism for the formation of microvesicles is generally coincident with the transverse migration of PS and membrane blebbing. Blebs are thought to result from a transient overload of the outer leaflet at the expense of the inner one. When the

cytoskeleton is no longer able to counteract the surface tension, shedding of micro vesicles also takes place [114].

2.3.3. Adhesion of phosphatidylserine exposed red blood cells

PS exposure on the RBC surface facilitates the adhesion of RBCs to vascular endothelium. Setty et al. [115] noted that in sickle RBCs the exposed PSs were seen as ligands for the RBC adhesion receptor CD36. Another research with sickle cell anaemia shows that under normal conditions the RBCs are generally considered non-adhesive for endothelial cell surfaces. However, the PS exposed sickle RBCs show a significant adhesion with endothelial cell surfaces [116]. Closse et al. [117] noted that in pathological conditions such as sickle cell disease, malaria and diabetes, an abnormal adherence of RBCs to endothelium is concomitant with loss of phospholipid asymmetry resulting in PS exposure. The adhesion is inhibited by PS liposomes and by annexin V giving clear evidence of the PS dependence of these interactions.

In the aspect of coagulation, under stimulating conditions, cells and microvesicles carrying exposed PS provide a catalytic surface promoting the assembly of the characteristic enzyme complexes of the coagulation cascade. Microvesicles shed from activated platelets constitute the main circulating population. They harbour major membrane glycoproteins, including functional adhesive receptors, and consequently disseminate a procoagulant potential that can be targeted according to the nature of counterligands [118]. They can bind to soluble or immobilized fibrinogen and aggregate with platelets [119]. The procoagulant potential of exposed PS cells or microvesicles is not restricted to platelet microvesicles because microvesicles from monocytes, lymphocytes, RBCs or endothelial cells also present PS at their surface [120].

2.3.4. Traditional and new concepts about red blood cells in thrombosis

According to the traditional opinion, coagulation is primarily a function of endothelial cells, platelets, and soluble coagulation factors, in which platelets take a central role. RBCs, in contrast, are generally regarded as innocent bystanders, passively entrapped in a developing thrombus as they flow through the vasculature.

Andrews et al. [86], in an excellent review article, summarized evidence suggesting that the RBCs play an important role in thrombosis. Duke et al. [121] noted that an increase of

haematocrit in thrombocytopenic patients showed an improvement in bleeding times after transfusion, even though their platelet counts remained low. Fifty years later, Hellem et al. [122] while examined anaemic patients with bleeding defects, they observed a decrease in bleeding time upon transfusion of washed RBCs. Because the platelet counts of these patients decreased slightly, the causal factor was again assumed to be the RBC. Blajchman et al. [123] reported that thrombocytopenic patients and related animal models displayed improved bleeding times after RBC transfusion levels [122, 123]. Evidence showed that PS exposure on the outer leaflet of platelets might serve as a catalytic surface for the assembly of coagulation factors. Therefore, platelets can initiate the coagulation cascade [118, 124]. Recently, Kaestner et al. [99] suggested a model cascade in thrombosis formation (see Fig. 6). The model points out that under certain conditions (such as injury) the activation of platelets leads to a release of lysophosphatidic acid and prostaglandin E₂. These substances react as mediators, which activate a non-selective voltage dependent cation (NSVDC) channel leading to a rapid increase of intracellular Ca²⁺. The increase of intracellular Ca²⁺ activates Gardos channel and scramblase. The activation of the Gardos channel leads to an efflux of intracellular KCl and subsequently leads to cell shrinkage. In combination with the activity of the scramblase, the consequences of this cascade are shrinkage and aggregation of RBCs. Taken all together, one can figure out that RBCs play an active role in clot formation.

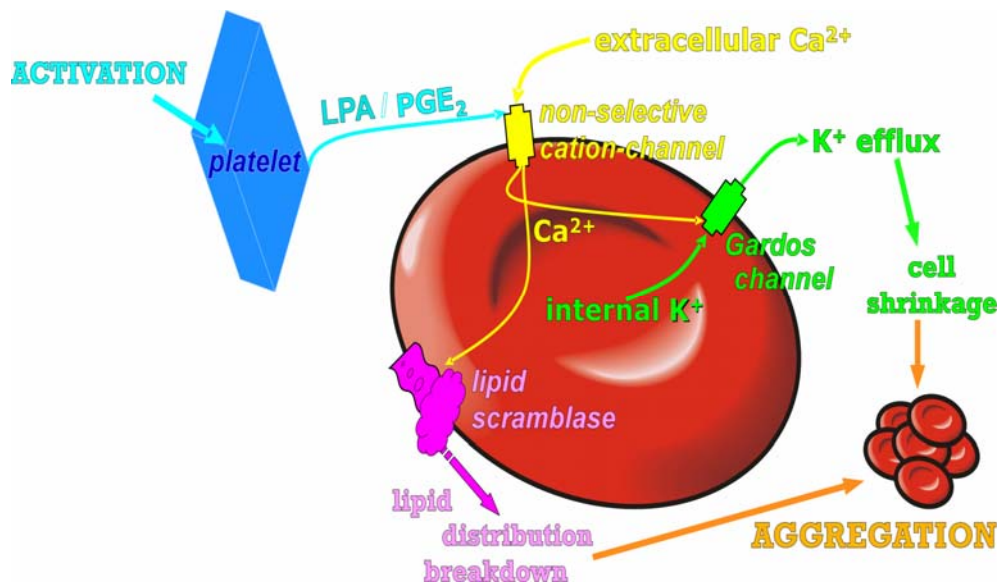


Fig. 6: Schematic cascade proposed for the aggregation of RBCs in activated conditions (provided by Prof. I. Bernhardt; proposed in [99]).

2.4. Biological role of Ca^{2+} in human red blood cells

2.4.1. Ca^{2+} homeostasis

The Ca^{2+} homeostasis of normal RBCs may appear deceptively simple because mature cells lack Ca^{2+} accumulation organelles and Ca^{2+} signalling functions (except the Ca^{2+} -activated K^+ channel). Their total Ca^{2+} content and Ca^{2+} permeability (P_{Ca}) are extremely low, and they have minimal cytoplasmic Ca^{2+} buffering capacity compared to other cell types [125].

The Ca^{2+} pump was originally discovered and extensively studied in RBCs. The maximal Ca^{2+} transport capacity (V_{max}) of the Ca^{2+} pump in human RBCs (approximately $10 \text{ mM [340 g Hb]}^{-1}\text{h}^{-1}$) is high compared with the normal pump-leak turnover rate of Ca^{2+} (approximately $50 \mu\text{mol [340 g Hb]}^{-1}\text{h}^{-1}$) [126].

The low intracellular Ca^{2+} concentration represents the balance between passive Ca^{2+} influx and active Ca^{2+} extrusion by the Ca^{2+} pump (see before). Passive Ca^{2+} influx is mediated through low capacity transport pathways with carrier properties [127, 128] and “leak”. Active Ca^{2+} extrusion is mediated by a large capacity (high V_{max}) [129].

The concentration of intracellular Ca^{2+} of RBCs under physiological conditions can be measured by different methods such as Ca^{2+} chelators, and atomic absorption spectroscopy. Fluorescent indicators for Ca^{2+} such as fura-2, indol 1, fluo-3, and fluo-4 have been commonly used. Kaestner et al. [130] pointed out that the application of fura-2 for intracellular Ca^{2+} measurement in RBCs was problematic because its excitation and emission properties were influenced by haemoglobin. Therefore, the accurate value of intracellular Ca^{2+} concentration is still uncertain. Until the problems are solved, it appears reasonable to consider the physiological intracellular Ca^{2+} level in human RBCs to be approximately 100 nM, probably within the range of 30 to 60 nM [131, 132].

2.4.2. Influence of intracellular Ca^{2+} on phosphatidylserine exposure

It has been shown in hundreds of publications that elevation of intracellular Ca^{2+} levels can induce rapid transbilayer redistribution of the phospholipids in human RBCs and platelets [133], resulting in the loss of normal phospholipid asymmetry [71, 134]. The asymmetry of membrane phospholipids is disturbed when RBCs are loaded with Ca^{2+} by using the

ionophore A23187. At moderate intracellular Ca^{2+} concentrations (50-100 μM), the effect appears to involve all major phospholipids in human RBCs, as shown by spin labelling and use of fluorescent phospholipid analogues [71, 135].

Lysophosphatidic acid and PGE_2 are important lipid mediators in various pathophysiological processes. They can stimulate an open of a Ca^{2+} channel in human RBCs. Therefore, in the presence of Ca^{2+} , they stimulate PS exposure and procoagulant microvesicle generation in RBCs [124, 136, 137].

Caspases are aspartate-specific cysteine proteinases that exist as latent zymogens, but once activated by eryptosis signals, they promote eryptosis by specific limited proteolysis of key cellular substrates. Under physiological conditions, the procaspase presents in mature RBCs. The overload of Ca^{2+} in the cells also leads to the activation of caspase, which is associated with impairment of aminophospholipid flippase activity leading to PS exposure [113, 138].

2.4.3. Influence of intracellular Ca^{2+} on protein kinase C

Two decades ago, the discovery of protein kinase C (PKC) opened a new research field of signal transduction. PKC is a large family of proteins with closely related structures but slightly distinct properties [78, 139]. Based on the structure and properties of their regulatory regions, PKC isoforms are divided into three subgroups (see Table 2).

Classical PKC enzymes or cPKC isoforms have been initially identified. The cPKCs have a C-2 domain binding with Ca^{2+} , and they are activated by Ca^{2+} , diacylglycerol or phorbol ester in the presence of PS. New protein kinase C isoforms or nPKCs do not possess a Ca^{2+} sensitive domain in their molecules, but they are activated by diacylglycerol. Atypical protein kinase C isoforms or aPKCs require PS for their activation but they do not respond neither to diacylglycerol and phorbol ester, nor to Ca^{2+} [107].

Recent experiments have noted that phorbol ester-mediated PKC activation stimulates RBC Ca^{2+} entry [136, 140-142] and PS exposure [143]. It has been known for a long time that human RBCs containing PKC mediate the phosphorylation of cytoskeletal proteins, such as band 4.1, 4.9, and the human Na^+/H^+ antiporter NHE-1 [107]. To date, $\text{PKC}\alpha$, $\text{PKC}\iota$, $\text{PKC}\mu$, and $\text{PKC}\xi$ have been reported to be expressed in RBCs. Upon activation, they influence cytoskeletal integrity and RBC functions. Although there were some reports about the activation of PKC leading to the apoptosis of RBCs, besides the artificial

activation of PKC by phorbol esters [143], no experimental data about the involvement of PKC activation and the exposure of PS in RBC are available [107].

Table 2: Protein kinase C isoforms in mammalian tissues (taken from [144]).

Subgroup	Amino acid residues	Ca ²⁺ and lipid activators	Tissue expression
cPKC		Ca ²⁺ , DAG, PS, FFAs, lyso PC	
α	622	"	Universal
βI	671	"	Some tissues
βII	671	"	Many tissues
γ	697		Brain only
nPKC			
δ	673	DAG, PS	Universal
ε	737	DAG, PS, FFA, PIP ₃	Brain and others
η (L)	683	DAG, PS, PIP ₃ , cholesterol sulfate	Skin, lung, heart
θ	707	?	Muscle, T-cell etc.
μ	912	?	NRK cells
aPKC			
ζ	592	PS, FFA, PIP ₃	Universal
λ, ι	587	?	Many tissues

PKC, protein kinase C; DAG, diacylglycerol; PS, phosphatidylserine; FFA, free unsaturated fatty acid; lyso PC, lysophosphatidylcholine; PIP₃, phosphatidylinositol-1,-,4,5-tetrakisphosphate ([145, 146]).

2.5. The ageing of red blood cells

2.5.1. Young and old red blood cells

In adult mammals, the circulating RBCs represent the product of a process of differentiation, which involves great biochemical and physiological changes. An undifferentiated stem cell in the bone marrow undergoes a series of cell divisions under the stimulus of the hormone erythropoietin to produce the sequential cell types: the erythroblast, the basophilic, polychromatophilic and orthochromatic normoblasts and the reticulocytes. Four mitoses occur during this transformation so that on average 16

reticulocytes are derived from each stem cell. During this process, the cells become smaller, the nucleus denser and the rate of haemoglobin synthesis increase. Finally, the nucleus is extruded, RNA production is ceased, and the immature RBC or reticulocyte is released into the circulation. Morphological changes during erythroid cell maturation are described also by Bessis [147]. During the differentiation process, there are alterations in membrane structure and function involving changes in membrane and lipid composition, changes in the transport of amino acids, sugars, Ca^{2+} , Na^+ and K^+ [148].

Methods such as gradient centrifugation, filtration, have been developed to separate the RBCs into young and old cell population [149-151]. Some differences among young and old RBCs are observed including change in geometry [150], reduced activity of Gardos channel [151], change in some enzymes [152], and vitamins with age [153]. A study on human RBC galactokinase in fetus and adult RBCs has revealed that the specific activity of galactokinase is three times higher in the fetal RBCs than in adult cells showing a significant difference in the Michaelis constant toward galactose [154]. The relationship between RBC aging and enzyme activities in rabbit, guinea pig, hamster, rats and mice blood was studied. Six enzymes: glucose-6-phosphate dehydrogenase (G-6-PD), 6-phosphogluconate dehydrogenase (6-PGD), hexokinase (Hx), glutamate oxaloacetate transaminase (GOT), lactate dehydrogenase (LDH) and acetylcholinesterase (AChE), were measured in the RBCs of different ages. It was found that activities of Hx, AChE and GOT activities were much higher in younger RBCs than in older cells; hence the activities of these enzymes may be used as an indicator of age of the cells [155].

The membrane redox activity in young and old RBCs is also evaluated. A reduction of membrane redox activity relating to ageing has been described [156, 157].

2.5.2. Ca^{2+} content in young and old red blood cells

Romero et al. [158] applied two methods using Percoll density gradients to separate light and dense RBCs from fresh human blood. Intracellular Ca^{2+} of RBCs in different fractions was quantitatively measured using fura-2. The results of five experiments showed that the free Ca^{2+} content was 8.4 ± 2.82 nM and 31.2 ± 13.0 nM in the 7 - 10% lightest and densest cells, respectively. However, it should be mentioned that concerning the interference of haemoglobin, fura-2 cannot be applied (Kaestner et al. [130]).

By using atomic absorption spectrometry early studies have shown a two-fold increase in Ca^{2+} content of the dense fraction in comparison to the light fraction of human RBCs

(after centrifugation in Percoll gradients). These authors also reported that the heaviest (old) cells take up more Ca^{2+} after being exposed to relatively high Ca^{2+} levels [149]. These results suggest that the RBC Ca^{2+} rises during ageing *in vivo*.

On the other hand, it is well known that a decrease of both ATP content [149] and activity of some key glycolytic enzymes occurs upon ageing of human RBCs. The decline in the concentration of phosphorylated compounds thus arising in senescent cells, would lead to a reduction in their Ca^{2+} chelating potential. Since the intracellular Ca^{2+} level is directly controlled by the activity of the ATP-dependent Ca^{2+} pump, it is expected that the decreased ATP content due to senescence may lead to an increase of the intracellular Ca^{2+} level [158]. In a concise report, Kirkpatrick et al. [159] investigated the concentration of adenosine triphosphate (ATP) in circulating RBCs. The result showed that the ATP level in the cells of the densest fraction (0.1-1% of circulating RBCs) decreased in comparison to unfractionated cells. However, the dense cells were also smaller, and the concentration of ATP in these cells was the same as in controls. Therefore, it seems unlikely that loss of cellular ATP is a crucial factor in removal of senescent RBCs from the circulation.

More recently, Kaestner et al. [130] has pointed out that the absorption of haemoglobin is close to the excitation of fura-2. Fluo-4 turns out to be the preferable indicator for fluorescent measurement in RBCs because of several reasons: (i) its excitation and emission properties are least influenced by haemoglobin and (ii) it is the only dye for which excitation light does not lead to significant auto-fluorescence of the RBCs. Taken all recent data together, it seems that the intracellular Ca^{2+} content in young and old RBCs is still a problem of debate.

2.5.3. Influence of ageing on membrane redox systems in red blood cells

RBCs are highly specialized cells, they are responsible for oxygen and carbon dioxide transport [160]. Glycolysis and the oxidative pentose phosphate pathway generate NADH and NADPH to reduce methaemoglobin. Therefore, RBCs deal with many free radicals during their life. At the end of their life span, the human RBCs are phagocytosed [161, 162].

Eukaryotic cells display a plasma membrane redox system (PMRS) that transfers electrons from intracellular substrates to extracellular electron acceptors. The physiological importance of PMRS is not fully understood, especially in RBCs [156]. However, the

PMRS appears to attenuate oxidative stress acting as a compensatory mechanism, lowering oxidative stress during the aging process [163, 164]. The PMRS accomplishes this by producing more NAD^+ for glycolytic ATP production via transfer of electrons from intracellular reducing equivalents to extracellular acceptors [157]. Fig. 7 shows the key enzymes of the plasma membrane redox system.

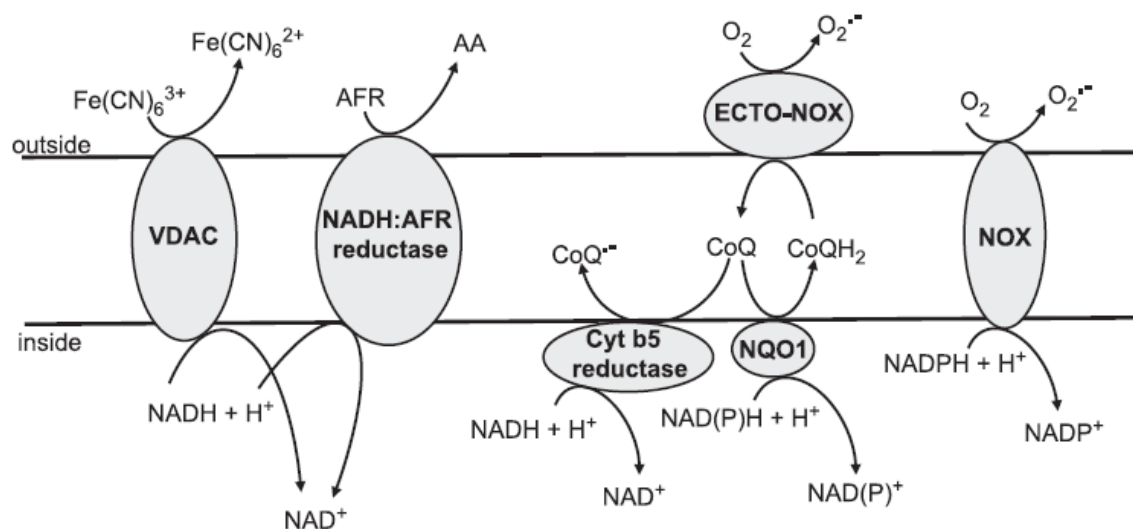


Fig. 7: Key enzymes of the plasma membrane redox system (taken from [165]). Membrane localisation and catalysed reactions for each enzyme are shown, in which CoQ takes the central role as an electron linker. AA: ascorbate; AFR: ascorbyl free radical; VDAC: voltage dependent anion selective channel or NADH: ferricyanide reductase; NQO1, NAD(P)H: ubiquinone, idoreductase or DT-diaphorase; NOX, NADPH oxidase; ECTO-NOX, NADH oxidase, CoQ: coenzyme Q.

Studies on the determination of the activity of PMRS in human RBCs as a function of age and the correlation of the activity with total plasma antioxidant capacity have been carried out to understand the role of PMRS in human aging. The activity of RBC PMRS is estimated by following the reduction of ferricyanide. The total antioxidant capacity of the plasma is estimated in terms of ferric reducing the ability of plasma (FRAP) values. A significant correlation is observed between PMRS activity of RBCs and human age. There is an age dependent decrease in total plasma antioxidant capacity measured in terms of FRAP values [156].

2.5.4. Relevance of ageing and apoptosis

The ageing of RBCs leads to the binding of autologous IgG and subsequently is the recognition and removal through phagocytosis, mainly by Kupffer cells in the liver. This process is triggered by the appearance of a senescent RBC-specific antigen. The functional and structural characteristics of senescent RBCs strongly suggest that this antigen originates on band 3, probably by Ca^{2+} induced proteolysis [166]. Generation of vesicles enriched in denatured haemoglobin is an integral part of the RBC aging process. These vesicles showing PS exposure are also removed by Kupffer cells. Moreover, senescent RBC-specific antigens are present on vesicles. Thus, vesicles and senescent RBCs may be recognized and removed through the same signals [166].

In sickle cell anaemia, when sickle cells are separated by density, the lightest and densest fractions tend to have the highest percentages of PS exposed cells. Loss of phospholipid asymmetry in dense cells may be a consequence of increased sickling or of the deactivation of ATP dependent APTL that is responsible for returning PS from the outer to the inner leaflet [81].

However, data obtained using biotin labelled RBCs in patients with sickle cell disease indicate that the exposure of PS does not lead to the immediate removal of high-density sickle RBCs from the circulation [167]. In murine sickle cell anaemia, short survival of PS exposed RBCs was observed. However, most of the decreased RBC survival in this model appeared to be independent of PS externalization. External PS may also be involved in thrombogenesis. Chiu et al. [168] showed that the dense fraction of sickle cells, which typically contains a high number of PS exposed cells, has procoagulant activity *in vitro*.

These and other data support the theory that RBC ageing is a form of apoptosis (also named eryptosis) that is concentrated in the cell membrane, and provide the context for future studies on initiation and regulation of the RBC ageing process. The clarification of the normal ageing mechanism is essential for understanding the fate of RBCs in pathological circumstances and the survival of donor RBCs after transfusion.

3. Materials and Methods

3.1. Materials

3.1.1. Chemicals and reagents

The common used substances and reagents are listed below:

Substances	Source	Stock solution in solvent
4,7-diphenyl-1,10-phenanthroline disulfonic acid disodium salt hydrate	Merck	
4-bromo-calcium ionophore A23187	Sigma-Aldrich	1 mM in ethanol
Acetic acid	VWR	
Amersham hyperfilm ECL	Amersham	
Ammonium persulfate (APS)	Roth	10% in H ₂ O
Annexin V-alexa 568	Roche	
Annexin V-FITC	Invitrogen	
BC Assay: Protein quantitation kit	Uptima	
BCECF, AM	Molecular Probes	1 mM in Pluronic
Beta-mercapto ethanol	Roth	
Bromophenolblue	Roth	
Charybdotoxin	Sigma-Aldrich	200 μ M in 1 M NaCl
Chelerythrine	Sigma-Aldrich	1 mM in DMSO
Citric acid	Roth	
DMSO	Roth	
Drabkin reagent	Sigma-Aldrich	1 ampul in 1 l H ₂ O
ECL advance western blotting detection kit	Amersham	
Ethanol	Sigma-Aldrich	
Ethylendiamintetraacetat-Na (EDTA)	Roth	
Ethylenglycoltetraacetat-Na (EGTA)	Roth	
Fibrinogen	Sigma-Aldrich	
Fluo-4, AM	Molecular Probes	1 mM in Pluronic
Glucose	Roth	

Glutaraldehyde	Sigma-Aldrich	
Glycine	Roth	
Heparin	Sigma-Aldrich	
HEPES	Roth	
Inorganic salts (NaCl, CaCl ₂ , KCl, FeCl ₃ ...)	Sigma-Aldrich/ Roth	
Inosine	Sigma-Aldrich	
Iodoacetate	Sigma-Aldrich	
K ₃ [Fe(CN) ₆]	Merck	
K ₄ [Fe(CN) ₆]	Merck	
L-polylysine	Sigma-Aldrich	
Lysophosphatidic acid (LPA)	Sigma-Aldrich	1 mM in H ₂ O
Methanol	Sigma-Aldrich	
NaOH	Roth	
Nigericin	Sigma-Aldrich	1 mM in ethanol
O-vanadate	Sigma-Aldrich	1 mM in PBS (*)
Percoll	Sigma-Aldrich	
Phenylmethylsulfonylfluorid (PMSF)	Sigma-Aldrich	
Phorbol 12-myristate 13-acetate	Sigma-Aldrich	1 mM in DMSO
Pluronic F-127, 20% in DMSO	Molecular Probes	
Poly-L-Lysin, 0,1% in H ₂ O	Sigma-Aldrich	
Prestained PAGE ladder	Fermentas	
Sodium acetate	Roth	
Sodium dodecylsulfate	Sigma-Aldrich	10% in H ₂ O
Staurosporine	Sigma-Aldrich	1 mM in DMSO
Tetramethylethylenediamine (TEMED)	Roth	
Thrombin	Sigma-Aldrich	148 IU in 0.9% NaCl
Tris (hydroxymethyl) aminomethane	Roth	
Triton X 100	Sigma-Aldrich	
Tween 20	Serva	
Valinomycin	Sigma-Aldrich	1 mM in DMSO

(*): O-vanadate is dissolved in PSB buffer. The pH 7.4 is adjusted by 0.1 M NaOH.

Main solutions used:

- Physiological solution (mM): NaCl 140, KCl 7.5, HEPES 10, Glucose 10 (pH 7.4, 0.1 M NaOH)
- PBS buffer (mM): NaCl 140, KCl 3.0, Na₂HPO₄ 7.5, and KH₂PO₄ 1.5, (pH 7.4, 0.1 M NaOH)
- B-buffer (mM): NaCl 145 in PBS 10, EDTA 0.5, 0.05% Glucose, (pH 7.4, 0.1 M NaOH).
- Annexin binding buffer (mM): NaCl 145, HEPES 10 CaCl₂ 2.5, (pH 7.4, 0.1 M NaOH)

Main reagents used:**A. Fluorescent dyes for measurement of Ca²⁺ and pH****Fluo-4, AM**

Fluo-4 is a special fluorescent dye for quantifying cellular Ca²⁺ concentrations in the 100 nM to 1 μM range with the K_d (Ca²⁺) of 345 nM [169]. Fluo-4 is similar in structure and spectral properties to the widely used fluorescent Ca²⁺-indicator dye, fluo-3, but it has certain advantages over fluo-3. Due to its greater absorption near 488 nm and the emission at 520 nm fluo-4 offers substantially brighter fluorescence emission when used with excitation by an argon ion laser or other sources in conjunction with the standard fluorescein filter set. The structure and fluorescence emission spectra of fluo-4 and fluo-3 are shown in Fig 8.

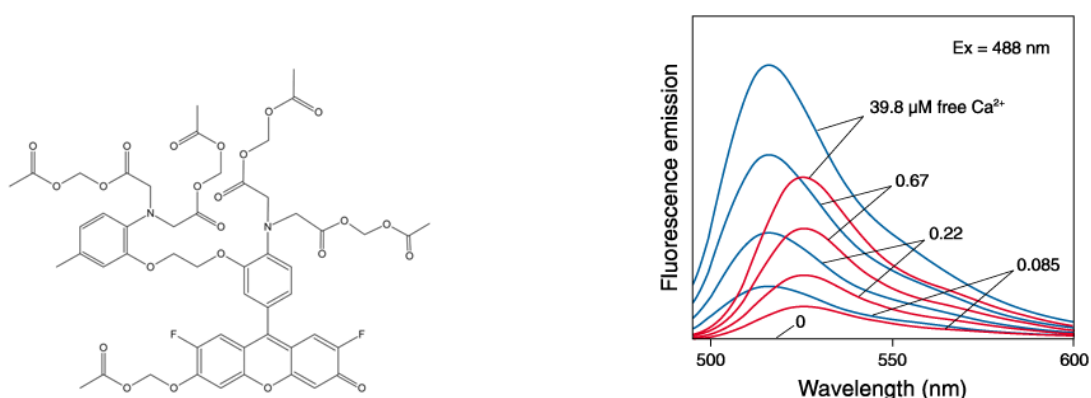


Fig 8: Structure and fluorescence emission spectra of fluo-4 and fluo-3. Left: molecular structure of fluo-4, right: fluorescence emission spectra of fluo-4 and fluo-3. The upper curve corresponds to fluo-4, the lower to fluo-3 for the same Ca²⁺ concentration. (<http://www.invitrogen.com/site/us/en/home/References/Molecular-Probes-The-Handbook/Indicators-for-Ca2-Mg2-Zn2-and-Other-Metal-Ions/Fluorescent-Ca2-Indicators-Excited-with-Visible-Light.html>).

BCECF, AM

Cell-permeable 2', 7'-bis-(2-carboxyethyl)-5-(and-6)-carboxyfluorescein acetoxymethyl ester (BCECF-AM) has been introduced by Roger Tsien and co-workers since 1982. So far, it is the most widely used fluorescent indicator for intracellular pH measurement. The structure and pH-dependent fluorescence excitation spectra of BCECF are shown in Fig. 9.

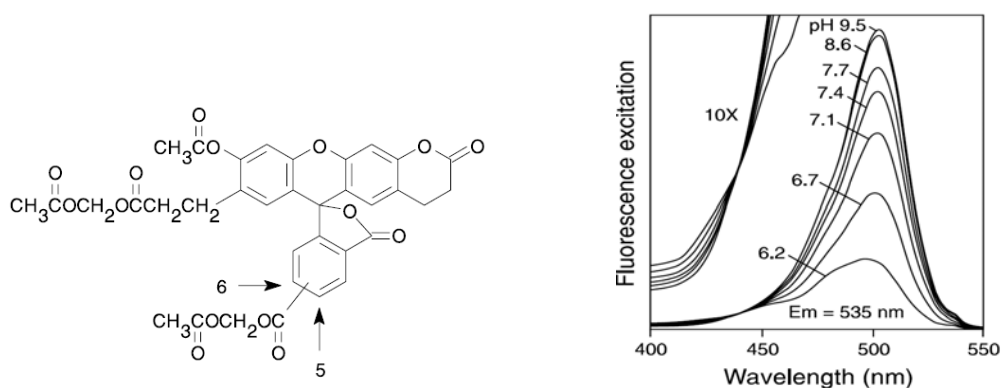


Fig. 9: Structure and pH-dependent fluorescence excitation spectra of BCECF.
(<http://probes.invitrogen.com/media/pis/mp01150.pdf>)

For BCECF, the pKa of 7.0 is ideally matched to the normal range of cytoplasmic pH (~6.8–7.4). The fluorescence excitation profile is pH-dependent (Fig. 9), allowing the implementation of ratiometric measurement techniques. The absorption maximum of the base form of BCECF is very close to the 488 nm argon ion laser, making it ideally suited for fluorescence microscopy applications. The acetoxymethyl ester derivative is a membrane permeant, allowing non-invasive bulk loading of cell suspensions. BCECF, AM is nonfluorescent by itself. It is converted to fluorescent BCECF via the action of intracellular esterases. Once inside the cell, the lipophilic blocking groups are cleaved by nonspecific esterases, resulting in a charged form that leaks out of cells much slower than its AM compound.

B. Annexin and its conjugates

Annexin V-FITC

Annexin V-FITC is a conjugate of annexin V with fluorescein isothiocyanate. Annexin V is a 35-36 kDa phospholipid binding protein with high affinity for PS in the presence of physiological concentrations of calcium. According to the manual instruction, the K_d for the binding of annexin V to PS has been estimated at $5 \cdot 10^{-10}$ M. The annexin V binding

assay is based on the rapid and selective binding to PS found in the outer cell membrane at the beginning of the apoptosis process.

Annexin V-alexa 568

Annexin V-alexa 568 is a conjugation of annexin V with an alexa fluorescent dye. The excitation and emission wavelengths of Annexin V-alexa 568 are 488 - 596 nm and over 600 nm, respectively. Like annexin V-FITC, annexin V-alexa 568 is also used to detect the PS exposure on the outer leaflet of the cell membrane. The structure of alexa 568 is shown in Fig. 10.

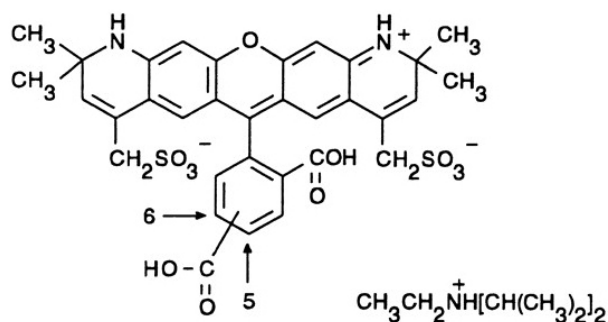


Fig. 10: The structure of alexa 568.

C. BD Retic-COUNT

BD Retic-COUNT (Becton Dickinson) is a trade name for 1-methyl-4[(3-methyl-2(3(H)-benzothiazolyli-dine) methyl]-quinolinium 4-methyl benzene sulfonate (Thiazole Orange). Retic COUNT is used to determine the number of reticulocytes in a population of RBCs. The immature RBCs contain fragments of RNA. The thiazole orange reagent will react with RNA molecules to form a complex of the RNA/thiazole orange (in the ratio 1:2). This complex exhibits an absorption band at 475 nm and a fluorescence emission band at 530 nm. This property makes it suitable for using with flow cytometers equipped with a 488 nm laser.

3.1.2. Main equipments and softwares used

- Fluorescence microscope: The fluorescence microscope model Eclipse TE 2000 E, Nikon was used to measure Ca^{2+} flux, intracellular Ca^{2+} , intracellular pH and kinetic processes. The fluorescence microscope combines with a focus-stabilizer (Nikon, T-PFC) and a very sensitive CCD camera (CCD97, Photometries, Cascade 512B) from Visitron systems. The included MetaVue software helps manipulations to become more feasible and precise.

- Flow cytometry: Intracellular Ca²⁺ and annexin positive cells are analysed by using a flow cytometer (FACScalibur 4CS E4021, Becton Dickinson and CellQuest software).
- Confocal laser scanning microscope (CLSM): The confocal microscope model ZEISS LSM 510 Meta was also used to investigate the intracellular Ca²⁺ content and annexin positive cells. Three different channels were used: transmission light, channel 1 argon laser (488 nm) for fluo-4, and channel 2 HeNe1 laser 543 for Alexa 543/568. Both single and multi channel scan were applied.
- Spectrophotometer: UV mini 1240, UV-Vis spectrophotometer, Shimadzu
- Sodium dodecyl sulfate polyacrylamide gel electrophoresis (SDS-PAGE) was carried out with BioRad Mini-Gel apparatus. The BioRad membrane transfer system was used for blotting.
- Different centrifuges were used:
 - Eppendorf centrifuge, model 5415D with rotor 78838,
 - Heraeus, Biofuge Stratos, Rotor # 3407,
 - Sorvall RC-5B refrigerated superspeed centrifuge, rotor SS-304, Dupont Instrument centrifuge
- The osmolarity of solutions was measured using an osmometer: Osmometer automatic, Knauer.
- Atomic force microscope: Bioscope IV, Veeco Instr., Santa Barbara, USA with Nano Scope controlling software.

3.2. Methods

3.2.1. Cell biology methods based on fluorescence microscopy and flow cytometry

A. Red blood cell preparation

Human venous blood was drawn from healthy donors. Heparin was used as anticoagulant. The blood samples were obtained from the Institute of Clinical Haematology and Transfusion Medicine of Saarland University Hospital.

Sickle cell anaemia blood was taken from young patients in the Department of Paediatric Oncology and Haematology of the Saarland University Hospital.

Sheep and cow blood samples were obtained from the sheep farm Ernst in Blieskastel, Germany.

Heparin anticoagulated rat and mouse blood samples were kindly given from the Department of Zoology and Physiology, and Department of Genetics, University of Saarland. In all experiments, antibiotics were not added to avoid possible interactions with the different assay systems.

Blood was washed by centrifugation at 2.000 g for 5 min at room temperature. The plasma was removed by aspiration. Subsequently, the RBCs were washed 3 times in physiological solution to remove the buffy coat. Finally, RBCs were re-suspended in physiological solution and the experiment started. Washed RBCs were depleted of ATP by pre-incubation in physiological solution without glucose in the presence of 1 mM iodoacetate and 10 mM inosine at 37°C for 90 min [3, 170]. Subsequently, RBCs were washed in the same solution 3 times by quick centrifugation (20 s, 12.000 g). Finally, RBCs were kept in physiological solution without glucose.

B. Intracellular Ca²⁺ measurement

In principle, the intracellular Ca²⁺ in the cells can be quantitatively measured using fura-2. Monitoring the intracellular free Ca²⁺ concentration in a fura-2 stained RBC population using a fluorescence spectrometer has been a standard method for more than a decade [171, 172]. Nevertheless, already in 1997 Blackwood et al. reported problems associated with fura-2 measurements in human RBCs [173]. The problems pointed to an effect of haemoglobin on the spectral properties of fura-2. The maximal absorption of haemoglobin is in the range of 410 - 430 nm. Therefore, fura-2 can not be applied for Ca²⁺ measurement in RBCs. In all experiments with RBCs, fluo-4, AM was used to measure intracellular Ca²⁺.

To measure the free cytosolic Ca²⁺ (intracellular Ca²⁺), the washed RBCs were suspended in physiological solution at 1% haematocrit with fluo-4, AM at 2.5 µM final concentration. The cell suspension was mixed by vortexing and incubated for 45 min at 37°C with occasionally shaking. Subsequently, the cells were washed 3 times with the physiological solution by quick centrifugation (20 s, 12.000 g) and re-suspended in physiological solution (haematocrit 0.5%).

The intracellular Ca²⁺ was measured by the addition of 50 µl of fluo-4 loaded cell suspension to 950 µl of physiological solution on a coverslip (0.025% haematocrit). The fluorescence intensity of fluo-4 in the cells was measured with the fluorescence microscope at room temperature. The fluo-4 loaded cells were excited with 488 nm light. The emission

fluorescence was detected at 530/15 nm. The fluorescence signals were normalized with background correction.

For the control, the fluorescence intensity of fluo-4 was measured under physiological condition in the presence of 2 mM extracellular Ca^{2+} . For the experiments with LPA, A23187, PMA or other substances, the samples were prepared like the control. However, just before starting the experiment, these substances were added. Every experiment was carried out with at least three different bloods. The data were analysed using MetaVue software.

In parallel with the fluorescence microscope, intracellular Ca^{2+} content was also measured using the flow cytometer (FACS). All parameters were adjusted using a calibration bead kit. The parameters for most measurements are listed below:

Parameters	Detector	Voltage	Amp Gain	Mode
P1	FSC	E00	2.5	lin/log
P2	SSC	450	1.0	lin/log
P3	FL-1	650	1.0	log

For each measurement, 30.000 RBCs were counted. At least 3 different bloods were used for each experiment. The data were analysed using BD Cell Quest Pro Software.

For the calibration of the intracellular Ca^{2+} concentration, a series of physiological solutions containing different Ca^{2+} concentrations was used. The final concentration of A23187 to calibrate the fluorescence intensity depending on the Ca^{2+} concentration was 2 μM .

C. Intracellular pH measurement

According to Tsien, the intracellular pH can be monitored by using the fluorescent dye 2,7-biscarboxyl-5(6)-carboxyfluorescein (BCECF) [174]. Washed RBCs at a haematocrit of 1% were loaded with cell-permeable acetoxymethyl ester of BCECF (BCECF, AM) in physiological solution at 5 μM final concentration for 45 min at 37°C. After incubation, the cells were washed 3 times with physiological solution as described above and resuspended in physiological solution (haematocrit 0.5%).

The pH measurements were started by the addition of 50 μl of BCECF loaded cell suspension to 950 ml of physiological solution on a coverslip (haematocrit 0.025%). Depending on the purpose of the experiments, different substances were added before starting the measurement. The fluorescence of BCECF in the cells was measured with the

fluorescence microscope (Eclipse TI 2000 E, Nikon) at room temperature. The BCECF loaded cells were alternately excited with 450 and 490 nm light. The emission wavelength was set at 535 nm. The ratio of the two fluorescence intensities (490/450) can be directly converted to pH_i value using a calibration. The ratio of two wavelengths is independent of dye leakage, photobleaching and cellular volume changes [174].

To convert the fluorescence ratio of BCECF loaded RBCs into intracellular pH values, a calibration was carried out by equalizing pH_i and pH_o using the K^+/H^+ ionophore nigericin (final concentration 10 μM) [175]. To calibrate the pH_i , cells were suspended into high K^+ solution (135 mM KCl, 10 mM NaCl, 10 mM glucose, 10 mM HEPES/NaOH). Different pH solutions (from 6 to 8.5) were used for the calibration. After adding nigericin, the cell suspension was kept at room temperature for 30 min to allow an exchange process of K^+ and H^+ between the cells and the outer solution until an equilibrium of distribution of K^+ and H^+ was established. The ratio of 490/450 was automatically calculated using Meta Vue Imaging Software with background correction. The calibration was carried out before each experiment. Fig. 11 shows the standard calibration curve for pH_i .

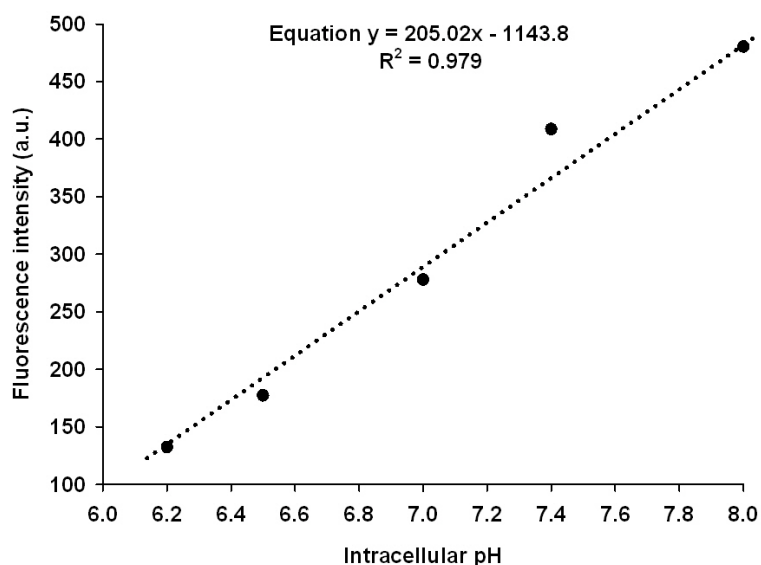


Fig. 11: Representative standard calibration curve for pH_i .

D. Determination of the exposure of PS on the outer leaflet of the cell membrane

The presence of PS on the outer leaflet of the RBC membrane surface is quantified based on the binding of PS with annexin V-FITC. The stimulated RBCs for PS exposure were washed in PBS buffer by quick centrifugation (20 s, 12.000 g). Subsequently, 500 μl of annexin binding buffer and 5 μl of annexin V-FITC were added into each sample. The

samples were mixed well and incubated at room temperature for 15 min. After incubation, the samples were put on ice and analysed.

The excitation and emission wavelength of annexin V-FITC are 488 and 530, respectively. Annexin V-FITC is excited by an argon laser; the fluorescence is detected using a 530/30nm band pass filter.

For each measurement, 30.000 RBCs were counted. The annexin V positive RBCs can be calculated in percentage by comparison of positive and negative signal events with the control. Cell Quest Pro software was used for data acquisition and analysis. The principle of this measurement is described in Fig. 12.

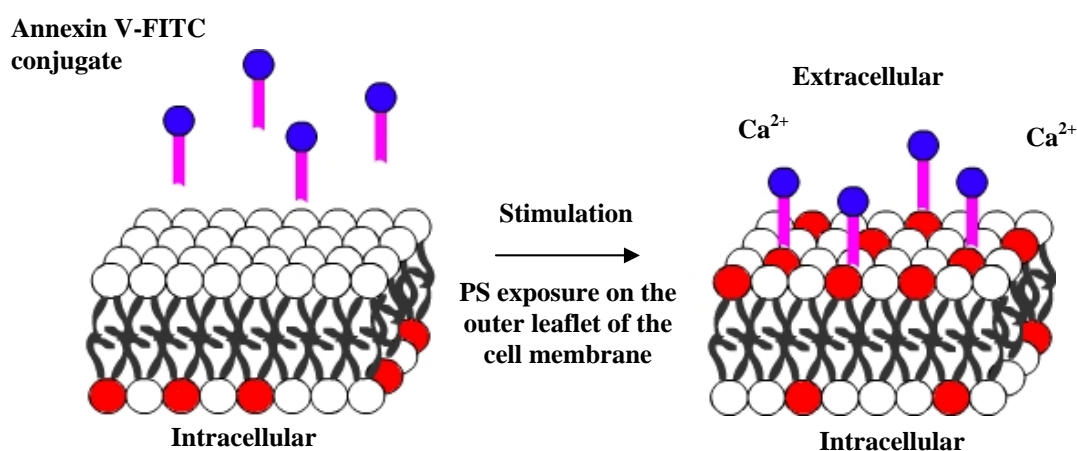


Fig. 12: Schematic representation of the annexin V-FITC assay. Red balls: phosphatidylserine, blue balls: annexin V-FITC conjugate, white balls: other membrane phospholipid.

E. Measurement of intracellular Ca^{2+} and PS exposure using CLSM

To investigate the relation between intracellular Ca^{2+} and exposure of PS, two fluorescent dyes, fluo-4 and annexin V-alexa 568, were used. First, the washed RBCs were loaded with fluo-4 following the procedure as described above (see 3.2.1B in this part). After washing, the fluo-4 loaded RBCs were investigated under different experimental conditions. After washing, RBCs were stimulated for PS exposure. After that stimulated RBCs were incubated with 5 μl of annexin V-alexa 568 in annexin binding buffer for 15 min at room temperature. Subsequently, the RBCs were washed to remove all unbound annexin V-alexa 568. The samples were analysed by using the confocal microscope. The samples were scanned by 3 different channels: transmission light, channel 1 for fluo-4, and channel 2 for alexa 568.

F. Investigation of the kinetics of PS exposure

To investigate the kinetics of the PS exposure processes, the washed RBCs were put on a coverslip in physiological solution in the presence of 2 mM Ca²⁺ and 5 µl of annexin V-FITC. Before starting the kinetic measurements, LPA or PMA or A23187 was added at a final concentration of 2.5 µM, 6 µM and 2.0 µM, respectively. The measurements were done by taking images after every 30 s using a very sensitive CCD camera. The kinetics of PS exposure was recorded up to 2.5 h with LPA and PMA. In case of A23187, the recording time lasted up to 4h. The results can be displayed as a continuous series of images or shown as a movie using MetaVue software.

G. Measurement of reticulocytes in red blood cell suspension

Reticulocytes are immature RBCs taking about 1% of the RBCs in the human body. Like mature RBCs, reticulocytes do not contain a nucleus. However, they are called reticulocytes because of a reticular (mesh-like) network of ribosomal RNA which can be observed under a microscope with certain dyes such as thiazole orange or methylene blue.

Briefly, 5 µl of well mixed whole blood was added to a 5 ml tube containing 1 ml of Retic-COUNT reagent. The solution was mixed well and incubated at room temperature for 30 min in the dark. The sample was gently vortexed immediately prior to analysis. The FSC and SSC amplifier gains were set to log mode. The noise and debris were excluded by adjusting the thresholds. Analysis is restricted to the population falling within a forward scatter (FCS) versus side scatter (SSC) gate. Cells within this RBC gate are analyzed to determine the amount of bound Retic-COUNT reagent that is measured by the fluorescence-1 (FL-1) detector.

Both the FL-1 fluorescence histograms of the gated data acquired from the unstained and stained sample were recorded. The equation for the percentage of positive reticulocytes result is:

$$\% \text{ gated stained tube} - \% \text{ gated unstained tube} = \% \text{ reticulocytes.}$$

The absolute reticulocyte counts can be obtained using the following equation:

$$\text{Absolute reticulocyte} = \frac{\% \text{ reticulocytes}}{100} \times (\text{RBCs } 10^{12} / \text{L})$$

H. Separation of young and old RBCs using Percoll density centrifugation

In a population of RBCs, cells are different from each other from their age. Depending on age, their density is also different. Young cells have a lower density in comparison to old cells. This makes it possible to separate them by gradient centrifugation into fractions with different densities according to their ages [149].

Percoll consists of colloidal silica particles coated with polyvinyl propylene (diameter 15-30 nm) and is inert for biological systems. It forms a gradient under centrifugation force in which the different dense RBCs distribute.

Leukocyte free RBCs were prepared by using a micropore filter to remove the leukocytes. 30 ml of Percoll buffer were mixed with 5 ml of washed RBCs and centrifuged at 40.000 g for 30 min at 4°C. The cell suspension in the centrifuge tubes was separated into 5 layers. These layers were individually taken and collected by washing three times with B-buffer at 2.000 g for 5 min at 4°C to remove remaining Percoll. Finally, the RBCs were resuspended in physiological solution.

3.2.2. Biochemistry methods

A. Haematocrit determination

The haematocrit was determined photometrically using Drabkin's reagent. This procedure is based on the oxidation of haemoglobin and its derivatives (except sulphaemoglobin) to methaemoglobin in the presence of alkaline potassium ferricyanide. Methaemoglobin reacts with potassium cyanide to form cyanmethaemoglobin, which has a maximum absorption at 540 nm. The color intensity measured at 540 nm is proportional to the total haemoglobin concentration. A volume of 100 µl of RBC suspension was added to 5 ml Drabkin's reagent. The RBCs were haemolyzed in Drabkin's reagent. The mixture was mixed well by vortexing. After 30 min incubation at room temperature, the absorption at 540 nm was measured by using a UV spectrometer. The blank sample contains only Drabkin's reagent. The haematocrit is calculated according to Ellory [176, 177]:

$$Hk = \frac{A \cdot f_{\text{Drabkin's}}}{CF}$$

where: A is the absorption of light at a wavelength of 540 nm, $f_{\text{Drabkin's}}$ is the dilution factor of RBCs in Drabkin's reagent and CF the conversion factor. CF contains the molecular mass of haemoglobin, the molar extinction coefficient, the mean haemoglobin content per unit volume of RBCs and the thickness of the cuvette. For human RBCs and the used cuvette, the CF factor is 247.

B. Plasma membrane redox activity assay

The plasma membrane redox system is ubiquitous, it transfers electrons from intracellular substrates to extracellular electron acceptors. The function of this redox system is involved in many biological events such as: redox state of sulfhydryl residues in membrane proteins, neutralization of oxidative stress outside the cells, stimulation of cell growth, cell ageing.

The method was created by Avron and Shavit [178] and modified by Rizvi et al. [156]. The principle of this method is to measure the amount of reduced potassiumhexacyanoferrat or $K_4[Fe(CN)_6]$ from $K_3[Fe(CN)_6]$ via the redox activity of the membrane.

Briefly, 20 μ l of washed RBCs were suspended in 1.98 ml of physiological solution containing 1 mM potassium ferrocyanide ($K_3[Fe(CN)_6]$) and 5 mM glucose (1% haematocrit). After 30 min incubation at 37°C in a shaking water bath, the suspension was quickly centrifuged (20 s, 12.000 g). 1 ml of the supernatant was added into the solution containing 0.3 ml of 100 mg 4,7-diphenyl-1,10-phenanthroline disulfonic acid disodium salt hydrate dissolved in 30 ml deionised water; 0.3 ml of 3 M sodium acetate pH 6.5; 0.15 ml of 0.2 M citric acid; 0.15 ml of 3.3 mM $FeCl_3$. The mixture was kept in the dark for 15 min. Subsequently, deionised water was added to give a volume of 2 ml. The absorption was measured at 535 nm using a spectrophotometer. The reference contained the same components except blood. The amount of reduced $K_4[Fe(CN)_6]$ was calculated based on a standard calibration curve (Fig. 13).

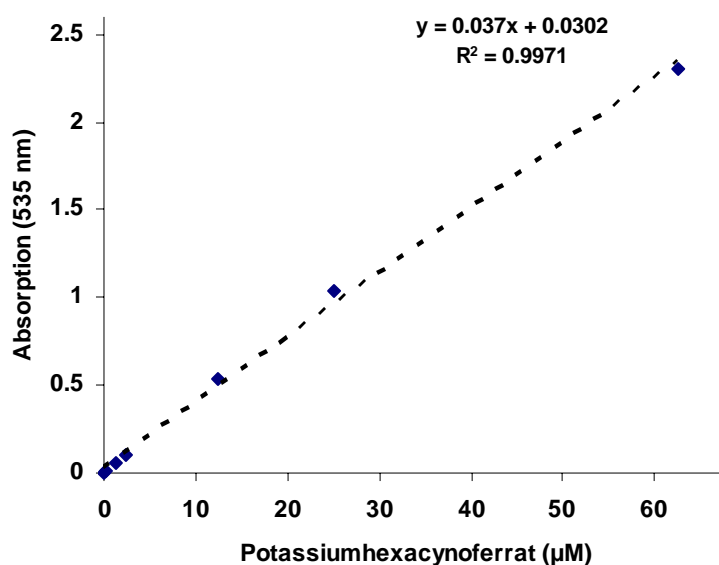


Fig. 13: Standard calibration curve of potassiumhexacyanoferrat.

C. Fibrinogen determination

Fibrinogen is a soluble plasma glycoprotein synthesised in the liver. In the blood coagulation cascade, prothrombin is activated to thrombin, which is responsible for converting fibrinogen into fibrin. Together with other factors, the blood clots are formed in the presence of fibrin. The amount of fibrinogen in washed blood after a number of washes can be quantified based on the method of Inada et al. [179].

Thrombin purchased from Sigma was dissolved in 0.9% NaCl solution at 148 IU/ml stock solution. The fibrinogen containing more than 90% of clottable protein with thrombin was prepared at 250 μ M stock solution in tris (hydroxymethyl) aminomethane/acid citrate-dextrose buffer. This buffer is a mixture of 5 volume of solution A and 1 volume of solution B. The solutions are described below:

- *Solution A* (in mM): NaCl 115, KCl 15, glucose 5, tris (hydroxymethyl) aminomethane (pH 7.4) 23.
- *Solution B* (in mM): trisodium citrate 85, citric acid 65, glucose 2%.
- *Solution C* (in mM): tris (hydroxymethyl) aminomethane (pH 7.0) 10, NaCl 40.

Sample preparation: 5 ml of whole blood were centrifuged at 2.000 g for 5 min at room temperature. After collecting the plasma, the cells were washed 3 times with 5 ml of physiological solution. Every time after centrifugation, the supernatant was collected for fibrinogen measurements.

Calibration: different fibrinogen solutions containing 0.1, 0.2, 0.5, 1, 2, 4, 6, 8, and 10 μ M were prepared by dilution from 1 mM stock solution using buffer A. 1 ml of solution C was added in a 1 cm path length cuvette, and then 0.5 ml of different fibrinogen concentration solutions were added and mixed well by inverting the cuvette slowly to avoid making foam or bubbles. Subsequently, 0.1 ml of 145 IU thrombin stock solution was added in the cuvette. The cuvette was immediately covered with parafilm and mixed well. The precipitation is formed after 2 - 3 min. The turbidity is measured at 450 nm using a spectrophotometer. The maximal absorption was recorded (A_{\max}).

Likewise, for experiments, 0.5 ml of each supernatant were added in 2 ml quartz cuvette containing 1 ml of buffer C. Next steps were carried out as described above. The amount of fibrin was calculated based on the standard line drawn from the calibration curve.

D. Ghost cell preparation and membrane protein extraction

Ghost cell preparation

RBC ghosts were prepared as described by Dodge et al. [2] with some modifications. Briefly, 10 ml of whole blood were washed 3 times with physiological solution, pH 7.4 at 4°C. After 3 times washing in physiological solution, RBCs were washed one time in 0.9% NaCl.

The washed RBCs were put in a 50 ml centrifuge tube. A volume of 25 ml of solution 1 (in mM) containing (Tris HCl 10, EDTA 1, PMSF 1, pH 8.0) was added. The centrifuge tubes were mixed by vigorously vortexing and put on ice for 30 min. In this solution, the RBCs were completely haemolysed. The supernatant was removed after centrifugation at 19,000 rpm using the Sorvall RC-5B (refrigerated super speed centrifuge, Rotor SS-304) for 30 min at 4°C. The procedure was repeated 1 time by adding 25 ml of solution 1. After vortexing, the suspension containing cell ghosts was centrifuged again at 19,000 rpm for 10 min at 4°C. The supernatant was discarded. After this step 25 ml of solution 2 (Tris HCl 50, NaCl 500, EDTA 1, PMSF 1, pH 8.0) was added and mixed well by vortexing. The purpose of this step is to remove remaining haemoglobin binding to ghost cells in the high ionic strength solution. The suspension was centrifuged at 19,000 rpm for 10 min at 4°C. The pellet was washed to remove salt by solution 1 two times.

Membrane protein extraction

A volume of 500 µl of extraction buffer (in mM) (Tris HCl 10, EDTA 1, PMSF 1, SDS 1%, pH 8.0) was added in the centrifuge tube containing haemoglobin free cell ghosts. The ghost suspension was mixed well by vortex and kept at 4°C overnight. Finally, the ghost cell suspension was centrifuged at 12,000 g for 30 min at 4°C. The supernatant was collected, aliquoted and stored at -20°C.

For SDS-PAGE, the concentration of ghost cell protein in the samples was quantified using the BC Assay (protein quantitation kit, UPTIMA). The amount of protein samples was loaded at the same concentration (10 µg) for each well.

E. Sodium dodecyl sulfate polyacrylamide gel electrophoresis (SDS-PAGE)

Ghost cell membrane proteins were separated using SDS-PAGE as described by Laemmli et al. [180]. The stacking and separating gel were prepared with 12% and 4.5% acrylamide, respectively. From each sample, after heating at 90°C for 4 min in sample buffer, 10 µg protein/well was loaded into the gel. The running gel program was set up at 100 V for 30 min and subsequently 150 V for 150 min at 4°C. Two gels were run in parallel. For Western blot experiments, one was used for blotting and the other for coomassie staining.

Buffers and solutions

- 30% acrylamide (containing 0.8% bisacrylamide)
- Tris HCl 1.5 M, pH 8.8
- Tris HCl 0.5 M, pH 6.8
- APS 10%
- TEMED
- 5X Sample Buffer: SDS 10%; β mercapto ethanol 10 mM; tris HCl 0.2 M, pH 6.8; bromophenolblue 0.05%.
- 1X Running Buffer: tris-HCl 25 mM, glycine 200 mM, SDS 0.1%, pH 8.3.

F. Immunoblot (Western blot)

So far, 5 isoforms of scramblases have been identified in human. In which, the expression of hPLSCR2 is restricted to testis, the hPLSCR4 has not been detected in peripheral blood lymphocytes [74]. Because the antibody against scramblase 5 is not available at the moment, only two antibodies against scramblase 1 and 3 have been used for detecting the scramblases. The antibody against human antigen PLSCR1 is a monoclonal antibody, which recognizes the N-terminus of scramblase 1 (35 kDa). The immunogenic sequence of scramblase 1 is not available (by Invitrogen). The antibody against human antigen PLSCR3 is a polyclonal antibody. The immunogenic sequence contains 295 amino acids:

MAGYLPPKGYAPSPPPYPVTPGYPEPALHPGPGQAPVPAQVPAPAPGFALFSPGP
 VALGSAAPFLPLPGVPSGLEFLVQIDQILIHQKAERVETFLGWETCNRYELRSGAGQP
 LGQAAEESNCCARLCCGARRPLRVRLADPGDRELLRLLRPLHCGCSCCPCGLQEME
 VQAPPGTTIGHVLQTWHPFLPKFSIQDADRQTVLRVVGPCWTCGCGTDTNFVVKTR
 DESRSVGRISKQWGGLVREALTDADDFGLQFPLDLVVRVKAVLLGATFLIDYMFPE
 KRGGAGPSAITS.

After finishing the SDS-PAGE, the polyacrylamide gel was taken out and soaked in transfer buffer with a nitrocellulose membrane (BioRad) for 10 min at room temperature. The proteins were transferred from the polyacrylamide gel onto the membrane by using a transfer system. The running time was set up at 80 V for 2 h at 4°C. Subsequently, the membrane was washed to remove methanol and blocked in blocking solution at 4°C overnight. On the next day, the blocked membrane was incubated in blocking solution containing primary antibody with 1000 times of dilution (see Table 4). The membrane was shaken for 2 h at 25°C. After incubation, the membrane was washed 3 times in PBS-T buffer (see before) for 45 min. The membrane was incubated in blocking solution containing the secondary antibody at 25°C for 2 h. The secondary antibody was prepared by dilution of 15.000 times in blocking solution.

After washing 3 times in PBS-T buffer for 45 min and 1 time with PBS for 10 min, the membrane was treated with ECL advance western blotting detection kit (Amersham, code: PRN2135) following the manual instruction. The films (Amersham hyperfilm ECL, code: 28-9068-38) were exposed 15 to 30 s. The films were developed and fixed following the instruction (Amersham, Biosciences Europe GmbH, Freiburg).

Table 4: Specificity, source and dilution of primary and secondary antibodies used in Western blot.

Antibodies	Clone, specificity	Species reactivity	Source	Dilution
Scramblase 1	Monoclonal (Clone 1E9) Mouse anti-human	Human	Invitrogen	1:1000
Scramblase 3	Polyclonal Mouse anti-human	Human	Abnova	1:1000
Peroxidase rabbit anti-mouse IgG1	Rabbit anti-mouse	Mouse	Sigma	1: 15000

Buffers and solutions

- 5X Transfer buffer (1 l): glycine 14.9 g, tris-base 29 g, pH 8.3
For 1 liter working solution: 200 ml of 5X transfer buffer, 200 ml of methanol, and 800 ml of H₂O.
- 10X PBS buffer (1 l): NaCl 80 g, KH₂PO₄ 2.4 g, KCl 2 g, Na₂HPO₄ 14.4 g, pH 7.4.
- PBS-Tween (1 l): 100 ml of 10X PBS buffer, 900 ml H₂O

3.2.3. Atomic force microscopy method

A. Basic principle

Atomic force microscopy (AFM) is based on the feature of scanning probe microscope (SPM). The pivotal property is the measurement of the interaction force between the tip and the sample when the tip is scanned over. Depending on the distance between the tip and the sample, both repulsive and attractive forces are created. In AFM technique, a fine tip is attached to the free end of a cantilever and brought very close to a surface. The cantilever is attached to a scanner piezo tube. A laser beam was applied on the back side of cantilever.

Attractive or repulsive forces resulting from interactions between the tip and the surface will cause a positive or negative bending of the cantilever. The bending of the cantilever will change the reflection of the laser beam. The reflected laser is later collected in a split photodiode detector and the photon signal is converted into a current [181].

Three modes of operation often used are contact, non-contact and tapping mode [182]. In this thesis, only the tapping mode is mentioned. In tapping mode, the cantilever is oscillating close to its resonance frequency. An electronic feedback loop ensures that the oscillation amplitude remains constant, such that a constant tip-sample interaction is maintained during scanning. Forces that act between the sample and the tip will not only cause a change in the oscillation amplitude, but also a change in the resonant frequency and phase of the cantilever. The amplitude is used for the feedback and the vertical adjustments of the piezoscanner are recorded as a height image. Simultaneously, the phase changes are presented in the phase image (topography). Except a slightly slow scanning speed, tapping mode shows many advantages for biological samples because it eliminates a large part of permanent shearing forces and causes less damage of the sample surface. High lateral resolution on most samples (1 nm to 5 nm) can be observed. Lateral forces are virtually eliminated, so there is no scraping [181].

B. Investigation of the surface structure of RBCs under physiological condition

Sample preparation

Washed RBCs of normal or sickle anaemia patients were fixed with 1% glutaraldehyde (final concentration) in physiological solution at room temperature for 5 min (0.1% haematocrit). Subsequently, RBCs were washed in physiological solution by centrifuging at 2.500 g for 2 min to remove glutaraldehyde. After every washing, the RBCs were vigorously vortexed. After the last wash, RBCs were suspended in physiological solution and applied on the glass slides. Finally, the slides were rinsed quickly with deionized water to remove crystallized salt and kept dry at room temperature.

Sample scanning

The tapping mode was used to scan the cell surfaces. The tip NSC16/NoAl from Micromash was used with the following characteristics: radius of curvature less than 10 nm; tip height 15- 20 μm ; full tip cone angle less than 20° ; reflective side is coated with Al. Both topography (height mode) and viscoelastic (amplitude mode) data were recorded simultaneously. The images were scanned at the resolution 512×512 pixels, scanning size in

the range 500 nm up to 10 μm , scanning rate in the range 0.44 to 0.75 Hz. For analysis, two parameters (volume and surface area) were analysed with Nano Scope software.

C. Investigation of the adhesion of RBCs under PS exposure conditions

Inducing PS exposure

Washed RBCs were stimulated for PS exposure by adding 2.5 μM LPA or 2 μM A23187 or 6 μM PMA in physiological solution in the presence of 2 mM Ca^{2+} . The cell suspensions (0.1% haematocrit) were mixed well and incubated at 37°C for 30 min. Subsequently, RBCs were washed and then fixed by adding glutaraldehyde at 1% final concentration. The following steps were carried out as described above (3.2.3.B). The control was RBCs in physiological solution containing 2 mM extracellular Ca^{2+} .

Sample scanning and observing

The surface structures of RBCs showing PS exposure were scanned using AFM as described above. The morphology and adhesion of stimulated RBCs were also observed under the microscope. The images were taken using a CCD camera.

3.2.4. Informatics tools

The amino acid sequences of scramblases were taken from the gene bank database (NCBI). The comparison for identity of amino acid sequences was carried out online with the support of Basic Local Alignment Search Tool (BLAST). Multi alignment of amino acid sequences was done by using ClustalX (version 2.0.11). The dendrogram (or phylogenetic tree) was drawn based on the neighbour joining method [183] by using ClustalX. The phylogenetic tree was displayed with the support of Treeview software (version 4.5).

3.2.5. Statistics

Data are displayed as arithmetic means \pm SD (standard deviation). Statistical analysis was performed using the unpaired t-test or one-way ANOVA. Tukey's test was used for multiple comparisons when ANOVA indicated statistically significant difference between or within groups. Differences were considered to be significant when $P \leq 0.05$.

4. Results

4.1. Investigation of Ca^{2+} uptake in human red blood cells

4.1.1. Calibration of intracellular Ca^{2+} content

For the calibration, physiological solutions containing different concentrations of Ca^{2+} from 50 nM to 5 mM were used. The fluorescence intensity of single cells was analysed by using a fluorescence microscope with the background correction. Fig. 14 shows a typical control experiment, in which Ca^{2+} is not added. The fluorescence intensity in single cells is almost stable during 30 min and is in the range of 8 and 25 arbitrary units (a.u.). Figs. 15 A, B, C represent the typical uptake of Ca^{2+} in the presence of 2 μM ionophore A23187 and 50 nM, 50 μM or 5 mM extracellular Ca^{2+} , respectively.

In the presence of 2 μM A23187, the delay time depends on the concentration of extracellular Ca^{2+} . At low concentrations, the delay time extends from 15 to 20 min (Fig. 15 A). At concentrations from 100 μM to 5 mM extracellular Ca^{2+} , there is no significant difference in both delay time and fluorescence intensity. In average, the highest fluorescence intensity reaches after 15 min.

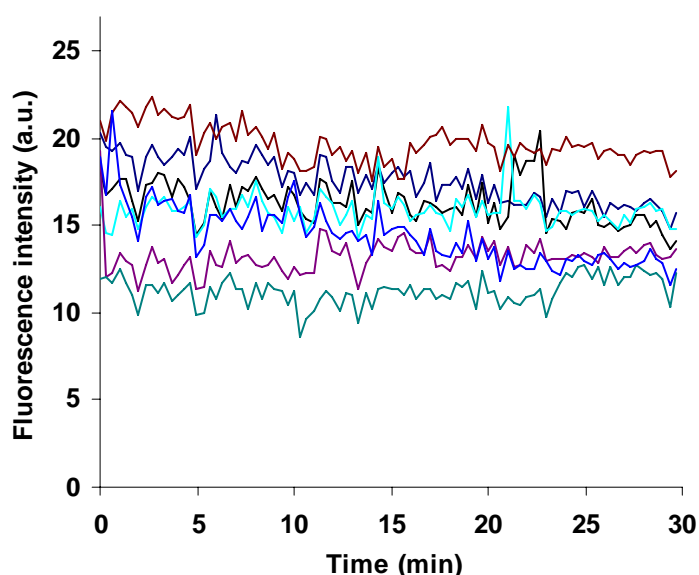


Fig. 14: Typical experiment showing the change of fluo-4 fluorescence intensity in RBCs. Each single curve represents one single cell.

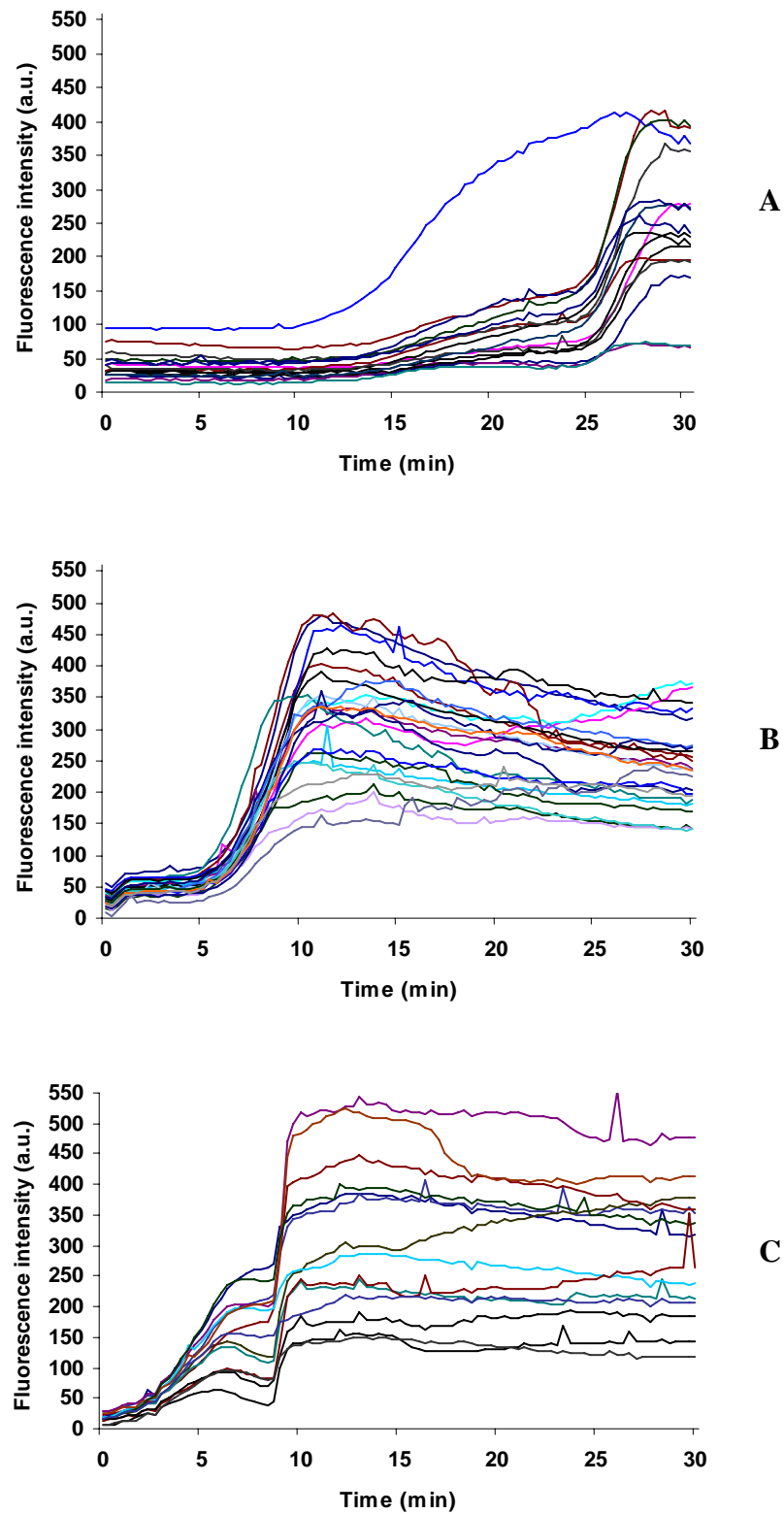


Fig. 15: Uptake of Ca^{2+} in RBCs for 30 min. RBCs were suspended in physiological solutions containing different concentrations of Ca^{2+} . The experiments were started after adding A23187 at 2 μM final concentration. **A, B, C:** physiological solution containing 50 nM, 50 μM , and 5 mM extracellular Ca^{2+} , respectively. Each single curve represents one single cell.

For quantitative measurement of the intracellular Ca^{2+} content of more cells, the fluo-4 loaded RBCs were suspended in physiological solutions containing different concentrations of Ca^{2+} and 2 μM A23187. After 15 min incubation at room temperature, the fluorescence intensity was measured by using a flow cytometer. In each experiment, a number of 30.000 RBCs was counted and analysed. Fig. 16 shows the overlay histogram of the fluorescence intensity of RBCs at different concentrations of extracellular Ca^{2+} .

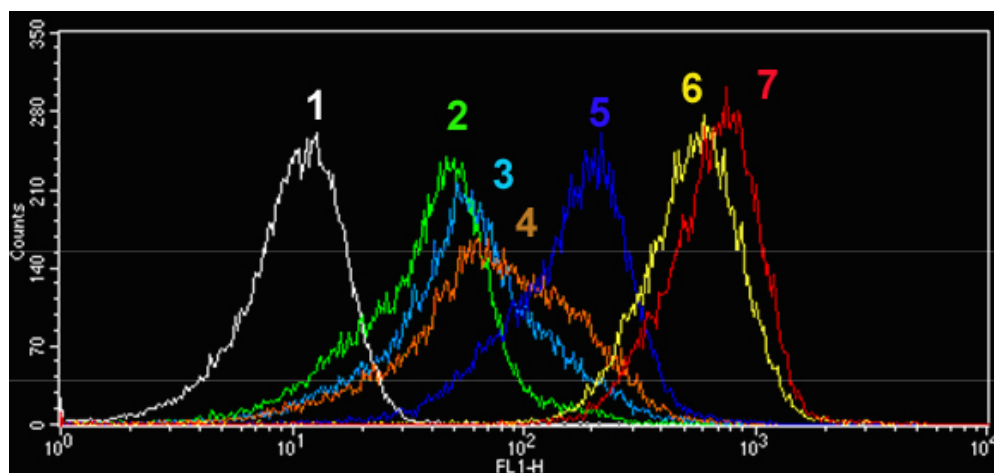


Fig. 16: A typical overlay histogram for Ca^{2+} calibration in RBCs. 1: Control in physiological solution; from 2 to 7: 50 nM, 500 nM, 5 μM , 50 μM , 1 mM and 2 mM Ca^{2+} added in the presence of 2 μM A23187 (FACS data analysis of 30.000 cells of one blood sample).

The fluorescence intensity from 3 different blood samples was analysed by flow cytometry. The mean values of the fluorescence intensity at different concentration of Ca^{2+} were analysed and showed in Fig. 17. One can see that the fluorescence intensity increases correspondingly with the concentration of extracellular Ca^{2+} . The fluorescence intensity of fluo-4 is not significantly different when the concentration of extracellular Ca^{2+} is in the range of 50 nM and 0.5 μM . At higher concentrations of extracellular Ca^{2+} (above 0.5 μM), the fluorescence intensity of fluo-4 increases and it saturates when the concentration of extracellular Ca^{2+} is above 100 μM .

In parallel, the relative cell volume was also analysed by using the mean value of the forward scatter (FSC). The data show that the cell volume decreases proportionally with the increase of the intracellular Ca^{2+} concentration (Figs. 18, 19), i.e. at high extracellular Ca^{2+} concentrations, maximum reduction was reached at 100 μM extracellular Ca^{2+} . Under such conditions, the RBCs show a spherical shape when they are observed under the microscope.

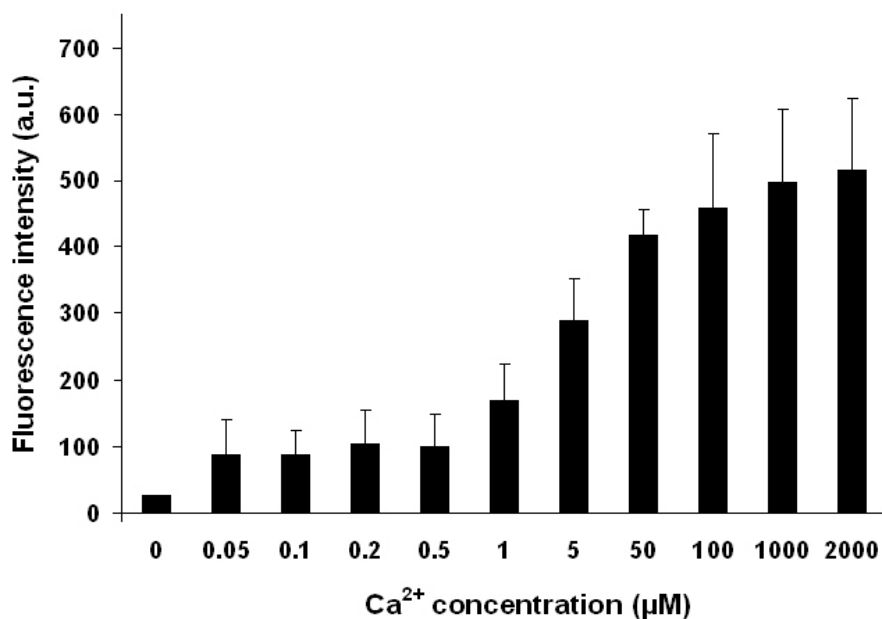


Fig. 17: Fluorescence intensity of fluo-4 in RBCs. The cells were incubated at different concentrations of extracellular Ca²⁺ in the presence of 2 µM A23187 after 15 min at room temperature. Bars show mean value of 3 different blood samples (30.000 cells of each blood sample were analysed). Error bars represent S.D.

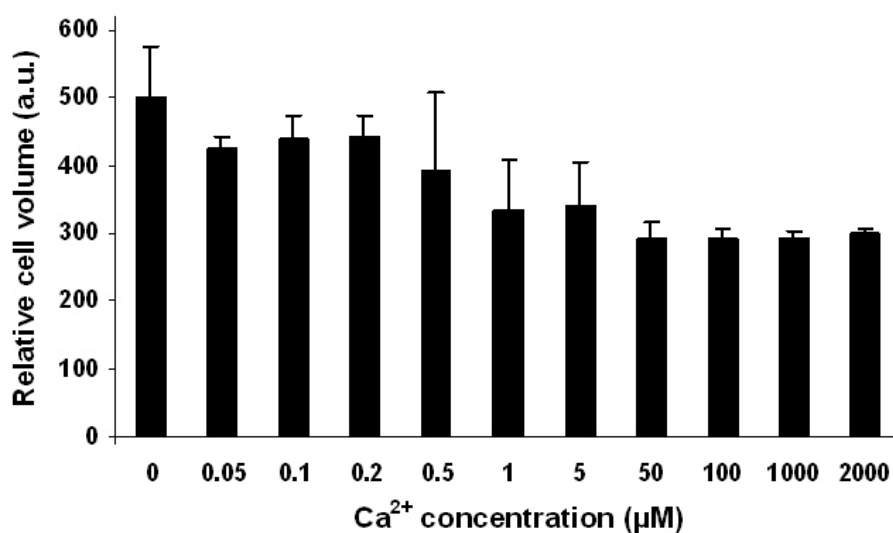


Fig. 18: The reduction of the cell volume. RBCs were incubated at different concentrations of extracellular Ca²⁺ in the presence of 2 µM A23187 after 15 min at room temperature. Bars show mean value of 3 different blood samples (30.000 cells of each blood sample were analysed). Error bars represent S.D.

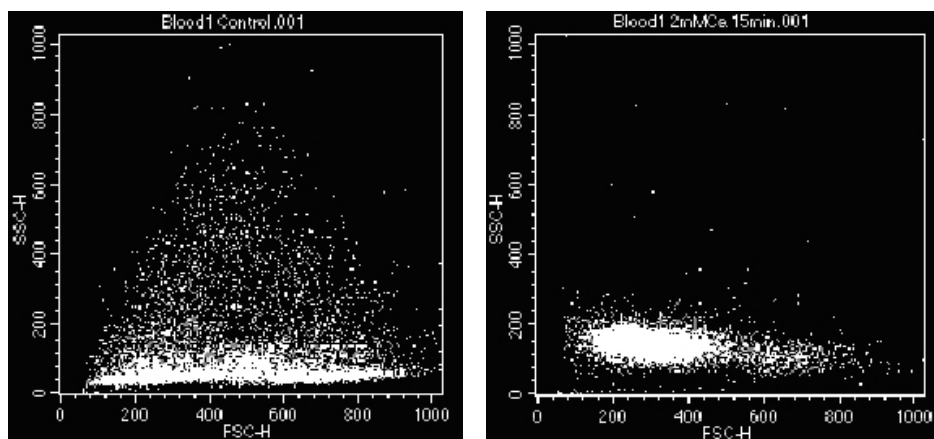


Fig. 19: The reduction of the cell volume in the presence of 2 mM extracellular Ca^{2+} and 2 μM A23187 after 15 min incubation. Original FACS data showing the side scatter vs. forward scatter. Left: control (physiological solution containing 2 mM Ca^{2+}), right: control with 2 μM A23187 after 15 min incubation at room temperature.

4.1.2. Influence of lysophosphatidic acid on the uptake of Ca^{2+}

The influence of LPA on the uptake of Ca^{2+} was investigated. A large concentration range of LPA from 1 μM to 20 μM was tested. The results showed that at 0.1% haematocrit, the concentration of LPA from 10 to 20 μM caused a strong haemolysis after 15 min incubation at 37°C. For Ca^{2+} uptake measurement with the fluorescence microscope, the fluo-4 loaded RBCs were suspended in the physiological solution containing 2 mM Ca^{2+} and applied on a cover slip. When the RBCs were settled down and kept in focus, 2.5 μM or 5 μM LPA were added and mixed gently by pipetting. The measurements were carried out immediately after LPA was added. The experiment was started at zero time.

FACS analysis the uptake of Ca^{2+} in the presence of LPA is presented in Fig. 20. The results show that there is an increase of Ca^{2+} uptake that can be observed after 45 - 60 s treatment RBC suspension with 2.5 μM LPA (0.1% haematocrit). The lag time is approximately 45 to 60 s depending on the blood. From Fig. 19 it can be seen that the percentage of RBCs reacting with LPA strongly depends on both haematocrit and the concentration of LPA. The intracellular Ca^{2+} varies from cell to cell. It suggests that the reaction of RBCs with LPA is different at single cell level (see Fig. 20). After a 7 min treatment of RBCs with 5 μM LPA, most cells are haemolysed (Fig. 20A). A reduction of the LPA concentration from 5 μM to 2.5 μM does not extend the delay time but the number of haemolysed RBCs is significantly reduced (Fig. 20B).

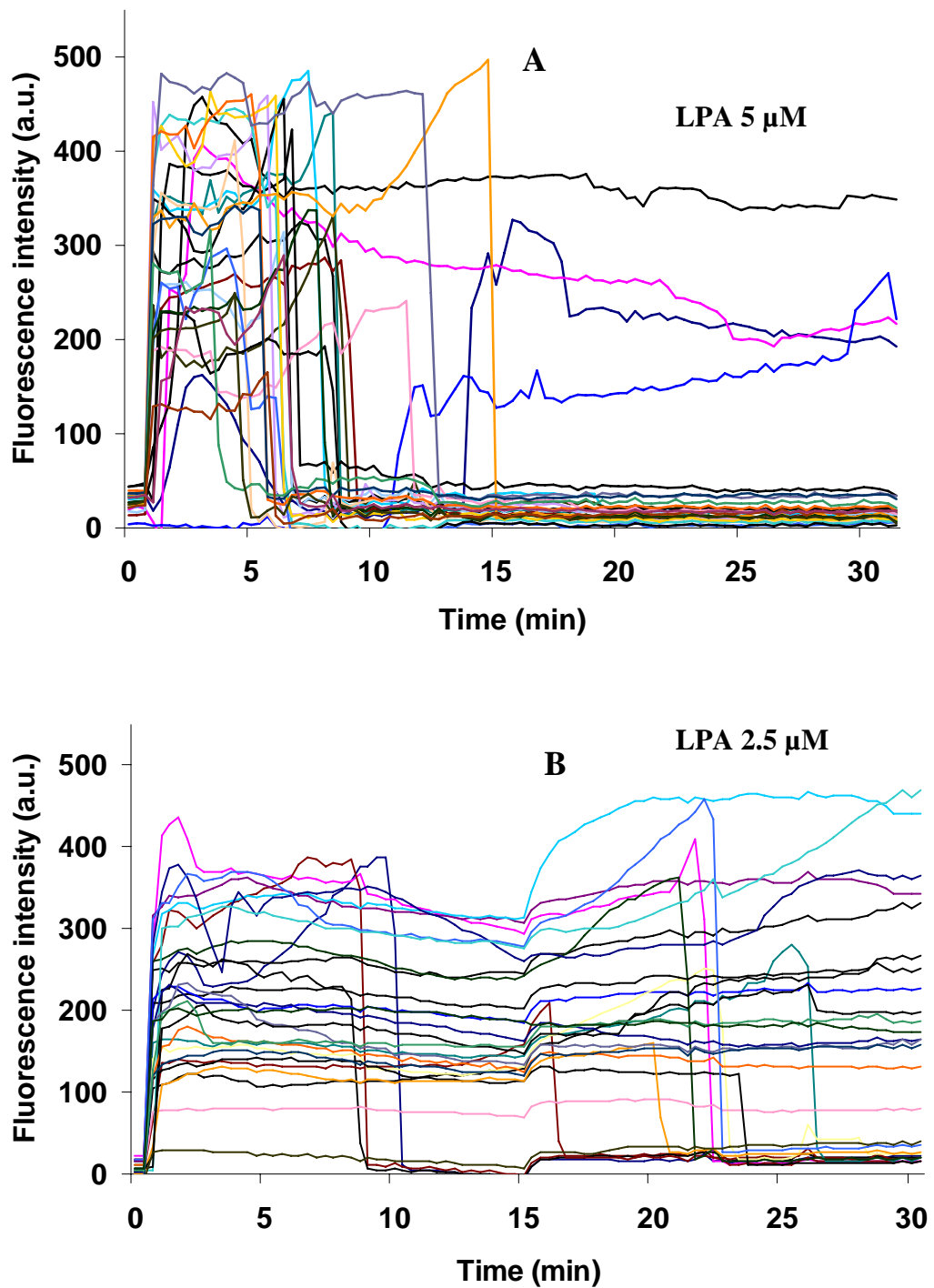


Fig. 20: The Ca^{2+} uptake of RBCs in the presence of LPA. RBCs were suspended in physiological solutions containing 2 mM Ca^{2+} . The experiments were started immediately after adding LPA. **A:** The Ca^{2+} uptake of RBCs in the presence of 5 μM LPA. **B:** The Ca^{2+} uptake of RBCs in the presence of 2.5 μM LPA. Each single curve represents one single cell.

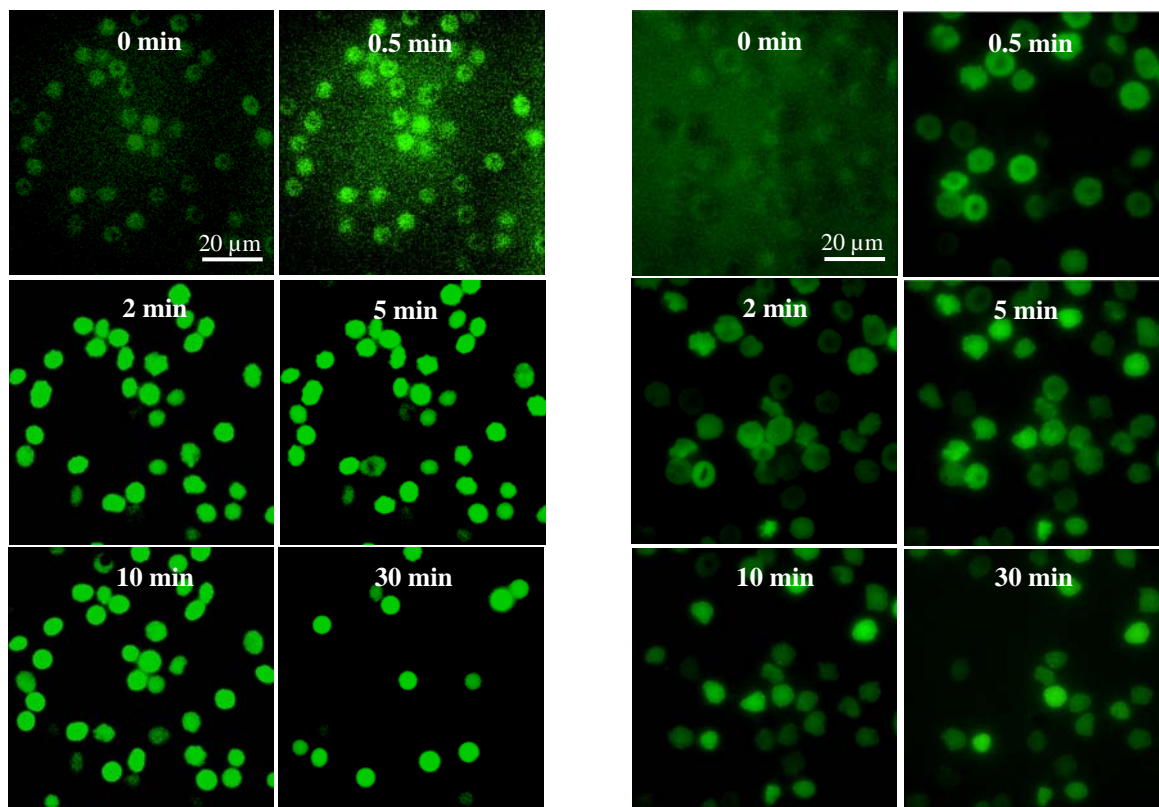


Fig. 21: Kinetics of the Ca^{2+} uptake in RBCs in the presence of LPA. RBCs were suspended in physiological solutions containing 2 mM Ca^{2+} . The kinetic experiments were started immediately after adding LPA. Left: 5 μM LPA, right: 2.5 μM LPA.

Fig. 21 shows the kinetics of Ca^{2+} uptake in the presence of LPA (fluorescence microscopy measurement). When 5 μM of LPA is applied the volume of cells reduces faster and the cells become spheroid in comparison to 2.5 μM LPA. After 10 min, the process of haemolysis starts. In the presence of 5 μM LPA, the fluorescence intensity of RBCs are higher in comparison with 2.5 μM . It also means that the level of Ca^{2+} uptake depends on the concentration of LPA.

4.1.3. Influence of phorbol 12-myristate 13-acetate on the uptake of Ca^{2+}

The influence of PMA, an activator of PKC, on the uptake of Ca^{2+} was analysed under the same condition as described above with LPA. After adding PMA (6 μM final concentration) in a RBC suspension (0.1% haematocrit) containing 2 mM extracellular Ca^{2+} , there is an increase of intracellular Ca^{2+} and the maximal fluorescence intensity was

reached after 20 min (Fig. 22). However, the intensity is much lower in comparison to LPA or A23187 (Figs. 15, 20). The summary of the Ca^{2+} uptake of RBCs is shown in Fig. 23.

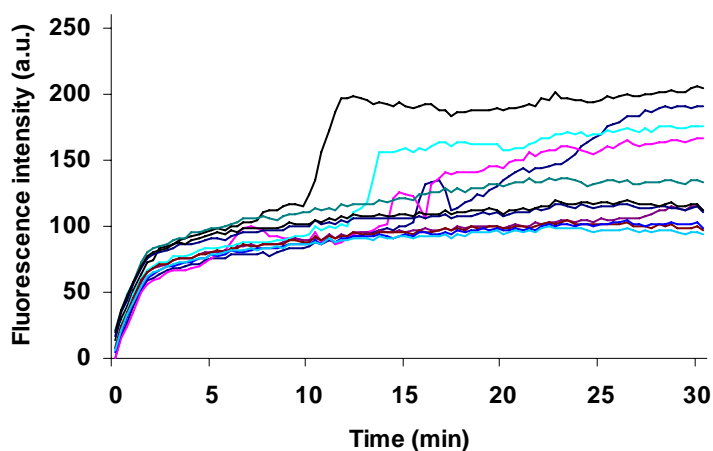


Fig. 22: A typical Ca^{2+} uptake experiment of RBCs in the presence of PMA. RBCs were suspended in physiological solutions containing 2 mM Ca^{2+} . The experiments were started immediately after adding 6 μM PMA. Each single curve represents one single cell.

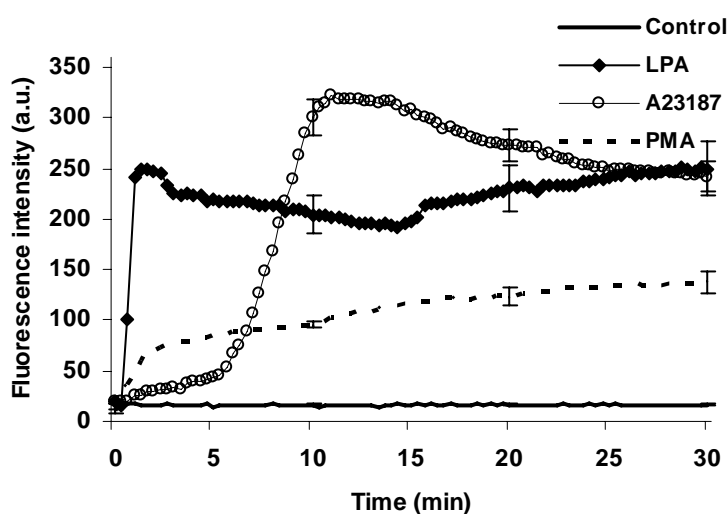


Fig. 23: Summary of the Ca^{2+} uptake of RBCs in the presence of 2.5 μM LPA, 2 μM A23187 or 6 μM PMA and 2 mM extracellular Ca^{2+} for 30 min. Curves show the mean values of more than 30 RBCs from 3 different blood samples, the error bars represent 25% of S.D.

To investigate the reaction of RBCs in the presence of A23187, LPA and PMA, the fluo-4 loaded RBCs were suspended in physiological solution containing 2 mM Ca^{2+} . Comparable experiments were carried out also with flow cytometry (FACS). After incubation with 2 μM A23187 or 2.5 μM LPA or 6 μM PMA for 15 min, the number of reacting cells and their

fluorescence intensity were analysed. Figs. 24 and 25 show the percentage of non-reacting and reacting RBCs in the presence of these substances as well as the fluorescence intensity, respectively.

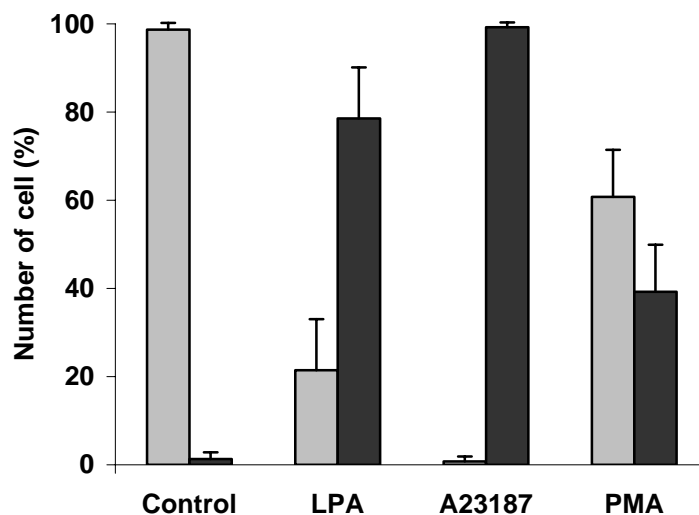


Fig. 24: Reaction of RBCs with LPA, A23187 or PMA. Grey bar: non-reacting RBCs, black bar: reacting RBCs. Bars show mean value of 3 different blood samples (30.000 cells of each blood sample were analysed). Error bars represent S.D.

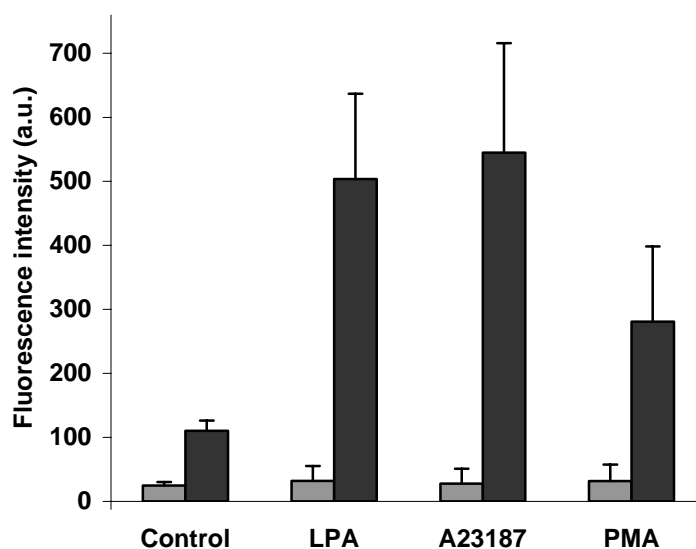


Fig. 25: Fluorescence intensity of non-reacting and reacting RBCs with LPA, A23187 or PMA. Bars show mean value of 3 different blood samples (30.000 cells of each blood sample were analysed). Error bars represent S.D.

Obviously, in the presence of A23187, almost all RBCs react (99.22%) while only 78.55% with LPA and 39.24% with PMA. For the reacting RBCs, the fluorescence intensity is very high in both LPA and A23817 treated cells. In case of PMA, the fluorescence intensity is

significantly lower. Fig. 26 shows a typical overlay histogram of RBCs reacting with these substances. The FACS data are in agreement with the data obtained from fluorescence microscopy investigation (cp. Fig. 23).

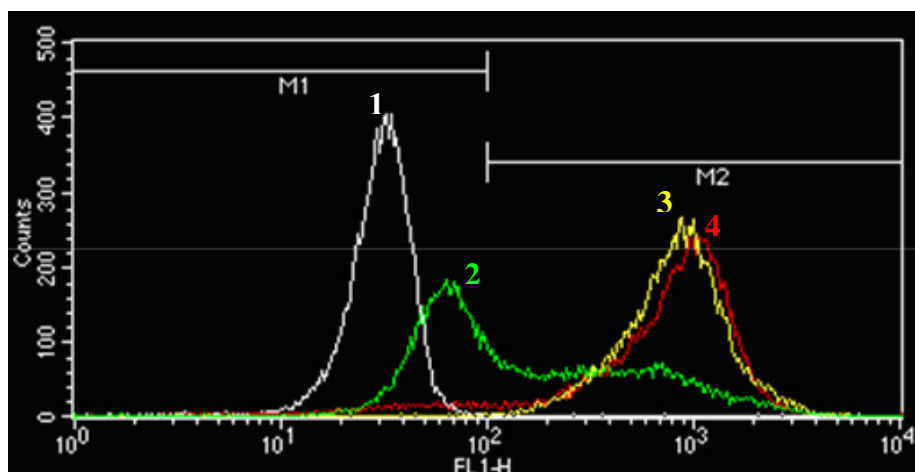


Fig. 26: Overlay histogram of the reaction of RBCs with LPA, A23187 or PMA.

1: control in physiological solution containing 2 mM Ca^{2+} , **2:** 6 μM PMA, **3:** 2.5 μM LPA, **4:** 2 μM A23187. M1 and M2 represent the number of the non-reacting and reacting RBCs.

The relative cell volume was also calculated by mean values of the forward scatter. After 30 min incubation with different substances, the RBCs showed a reduction of their volume. The data are presented in Fig. 27. It can be seen that the cell volume decrease is more pronounced in the presence of A23187 compared to LPA or PMA treatment.

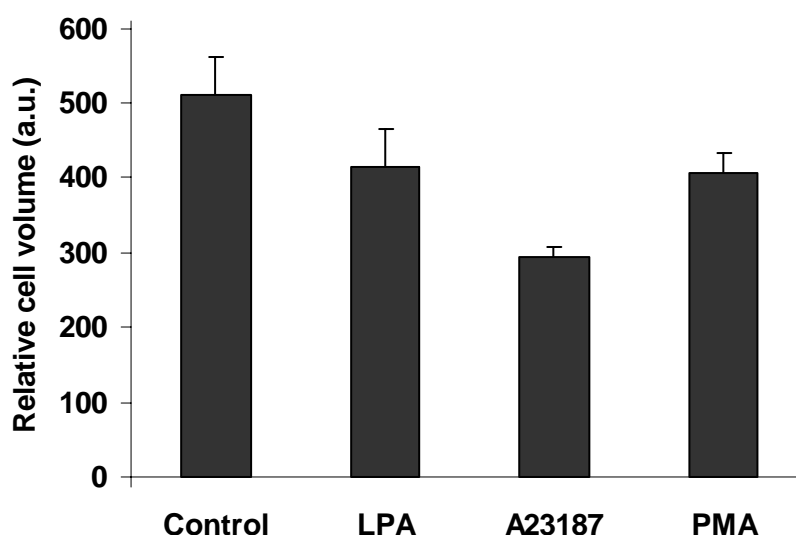


Fig. 27: Relative cell volume of RBCs in the presence of LPA, A23187 or PMA. Data were calculated by using the mean value of the forward scatter of 3 different blood samples (30.000 cells of each blood sample were analysed). Error bars represent S.D.

4.1.4. Investigation of the Ca^{2+} content in sickle red blood cells

To measure the Ca^{2+} content in sickle RBCs, the sickle blood samples were loaded with fluo-4 as described before and analysed using fluorescence microscopy. The experiments were carried out in physiological solutions in the absence of Ca^{2+} . Fig. 28 shows a typical image of RBCs in a sickle blood on a glass surface. Fig. 29 shows the Ca^{2+} content in RBCs of a sickle blood sample over 30 min of the experiment.

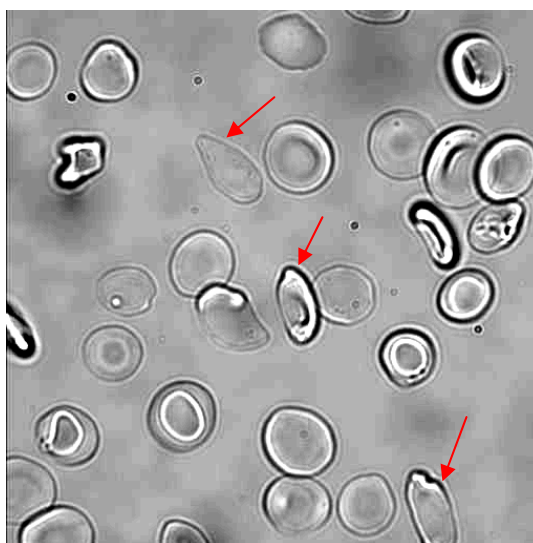


Fig. 28: Bright field image of a sickle blood sample on glass surface (cover slip). Red arrows indicate sickle RBCs.

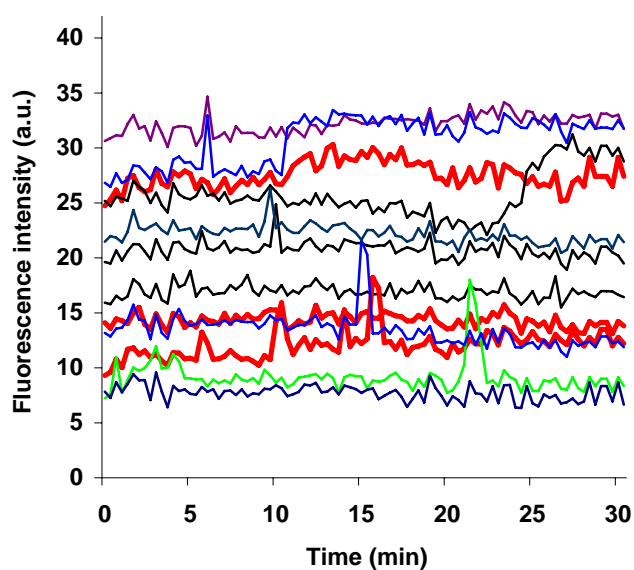


Fig. 29: Typical Ca^{2+} content of RBCs in a sickle blood sample. The red curves represent sickle RBCs. Other curves represent normal cells.

The physiological Ca^{2+} content in normal and sickle blood samples were also investigated by flow cytometry analysis. A number of 90.000 RBCs from 3 different blood samples was analysed. Results show that there is no significant difference in the Ca^{2+} content in RBCs of normal and sickle blood samples (Fig. 30).

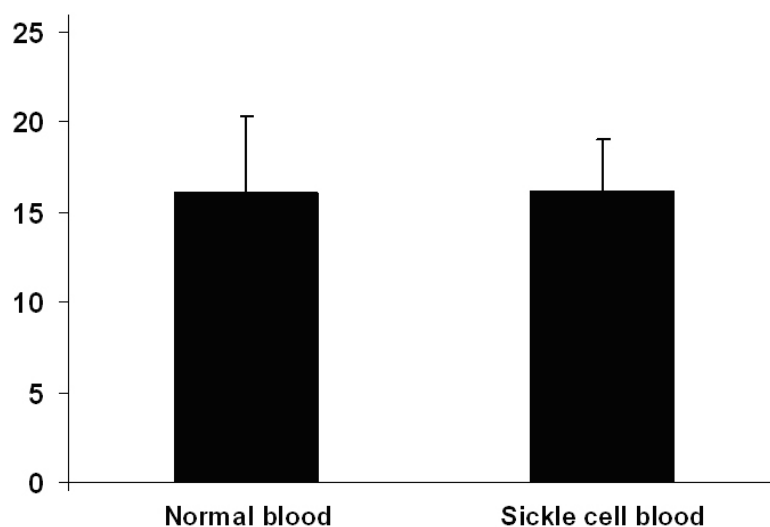


Fig. 30: Ca^{2+} content in normal and sickle blood sample. Bars show mean value of 3 different blood samples (30.000 cells of each blood sample were analysed). Error bars represent S.D. T-test analysis shows that the mean values of Ca^{2+} content in normal and sickle cell blood is not statistical significant.

Investigation of the surface structure of normal and sickle RBCs under physiological conditions

The surface structure of normal and sickle RBCs was investigated under physiological conditions using the AFM technique. The tapping mode was applied using the ultra sharp silicon cantilever NSC16/50 from Micromasch. Fig. 31 shows an AFM image of human sickle cell anemia blood and Fig. 32 shows the surface plot of normal and sickle cells, respectively.

The clear difference in the shape of normal and sickle RBCs can be seen by comparing the upper left and lower left images of Fig. 32. Upper right and lower right images show the height mode of normal and sickle RBCs at high resolution. Data from volume and surface area analysis show that there are also differences in the protein distribution of the surfaces (data not shown).

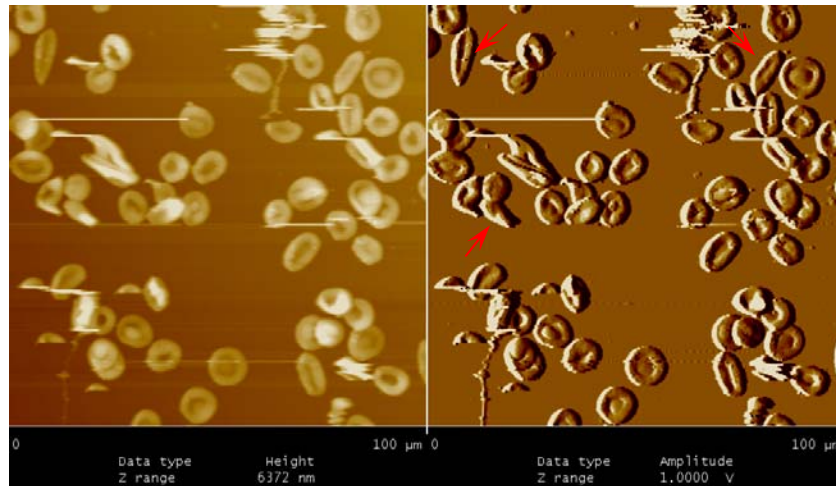


Fig. 31: AFM image of human sickle blood sample. The cells were fixed by 1% glutaraldehyde. Left: amplitude mode ($100 \times 100 \mu\text{m}$), right: height mode ($100 \times 100 \mu\text{m}$). The red arrows indicate sickle cells.

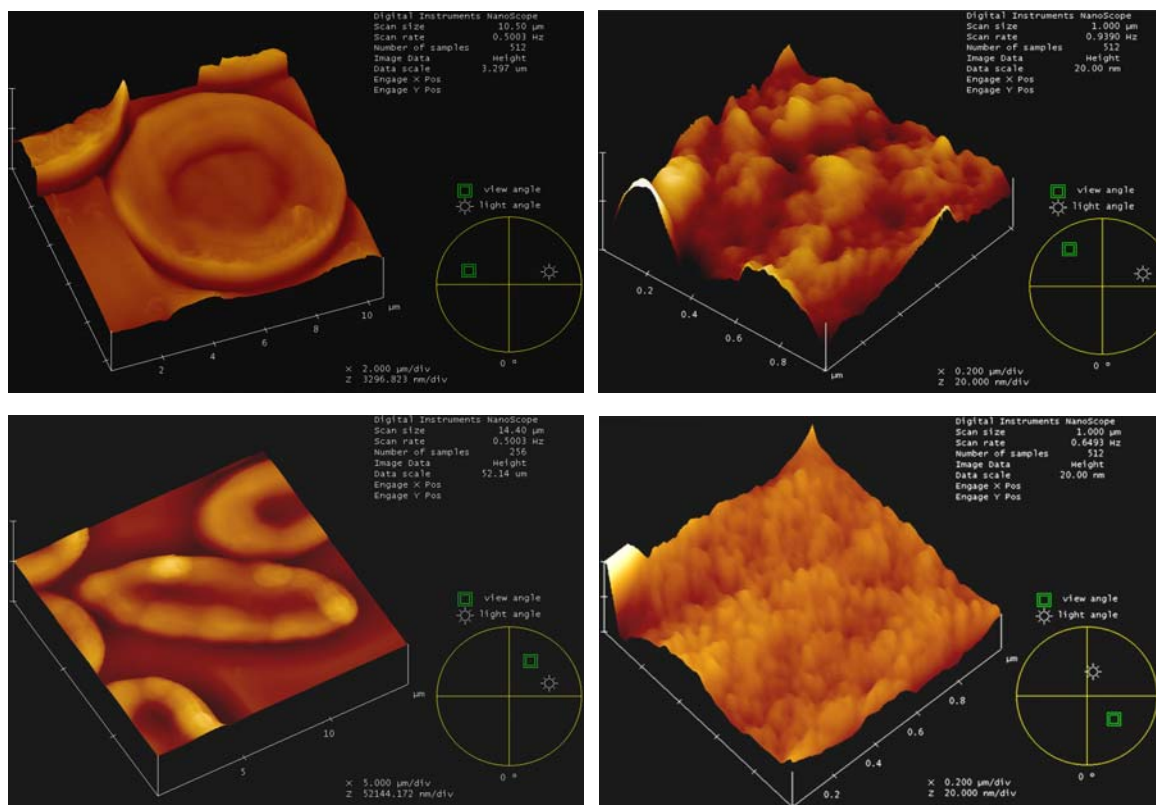


Fig. 32: AFM image of a normal and a sickle RBC. The cells were fixed by 1% glutaraldehyde. Upper left: whole cell plot ($15 \times 15 \mu\text{m}$) of a normal RBC, upper right: high resolution plot ($1 \times 1 \mu\text{m}$) of the normal RBC. Lower left: whole cell plot ($10 \times 10 \mu\text{m}$) of a sickle RBC, lower right: high resolution plot ($1 \times 1 \mu\text{m}$) of the sickle RBC.

4.1.5. Investigation of Ca^{2+} uptake in sheep red blood cells

The Ca^{2+} uptake in sheep RBCs was also investigated. Basically, the reaction of sheep RBCs is similar to human RBCs. In the presence of A23187, almost all cells react and show the highest fluorescence in comparison to LPA or PMA. Fluorescence microscopy investigation with LPA is shown in Fig. 33. The reaction of the cells and the fluorescence intensity vary from cell to cell. The delay time is longer in comparison to human RBCs. In addition, there is a large number of cells reacting very slowly and the fluorescence intensity is much lower in comparison to human RBCs.

Figs. 33 and 34 show a typical kinetics of Ca^{2+} uptake measurements in the presence of $2.5 \mu\text{M}$ LPA over 30 min at room temperature.

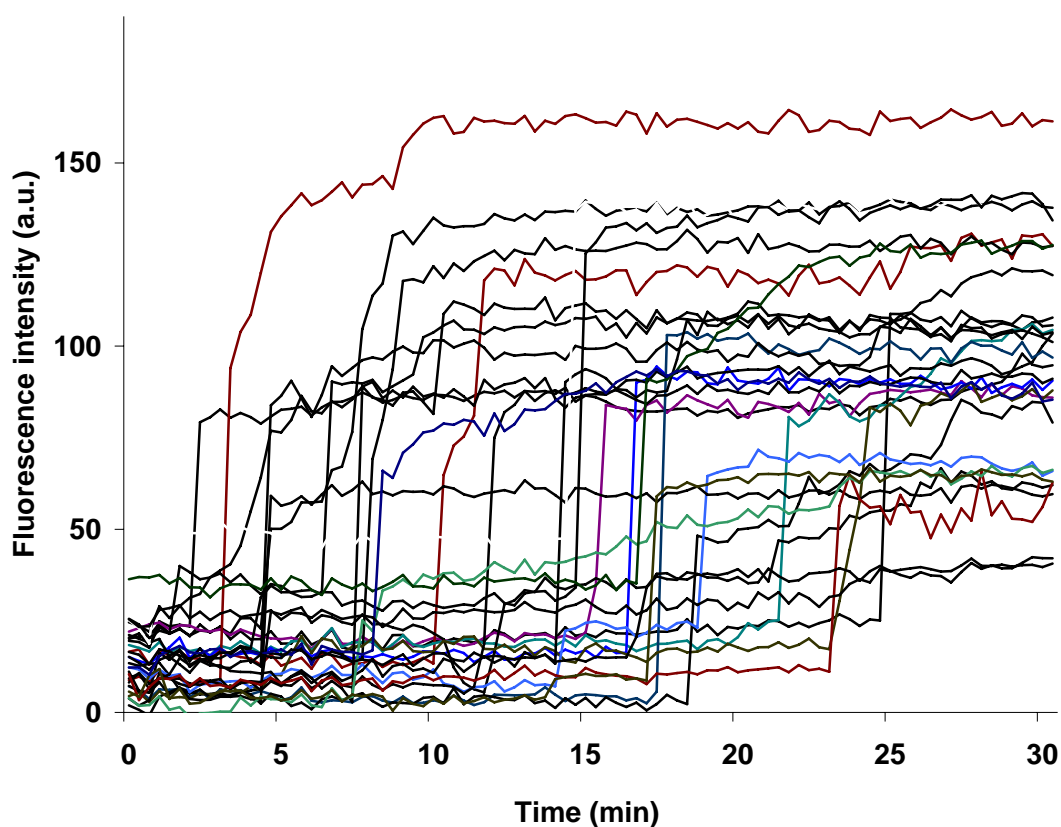


Fig. 33: Ca^{2+} uptake of sheep RBCs in the presence of $2.5 \mu\text{M}$ LPA (fluorescence microscopy measurement). Each single curve represents one single cell.

It can be clearly seen that the reaction of sheep RBCs is similar to human RBCs. The reaction with LPA is different at single cell level. In addition, the fluorescence intensity in sheep RBCs is much lower in comparison with human cells (cp. Fig. 20). The haemolysis is also observed in sheep RBCs (Fig. 34).

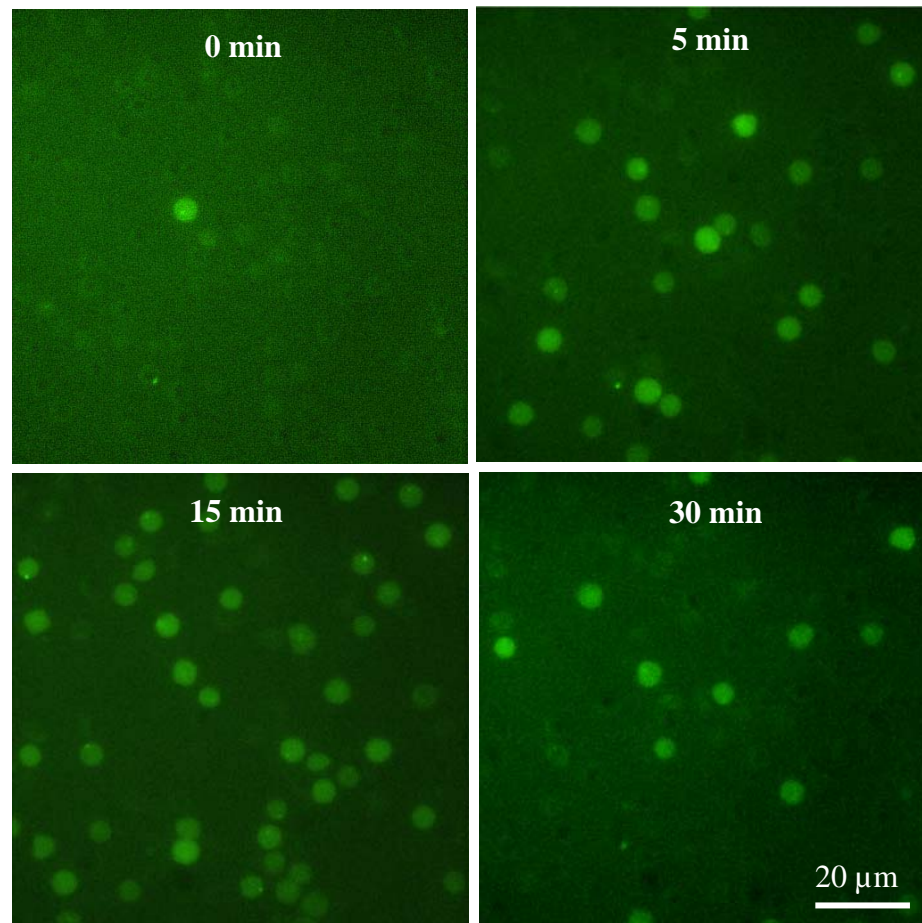


Fig. 34: Kinetics of Ca^{2+} uptake of sheep RBCs in the presence of $2.5 \mu\text{M}$ LPA (fluorescence microscopy measurement).

It can be seen that after 5 min treatment with $2.5 \mu\text{M}$ LPA, the intracellular Ca^{2+} increases in some cells. After 15 min, almost all cells react and show high fluorescence intensity. The haemolysis was also observed, especially after 15 min. At the end of the experiment (after 30 min), more than 60% of sheep RBCs were haemolysed.

Measurement of the Ca^{2+} content of sheep RBCs was also carried out using FACS. Data analysis shows that in the presence of $2.5 \mu\text{M}$ LPA or $2 \mu\text{M}$ A23187 or $6 \mu\text{M}$ PMA, the numbers of cells reacting are 10.53%, 98.33% and 40.65%, respectively (Fig. 35 A). The fluorescence intensity increases in comparison to the control but it is much lower in comparison to human RBCs under the same experimental conditions (Fig. 35 B) (cp. Fig. 24).

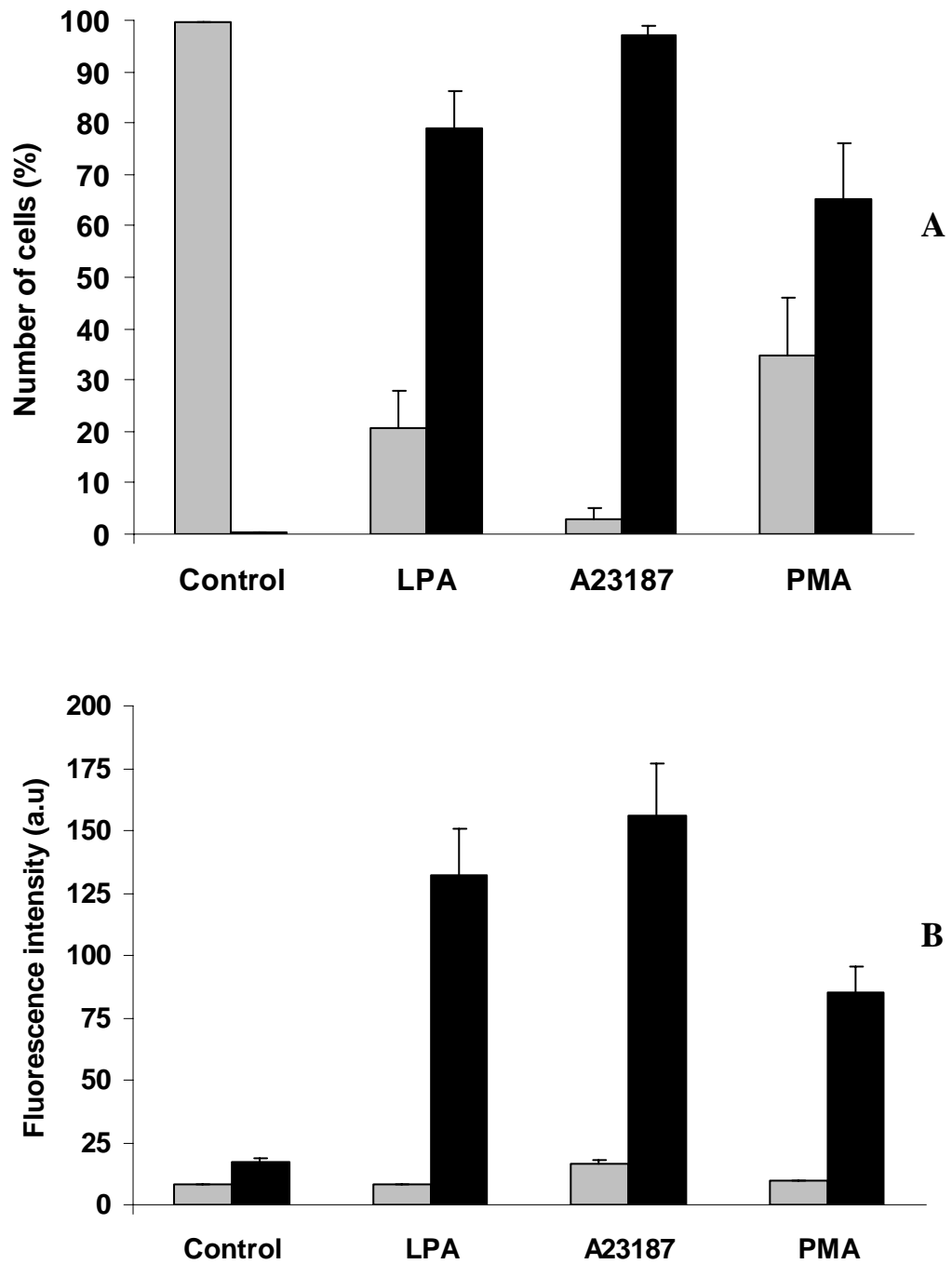


Fig. 35: Reaction of sheep RBCs with 2.5 μ M LPA, 2 μ M A23187 and 6 μ M PMA after 15 min incubation (FACS measurement). A: Reaction of sheep RBCs, B: Fluorescence intensity of reacting and non-reacting cells. Bars show mean value of 3 different blood samples (30.000 cells of each blood sample were analysed). Error bars represent S.D.

4.2. Investigation of phosphatidylserine exposure in red blood cells

4.2.1. Phosphatidylserine exposure in red blood cells under stimulated conditions

The RBCs were stimulated for PS exposure by 2.5 μM LPA, 2 μM A23187 or 6 μM PMA in the presence of 2 mM extracellular Ca^{2+} for 30 min at 37°C. The PS exposure in the outer leaflet of the RBC membrane was analysed by flow cytometry. The results are shown in Fig. 36.

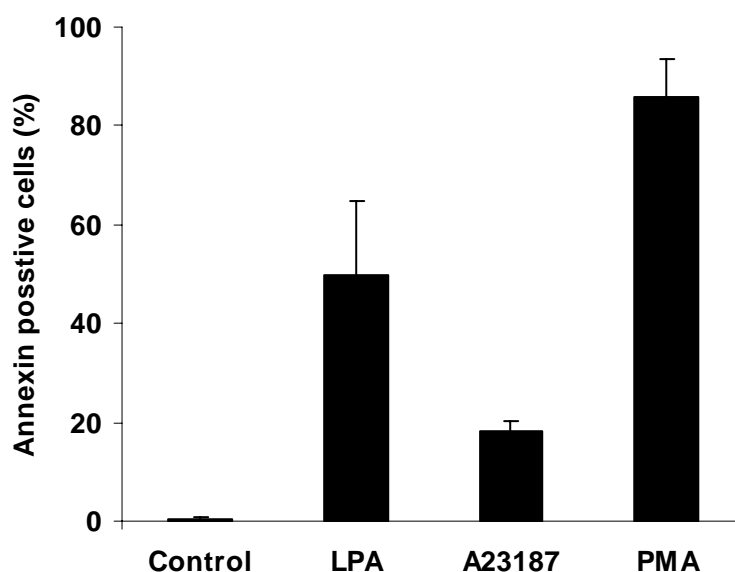


Fig. 36: PS exposure of RBCs stimulated with LPA, A23187 and PMA. Bars show mean value of 3 different blood samples (30.000 cells of each blood sample were analysed). Error bars represent S.D.

Under inducing conditions, the annexin positive cells (%) are 0.31 ± 0.19 , 50.78 ± 14.03 , 18.34 ± 2.01 and 85.89 ± 7.56 for control, LPA, A23187, and PMA, respectively. In case of LPA, the number of cells showing PS exposure varies and depends on the blood samples. However, RBCs treated with PMA show PS exposure in the range of 80 and 95% and no significant haemolysis of the RBCs can be observed. The original measurement data for PS exposure (histogram analysis) are presented in Fig. 37. The original measurement data for PS exposure and microvesicle formation (dot plot analysis) are presented in Fig. 38.

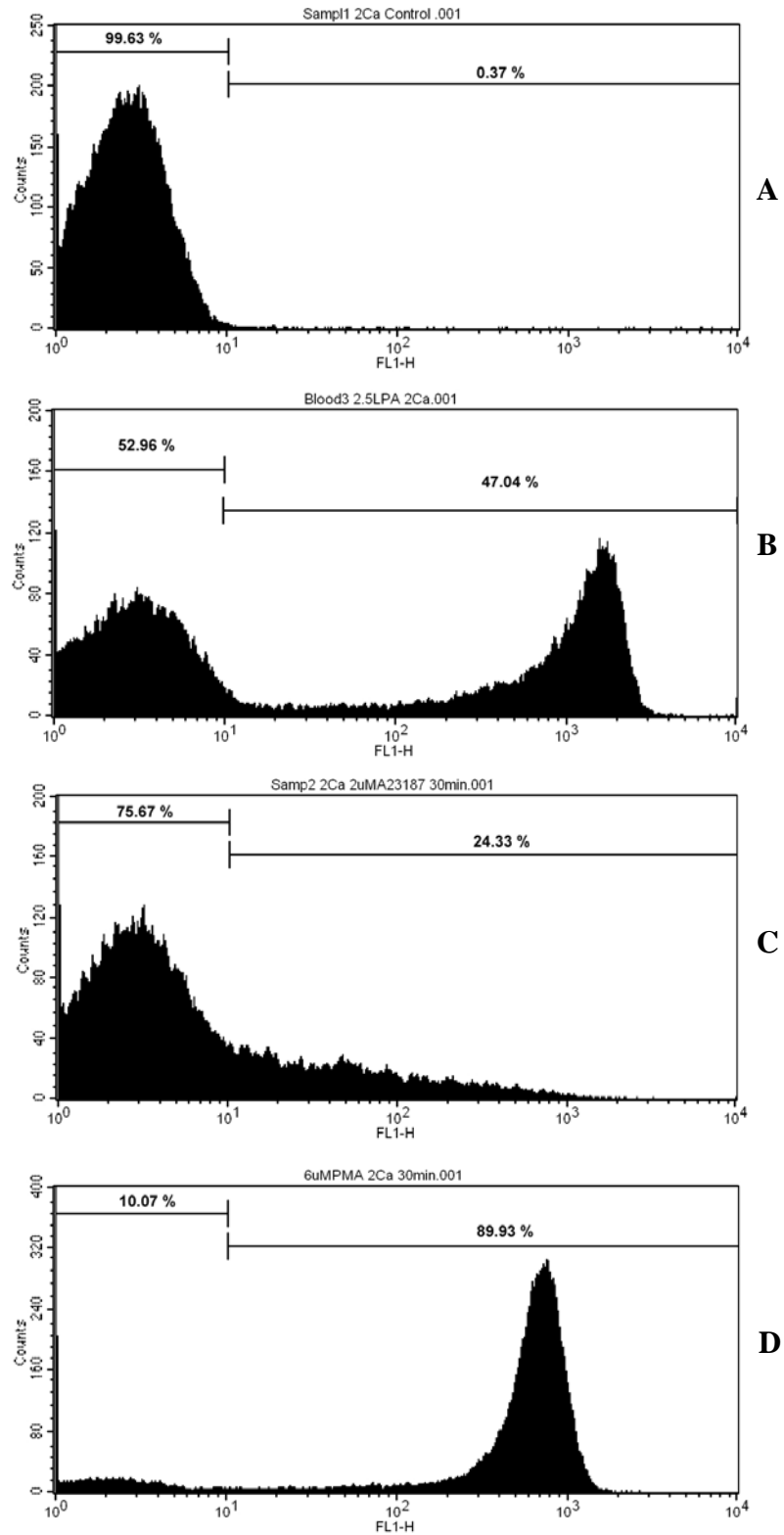


Fig. 37: Typical histograms for PS exposure of RBCs. A: control in physiological solution, **B:** 2.5 μM LPA, **C:** 2 μM A23187, and **D:** 6 μM PMA (cells were treated for 30 min at 37°C in the presence of 2 mM Ca^{2+}).

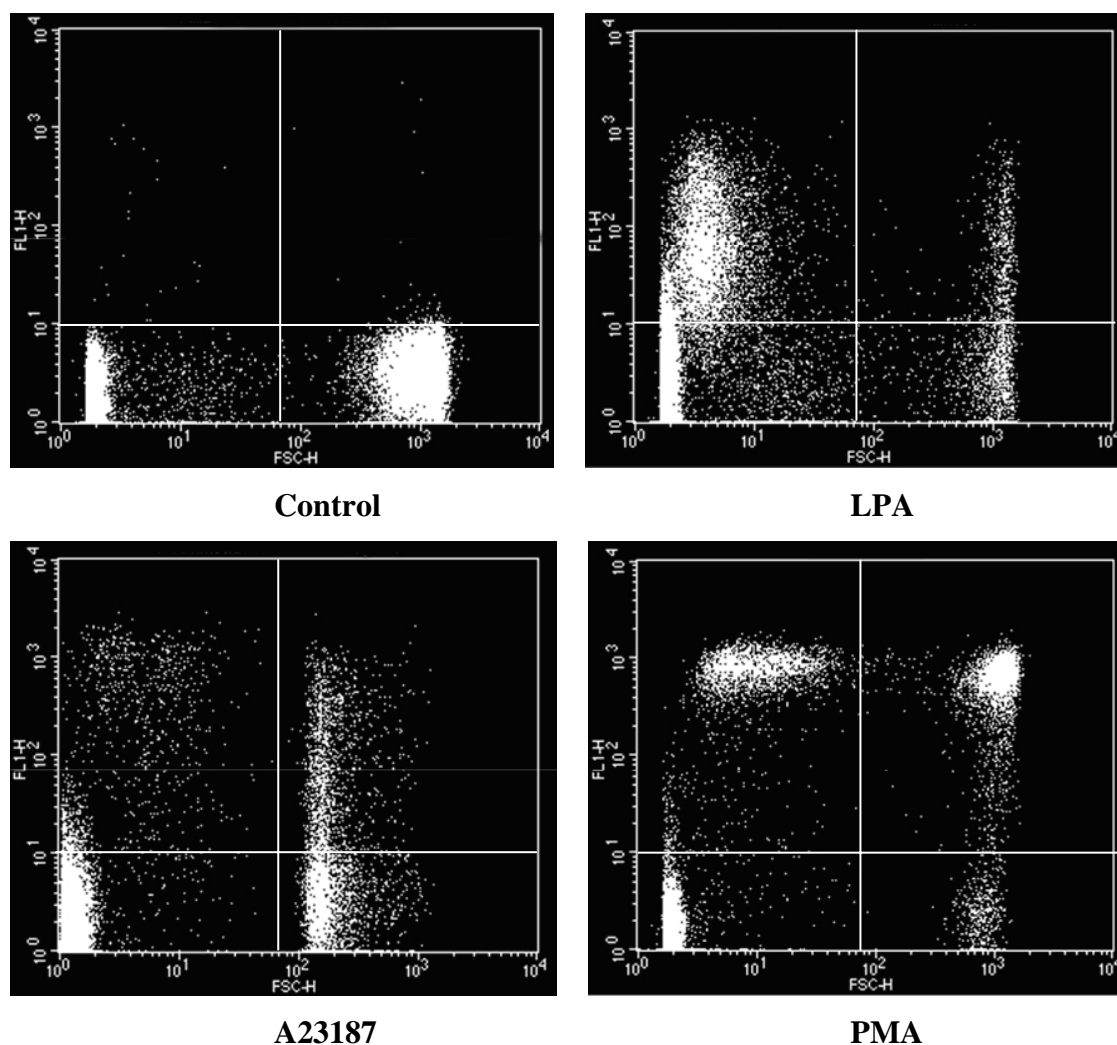


Fig. 38: Typical dot plots showing PS exposure and microvesicle formation. Upper left: control in physiological solution containing 2 mM Ca^{2+} , upper right: 2.5 μM LPA. Lower left: 2 μM A23187, lower right: 6 μM PMA (cells were treated for 30 min at 37°C). In each plot, upper left: microvesicles, upper right: cells showing PS exposure, lower left: debris or very small particles, lower right: cells with no PS exposure.

Although the fluorescence intensity of fluo-4 in RBCs stimulated by PMA is much lower in comparison to LPA and A23187, the number of cells showing PS exposure is significantly higher. It suggests that the PS exposure in case of PMA treatment does not depend on the level of intracellular Ca^{2+} only.

Experiments were also done in the absence of Ca^{2+} . After being loaded with fluo-4, RBCs were treated with 6 μM PMA and 1 mM EGTA in the absence of Ca^{2+} to remove completely Ca^{2+} in the solution. The results revealed that the intracellular Ca^{2+} content is the same as the control sample (without PMA) (Fig. 39). However, in the absence of extracellular Ca^{2+} the

number of cells showing PS exposure is only about 50% (Figs. 40, 41). This would suggest that the PS exposure in the case of PMA treatment involves a Ca^{2+} independent pathway.

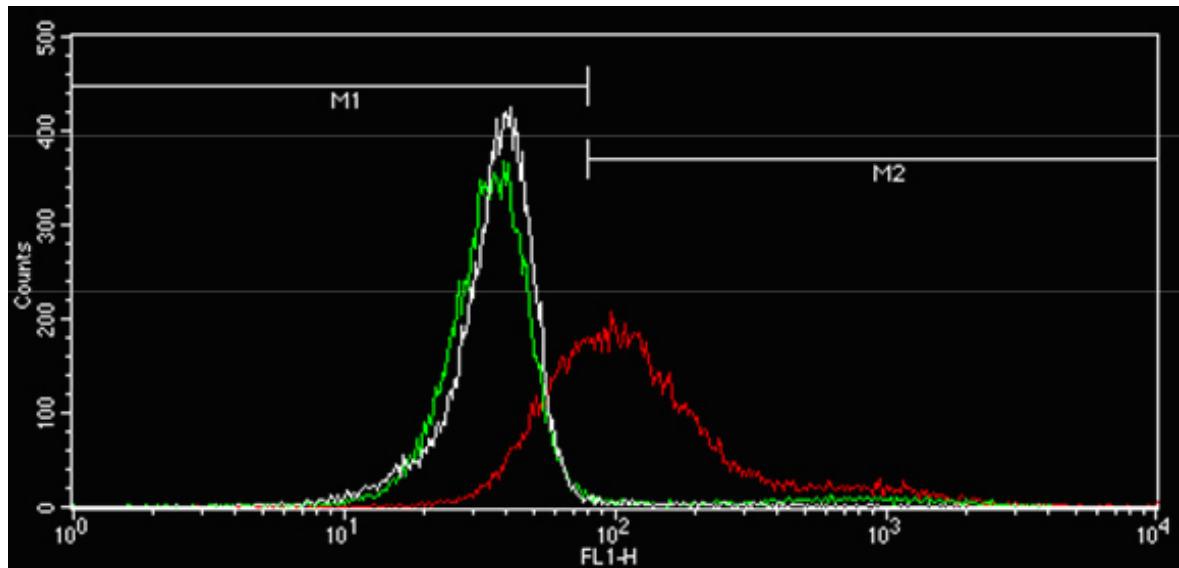


Fig. 39: Histogram overlay of fluo-4 fluorescence intensity of RBCs in the presence of PMA. White: control (without PMA), red: 2 mM Ca^{2+} and 6 μM PMA, green: 1 mM EGTA and 6 μM PMA.

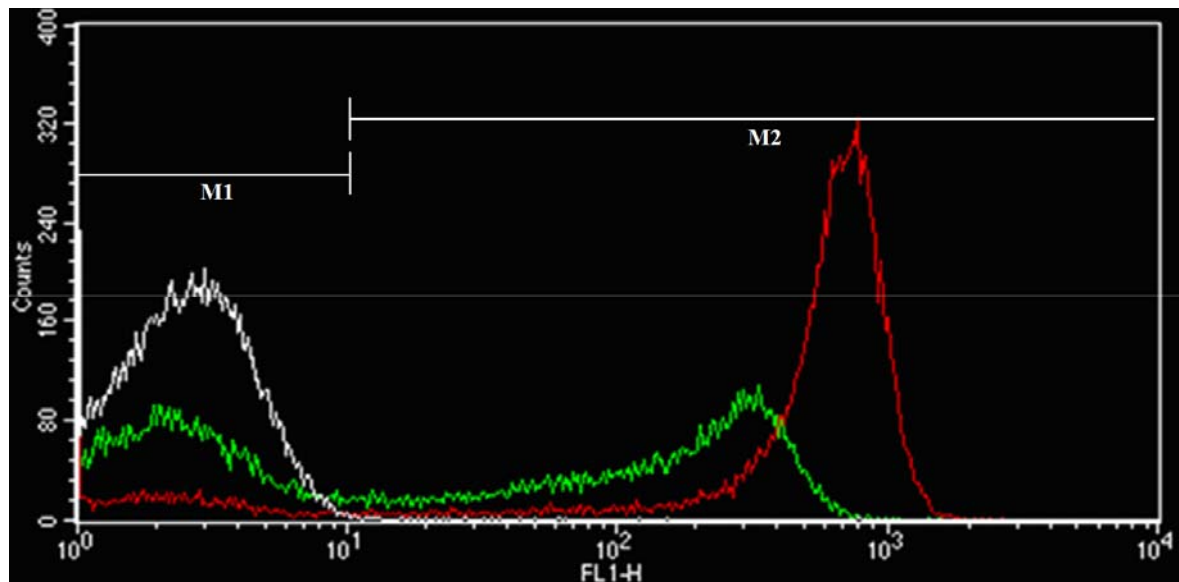


Fig. 40: Histogram overlay for PS exposure of PMA stimulated RBCs in the presence and absence of extracellular Ca^{2+} . White: control (without PMA), red: 2 mM Ca^{2+} and 6 μM PMA, green: 1 mM EGTA and 6 μM PMA.

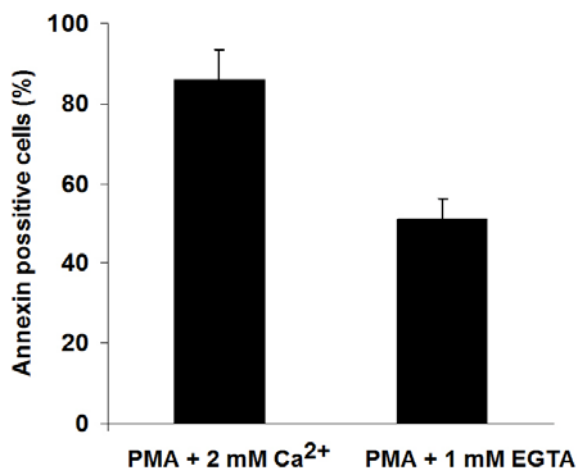


Fig. 41: PS exposure of RBCs stimulated by PMA (in the presence and absence of extracellular Ca²⁺). Bars show mean value of 3 different blood samples (30.000 cells of each blood sample were analysed). Error bars represent S.D.

4.2.2. Kinetics of phosphatidylserine exposure

The kinetics of PS exposure of RBCs under inducing conditions was investigated by using both fluorescence microscopy and flow cytometry. Fig. 42 shows the process of PS exposure in RBCs treated with 2 μ M A23187 in the presence of 2 mM Ca²⁺ during 24 h.

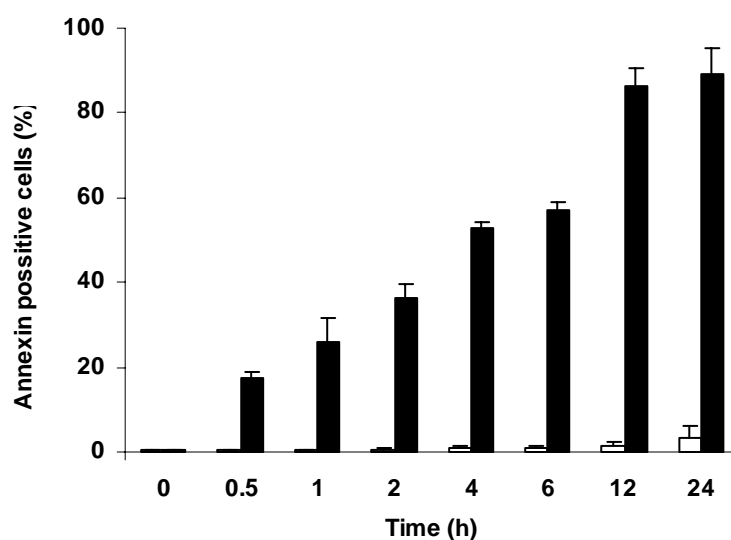


Fig. 42: Kinetics of PS exposure of human RBCs (FACS measurement). White bars: in the absence of Ca²⁺, black bars: in the presence of 2 mM Ca²⁺. Bars show mean value of 3 different blood samples (30.000 cells of each blood sample were analysed). Error bars represent S.D.

It is clear that the number of cells showing PS exposure increases correspondingly with the incubation time. The saturation of PS exposure is reached after 12 h of incubation. The

haemolysis is also seen after 12 h. The details of the PS exposure process of RBCs under inducing conditions (A23187 and LPA treatment) are shown in Fig. 43 (recorded by using a fluorescence microscope). In the presence of 2 μM A23187 and 2 mM extracellular Ca^{2+} , one can see the cell membrane blebbing and the formation of microvesicles after 30 min. The extension of blebs forms rod like structures, which can be clearly observed when they bind with annexin V-FITC (Fig. 43).

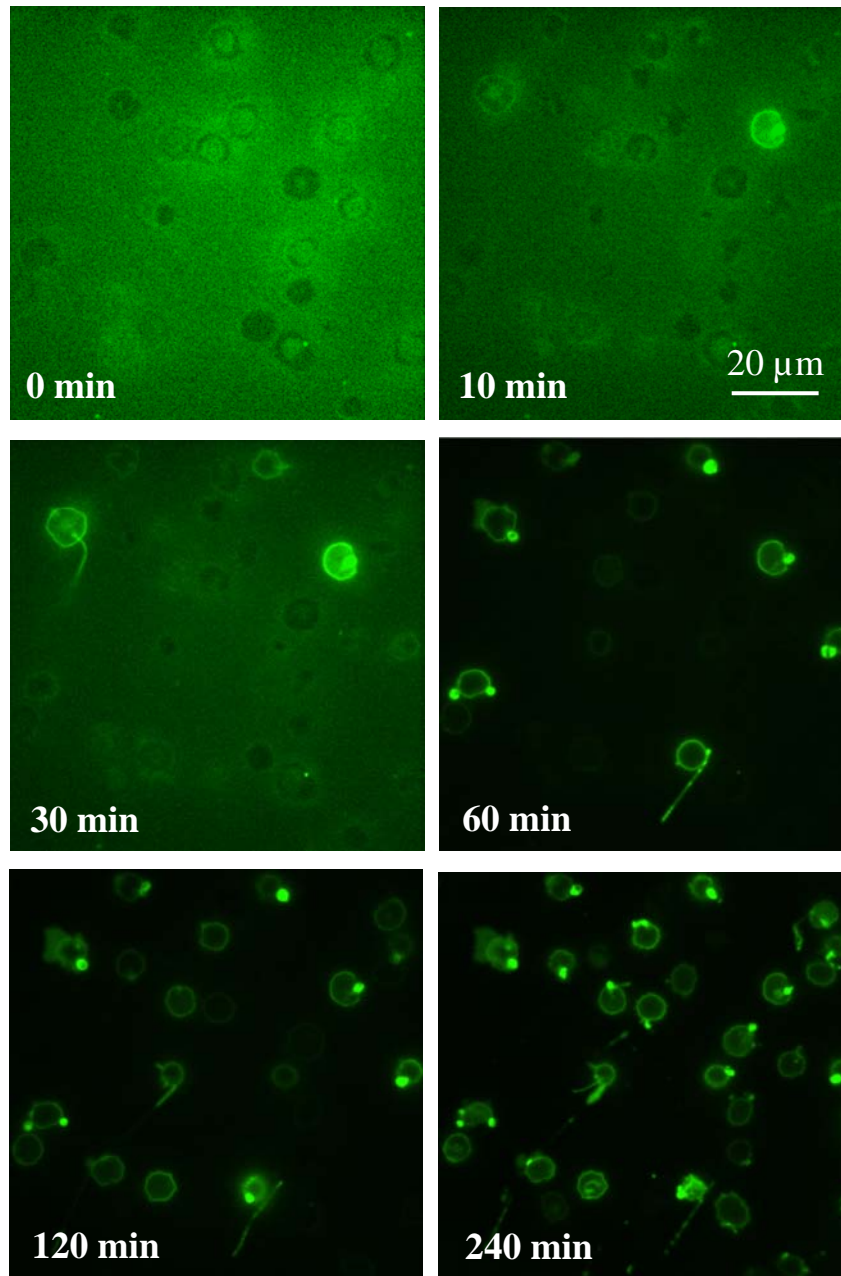


Fig. 43: Kinetics of PS exposure of RBCs treated with A23187 (fluorescence microscope measurement). RBCs were treated with annexin V-FITC, 2 μM A23187, and 2 mM extracellular Ca^{2+} . The experiments were done at room temperature.

The kinetics of PS exposure process in the presence of LPA is similar but it is faster than in the case of A23187. The formation of membrane blebbing and microvesicles can be also observed (Fig. 44). However, the rod like structures are not seen clearly as for A23187 treatment.

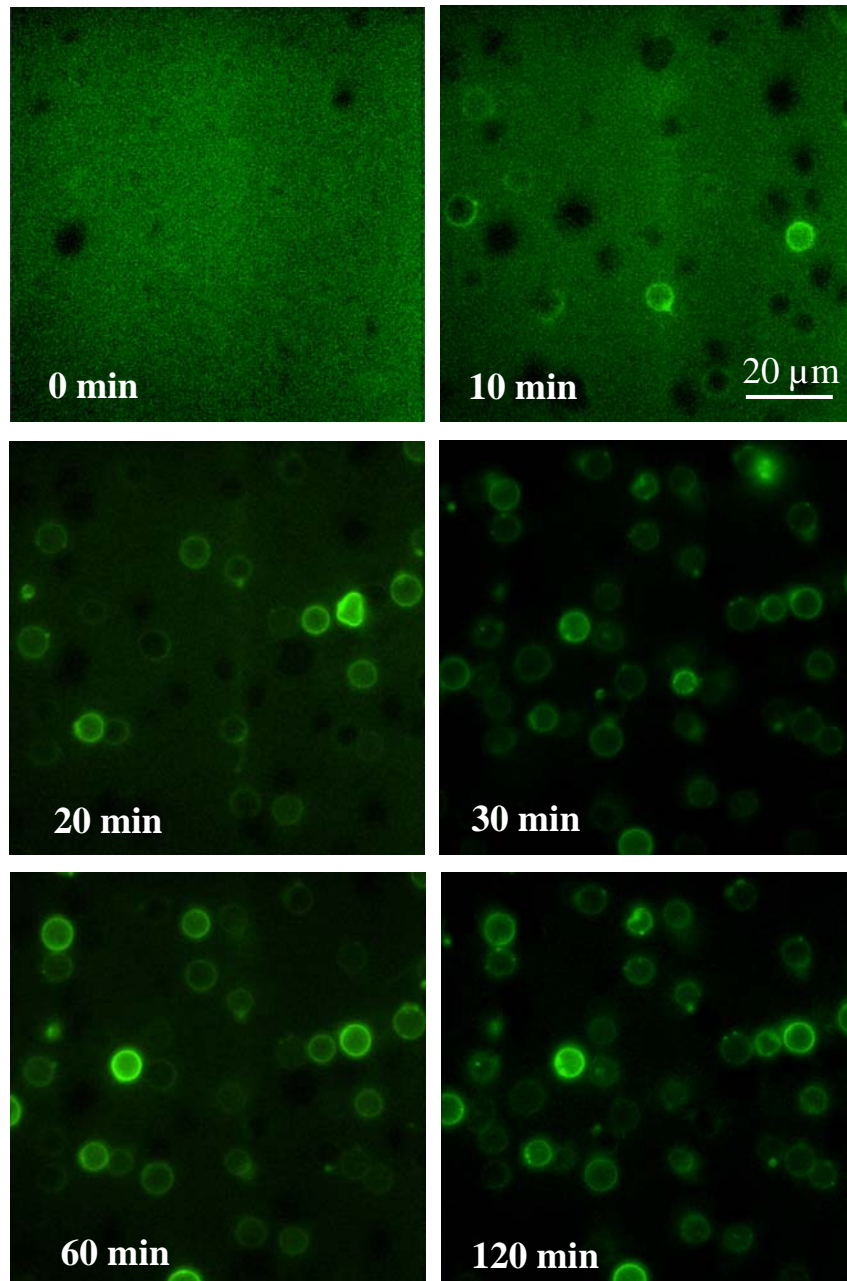


Fig. 44: Kinetics of PS exposure of RBCs treated with LPA (fluorescence microscope experiment). RBCs were treated with Annexin V-FITC, 2.5 μM LPA, and 2 mM extracellular Ca^{2+} . The experiments were done at room temperature.

Sickle RBCs and PS exposure

Under physiological conditions, the exposure of PS on RBCs of normal and sickle blood samples was measured. Washed RBCs were incubated with annexin V-FITC for 15 min at room temperature. The results show that the number of RBCs showing PS exposure is less than 0.5% in all normal blood samples. In case of sickle blood samples, the number of cells showing PS exposure is about 2.5% (FACS analysis, data not shown).

Under physiological conditions, the number of RBCs showing PS exposure is very low. To investigate the reaction of normal and sickle RBCs of sickle cell patients under conditions stimulating for PS exposures, the washed RBCs were treated with 2 μM A23187 and 2 mM Ca^{2+} at 37°C for 30 min (Fig. 45). The result shows that all sickle RBCs show PS exposure while some normal RBCs of this patient do not (only a certain amount). This statement is based on investigation of about 60 sickle cells from 3 different blood samples. The explanation for this phenomenon is unclear.

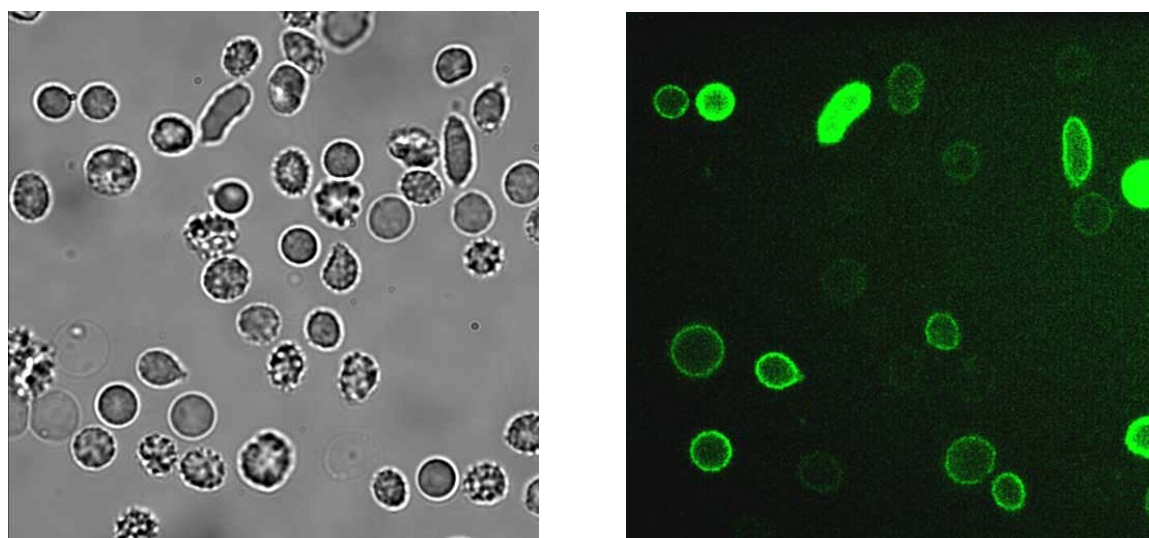


Fig. 45: PS exposure of RBCs in sickle blood sample. RBCs of sickle blood sample were treated with 2 μM A23187 in the presence of 2 mM extracellular Ca^{2+} for 30 min at 37°C. Left: transmission light image, right: fluorescence image (cells stained with annexin V-FITC).

4.2.3. Intracellular pH in phosphatidylserine exposed human red blood cells

The kinetics of intracellular pH under inducing conditions with LPA, A23187 or PMA was investigated by using a fluorescence microscope. 2 min after addition of 2.5 μM LPA, the

pH_i started to decrease. The lowest pH_i value observed was about 6.4 after 8 min and kept constant for 20 min. The pH_i also reduced when 2 μM A23187 was added. However, the delay time lasted approximately 7 min before a reduction from 7.12 to 6.20. After this, the pH_i increased again to 6.8 and stayed in the range of 6.5 and 6.6. In case of PMA treatment, the pH_i reduced slowly from 7.15 to 6.6 after 25 min and finally increased to be about 6.8. In the control, the pH_i was relatively stable with a slight decline over 30 min (Fig. 46). The described effects shown for one blood sample were observed for 3 different bloods. The reduction of pH_i can be explained by the loss of K^+ , Cl^- and the uptake of H^+ .

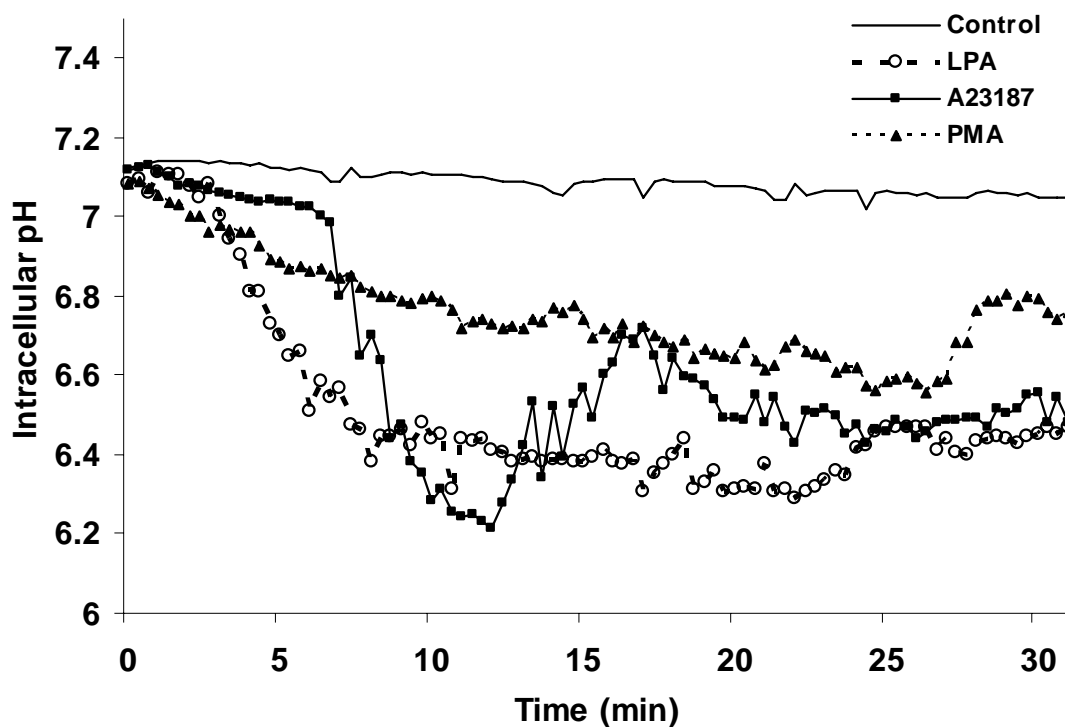


Fig. 46: Kinetics of pH_i of RBCs under different conditions. Control: physiological solution with 2 mM Ca^{2+} . Experiment samples with 2.5 μM LPA or 2 μM A23187 or 6 μM PMA. Mean value of about 30 cells (to each curve) from one blood.

4.2.4. Investigation of phosphatidylserine exposure under other conditions

Influence of valinomycin on PS exposure

To investigate the influence of K^+ efflux on PS exposure, cells were treated with valinomycin at different concentrations. Valinomycin was added to a RBC suspension in physiological solution (145 mM NaCl, 7.5 mM KCl, 10 mM glucose, 10 mM HEPES, pH 7.4). The RBC suspension (0.1% haematocrit) was incubated at 37°C. After 6, 18 and 24 h,

the RBCs were collected for the PS exposure measurements. The results show that the number of cells showing PS exposure is very low. After 24 h the PS exposure is in the range of 12 and 14%. There was not much difference in the number of RBCs showing PS exposure in dependence of the valinomycin concentrations (Fig. 47).

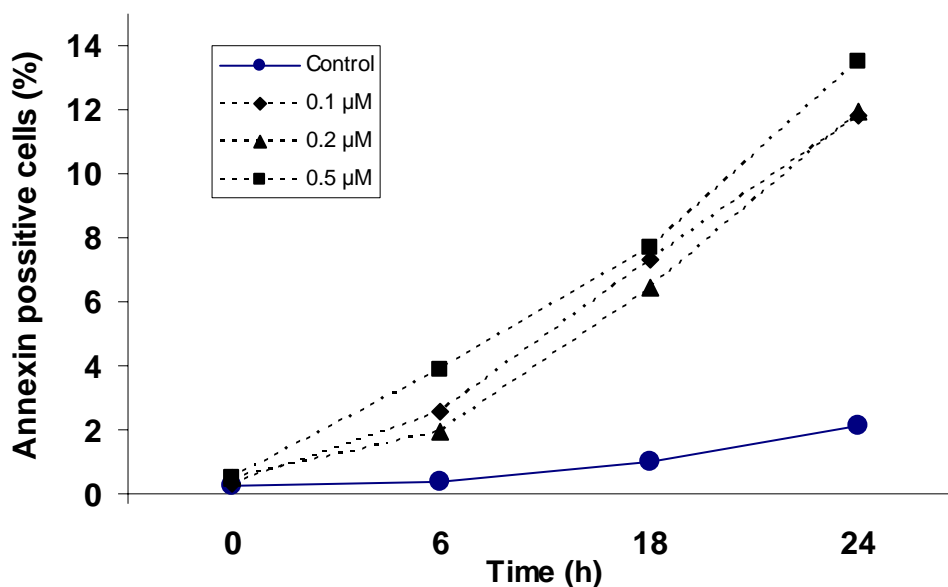


Fig. 47: Influence of the valinomycin concentrations on the PS exposure. FACS analysis of 30.000 cells from 1 blood sample.

It is evident that a stimulation of K^+ efflux by valinomycin contributes to the effect of PS exposure. However, this is of significance only after long time incubation and does not play a substantial role after 30 min.

By removing NaCl and adding KCl instead to the physiological solution to keep the osmotic pressure constant, solutions containing 7.5, 75 and 150 mM KCl were prepared. RBCs were stimulated for PS exposure by adding 2 μ M A23187 or 2.5 μ M LPA (Figs. 48, 49).

To see whether the PS exposure is somehow connected with the K^+ efflux via the Ca^{2+} activated K^+ channel, experiments were carried out where PS exposure was measured after LPA treatment in solution of different KCl concentrations. At 150 mM KCl outside, the opening of the Ca^{2+} -activated K^+ channel would not allow to extrude K^+ from intracellular to extracellular. After 30 min incubation at 37°C, RBCs were collected for PS exposure measurement. In case of LPA, in a high KCl containing solution, the PS exposure is reduced in comparison to the physiological solution containing 7.5 mM KCl (Fig. 48). A significant difference was observed in solutions containing 7.5 and 150 mM KCl.

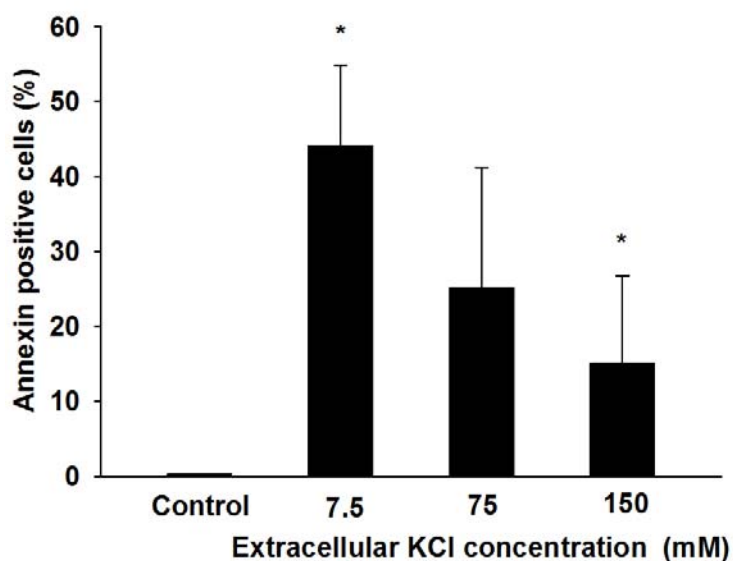


Fig. 48: Influence of different extracellular K^+ concentrations on PS exposure of RBCs in the presence of $2.5 \mu\text{M}$ LPA. RBCs were stimulated for PS exposure by $2.5 \mu\text{M}$ LPA in the presence of 2 mM Ca^{2+} . Bars show mean value of 3 different blood samples (30.000 cells of each blood sample were analysed). Error bars represent S.D. (*) T-test analysis shows that the mean values between the two samples are statistically significant different ($P < 0.05$).

In the presence of $2 \mu\text{M}$ A23187, there is also a reduction of PS exposure in high KCl containing solution. In a solution containing 150 mM KCl, the reduction was about 25% in comparison to the physiological solution containing 7.5 mM KCl (Fig. 49).

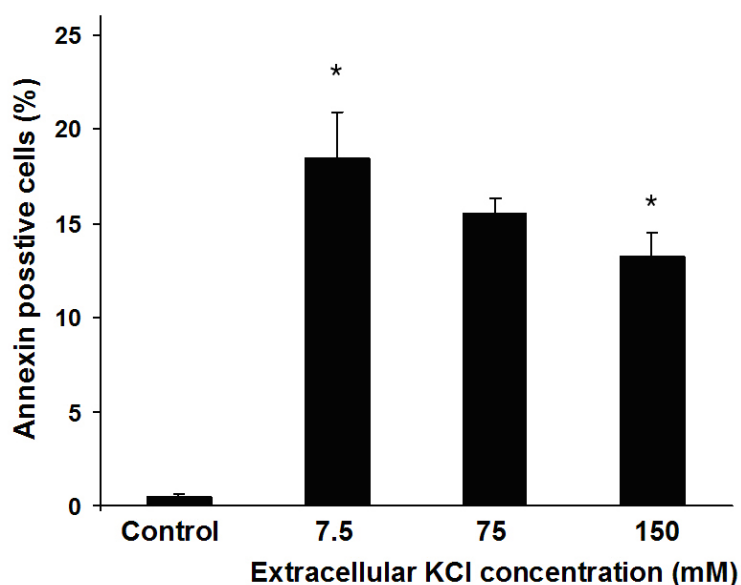


Fig. 49: Influence of different extracellular K^+ concentration on PS exposure in the presence of $2 \mu\text{M}$ A23187. Bars show mean value of 3 different blood samples (30.000 cells of each blood sample were analysed). Error bars represent S.D. (*) T-test analysis shows that the mean values of the two samples are significant different ($P < 0.05$).

In principle, the Ca^{2+} -activated K^+ channel (Gardos channel) is activated when the intracellular Ca^{2+} increases. Charybdotoxin potently inhibits both Gardos and voltage-activated K^+ channels. To investigate the influence of Gardos channel on the PS exposure of RBCs, 100 and 200 nM of charybdotoxin were added to a RBC suspension (0.1% haematocrit) 30 min before inducing PS exposure by 4 μM A23187 for 2 h. The results show that when the Gardos channel is inhibited, the number of cells showing PS exposure is significantly reduced, approximately by 40% (Fig. 50 A, B).

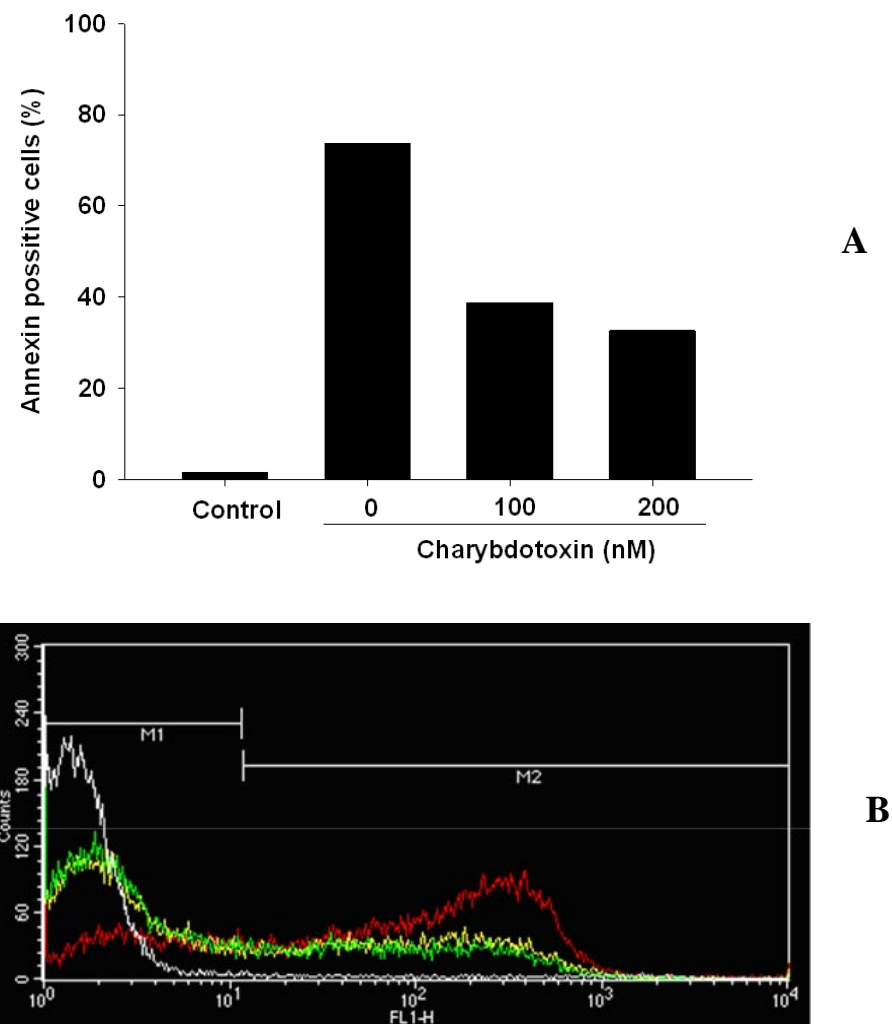


Fig. 50: Influence of charybdotoxin on PS exposure in the presence of A23187.

A: Control, RBCs in physiological solution containing 2 mM Ca^{2+} . Charybdotoxin at different concentrations 0 nM, 100 nM, and 200 nM was used. **B:** Histogram of FACS analysis shows the overlay of the control and charybdotoxin treatment. White: control (RBCs in physiological solution containing 2 mM Ca^{2+}), red: 4 μM A23187, green: 100 nM charybdotoxin and 4 μM A23187, yellow: 200 nM charybdotoxin and 4 μM A23187.

Influence of osmotic pressure on PS exposure

By removing NaCl from the physiological solution or adding sucrose to the physiological solution, different osmotic pressure solutions were prepared. Based on the mean value of the forward scatter, the cell volume change was observed. Fig. 51 shows the influence of osmolarity on the volume of the cells. The physiological solution was estimated with an osmolarity of 305 mOsm/kg. In low osmolarity solution, the volume of the cells increased. A strong reduction of cell volume (more than 50%) was observed when 500 mM sucrose was added to physiological solution. At 793 mOsm (physiological solution containing 700 mM sucrose), the cells showed haemolysis. There was no significant difference in the cell volume after 30 min and 24 h incubation.

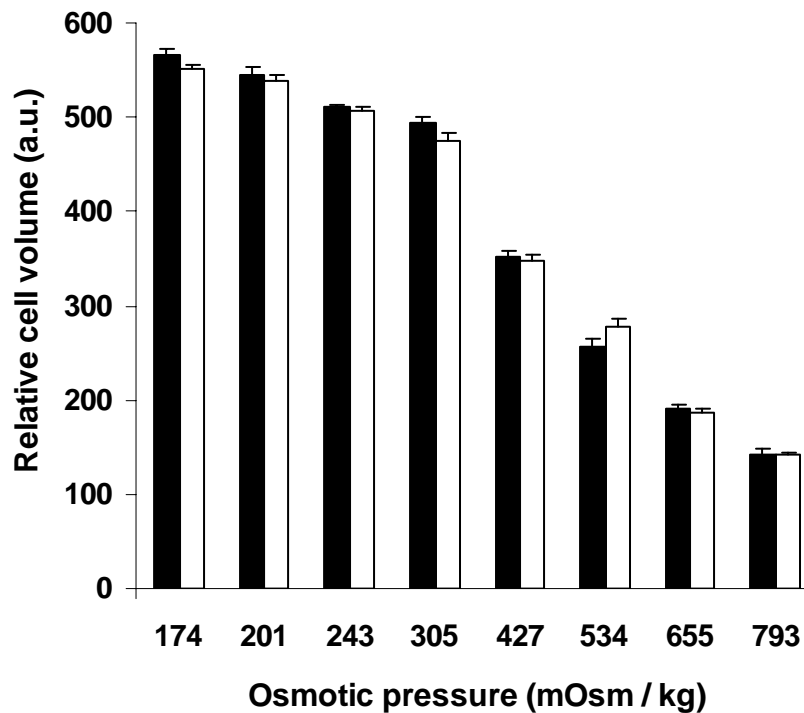


Fig. 51: Influence of osmolarity on cell volume after 24 h. Black bars: without Ca²⁺, white bars: with 2 mM Ca²⁺. Bars show mean value of 3 different blood samples (30.000 cells of each blood sample were analysed). Error bars represent S.D.

The PS exposure of RBCs under different osmotic solutions was measured after 24 h of incubation at 37°C. The results show that in low osmolarity solution there is also no significant PS exposure even after long time incubation in comparison to the control in physiological solution. In contrast, the number of cells showing PS exposure increases proportionally with the osmolarity. In the presence of 2 mM extracellular Ca²⁺, the PS

exposure is significantly enhanced (Fig. 52). It should be mentioned that after 30 min or 1 h of incubation, no significant PS exposure was observed in both low and high osmolarity solutions.

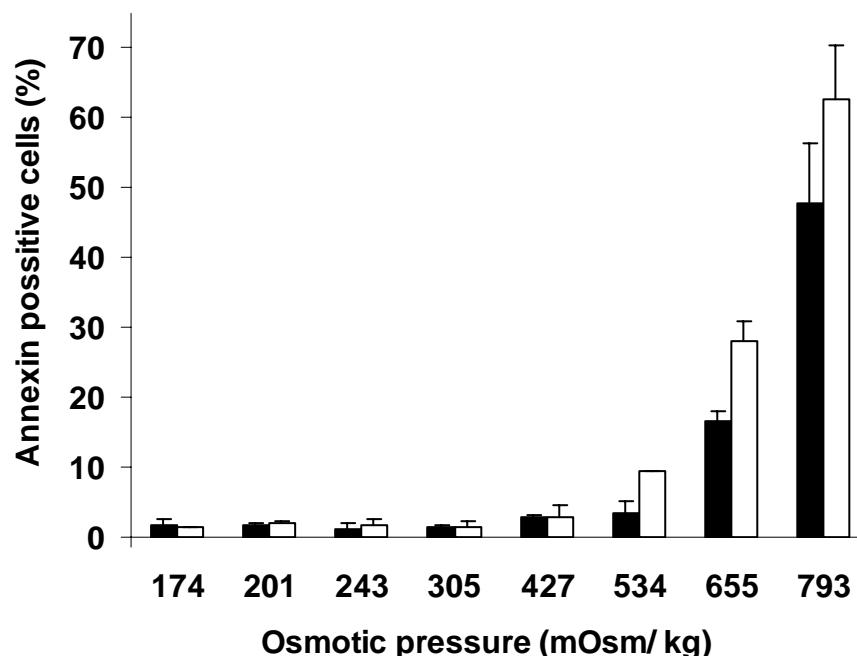


Fig. 52: Influence of osmotic pressure on PS exposure after 24 h. Black bars: without Ca²⁺, white bars: with 2 mM Ca²⁺. Bars show mean value of 3 different blood samples (30.000 cells of each blood sample were analysed). Error bars represent S.D.

Influence of protein kinase C inhibitors on PS exposure

Chelerythrine and staurosporine are known as potential inhibitors of protein kinase C [124, 184]. Before inducing PS exposure of RBCs by 2.5 μ M LPA or 2 μ M A23187 or 6 μ M PMA and 2 mM Ca²⁺ as mentioned above, the cells were pre-incubated with chelerythrine or staurosporine (10 μ M final concentrations) at 37°C for 15 min.

Data analysis show that both chelerythrine and staurosporine inhibit the number of cells showing PS exposure. At the same concentration, the inhibition activity of chelerythrine is higher in comparison to staurosporine. In the group experiments with PMA, the inhibition activity of chelerythrine and staurosporine is clearly observed. However, in the group experiments with LPA and A23187, the inhibition activity of staurosporine and chelerythrine was not statistically significant (Fig. 53).

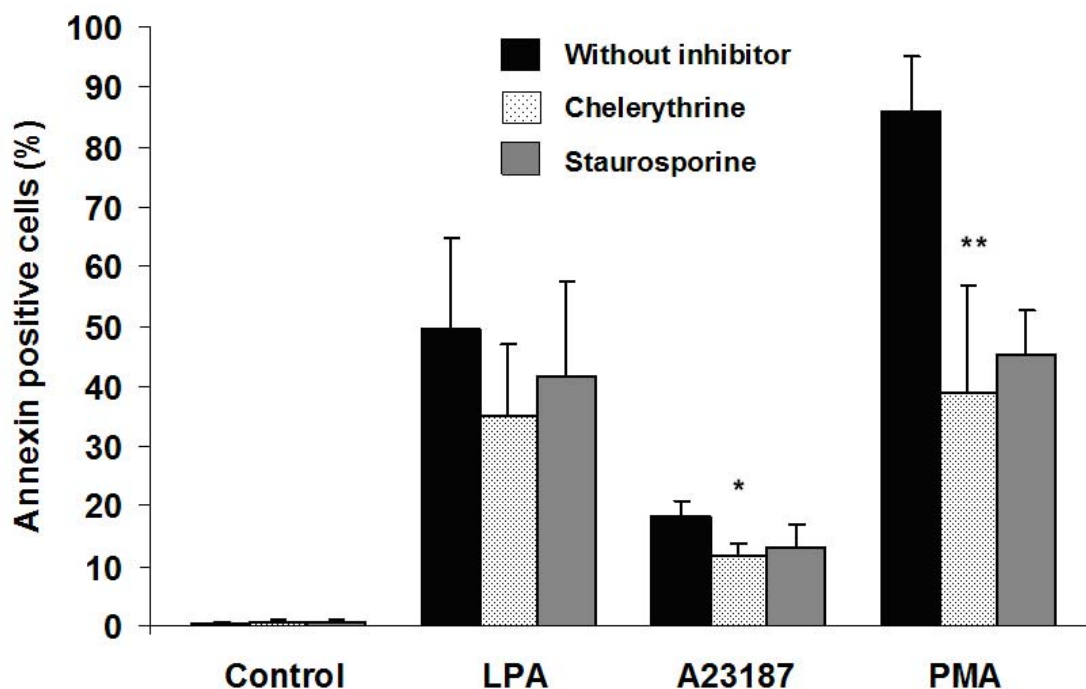


Fig. 53: Influence of 10 μM chelerythrine and 10 μM staurosporine on PS exposure of human RBCs. RBCs are treated with 2.5 μM LPA or 2 μM A23187 or 6 μM PMA and 2 mM extracellular Ca^{2+} . Bars show mean value of 3 different blood samples (30.000 cells of each blood sample were analysed). Error bars represent S.D. Paired t-test shows no statistical significant difference among the mean values of the samples treated with LPA in the presence or absence of inhibitors. (*) Paired t-test shows a statistical significant difference between the mean value of the samples without and with chelerythrine treatment. (**) Paired t-test shows a statistical significant difference between the mean values of the sample without and with inhibitors. Data analysis shows that there is no significant difference in the inhibition activity between chelerythrine and staurosporine.

Influence of low ionic strength, glucose free and ATP depletion solutions on PS exposure

Low ionic strength (LIS) solution is a term to describe a physiological solution in which NaCl was replaced by sucrose [185]. After 24 h incubation at 37°C in LIS solution, the RBCs were analysed by flow cytometry. The results show that in LIS solution, the number cells showing PS exposure is very low. In the solution containing no glucose, approximately 5% of the cells showing PS exposure can be observed. The presence of 2 mM extracellular Ca^{2+} enhances PS exposure. Under ATP depleted conditions with 1 mM EGTA, the PS exposure increases up to 9%. When 2 mM Ca^{2+} was added, the PS exposure increased significantly. However, under such condition, haemolysis can be observed (Fig. 54). After short time incubation (2 h) under the mentioned conditions, the number of cells showing PS exposure was not significant.

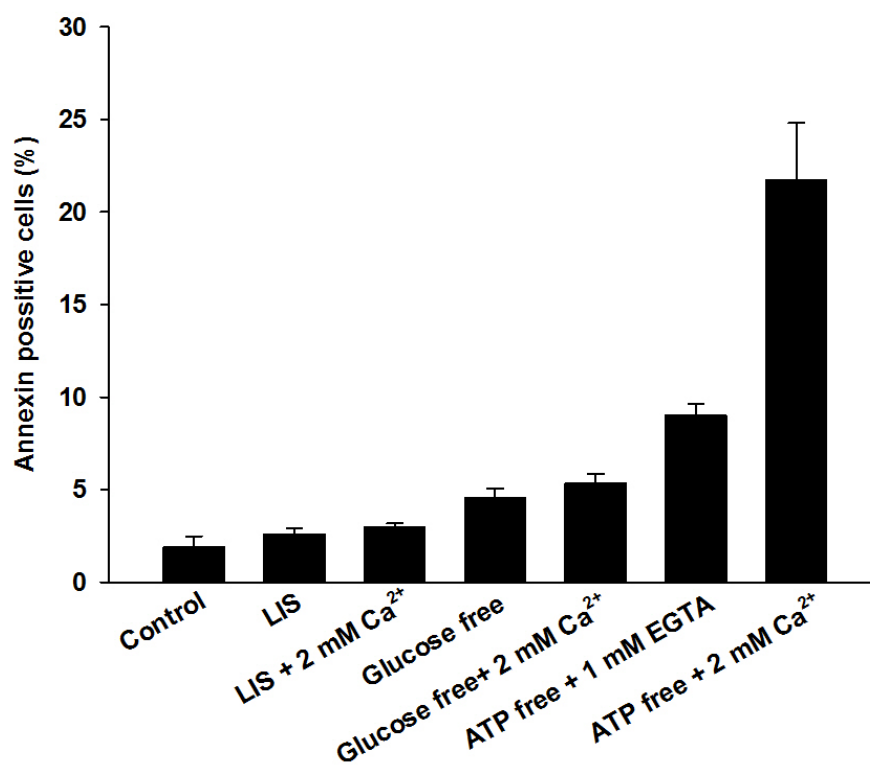


Fig. 54: Influence of low ionic strength, glucose free and ATP depleted solutions on PS exposure of human RBCs. Flow cytometry analysis after 24 h incubation. Bars show mean value of 3 different blood samples (30.000 cells of each blood sample were analysed). Error bars represent S.D.

Influence of ZnCl₂ and tert-butyl perhydroxide on PS exposure

RBCs were incubated with tert-butyl hydroperoxide at a final concentration of 0.5 mM for 2 h at 37°C. Tert-butyl hydroperoxide is known as a substance inducing oxidative stress [106]. In all experiments with different blood samples, the number of cells showing PS exposure is very high (more than 90%), no haemolysis was observed under this condition (Fig. 55). However, the colour of RBCs after treatment changed from red to red-grey. The influence of Zn²⁺ on PS exposure was also studied. Zn²⁺ is known to activate the ceramide formation and caspase activation [109]. After 24 h incubation at 37°C, the number of cells showing PS exposure increases significantly depending on the concentration of extracellular Zn²⁺ (Fig. 55).

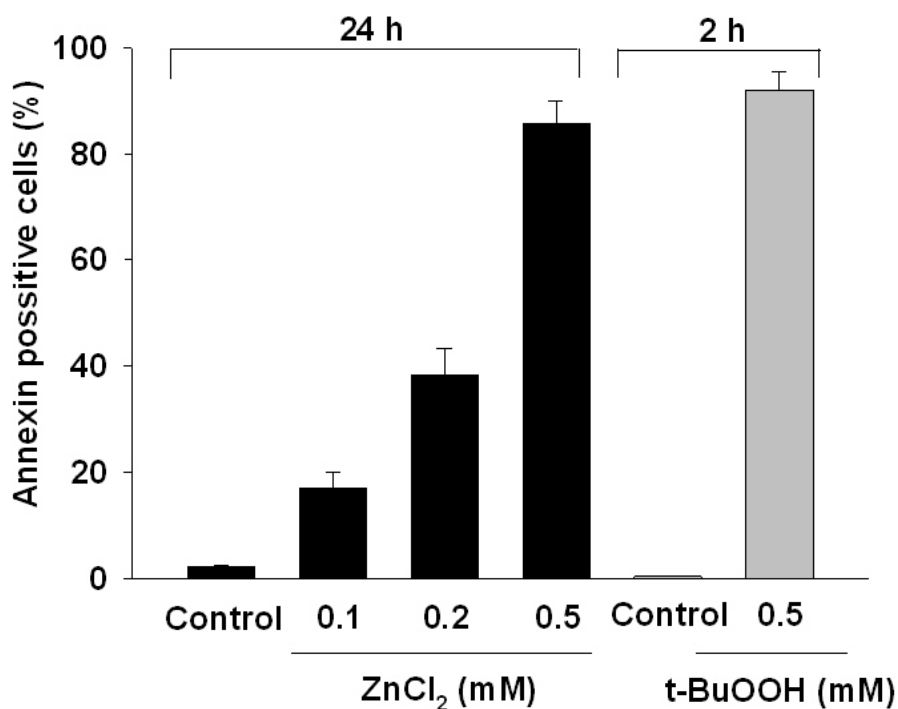


Fig. 55: Influence of ZnCl₂ and tert-butyl hydroperoxide on PS exposure of human RBCs. Bars show mean value of 3 different blood samples (30.000 cells of each blood sample were analysed). Error bars represent S.D. (t-BuOOH: tert-butylhydroperoxide).

4.2.5. Relevance of intracellular Ca²⁺ for the phosphatidylserine exposure

By using flow cytometry and fluorescence microscopy, the fluorescence signal of fluo-4 and annexin V-FITC was only analysed separately because the excitation and emission wavelength of fluo-4 and FITC are the same range (488 nm and 520 nm, respectively). Therefore, the question is whether cells containing higher Ca²⁺ content also show more PS exposure. To answer this question, the RBCs were double labelled with both fluo-4 and annexin V-Alexa 568 (see Materials and Methods).

After being stimulated for PS exposure by 2.5 μM LPA, 2 μM A23187 or 6 μM PMA in the presence of 2 mM Ca²⁺ for 30 min at 37°C, RBCs were double labelled and scanned by using a confocal scanning fluorescence microscope as described (see 3.2.1 E). It is very clear that in case of A23187, almost all RBCs react and show a high fluorescence signal of fluo-4. It means that intracellular Ca²⁺ in these RBCs increases. Nevertheless, under these conditions, some cells with a high fluorescence signal for Ca²⁺ but a small or even no PS exposure can be observed (Fig. 56).

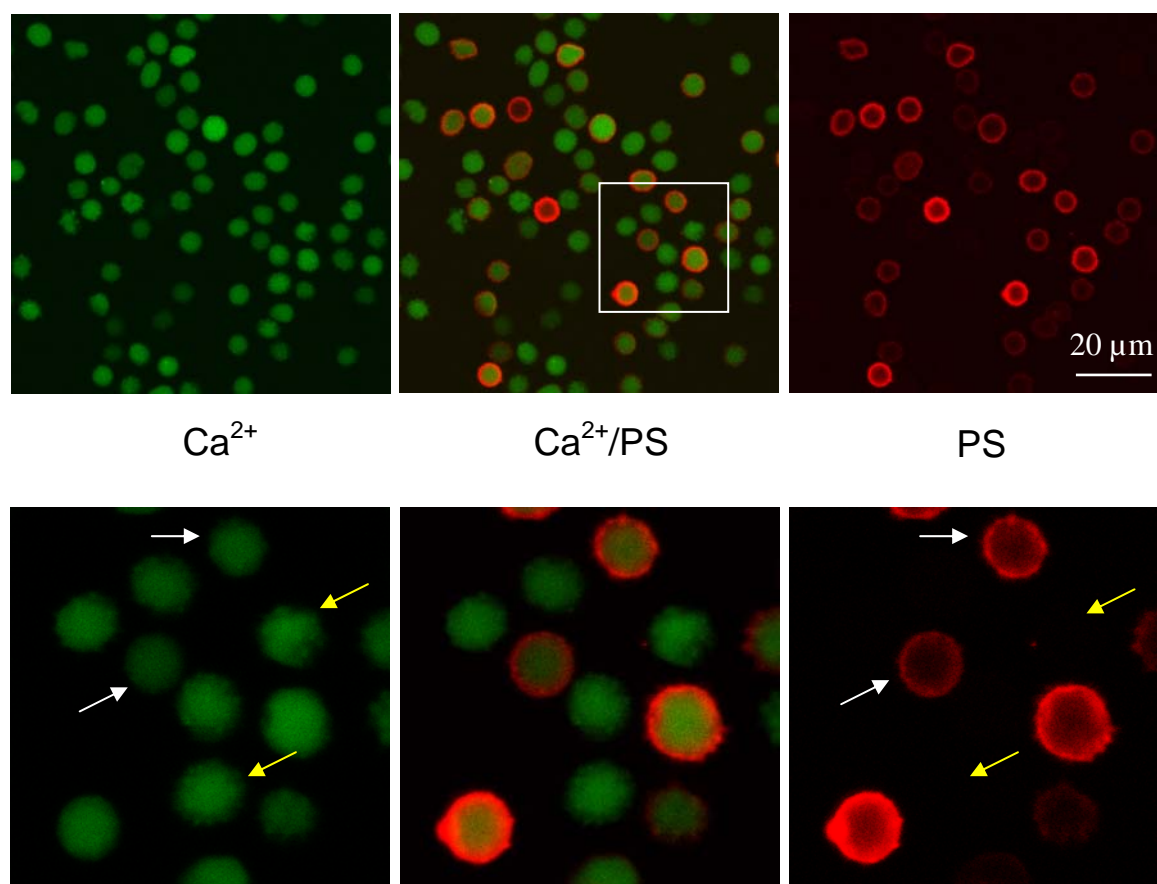


Fig. 56: Double labelled human RBCs with fluo-4 and annexin V-alexa 568 after being stimulated for PS exposure with A23187. RBCs are treated with 2 μM A23187 in the presence of 2 mM Ca^{2+} at 37°C for 30 min. The Ca^{2+} content is determined by using fluo-4 at 488 nm, the PS exposure is determined by using annexin V alexa at 568 nm. Upper row: Ca^{2+} : channel 1, green signal (488 nm), PS: channel 2, red signal (543 nm), Ca^{2+}/PS : double scan channel 1 and 2. Lower row: magnification of square marked area. White arrows: cells showing both fluo-4 fluorescence intensity and PS exposure. Yellow arrows: cells showing fluo-4 fluorescence but no PS exposure.

In case of LPA treatments, the statistical data of the images indicate more than 60% of RBCs showing PS exposure. In which, there are some RBCs showing high fluo-4 fluorescence intensity but no PS exposure or vice versa (Fig. 57).

The relation of Ca^{2+} content and PS exposure for PMA treated RBCs was also investigated. In the absence of Ca^{2+} after treating 30 min, there are about 40% of cells showing PS exposure although the intracellular Ca^{2+} content in these cells is very low (Fig. 58). The results are agreement with the analysis data in FACS measurements (Figs. 35, 39).

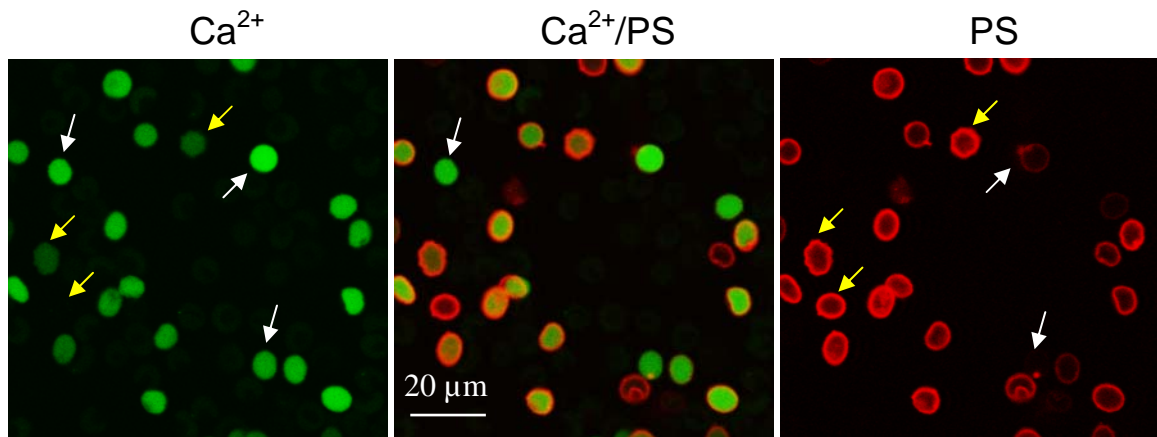


Fig. 57: Double labelled human RBCs with fluo-4 and annexin V-alexa 568 after being stimulated for PS exposure with LPA. RBCs are treated with 2.5 μM LPA in the presence of 2 mM Ca^{2+} at 37°C for 30 min. Ca^{2+} : channel 1, green signal (488 nm), PS: channel 2, red signal (543 nm), Ca^{2+}/PS : double scan channel 1 and 2. White arrows: cells showing fluo-4 signal but no or very less PS exposure. Yellow arrows: cells showing low or no fluo-4 signal but PS exposure. Most cells show both green and red signal.

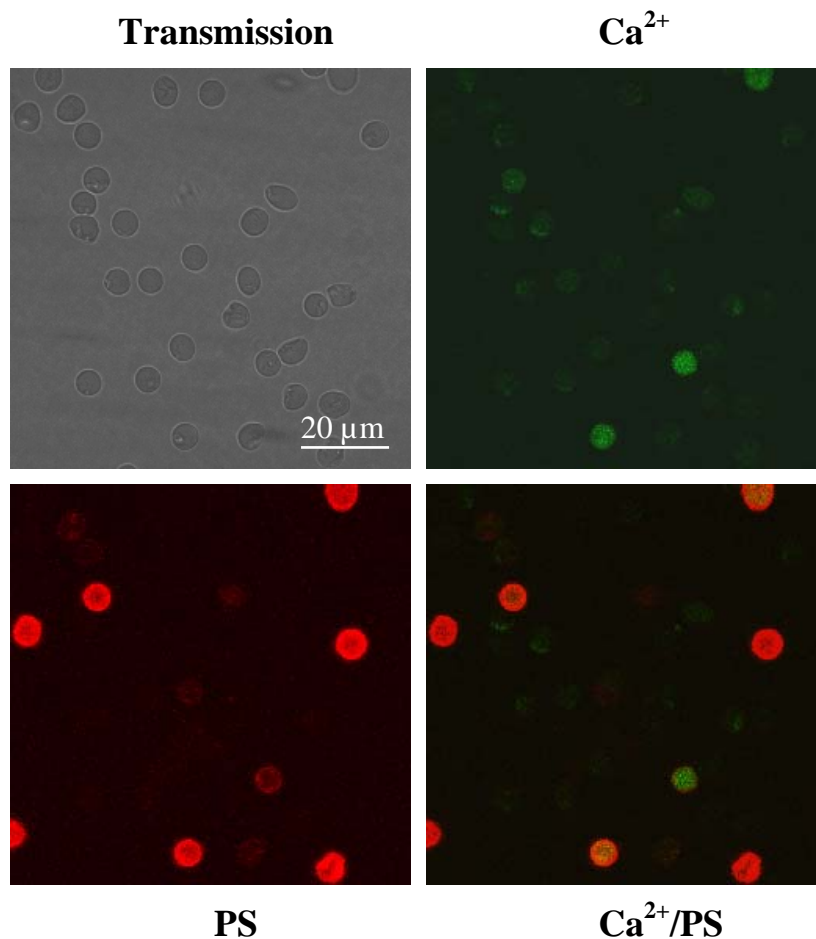


Fig. 58: Double labelled human RBCs with fluo-4 and annexin V-alexa 568 after being stimulated for PS exposure with 6 μM PMA in the absence of Ca^{2+} . Upper left: Light transmission; Upper right, Ca^{2+} : channel 1 (488 nm), green signal; Lower left (PS): channel 2 (543 nm), red signal. Lower right (Ca^{2+}/PS): double scan channel 1 and 2.

In the presence of 2 mM extracellular Ca^{2+} , the number of RBCs showing PS exposure after PMA treatment increases up to more than 80%. Both RBCs with high and low fluo-4 fluorescence show PS exposure (Fig. 59). It means that the increase of intracellular Ca^{2+} enhances the number of cells showing PS exposure (in comparison to the experiments without Ca^{2+}). These results are agreement with other experiments done with normal fluorescence microscope and flow cytometer.

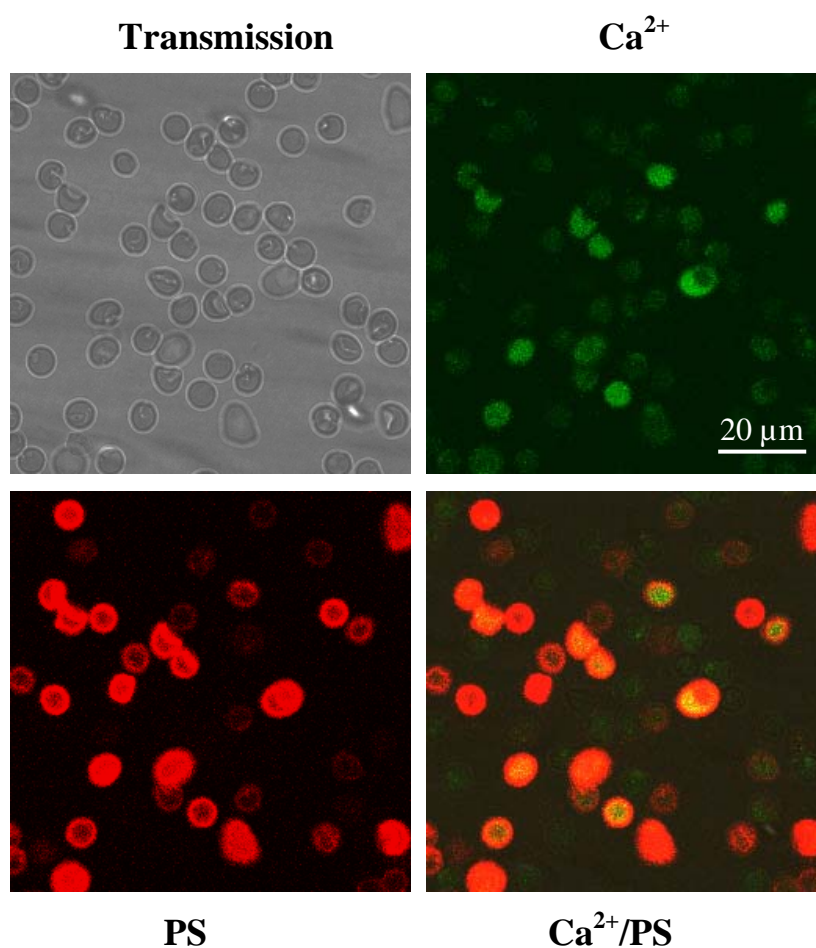


Fig. 59: Double labelled human RBCs with fluo-4 and annexin V-alexa 568 after being stimulated for PS exposure with 6 μM PMA in the presence of 2 mM Ca^{2+} . Upper left: light transmission; upper right (Ca^{2+}): channel 1 (488 nm), green signal; lower left (PS): channel 2 (543 nm), red signal; lower right (Ca^{2+} /PS): double scan channel 1 and 2.

4.2.6. Phosphatidylserine exposure in sheep red blood cells

Sheep RBCs were also investigated under conditions stimulating for PS exposure. Interestingly, when A23187 was applied, almost all cells reacted and showed high signals of fluo-4. However, only a few cells or even no cell showing PS exposure could be observed (Fig. 60, upper row). This phenomenon also happened under conditions

stimulating for PS exposure by PMA (data not shown). In case of LPA treatment, there were less than 10% of cells showing PS exposure (Fig. 60, lower row).

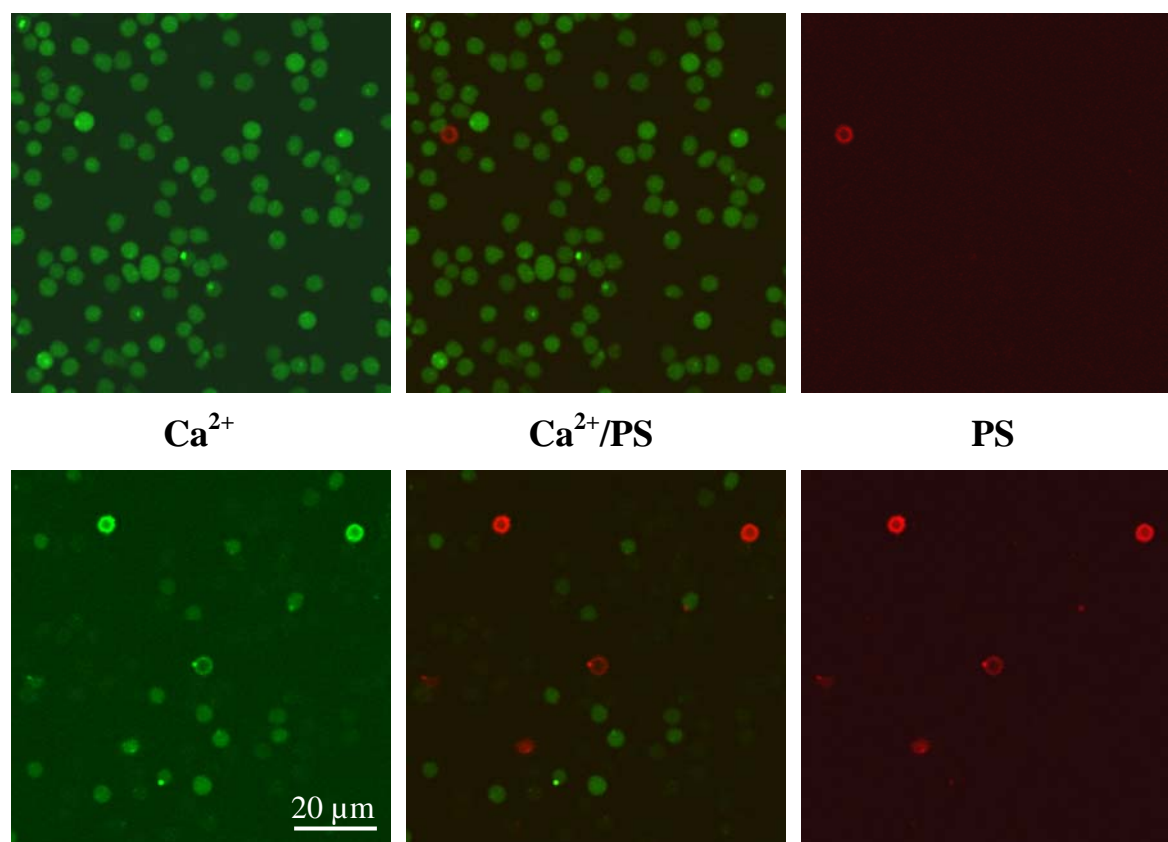


Fig. 60: Double labelled sheep RBCs with fluo-4 and annexin V-alexa 568 after being stimulated for PS exposure with A23187 or LPA. Upper row: Sheep RBCs treated with 2 μM A23187 in the presence of 2 mM extracellular Ca²⁺ for 30 min at 37°C. Lower row: Sheep RBCs treated with 2.5 μM LPA in the presence of 2 mM extracellular Ca²⁺ for 30 min at 37°C. Ca²⁺: channel 1(488 nm), green signal; PS: channel 2 (543 nm) red signal; Ca²⁺/PS: double scan channel 1 and 2.

4.3. Adhesion of phosphatidylserine exposed red blood cells

4.3.1. Determination of fibrinogen concentration in washed cell suspensions

Fibrinogen is converted into fibrin by the activation of thrombin. Together with platelets, fibrin is involved in the clotting of blood when it is polymerized to form a network of fibrins. Regarding the traditional opinion, the RBCs are “trapped” by this network and therefore they prevent bleeding. According to this opinion, it seems that RBCs play a passive role in blood clot formation only. However, experiment data shows that the RBCs

showing PS exposure on outer leaflet of the membrane can adhere together in the absence or at a very low concentration of fibrin (see Fig. 63). The concentration of remaining fibrinogen or fibrin in washed RBCs is determined (see Materials and Methods). Fig. 61 shows the calibration curve of fibrinogen. Fig. 62 shows the results of the determined fibrinogen concentration of washed blood.

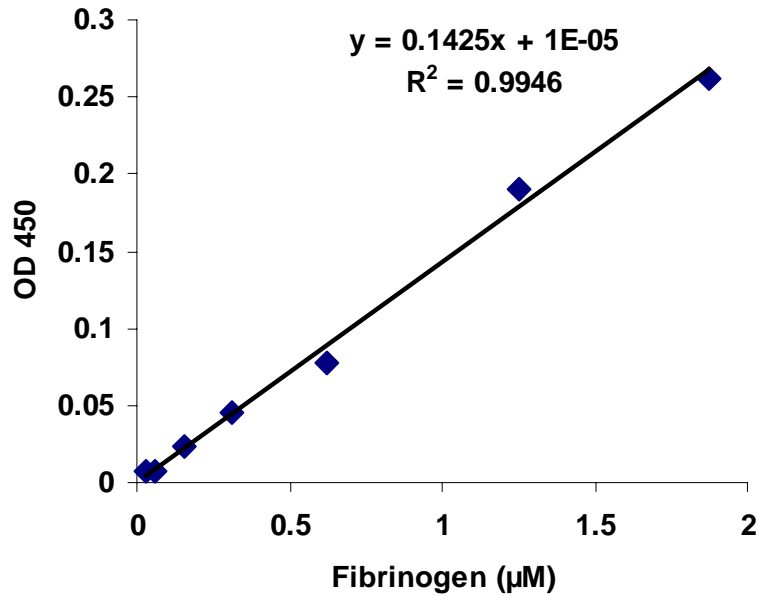


Fig. 61: The calibration curve of fibrinogen.

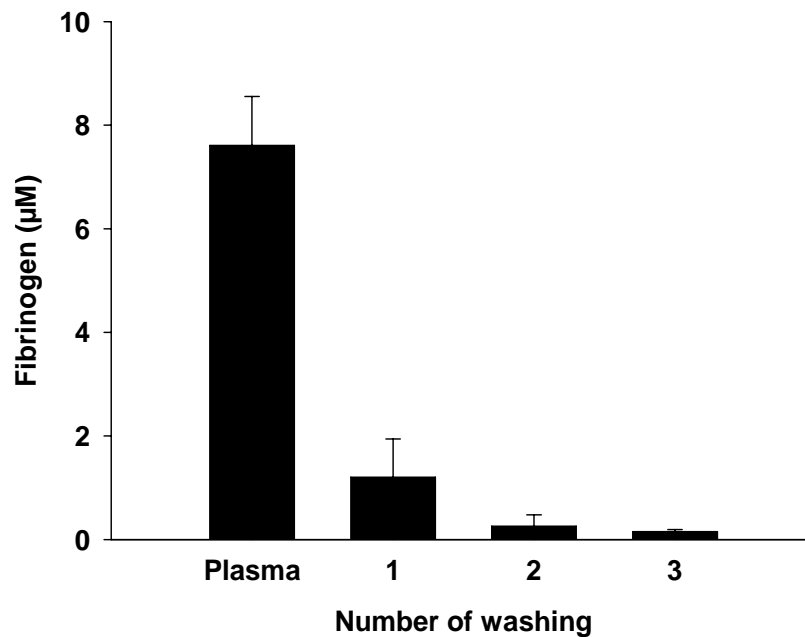


Fig. 62: Fibrinogen concentration in washed RBCs. Bars show mean value of 3 different experiments with 3 different blood samples. Error bars represent S.D.

Based on the calibration curve, the fibrinogen concentration in the third washing of RBCs is less than 0.15 μM . In our experiments, the haematocrit is approximately 0.1%, therefore the final concentration of fibrinogen in the experiment suspension is less than 0.15 nM. In average, the molecular weight of fibrinogen is about 340 kDa and therefore the amount of fibrinogen is less than 4.41×10^{-7} g/l. Such amount is not sufficient to be polymerized even in the presence of thrombin.

4.3.2. Adhesion of red blood cells

Human RBCs

As described (see Materials and Methods), after being stimulated for PS exposure by 2.5 μM LPA, 2 μM A23187 or 6 μM PMA in the presence of 2 mM Ca^{2+} for 30 min at 37°C, RBCs were fixed by glutaraldehyde and put on glass slides. Under bright field microscope, it is very clear to see that the shapes of RBCs are different among the experiment and control samples. Cell shrinkage, membrane blebbing, and microvesicle formation are also observed (Fig. 63). It is interesting that only RBCs treated with LPA, A23187 or PMA were stuck together or formed structures like clots or strings (roulaux). There was no adhesion of cells in the control samples. It is necessary to notice that the adhesion of PS exposed RBCs occurs in the absence of fibrinogen or fibrin. It would suggest that PS is involved in the adhesion process.

There are many possible questions for these observations such as why the RBCs showing PS exposure adhere together. How strong is the adhesion force among the cells? Is it strong enough to overcome the forces occurring during the vortex procedure when the cells were washed? Or, what is the basis of the adhesion force and which molecules are involved in these processes?

The surface structures of RBCs showing PS exposure were also investigated by using AFM. Fig. 64 shows both height mode and phase mode of RBCs treated with 2 μM A23187 for 30 min in the presence of 2 mM extracellular Ca^{2+} . It is evident to see the reduction of cell volume, membrane blebbing and vesicle formation in scanned cells. The adhesion area of two cells is also scanned (Fig. 64).

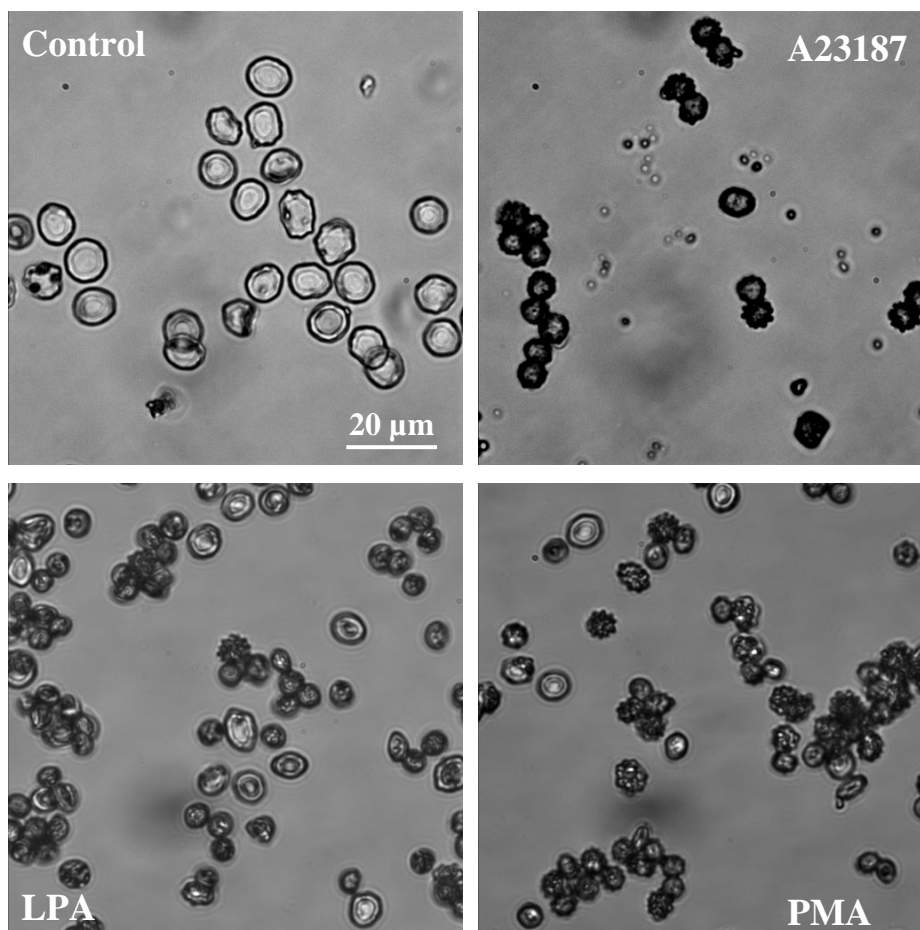


Fig. 63: Adhesion of human RBCs. Human RBCs are stimulated for PS exposure by 2 μM A23187 or 2.5 μM LPA or 6 μM PMA in the presence of 2 mM extracellular Ca^{2+} for 30 min at 37°C. The cells were fixed in physiological solution containing 1% glutaraldehyde.

Sheep RBCs

Under the same conditions applied for human RBCs, sheep RBCs also adhere together after treatment with 2.5 μM LPA, 2 μM A231857 or 6 μM PMA in the presence of 2 mM extracellular Ca^{2+} for 30 min at 37°C. The images of sheep RBC adhesion are shown in Fig. 65. In case of LPA, the number of sheep RBCs showing PS exposure was shown less than 10% (see Fig. 60). Therefore, the adhesion of sheep RBCs can be supposed to be the same as in case of human RBCs when they are treated by LPA. Interestingly and surprisingly, in the cases of A23187 or PMA treatments although the number of cells showing PS exposure is very low or even no PS exposure (Fig. 60, upper row) but they are still adhere together (similar to LPA treatment) (Fig. 65). There are some open questions for this phenomenon such as how much PS exposure on the outer leaflet of the membrane

is sufficient for the adhesion? Does the adhesion depend only on the PS exposure or depend on other unknown factor(s)?

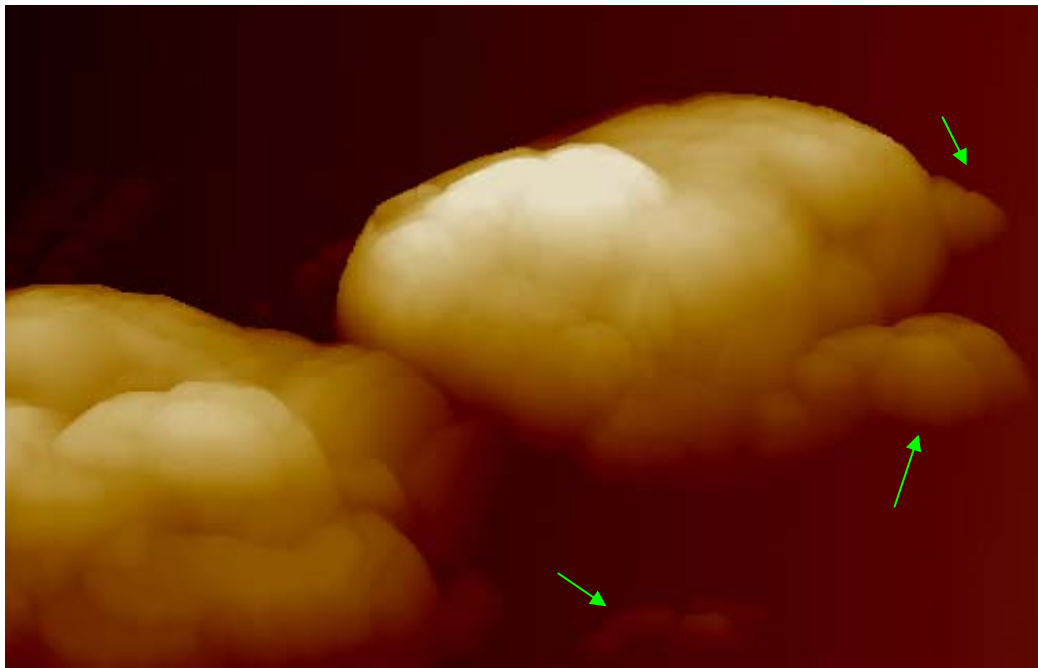
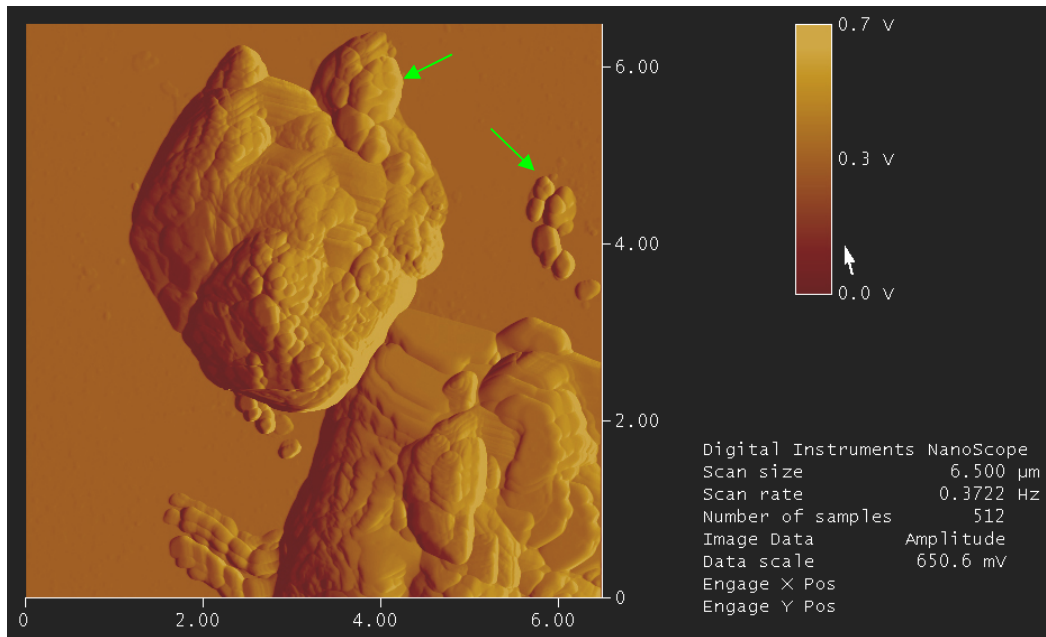


Fig. 64: AFM scanning image of human RBCs treated with 2 μM A23187 in the presence of 2 mM extracellular Ca^{2+} for 30 min. The cells were fixed in physiological solution containing 1% glutaraldehyde. Upper: top view of the amplitude mode, scan size 6.5 μm , lower: the adhesion area of two RBCs (topography of the adhesion area). The blue arrows show membrane blebbing and vesicles.

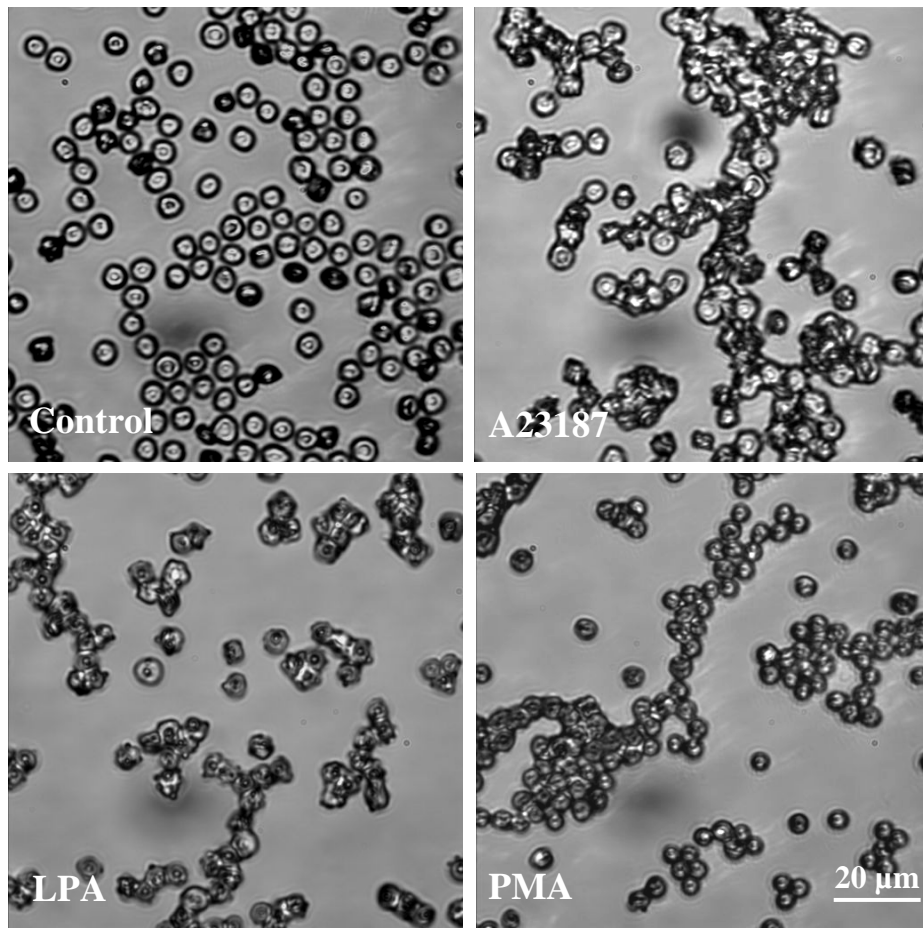


Fig. 65: Adhesion of sheep RBCs. Sheep RBCs are stimulated for PS exposure by 2 μM A23187 or 2.5 μM LPA or 6 μM PMA in the presence of 2 mM extracellular Ca^{2+} for 30 min at 37°C. The cells were fixed in physiological solution containing 1% glutaraldehyde.

4.4. Detection of scramblase in red blood cells

4.4.1. Alignment of amino acid sequences of scramblases in human red blood cells

So far, at least 5 isoforms of phospholipid scramblase (PLSCR) from different human tissues have been discovered [74]. The isoform 5 was identified in 2003 by Strausberg et al. [75]. The amino acid sequences of these isoforms were aligned by ClustalX (Fig. 66).

In humans, hPLSCRs constitute a family of 5 homologous proteins which are named as hPLSCR1 - hPLSCR5 [74]. The predicted open reading frames of hPLSCR2 (224 aa), hPLSCR3 (295 aa) and hPLSCR4 (329 aa) show 74%, 52% and 47% homology, respectively, to hPLSCR1 (Table 3). There are 5 highly conserved regions in all hPLSCRs (Fig. 66): the DNA binding motif comprises residues M⁸⁶-E¹¹⁸, the nuclear localization signal (NLS) motif, the cysteine-palmitoylation motif, the Ca²⁺ binding motif, and the transmembrane domain [210].

4.4.2. BLAST analysis of phospholipid scramblases

Comparison of the amino acid sequences of hPLSCRs with the protein databases was done online by using Basic Local Alignment Search Tool for protein (BLASTp). 5 amino acid sequences of 5 hPLSCRs were used as query sequences against the protein database. The results are summarized in tables 3, 4, 5, 6, and 7. In each table, the species showing high identity with the query sequence are shown together with their proteins and their sequence length. The identity of amino acid sequences of the species is displayed in percent. The score is an indication representing how good the alignment is. Therefore, the higher score shows the better alignment. The expect value (E value) is an indication of the statistical significance of a given pairwise alignment and reflects the size of the database and the scoring system used. The lower the E value shows the more significant the hit is [186, 187]. The accession numbers of the sequences in protein database are also listed in the tables.

The analysis results from tables 3-7 show that PLSCRs are present in a large variety of species. The hPLSCRs have the highest identities with the PLSCRs of monkey (*P. troglodytes*, *M. mulatta*), cow (*B. taurus*), horse (*E. caballus*), mouse and rat (*M. musculus*, *R. norvegicus*), dog (*C. familiaris*) and frog (*X. laevis*). It should be noted that species belonging to monkey, cow, horse, rat, and mouse families also have 5 isoforms of PLSCRs.

Table 3: BLAST analysis of the hPLSCR1 against the protein database.

Species	Protein	Sequence length	Identities (%)	Score (bits)	Expect value	Gap (%)	Accession number
<i>Pan troglodytes</i>	PLSCR 1	311	100	637	0.0	0	XP_001135562
<i>Macaca mulatta</i>	PLSCR 1	318	97	583	1e-164	0	XP_001111222
<i>Bos taurus</i>	PLSCR 1	293	75	486	1e-135	6	NP_001029608
<i>Equus caballus</i>	PLSCR 1	336	67	450	8e-125	11	XP_001492359
<i>Rattus norvegicus</i>	PLSCR 1	335	76	447	6e-124	6	NP_476542
<i>Canis familiaris</i>	PLSCR 1	356	72	447	6e-124	10	XP_854267
<i>Mus musculus</i>	PLSCR 1	327	74	434	6e-120	2	AAH02017
<i>Xenopus laevis</i>	PLSCR 2	354	63	385	1e-94	4	NP_001090508
<i>Homo sapiens</i>	PLSCR 2	317	74	362	3e-98	2	AAH55415
<i>Homo sapiens</i>	PLSCR 5	271	59	308	4e-82	2	NP_001078889
<i>Homo sapiens</i>	PLSCR 3	295	52	281	6e-74	5	BAG37205
<i>Homo sapiens</i>	PLSCR 4	329	47	259	3e-67	6	AAF89960.1

Table 4: BLAST analysis of the hPLSCR2 against the protein database.

Species	Protein	Sequence length	Identities (%)	Score (bits)	Expect value	Gap (%)	Accession number
<i>Pan troglodytes</i>	PLSCR 2	309	98	460	6e-128	0	XP_516803
<i>Macaca mulatta</i>	PLSCR 2	300	96	390	8e-107	0	XP_001111255
<i>Bos taurus</i>	PLSCR 1	293	79	383	6e-105	0	NP_001029608
<i>Homo sapiens</i>	PLSCR 1	318	84	375	1e-102	0	NP_066928
<i>Mus musculus</i>	PLSCR 1	328	79	362	1e-98	0	BAB22897
<i>Rattus norvegicus</i>	PLSCR 1	335	79	360	6e-98	0	NP_476542
<i>Equus caballus</i>	PLSCR 1	336	73	353	6e-96	0	XP_001492359
<i>Mus musculus</i>	PLSCR 2	307	72	350	6e-95	0	AAH02012
<i>Canis familiaris</i>	PLSCR 1	356	80	337	7e-91	0	XP_854267
<i>Gallus gallus</i>	PLSCR 1	305	74	335	2e-90	0	XP_001231237
<i>Xenopus laevis</i>	PLSCR 2	354	66	333	7e-90	0	NP_001090508
<i>Homo sapiens</i>	PLSCR 5	271	62	296	1e-78	0	NP_001078889
<i>Homo sapiens</i>	PLSCR 3	295	52	259	1e-67	0	BAG37205

Table 5: BLAST analysis of the hPLSCR3 against the protein database.

Species	Protein	Sequence length	Identities (%)	Score (bits)	Expect value	Gap (%)	Accession number
<i>Pan troglodytes</i>	PLSCR 3	473	99	592	1e-167	0	XP_001174792
<i>Macaca mulatta</i>	PLSCR 3	295	98	588	2e-166	0	XP_001118026
<i>Bos taurus</i>	PLSCR 3	303	92	522	2e-146	0	NP_001039518
<i>Equus caballus</i>	PLSCR 3	337	91	516	1e-144	0	XP_001503118
<i>Mus musculus</i>	PLSCR 3	296	93	505	2e-141	0	NP_076053
<i>Rattus norvegicus</i>	PLSCR 3	335	92	481	3e-134	0	NP_001012139
<i>Canis familiaris</i>	PLSCR 3	239	94	433	9e-120	0	XP_546589
<i>Xenopus laevis</i>	PLSCR 2	354	53	293	2e-77	5	NP_001090508
<i>Homo sapiens</i>	PLSCR 1	318	50	266	2e-69	8	NP_066928
<i>Homo sapiens</i>	PLSCR 5	271	50	249	3e-64	0	NP_001078889

Table 6: BLAST analysis of the hPLSCR4 against the protein database.

Species	Protein	Sequence length	Identities (%)	Score (bits)	Expect value	Gap (%)	Accession number
<i>Macaca mulatta</i>	PLSCR 4	329	96	642	0	0	XP_001111439
<i>Pongo abelii</i>	PLSCR 4	329	97	621	3e-176	0	NP_001153278
<i>Pan troglodytes</i>	PLSCR 4	473	99	592	1e-167	0	XP_001174792
<i>Bos taurus</i>	PLSCR 4	333	81	564	9e-154	0	NP_001075201
<i>Canis familiaris</i>	PLSCR 4	477	84	530	6e-149	0	XP_854260
<i>Mus musculus</i>	PLSCR 4	326	79	528	4e-148	1	NP_848826
<i>Rattus norvegicus</i>	PLSCR 4	326	79	514	6e-144	1	NP_001012000
<i>Equus caballus</i>	PLSCR 4	471	88	503	2e-140	0	XP_001917611
<i>Rattus norvegicus</i>	PLSCR 2	311	47	271	5e-71	7	NP_001014116
<i>Bos taurus</i>	PLSCR 1	293	48	265	4e-69	10	NP_001029608
<i>Mus musculus</i>	PLSCR 2	307	47	263	2e-68	7	Q9DCW2
<i>Homo sapiens</i>	PLSCR 1	318	47	259	3e-67	6	NP_066928
<i>Homo sapiens</i>	PLSCR 5	271	43	208	8e-52	6	NP_001078889
<i>Homo sapiens</i>	PLSCR 3	295	40	198	5e-49	5	BAG37205

Table 7: BLAST analysis of the hPLSCR5 against the protein database.

Species	Protein	Sequence length	Identities (%)	Score (bits)	Expect value	Gap (%)	Accession number
<i>Pan troglodytes</i>	PLSCR 5	271	96	542	1e-152	0	XP_516805
<i>Mus musculus</i>	PLSCR 5	274	87	489	9e-137	1	XP_287936
<i>Equus caballus</i>	PLSCR 5	471	88	488	3e-136	2	XP_001492341
<i>Bos taurus</i>	PLSCR 5	270	81	411	3e-113	3	XP_599511
<i>Canis familiaris</i>	PLSCR 5	477	84	530	6e-149	0	XP_854280
<i>Rattus norvegicus</i>	PLSCR 1	318	79	388	3e-106	0	NP_001012000
<i>Rattus norvegicus</i>	PLSCR 2	222	90	388	3e-106	0	XP_001067563
<i>Bos taurus</i>	PLSCR 1	293	57	308	4e-82	1	NP_001029608
<i>Xenopus laevis</i>	PLSCR 2	354	55	298	4e-79	3	NP_001090508
<i>Homo sapiens</i>	PLSCR 2	317	54	256	1e-66	3	AAH55415
<i>Homo sapiens</i>	PLSCR 3	295	48	249	2e-64	2	NP_065093

Based on the alignment of their amino acid sequences, the phylogenetic relationship of some PLSCRs in different species was analysed (Fig. 67). Multi sequence alignment was done by using ClustalX version 2.0.11. The dendrogram (phylogram) are plotted by using Treeview version 4.5 (see Materials and Methods).

The results from Fig. 67 indicate that the isoforms of PLSCRs are located in groups. For example, PLSCR1 from human is located within a group including PLSCR1 isoforms of monkey (*M. mulatta*), chimpanzee (*P. troglodytes*). This group is very close to the group including PLSCR1 isoforms of cow (*B. taurus*), dog (*C. familiaris*) horse (*E. caballus*), rat (*R. norvegicus*), and mouse (*M. musculus*).

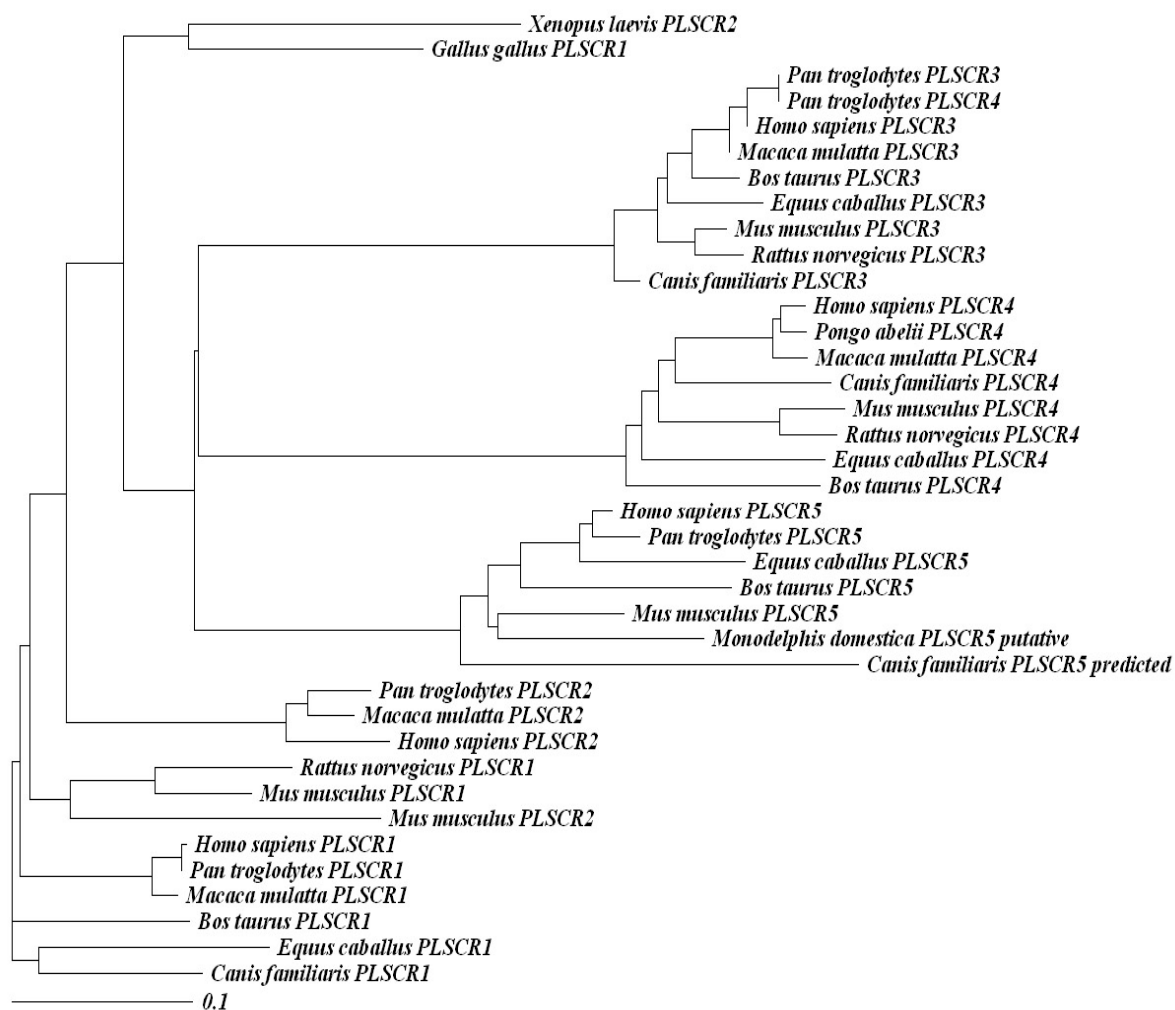


Fig. 67: Phylogram of the phospholipid scramblase family in some animals.

4.4.3. Detection of scramblases using Western blot analysis

The main purpose of the experiment is to screen for the presence of PLSCRs in sheep RBCs because so far no publication has mentioned the presence of these proteins in sheep. In addition, BLAST analysis of human PLSCR1 and PLSCR3 against sheep-specific protein database show no significant similarity. Therefore, the existence of PLSCR in sheep is still a question, especially in sheep RBCs. The results from PS exposure experiments with sheep RBCs (see Fig. 60) raise a question whether PLSCR(s) exist or not. In the frame of the thesis, only two isoforms PLSCR1 and PLSCR3 were used to screen. The reasons are: in 5 isoforms of scramblases have been identified in human, the expression of hPLSCR2 is restricted to testis, the hPLSCR4 has not been detected in

peripheral blood lymphocytes, and the antibody against scramblase 5 is not available at the moment.

The antibodies raised against human PLSCR1 and PLSCR3 were used to screen the PLSCR1 and PLSCR3 in different species. Therefore, analysis the identity of the amino acid sequences of PLSCR1 and PLSCR3 in these species is necessary.

Alignments of amino acid sequences of PLSCR1 among human, cow, rat, and mouse are shown in Figs. 68. There is a high identity of amino acid sequences at the C-terminus of PLSCR1 in analysed species. However, the identity at N-terminus is very low.

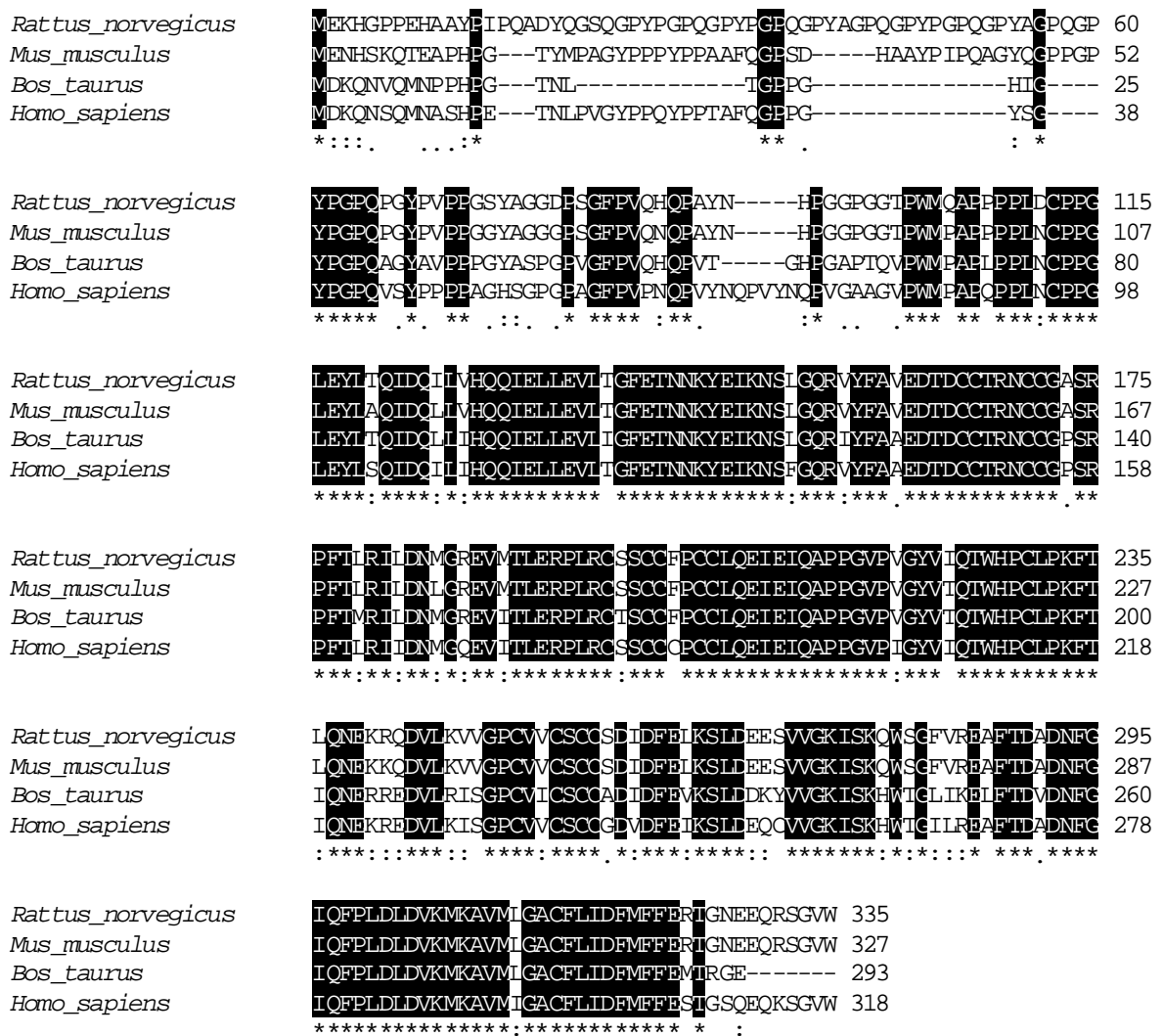


Fig. 68: Alignment of amino acid sequences of PLSCR1 in different species. (*) amino acids are identical in all sequences in the alignment, (:) conserved substitutions, (.) semi-conserved substitutions. The amino acid sequences of PLSCR1 from *Rattus norvegicus* (rat), *Mus musculus* (mouse), *Bos taurus* (cow), and *Homo sapien* (human) were taken from protein database under accession numbers NP_476542, AAH02017, NP_001029608, and NP_066928, respectively.

analysed species, antibody against human PLSCR1 did not react with mouse, rat, cow, and sheep RBC ghost membrane proteins (Fig. 70, data from cow not shown). The reason for the non-reaction of the antibody with other ghost membrane proteins from other species may be due to the low identity of amino acid sequences at the N-terminus of the proteins (see Fig. 68). In addition, the antibody used to screen PLSCR1 is a monoclonal antibody, so it is possible that the epitope necessary for the recognition of the antibody is not present in the PLSCR1 of mouse, rat, sheep, and cow. Therefore, the monoclonal antibody raised against PLSCR1 from the clone 1E9 (see Materials and Methods) is not suitable for screening the PLSCR1 of other species. Further investigations for the presence of PLSCR1 in sheep RBCs are required.

The antibody against PLSCR3 reacts with all ghost proteins from human, mouse, rat and cow (data with cow RBCs not shown). Fig. 70 shows a clear band at 58.56 kDa indicating that the presence of PLSCR3 can be observed. The results from Western blot analysis suggest that the scramblase isoform 3 is present in sheep RBCs. However, the activity of this enzyme as well the condition for the activation of the enzyme is not investigated.

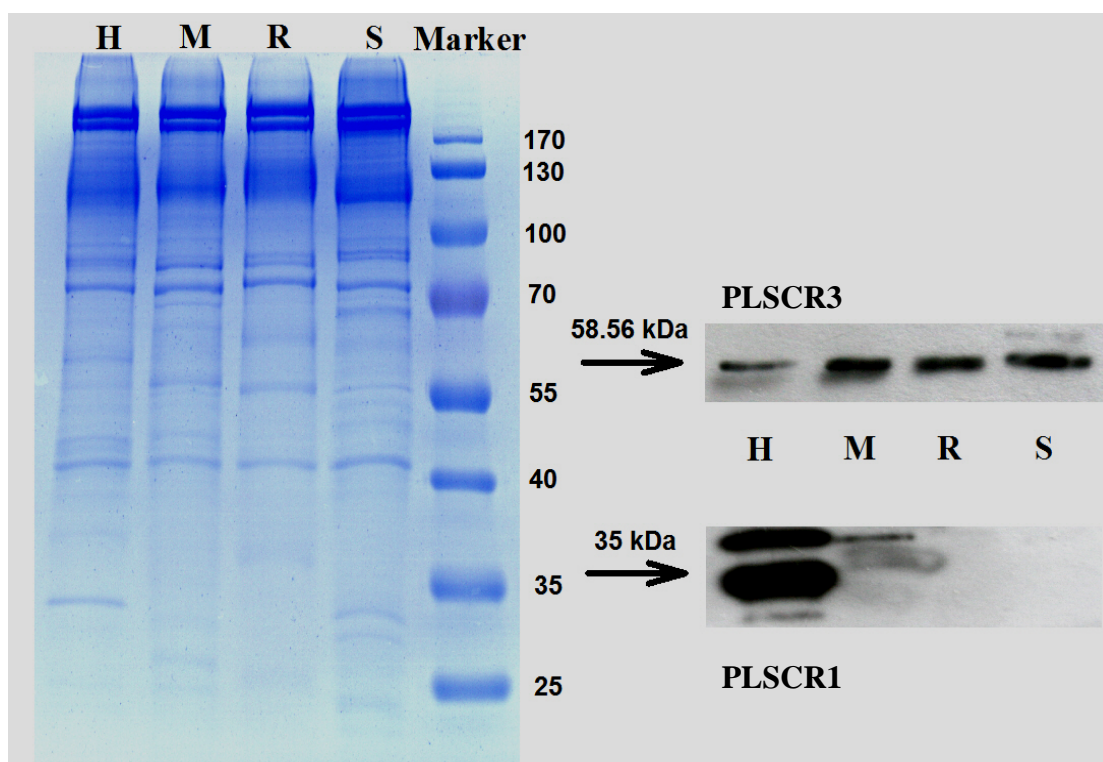


Fig. 70: SDS-PAGE and Western blot analysis of PLSCR1 and PLSCR3. Left: SDS-PAGE analysis of ghost membrane proteins of human (H), mouse (M), rat (R) and sheep (S). Upper right: Western blot analysis of PLSCR3, Lower right: Western blot analysis of PLSCR1.

4.5. Young and old red blood cells

4.5.1. Separation of red blood cells into young and old cell fractions

Fig. 71 shows a typical image of a centrifuge tube after centrifugation of RBCs in a Percoll gradient. Fraction 1 and 5 contain the youngest and oldest cells, respectively. Other fractions contain cells at various ages.

The proteins from fractions were isolated from ghost cell membranes. According to Lutz et al. [188] the ratio of band 4.1a/4.1b was used to distinguish the young and old cells. Young cells contain more band 4.1a, old cells contain more band 4.1b.

On SDS-PAGE, human RBC protein 4.1 can be resolved into the two polypeptides 4.1a and 4.1b which differ by 2 kDa in the C-terminal domain [189]. According to Inaba et al. [189], the molecular weights of band 4.1a and 4.1b are 81 and 79 kDa, respectively.

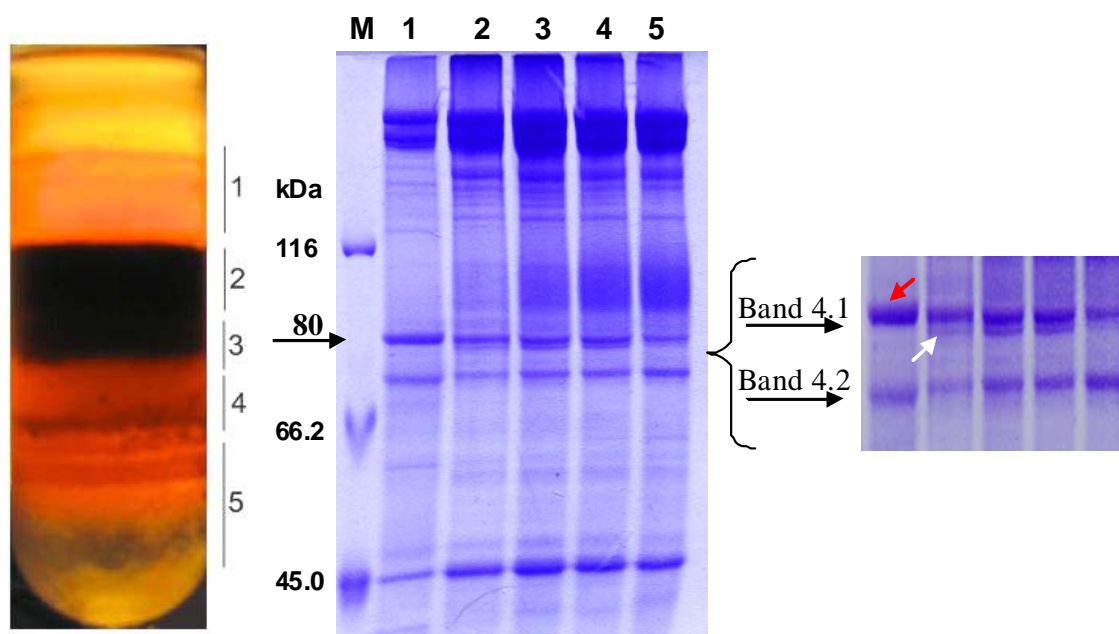


Fig. 71: Separation of RBCs by Percoll gradient ultracentrifugation and SDS-PAGE of ghost membrane proteins of the different fractions (1-5). Left: A typical image of the centrifuge with 5 fractions containing cells at different age from 1-5: from the lightest to the heaviest cells (the youngest and the oldest cells). Middle: SDS-PAGE of proteins isolated from ghost cell membranes of different fractions. Right: A section of SDS-PAGE containing band 4.1a and 4.1b. The red arrow indicates band 4.1a, the white arrow indicates band 4.1b.

4.5.2. Determination of reticulocytes in fractions of different cell age

The lightest fraction contains the youngest RBCs and a certain amount of immature RBCs. The immature RBCs contain fragments of RNA; the thiazole orange reagent will react with RNA molecules to form a complex of the RNA/thiazole orange, which can be analysed by FACS.

The amount of reticulocytes in different fractions was determined. Fraction 1 contains more reticulocytes than the other fractions ($0.93 \pm 0.53\%$), fractions 4 and 5 have a very less amount of reticulocyte (0.26 ± 0.14) (Fig. 71). These results suggest that centrifugation RBCs using Percoll gradient is a reliable method to separate RBCs depending on their density.

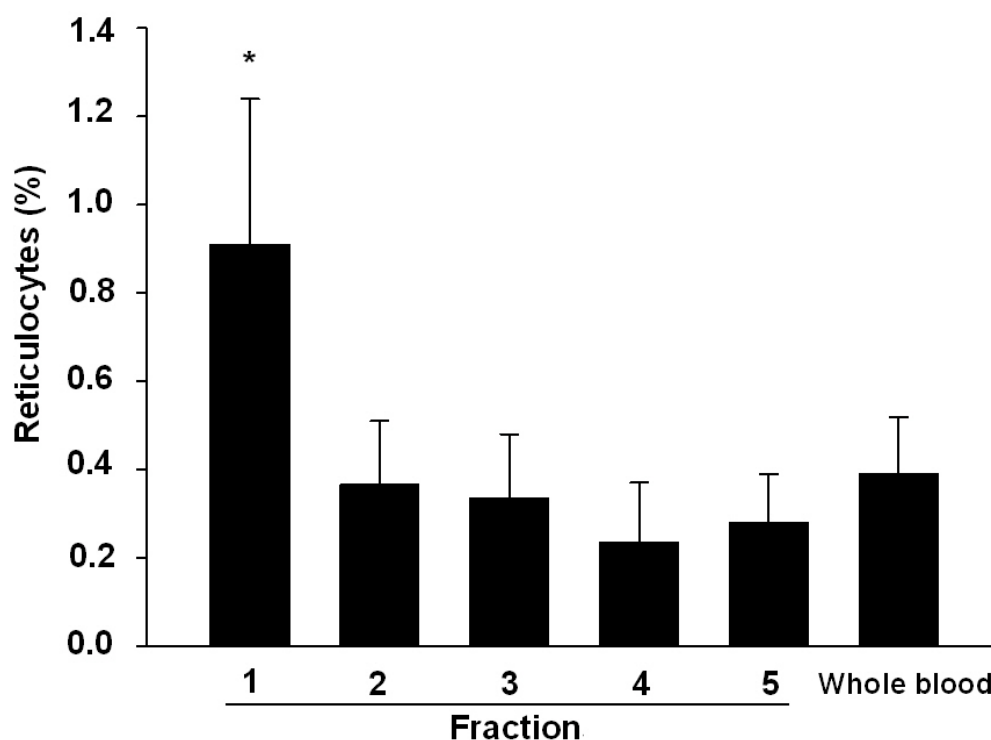


Fig. 72: Reticulocyte content (in percent) in different fraction of RBCs separated using a Percoll gradient. Bars show mean value of 3 different blood samples (data analysis of 100.000 cells of each blood sample). Error bars represent S.D. Fraction 1 contains the youngest cells; fraction 5 contains the oldest cells. Whole blood: washed RBCs before being separated into fractions. (*) T-test showed a statistically significant difference ($P < 0.05$) among fraction 1 and all others. There is no significant different among fraction 2, 3, 4, 5, and whole blood.

4.5.3. Investigation of the relative volume of young and old red blood cells

Another factor related to young and old RBCs is the size of the cell. In principle, the size of the young RBCs is larger than of the old ones. The FSC value is an important parameter reflecting the size of the cells. Analysis of the mean value of FSC (in FACS measurement) of the fractions shows that RBCs is decreasing from fraction 1 to fraction 5 (Fig. 73). This result confirms that young and old RBCs are present mostly in fraction 1 and 5, respectively.

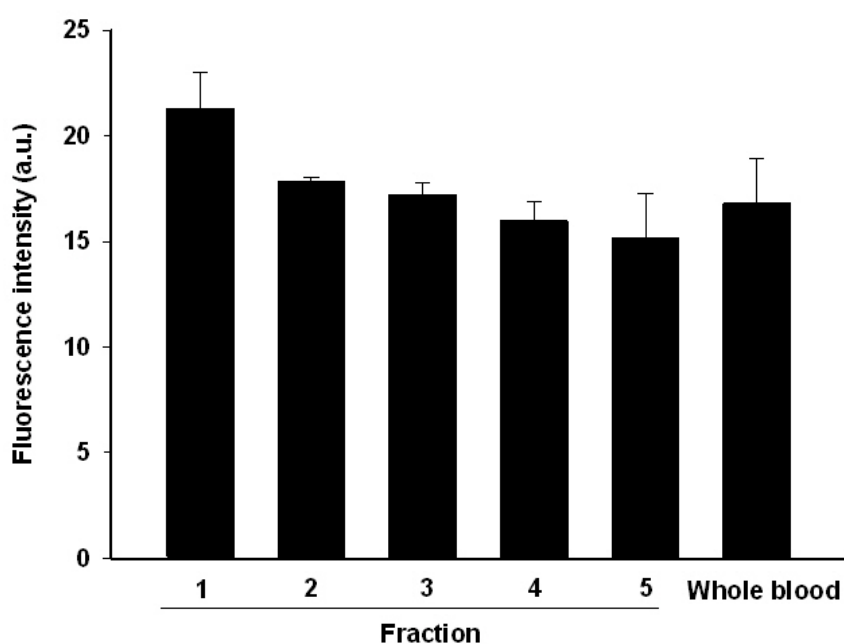


Fig. 73: Relative cell volume of RBCs in different fractions. Bars show mean value of 3 different blood samples (30.000 cells of each blood sample were analysed). Fraction 1 contains the youngest cells; fraction 5 contains the oldest cells. Whole blood: washed RBCs before being separated into fractions. Error bars represent S.D.

4.5.4. Determination of Ca^{2+} content in young and old red blood cells

The leukocyte free RBCs were separated into different fractions by Percoll density centrifugation (see Material and Methods). The RBCs taken from different fractions were loaded with fluo-4 and analysed by flow cytometry and fluorescence microscopy. It seems very interesting that the Ca^{2+} content of RBCs in fraction 1 is the highest (Fig. 74). The Ca^{2+} content is slightly reduced in fractions 2, 3, 4 and lowest in fraction 5. This finding is

not in agreement with some previous reports showing that the old RBCs contain more Ca^{2+} than the young cells [158, 190]. However, the Ca^{2+} content in RBCs taken from fractions, which are separated directly from washed RBCs (without filter to remove leukocyte) is not significantly different (data not shown). This result could be due to enhance of membrane permeability for Ca^{2+} under shear stress condition of filtration (the interaction of cells with the filter pore).

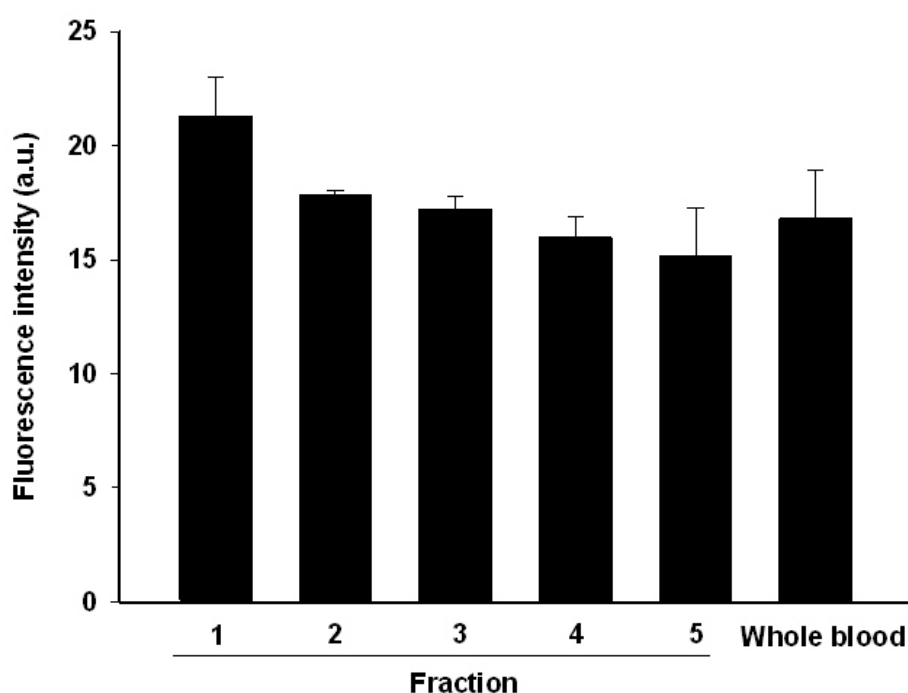


Fig. 74: Fluorescence intensity of fluo-4 in different fractions. Bars show mean value of 3 different blood samples (30,000 cells of each blood sample were analysed). Fraction 1 contains the youngest cells; fraction 5 contains the oldest cells. Whole blood: The leukocyte free RBCs before being separated into fractions. Error bars represent S.D. One way ANOVA test showed that there is a significant difference ($P < 0.05$) among the fractions. T-test showed that there is a significant difference among fraction 1 and all others. There is no significant difference among fractions 2, 3, 4, 5 and whole blood.

4.5.5. Phosphatidylserine exposure of young and old red blood cells

To investigate the PS exposure of RBCs taken from different fractions, the cells are incubated with annexin V-FITC. The result shows that the number of cells showing PS exposure are highest in fraction 1 followed by fraction 5 and 4, while RBCs in fraction 3 and 2 (middle aged cells) show lowest PS exposure (Fig. 75).

Under normal condition, the number of cells showing PS exposure is less than 0.3% (cp. Figs. 36 and 37). However, under conditions used to separate cells by age, i.e. filtering to remove leukocytes, the percentage of cells showing PS exposure in the whole blood as well as in different fractions is higher. This could be due to the shear forces applied when the RBCs were filtered. It may suggest that the youngest and oldest cells are more stress sensitive.

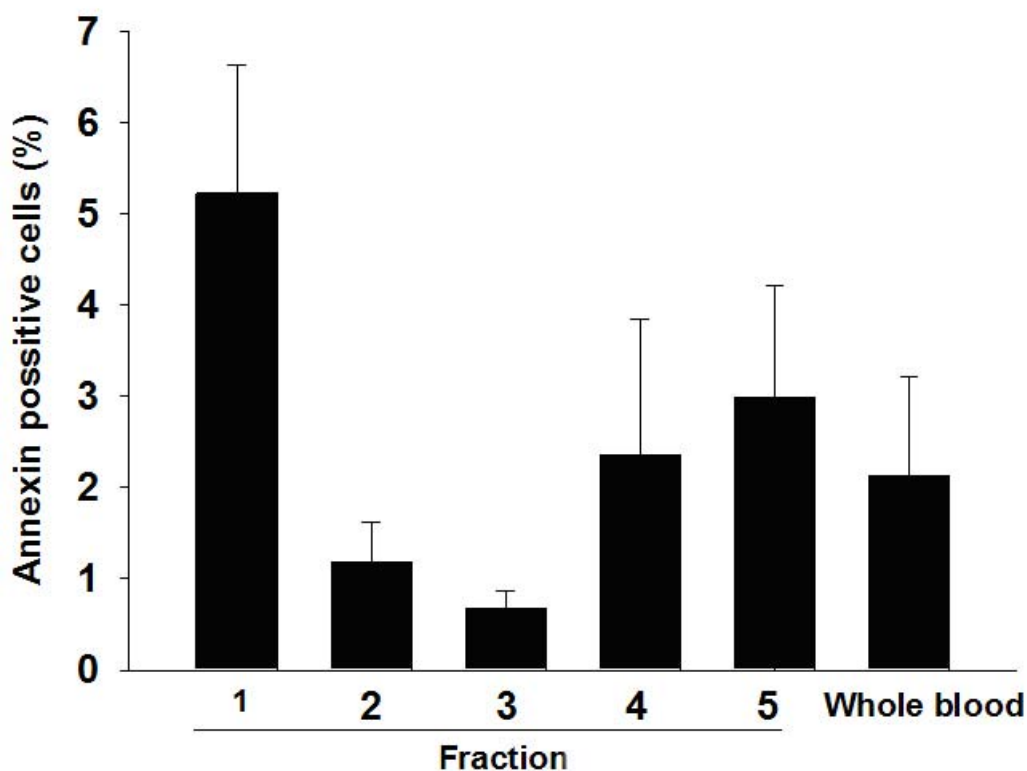


Fig. 75: PS exposure of RBCs taken from different fractions. Bars show mean value of 3 different blood samples (30.000 cells of each blood sample were analysed). Fraction 1 contains the youngest cells; fraction 5 contains the oldest cells. Whole blood: The leukocyte free RBCs before being separated into fractions. Error bars represent S.D. ANOVA and t-test showed that there is no significant difference among different fractions.

Reaction of RBCs taken from different fractions with LPA

As shown above, in a population of RBCs, the reaction of cells with LPA was different for each cell (Fig. 75). Based on the hypothesis that this difference is due to the cell age, the reaction of RBCs in fractions 1-5 with LPA was investigated. RBCs from each fraction were stimulated for PS exposure with 2.5 μ M LPA for 30 min at 37°C. Flow cytometry analysis shows that the highest amount of RBCs showing PS exposure were observed in

fractions 2 and 5 (Fig. 76). The result shows that the number of cells showing PS exposure is highest in fractions 2 and 5. It means that the reaction of cells in fractions is different. The explanation for this result is not clear now.

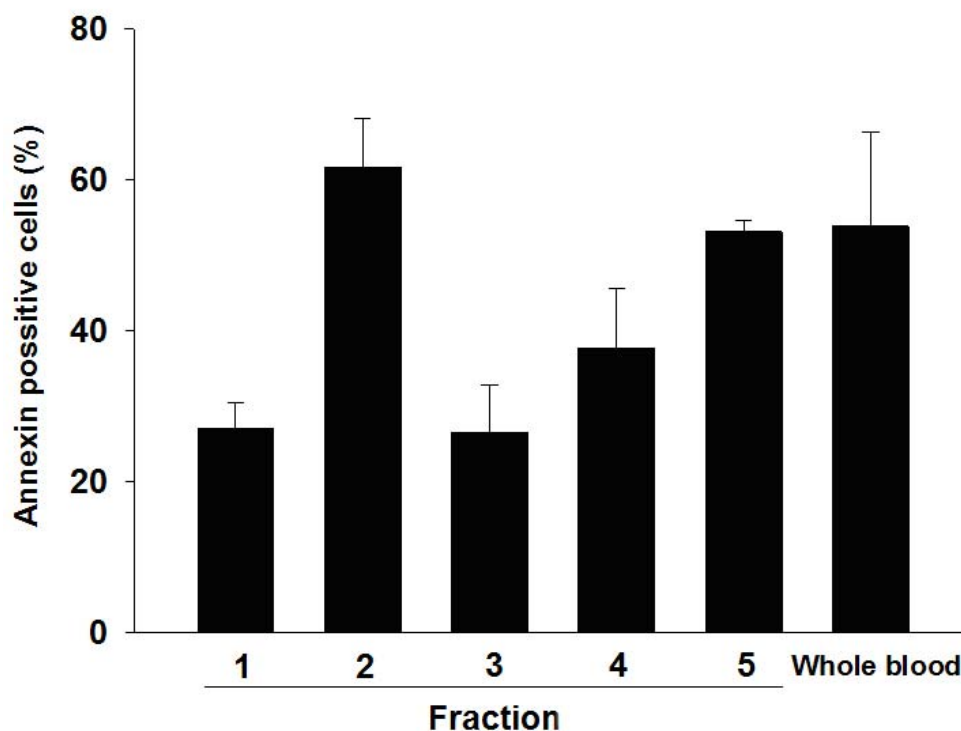


Fig. 76: PS exposure of RBCs taken from different fractions stimulated with LPA. Bars show mean value of 3 different blood samples (30.000 cells of each blood sample were analysed). Fraction 1 contains the youngest cells; fraction 5 contains the oldest cells. Whole blood: washed RBCs before being separated into fractions. Error bars represent S.D. One way ANOVA test showed that there is a significant difference among fractions. Pairwise multiple comparison tests pointed out that the reaction of RBCs in fraction 1 was different from fractions 2, 5 and whole blood.

4.5.6. Phosphatidylserine exposure of stored red blood cells

The serum pH values of blood samples after different storage time at 4°C were measured. A reduction of pH depending on the time of the storage was observed. For fresh blood, the pH of serum is about 7.4 while the blood stored for 28 days, shows a pH value of about 7.15 (Fig. 77 A). The number of cells showing PS exposure increases proportionally with the storage time (Fig. 77 B).

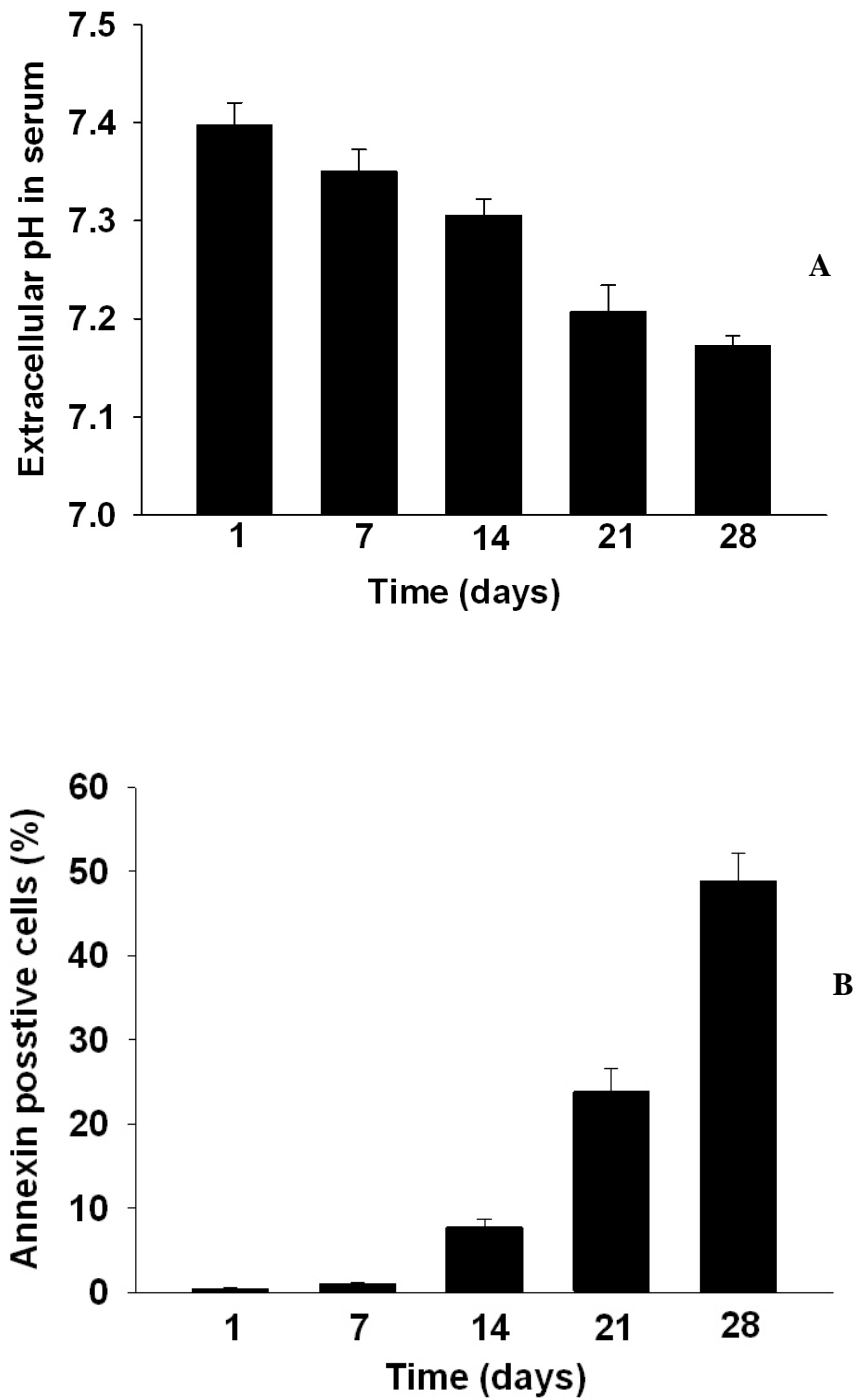


Fig. 77: PS exposure in RBCs after different storage time. Bars show mean value of 3 different blood samples (30.000 cells of each blood sample were analysed). Error bars represent S.D. Fraction 1 contains the youngest cells; fraction 5 contains the oldest cells. **A:** pH of serum after different blood storage time. ANOVA analysis showed that there is a significant difference of pH value among samples. **B:** Number of cells showing PS exposure (%) after different blood storage time. ANOVA analysis showed that there was a significant difference among samples.

4.5.7. Membrane redox activity of young and old red blood cells

The membrane redox activity in fractions and whole blood was determined. The results show that the redox activity reduces gradually regarding the age of RBCs separated by Percoll gradient centrifugation. Fraction 1 containing the youngest RBCs has the highest redox activity. The oldest RBCs (fraction 5) have the lowest redox activity (Fig. 78).

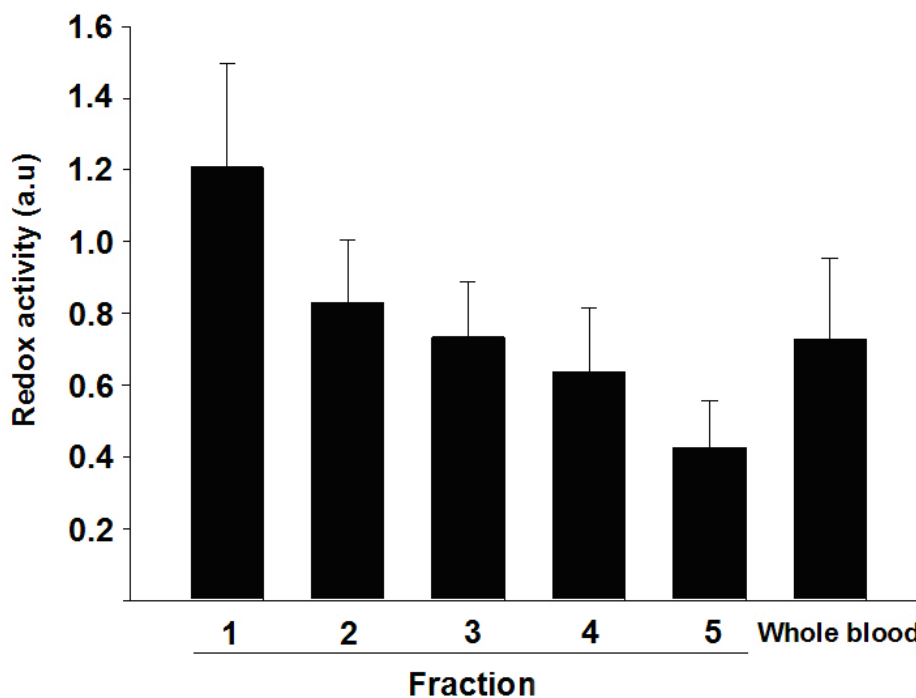


Fig. 78: Membrane redox activity of RBCs in different fractions. Bars show mean value of 3 different blood samples (30.000 cells of each blood sample were analysed). Error bars represent S.D. Fraction 1 contains the youngest cells; fraction 5 contains the oldest cells. Whole blood: washed RBCs before being separated into fractions. ANOVA analysis shows that there is a significant difference of redox activity among fractions. T-test shows that there was as significant difference between fraction 1 and 5.

4.5.8. Surface structure of young and old red blood cells

The surface structure of young and old RBCs was also investigated by AFM technique. RBCs of different fractions were scanned. Analysis data of volume and surface area point out that in healthy people there is no significant difference in the surface structure of young and old RBCs (analysis data now shown). Fig. 79 shows two typical images of young and old RBCs taken from fractions 1 and 5, respectively.

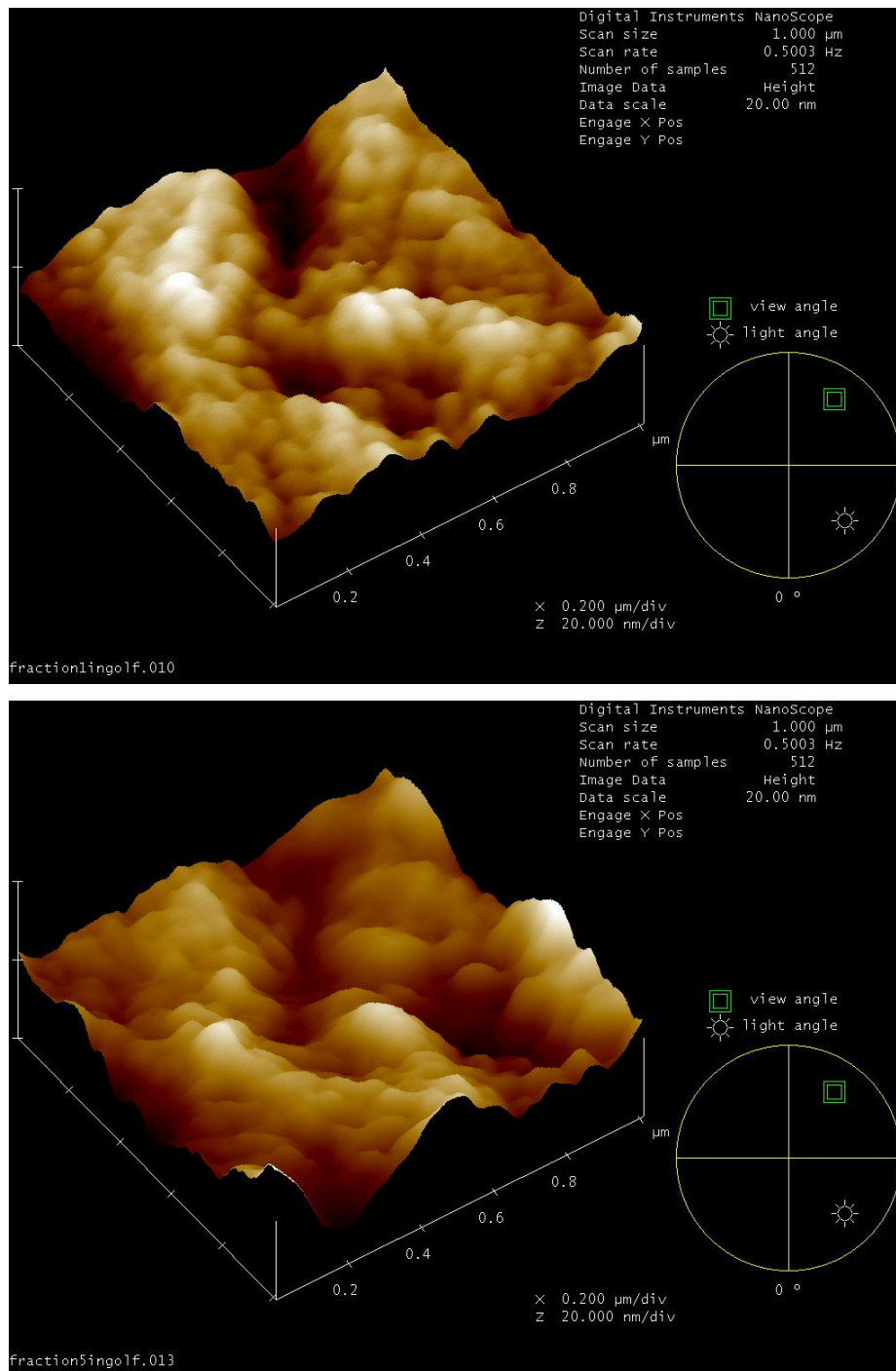


Fig. 79: Surface structure of young and old RBCs. Upper: a typical RBC taken from fraction 1, Lower: a typical RBC taken from fraction 5. The scan size is $1 \times 1 \mu\text{m}$, the scan rate 0.5 Hz and the data scale at nm (height).

5. Discussion

5.1. Role of Ca^{2+} in red blood cells under physiological conditions

The importance of Ca^{2+} for biological tissues was first discovered by Sydney Ringer in the early 1880s [191]. By conducting experiments on isolated hearts, he observed that adding a small amount of Ca^{2+} to distilled water dramatically prolonged the time that hearts continue to beat. This was a milestone and led to the introduction of a famous physiological solution, acknowledged by generations of physiologists as “Ringer’s solution”. Later on, it was shown that Ca^{2+} acts as universal intracellular messenger for many biological processes such as cell proliferation, neuron signal transmission, gene transcription, ion channel function, and muscle contraction. To control multifunctions specifically, the distribution and the content of Ca^{2+} in the cells is highly regulated.

RBCs are quite special because they lack a nucleus and organelles including Ca^{2+} accumulation structures. Therefore, the Ca^{2+} homeostasis of normal RBCs is thought to be relatively simple. In comparison to other cell types, the content of intracellular Ca^{2+} in RBCs is also extremely low (see below). RBCs can keep intracellular Ca^{2+} at such low levels because of the low membrane permeability and action of the powerful Ca^{2+} pumps.

The study of the cytosolic free Ca^{2+} levels in normal and sickle RBCs based on nuclear magnetic resonance (NMR) technique measurement showed that the mean value of ionized free Ca^{2+} in oxygenated normal and sickle RBCs were 21 ± 2 nM and 18 ± 2 nM respectively. Only a slight increase of the Ca^{2+} permeability in sickle RBCs under oxygenated condition was observed [192]. However, it has been found that the total Ca^{2+} content is significantly higher in sickle RBCs in comparison to normal RBCs [192].

In the present work, investigating the Ca^{2+} content in normal and sickle RBCs under physiological condition using fluo-4, it could be shown that there was no significant difference of free intracellular Ca^{2+} in these cells. The average value of fluorescence intensity in both normal and sickle RBCs when measured with both fluorescence microscopy and flow cytometry is very low, about 15 arbitrary units (a.u.) (see Figs. 29, 30). In malaria patients, the parasites *Plasmodia* spend most of their asexual life cycle within the RBCs, where they proliferate and mature. It is clear that the absence of Ca^{2+} or very low Ca^{2+} levels inhibit

Plasmodia function and survival. To overcome such situations, the parasites maintain a high Ca^{2+} content (about 40 μM) within the parasitophorous vacuole, a compartment formed during invasion, in which the parasites grow and divide [193]. These findings suggest that under normal conditions RBCs probably do not need Ca^{2+} for their activity.

5.2. Increase of intracellular Ca^{2+} and its consequences

It is clear that treatment of RBCs with the ionophore A23187 leads to a dramatic increase of intracellular Ca^{2+} (see Fig. 15). The increase of the Ca^{2+} content leads to the activation of Gardos channel resulting in K^+ efflux (followed by Cl^-) and the consequent reduction of the RBC volume (Fig. 18). It has been described that the threshold of the Gardos channel activation is around 40 nM of free Ca^{2+} in normal cells [170]. The increase of intracellular Ca^{2+} also activates many other processes such as scramblase [14, 194, 195] and $\text{PKC}\alpha$ [143, 196]. The consequence is the exposure of PS on the outer leaflet of the cell membrane. The exposure of PS is also a significant signal for a determined cell death called eryptosis [90, 92-95, 197]. It is necessary for the recognition and engulfment of macrophages [85, 90, 94, 197-199]. In platelets (thrombocytes), the PS exposure is supposed to provide a catalytic surface promoting the assembly of the characteristic enzyme complexes of the coagulation cascade [86, 200, 201].

LPA a water-soluble lipid second messenger is released from activated platelets [202], fibroblasts, adipocytes, and cancer cells [203]. A very fast influx of Ca^{2+} could be observed when RBCs were treated with LPA (Figs. 20, 21). According to Yang et al. [136], the Ca^{2+} influx should be due to a channel mediated transport rather than a leak transport. LPA is believed to bind to a G protein-coupled receptor that activates a C-type phospholipase [204, 205] that in turn generates diacylglycerol and 1,4,5-inositoltrisphosphate. These substances are then believed to activate protein kinase C and to promote the release of Ca^{2+} into the cell [136]. Kaestner et al. [206-208] demonstrated that LPA opens the non-selective voltage dependent cation (NSVDC) channel in human RBCs.

RBCs treated with PMA in the presence of 2 mM extracellular Ca^{2+} also show an increase of intracellular Ca^{2+} content (Fig. 22). However, the fluorescence intensity is

much lower compared to A23187 or LPA treatment (Figs. 15, 17, 20, 23). According to Andrews et al. [140] the ω -agatoxin-TK-sensitive, Cav2.1-like (P/Q-type) Ca^{2+} channel is present in the RBC membrane and it may function under the control of kinases and phosphatases. This Ca^{2+} channel is responsible for the uptake of Ca^{2+} into RBCs in the presence of PMA. However, the activity of this channel has not been fully investigated. In a study with rat pulmonary artery endothelial cells, when the cells were treated by PMA, there was also an influx of Ca^{2+} . The data were consistent with the hypothesis that PMA induced the Ca^{2+} influx through the voltage dependent L-type Ca^{2+} channel in endothelial cells [141]. Romero et al. [142] reported that both voltage dependent L-type and R-type Ca^{2+} channels exist in young and old RBCs. These observations suggest that the voltage dependent L-type Ca^{2+} channel and the ω -agatoxin-TK-sensitive, Cav2.1-like (P/Q-type) Ca^{2+} channel are activated when RBCs were treated with PMA leading to the influx of Ca^{2+} . When sheep RBCs are treated with A23187, LPA or PMA, influxes of Ca^{2+} were also observed (Figs. 33, 34). It suggests that the voltage dependent L-type Ca^{2+} channel and the non-selective voltage dependent cation (NSVDC) channel may exist in both human and sheep RBCs.

Sodium orthovanadate is an inhibitor of protein tyrosine phosphatases, alkaline phosphatases and a number of ATPases. It has been used widely as non specific inhibitor for the Ca^{2+} pump [209]. RBCs treated with 1 mM sodium orthovanadate showed a small influx of Ca^{2+} (data now shown). Likewise, under this condition, the number of RBCs showing PS exposure was also very low even after long time incubation (6 h) (data not shown). Probably the threshold for activating the processes leading to PS exposure is not reached.

5.3. Scramblases in red blood cells

Data mining of protein database indicates that scramblases exist in almost all vertebrates. BLAST result reveals that PLSCRs in human have a high identity with those in monkey, mouse, horse, cow, and dog. Phylogenetic analysis also indicates that isoforms of PLSCRs in human are very close to other isoforms of PLSCRs in animals (Fig. 67).

In human, at least 5 isoforms of scramblases and some putative protein like scramblases showing a high identity with these 5 isoforms have been discovered. Northern blots revealed that the expression of hPLSCR2 is restricted to testis, whereas hPLSCR1, 3 and 4 are expressed in most of the 16 tissues examined including heart, brain, placenta, lung, liver, skeletal muscle, pancreas, spleen, thymus, prostate, testis, uterus, small intestine, colon, and peripheral blood [74]. Notable exceptions are hPLSCR4, which is not detected in peripheral blood lymphocytes, and hPLSCR1 and hPLSCR3, which are not detected in brain [74]. This would suggest that in human RBCs there exist the scramblase isoforms 1 and 3.

Two antibodies against hPLSCR1 and hPLSCR3 (raised from mouse) were used for Western blot analysis to detect the presence of these isoforms in different animals including rat, mouse, sheep, and cow. The results show that the scramblase isoform 3 is present in all investigated species, including sheep. The antibody against hPLSCR1 reacted only with human ghost cell protein but did not react with ghost cell protein of rat, mouse, cow, and sheep (Fig. 70). As mentioned before, this is due to the low identity of amino acid sequences at N-terminus of the PLSCR1s in human, rat, mouse, and cow (Fig. 68). Although the antibody did not react with sheep ghost proteins, it is still not possible to state that the scramblase 1 is absent in sheep RBCs. The reason is that the antibody against hPLSCR1 is a monoclonal antibody. Therefore, it is possible that the necessary epitope (amino acid sequence or the structure of recognition domain) for the recognition of the antibody is not present in the PLSCR1s of mouse, rat, cow, and sheep. Nevertheless, the Western blot results show that at least there exist scramblase isoform 3 in sheep RBCs. The activation of this isoform may be not only dependent on the intracellular Ca^{2+} level but also on other unknown factors.

The specific activity of the scramblases is unknown. However, 4 motifs including Ca^{2+} binding motif and 1 transmembrane domain are highly conservative among these scramblases [210]. The Ca^{2+} binding motif present in all scramblase isoforms suggests that the activity of scramblase strongly depends on the concentration of intracellular Ca^{2+} .

The detailed mechanism of phospholipid scrambling and the difference of the activity among various PLSCRs are not fully understood. The exact threshold of the free Ca^{2+} concentration in cytoplasm for the activation of scramblases is also not precisely known

because different cell types have different Ca^{2+} concentrations. In human RBCs, intracellular Ca^{2+} concentrations above 50–100 μM have been shown to induce transbilayer redistribution of phospholipids [14, 71]. The experiments using A23187 at different concentrations of extracellular Ca^{2+} (from 50 nM to 1 μM) showed that the number of RBCs showing PS exposure is not significant after 30 min. There are two possible explanations for these observations. First, at low concentrations of extracellular Ca^{2+} , the time needed for an influx of Ca^{2+} is longer (Fig. 15A). Second, the amount of free intracellular Ca^{2+} is still not enough to activate scramblases. Higher concentrations of extracellular Ca^{2+} (above 50 μM) lead to a significant influx of Ca^{2+} (Figs. 15B, C and 16). A significant PS exposure is also observed at these concentrations. There was no significant difference in the reaction behaviour (delay time) or the level of the intracellular Ca^{2+} (based on the mean value of fluo-4 fluorescence intensity) when the extracellular concentration of Ca^{2+} was higher than 100 μM (Fig. 17). The reason for that is probably due to the saturation of the fluorescence intensity.

These data are also compatible with the data of Woon et al [14]. He reported that the phospholipid scrambling was found to be half-maximally activated at 63-88 μM free intracellular Ca^{2+} . Such concentrations are a bit higher than the range of 20-60 μM reported by Bassé et al. [195] for a 37 kDa scramblase protein isolated and reconstituted from human RBCs. In another report, Verhoven et al. [211] showed that the concentration of intracellular Ca^{2+} within the range of 50 and 100 μM is enough to activate the scramblase in resealed ghosts and human RBCs. However, the presence of as little as 5-10 μM Ca^{2+} in erythrocyte ghosts resulted in a loss of the phospholipid asymmetry [212]. The possible reasons for these observations may be due to the different activities of scramblase isoforms existing in RBCs.

5.4. Phosphatidylserine exposure in red blood cells

As mentioned before, when the intracellular Ca^{2+} increases, the Gardos channel is activated and leads to an efflux of K^+ . Elevation of the intracellular Ca^{2+} level also activates the scramblases. The consequences are cell shrinkage, membrane blebbing, PS exposure, and the formation of microvesicles. Figs. 16, 17, 20, 21, 22, 23 and 26 show that the intracellular Ca^{2+} level increases when RBCs are treated with 2.5 μM LPA, 2 μM A23187

or 6 μM PMA in the presence of 2 mM extracellular Ca^{2+} . The influx of Ca^{2+} activates phospholipid scramblases (PLSCR) leading to PS exposure on the outer leaflet of RBCs, and microvesicle formation (Figs. 36-38). Details of the kinetic process of PS exposure in human RBCs are presented in Figs. 43, 44, in which, cell shrinkage, membrane blebbing and microvesicle formation can be clearly observed.

However, the experiments with PMA demonstrate that in the absence of Ca^{2+} and 1 mM EGTA (no influx of Ca^{2+} , Fig. 39), more than 50 % of RBCs showing PS exposure is observed (Figs. 40, 41). In the presence of 2 mM Ca^{2+} more than 85 % of the RBCs showing PS exposure after PMA treatment (Figs. 40, 41). It means that the exposure of PS in RBCs does not only depend on the activity of scramblases but also on other pathway(s).

The intensity of fluo-4 when RBCs treated with LPA or A23187 in the presence of 2 mM Ca^{2+} is very high (Fig. 23). In addition, treatment of RBCs with A23187 showed that the number of reacting cells as well as the fluorescence intensity of fluo-4 is higher than treatment of RBCs with LPA (Figs. 23, 24). However, the number of RBCs showing PS exposure in case of A23187 treatment is much lower (Fig. 36, 37). The results suggest that the PS exposure does not only depend on the intracellular Ca^{2+} . The reason why the number of the RBCs showing PS exposure is higher in LPA treatments is probably due to the binding of LPA to the G protein-coupled receptor. This receptor activates a C-type phospholipase [204, 205]. C-type phospholipase in turn generates diacylglycerol and 1,4,5-inositoltrisphosphate. Two substances are then believed to activate protein kinase C [136]. The activation of protein kinase causes many different effects leading to PS exposure (Fig. 80).

Interestingly, the results from treatment of RBCs with LPA and A23187 in the presence of Ca^{2+} showed that one population of RBCs there exist some cells showing a high fluorescence intensity of fluo-4 (for Ca^{2+}), but no or very low fluorescence intensity of annexin V-alexa 568 (for PS exposure) can be observed. In contrast, there are some cells showing PS exposure but the Ca^{2+} content in these cells is very low (Fig. 56, 57,). However, long time incubation with A23187 or LPA (more than 30 min) leads to more RBCs showing PS exposure but haemolysis can occur. Another study with LPA and A23187 also came to the conclusion that the reactions of RBCs to the substances are both

time and concentration dependent [124]. It suggests that the reaction of RBCs differs at the single cell level.

Surprisingly, in the presence of EGTA, RBCs treated with 6 μM PMA also show PS exposure although the fluo-4 signal (for Ca^{2+} level) is very low. This result is also comparable with the data analysis of the flow cytometry experiment (Fig. 40). Results from treatment of RBCs with PMA (Figs. 58, 59), LPA and A23187 (Figs. 56, 57) give more evidence supporting for the hypothesis that the PS exposure does not only depend on the intracellular Ca^{2+} content but also other factor(s). Although the exact mechanism for the PMA induced Ca^{2+} influx is unclear, the Ca^{2+} content is high enough to create a temporary imbalance between the Ca^{2+} influx and the outward flux driven by the Ca^{2+} pump. Enhanced intracellular Ca^{2+} levels can induce PKC activation in the RBCs. It suggested that the initially enhanced Ca^{2+} levels could recruit more PKCs and translocate them from cytoplasm to the membrane as well as to induce a positive feedback [143] (also see Fig. 80). In other words, the increase of intracellular Ca^{2+} in case of PMA stimulates a propagation signal for the activation of PKC.

In a report, Frasch et al. [78] pointed out that protein PKC δ plays an important role in the activated transbilayer movement of phospholipids and surface PS exposure by directly enhancing the activity of phospholipid scramblase. Specific inhibition of PKC δ by rottlerin prevented both apoptosis and the activation of scramblase in Jurkat cells [78]. According to Govekar et al. [213] so far only 4 isoforms of PKCs have been discovered in human red blood cells. These are PKC α , PKC μ , PKC ζ and PKC ι . PKC α is activated by Ca^{2+} , FFA and DAG. PKC ζ is activated by PIP3 and FFA. Both types of PKC are activated by PS. Activation of PKC μ and PKC ι is unknown [144] (see Table 2) The activation of PKC could inhibit the activity of aminophospholipid translocases (ALPTs) and lead to enhance PS exposure. The data indicated that after 30 min incubation with 6 μM PMA almost all RBCs showed PS exposure (Figs. 40, 41). As mentioned before (see Theoretical background) the PS exposure stimulated by the inhibition of ALPTs is a time dependent process. Hence, the PS exposure in case of RBCs stimulated by PMA does not strongly depend on the activity of ALPTs. Experiments also show that chelerythrine significantly reduces the number of RBCs showing PS exposure (Fig. 53). In addition, chelerythrine does not inhibit the Ca^{2+} influx when RBCs were stimulated with PMA (data not shown).

Therefore, the process of PKC inducing PS exposure in RBCs does not directly depend on the intracellular Ca^{2+} level.

The experiments with sheep RBCs under the same conditions (LPA, A23187 and PMA treatment) give additional interesting results for the relation between intracellular Ca^{2+} and PS exposure (Figs. 33-35, 60). When sheep RBCs are treated with A23187, all cells react and show a high signal of fluo-4 fluorescence but there are nearly no cells showing PS exposure (Fig. 60 upper row). The number of sheep RBCs showing PS exposure is less than 10 % when LPA is applied (Fig. 60 lower row). Sheep RBCs treated with PMA in the presence of 2 mM Ca^{2+} do not result in PS exposure (data not shown). Some possible conclusions for the PS exposure in human and sheep RBCs can be figured out. First, the PS exposure in RBCs depends on the level of intracellular Ca^{2+} . However, only the elevation of the Ca^{2+} level does not seem to be enough for PS exposure in the case of sheep RBCs. It does not mean that the scramblase(s) in sheep RBCs is not functioning. It should be noted that the lipid components in the membrane of sheep RBCs are different from human RBCs (but similar to cow). In the outer leaflet, there is about 100 % of SM and nearly no PC while in the inner leaflet PS and PE are located (Fig. 1). This distribution of lipids may influence the lipid transport between the two membrane leaflets leading to only a small number of cells showing PS exposure. Second, there exists one (or more) pathway(s) leading to the exposure of PS independent of Ca^{2+} , or in other words, the exposure of PS is not only regulated by phospholipid scramblases but also by another mechanism involving PKC. Third, the reaction of RBCs in a population does not follow the “all or nothing” manner, they reacted differently (at least some) at the single cell level. The explanation for that finding may come from the difference among RBCs related to their age.

Cellular acidification in the apoptosis was mentioned by Bucky et al. [214]. They investigated the involvement of the Na^+/H^+ exchanger in the process of PS exposure during human platelet activation. However, the relationship between Ca^{2+} mobilization and NHE1 function during platelet activation is not well established. Experiments show that under stimulating conditions by LPA, A23187 or PMA treatment, the pH_i is reduced (Fig 46). A proportional decline of pH_i with the increase of intracellular Ca^{2+} could be figured out. It means that the reduction of pH_i is compatible with the increase of intracellular Ca^{2+} (see Fig. 23). Zsemberly et al. [215] reported that a raising intracellular Ca^{2+} concentration up to 1 μM leads to a parallel activation of Cl^- channels and HCO_3^- extrusion. Wagner et al. [216]

indicated that PKC activated a Cl^- channel in fibrosis airway epithelial cells. Hence, there is a connection between the Cl^- efflux and the change of pH_i . Experiments using a specific fluorescent dye for Cl^- such as MEQ (6-methoxy-N-ethylquinolinium chloride) should be used to investigate the fluctuation of Cl^- under stimulating conditions (LPA, A23187, PMA treatment).

The PS exposure has also been investigated under other conditions. It has been pointed out that the LIS induced cation transport is mediated by the $\text{K}^+(\text{Na}^+)/\text{H}^+$ exchanger. At very low ionic strength, there might be an increased opening of the non-selective voltage dependent cation (NSVDC) channel allowing Ca^{2+} to go in the RBCs [217]. Based on these findings one could explain the low number of RBCs showing PS exposure in LIS solution (Fig. 54). Glucose-free solution showed a very low effect on PS exposure. This can be easily explained because the remaining ATP in RBCs is enough for the function of the Ca^{2+} pump and amino phospholipid translocase for at least 24 h. When all ATP is removed the PS exposure occurred and this process was enhanced in the presence of Ca^{2+} . The result suggests that the asymmetric distribution of the membrane lipid is disturbed by the absence of ATP. There are two processes, which relate to ATP consumption. First, without ATP the Ca^{2+} pump can not work and the consequences are the elevation of intracellular Ca^{2+} and activation of the scramblases. Second, when the amino phospholipid translocases do not function because of the lack of ATP, after a certain time the PS and PE can not be transported back to the inner leaflet. Under these conditions, the movement of the phospholipids is simply based on diffusion and therefore it requires a long time.

Valinomycin is an ionophore, which is selective for K^+ ions over Na^+ ions. It functions as a K^+ specific transporter and facilitates the movement of K^+ through lipid membranes "down" its electrochemical potential gradient. The physiological solution contains 7.5 mM KCl while the concentration of K^+ in RBC cytoplasm is much higher, around 150 mM. An efflux of K^+ occurs when RBCs are treated with valinomycin. This process mimics somehow the action of Gardos channel when the intracellular Ca^{2+} is elevated. A significant percentage of cells showing PS exposure (about 15 %) is seen after a 24 h treatment with valinomycin without extracellular Ca^{2+} (Fig. 47). This means that the K^+ efflux is one contributing factor leading to PS exposure in RBCs. It also suggests that the volume of the cells is critical for surviving of RBCs in terms of apoptosis.

An experiment in the presence of Ca^{2+} and the Gardos channel inhibitor charybdotoxin confirms the role of K^+ efflux for the PS exposure (Fig. 50). The efflux of K^+ induced by A23187 and conducted by the Gardos channel was significantly inhibited by charybdotoxin (Fig. 50). This effect of inhibition of PS exposure can also be seen in the solution containing a high KCl concentration (Fig. 49). Also in case of PS exposure stimulated by LPA, an inhibition of this process can be seen in a solution containing high KCl (Fig. 48). More than 50 % of RBCs showing PS exposure is reduced when 150 mM extracellular KCl.

Osmotic pressure has also an influence on the PS exposure of RBCs [100]. When RBCs are suspended in hypotonic solutions, an increase of the cell volume can be observed (Fig. 51). In contrast, in hypertonic solutions, a dramatic reduction of cell volume can be seen (Fig. 51). The PS exposure occurs only in hypertonic solution, the presence of Ca^{2+} accelerates significantly the number of cells showing PS exposure (Fig. 52). It suggests that hypertonic solution elevates an influx of Ca^{2+} by activation of a non-selective cation channel [131].

Chelerythrine and staurosporine are potential inhibitors for protein kinase C. Experiments showed that in the presence of chelerythrine the number of RBCs showing PS exposure was reduced. When RBCs are treated with PMA in the presence of chelerythrine, the number of RBCs showing PS exposure reduces at least 50 % (Fig 53). In case of LPA or A23187, the inhibition activity for PS exposure of chelerythrine and staurosporine is less pronounced (Fig 53). Hence, the PS exposure does not strongly depend on the activity of protein kinase C when RBCs are treated with LPA or A23187.

Kempe et al. [110] reported that Pb^+ ions activate erythrocyte K^+ channels, probably the Gardos channel, leading to erythrocyte shrinkage, and also activate the erythrocyte scramblase, leading to PS exposure. Treatment of RBCs with tert-butyl hydroperoxide also leads to the exposure of PS due to the oxidative activity. More than 90 % of the cells showing PS exposure after a treatment with 0.5 mM tert-butyl hydroperoxide for 2h min at 37°C (Fig. 55). The presence of Zn^{2+} also stimulated a significant number of cells showing PS exposure. According to Mandal et al. [113] the exposure of PS in the presence of Zn^{2+} was due to the activation of caspases and the inhibition of flippase activity.

Taken together, the proposed pathways involved in the process of PS exposure in RBCs can be summarized (Fig. 80).

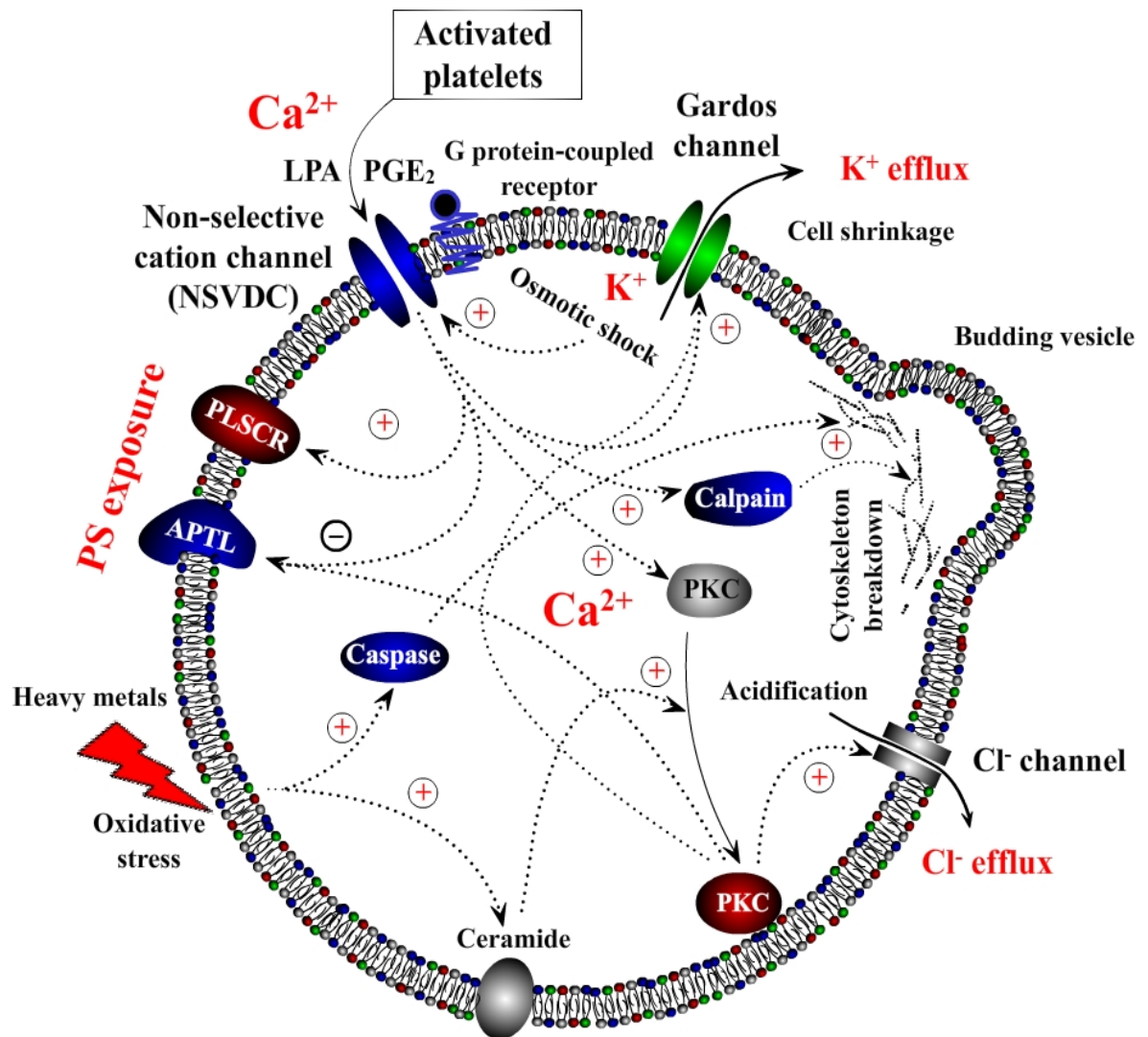


Fig. 80: Possible pathways leading to PS exposure in RBCs. LPA or PGE₂ released from activated platelets (possible together with G protein-coupled receptor) activates a non-selective voltage dependent cation (NSVDC) channel. The opening of this channel leads to an increase of the intracellular Ca²⁺. The increase of intracellular Ca²⁺ level leads to an activation of phospholipid scramblase (PLSCR) and protein kinase C (PKC). The activated PKC moves from the cytoplasm to the membrane. Aminophospholipid translocase (APTL) is inhibited by high concentrations of intracellular Ca²⁺, PKC, and ATP depletion. PKC also activates and opens Cl⁻ channels leading to an efflux of Cl⁻. It seems likely that the efflux of Cl⁻ leads to the intracellular acidification. Under stress conditions (oxidative substances), ceramide is formed. Ceramide consists of sphingosine and fatty acid. Ceramide activates PKC. Caspases, a family of cysteine proteases, are also activated under stress condition. Calpains are a family of calcium-dependent, non-lysosomal cysteine proteases. They are also activated by Ca²⁺. Caspase and calpain break down the cytoskeleton by a proteolysis activity leading to membrane blebbing and vesicle formation.

5.5. Adhesion of red blood cells

RBCs treated by LPA, A23187 or PMA adhere together (Figs. 63, 65). There was no adhesion observed in the controls. The reasons for the adhesion among RBCs are unknown. There are many open questions relating to this phenomenon such as why do the RBCs showing PS exposure adhere together, how strong is the adhesion force among the cells? What is the nature of the adhesion force? Alternatively, which molecules are involved in these processes? To find the answers or at least explanations for that, the following arguments should be considered.

The aspects of PS exposure

Closse et al. [117] pointed out that under pathological conditions such as sickle cell disease, malaria and diabetes, an abnormal adherence of RBCs to the endothelium is concomitant with the loss of phospholipid asymmetry resulting in PS exposure. The adhesion was inhibited by PS liposomes and by annexin V giving clear evidence of the PS dependency of these interactions. Treatment of RBCs with the Ca^{2+} ionophore A23187 showed that RBCs showing PS exposure massively adhered to human umbilical vein endothelial cells (HUVEC) in a Ca^{2+} dependent manner. This adhesion was also inhibited by PS liposomes and by annexin V, supporting for the PS dependency of these interactions. Similar investigations were carried out by Manodori et al. [80]. They studied the role of PS exposure in Ca^{2+} ionophore treated normal RBCs adhering to HUVEC monolayer. When the HUVEC monolayer was incubated with PS exposed RBCs, the endothelial cells (EC) retracted and the RBCs adhered primarily in the gaps opened between the ECs. A linear correlation was found between the number of PS exposing RBCs in the population and the number of adhering RBCs to the monolayer. Pre-treatment of RBCs with annexin V significantly decreased adherence by covering PS on the surface of the RBCs. Similarly, PS containing lipid vesicles decreased RBC binding by competing for the PS binding sites in the monolayer. PS exposed RBCs and PS containing lipid vesicles adhered to immobilized thrombospondin (TSP) and matrix TSP, respectively, and adherence of PS exposed RBCs to the EC monolayer was reduced by antibodies to TSP and to the receptor of ECs (avb3) [80].

In a study of phospholipid vesicle aggregation, Ohki et al. [218] showed that in the presence of divalent ions the aggregation of vesicles containing PS can be explained by the

dynamic interactions of the vesicle membrane by electrostatic forces. Nir et al. and Bentz et al. [219, 220] noted that the fusion of PS containing vesicles does not occur when the medium contains only monovalent cations (at pH 7.4). Ca^{2+} is an important factor for the aggregation of PS containing vesicles. In a mini-review, Papahadjopoulos et al. [221] showed that Ca^{2+} could induce aggregation of phosphatidylserine containing vesicles and play an important role in the formation of a “bridge” structure between two phosphatidylserines (PS--- Ca^{2+} ---PS). Together with other report about PS exposure and its ability for adhesion with endothelial cells, it suggests that PS is one important factor for cell adhesion.

The aspects of cell receptors

In a very interesting report, Setty et al. [115] showed that sickle RBCs adhered with non-activated endothelial cells. It is known that under normal conditions, there is a subpopulation of RBCs in sickle cell blood showing PS exposure. When sickle RBCs were treated with annexin V (to cover PS) or anti-CD36, there was an inhibitory effect on the adhesion process of $36 \pm 10\%$ and $23 \pm 8\%$, respectively. In case both annexin V and anti-CD36 were used, an additive effect was observed. Hence both exposed PS and CD36 take part in the adhesion with endothelium and CD36 exists at a significant amount on sickle RBCs [115].

In a study on *Plasmodium falciparum*, van Schravendijk et al. [222] used the monoclonal antibodies (MoAbs) anti-CD36 to test the presence of this cluster on the human RBC membrane. Mature RBCs have previously been considered to be negative for CD36. However, using fluorescence activated cell sorter (FACS) analysis with the anti-CD36 MoAbs 8A6, OKM5, and OKM8 they found that there exist CD36 in mature RBCs, but the level of expression of CD36 is low. However, there are also enough CD36-like molecules on the surface of normal RBCs to mediate adherence to a surface presenting suitable receptors, such as anti-CD36 MoAbs. It is also possible that CD36 on RBCs may act together with other receptors in mediating adhesion phenomena because many cell adhesion processes involve multiple receptors [116, 222].

A report by Tail et al. [223] showed that CD36 has been proposed as one receptor protein that recognizes PS and other anionic phospholipids. They investigated the binding of phospholipid vesicles to the monocytic leukaemia cell lines THP-1 and J774A.1 using vesicles containing 50% PS, PI, or phosphatidylglycerol (PG), and with balance of phosphatidylcholine (PC). Specific, high affinity binding was observed for vesicles

containing PS, PI, or PG. Normal RBCs or annexin V treated vesicles showing minimal binding to the human monocytic leukaemia cell line (THP-1) were used as control. High concentration of o-phospho-l-serine (1 mM) had no effect on the binding of PS vesicles, indicating that high affinity binding requires a surface containing multiple phosphoserine groups rather than a single molecule.

A monoclonal antibody to CD36 blocked up to 60 % of the specific binding of PS vesicles but had minimal or no effect on the binding of PG or PI vesicles. This antibody also selectively inhibited the phagocytosis of PS containing vesicles as measured by fluorescence microscopy, indicating that CD36 is functionally significant for phagocytosis of this vesicle type. In addition, collagen and thrombospondin, two other putative ligands of CD36, were unable to inhibit the binding of PS vesicles. These evidences suggest that CD36 is the primary protein responsible for the high affinity binding of PS vesicles to these monocyte-like cells. In addition, CD36 appears to be specific for PS among anionic phospholipids [223]. Other reports also pointed out that the presence of CD36, CD44, and VLA-4 plays an important role in cell mediating adhesion, especially in sickle cell anaemia to components of the extracellular matrix [116].

Recently, the adhesion force between two RBCs which were stimulated by LPA or A23187 treatment was measured by using atomic force microscopy. The results show that at least a force larger than 100 pN was measured (P. Steffen and D. Moersdorf, unpublished, private communication). In the control experiment, the adhesion forces were determined to be one order of magnitude lower. This evidence is very convincing to demonstrate the self-adhesion ability of RBCs showing PS exposure.

Treatment of sheep RBCs with 2.5 μM LPA in the presence of 2 mM Ca^{2+} results in about 10% of cells showing PS exposure (Fig. 60, lower row). When sheep RBCs are treated with A23187 or PMA, there is no or very less cell showing PS exposure (Fig. 60, upper row). However, it is very interesting that sheep RBCs adhere together under these conditions (Fig. 65). An open question here is which amount of PS exposure on the outer leaflet of RBCs is enough to induce the adhesion? Another question is whether a few numbers of PSs together with other phospholipids are enough for the adhesion process? To answer these questions the nature of the adhesion process should be elucidated. In addition, the role of cell receptors should also be under consideration.

Taken all together, the adhesion of RBCs to other tissues and to themselves is related to the presence of exposed PS (may be together with other anionic or zwitterionic phospholipids)

and the interaction of receptors on the membrane of the RBCs as well. Fig. 81 shows a proposed model for the adhesion of RBCs under stimulated conditions.

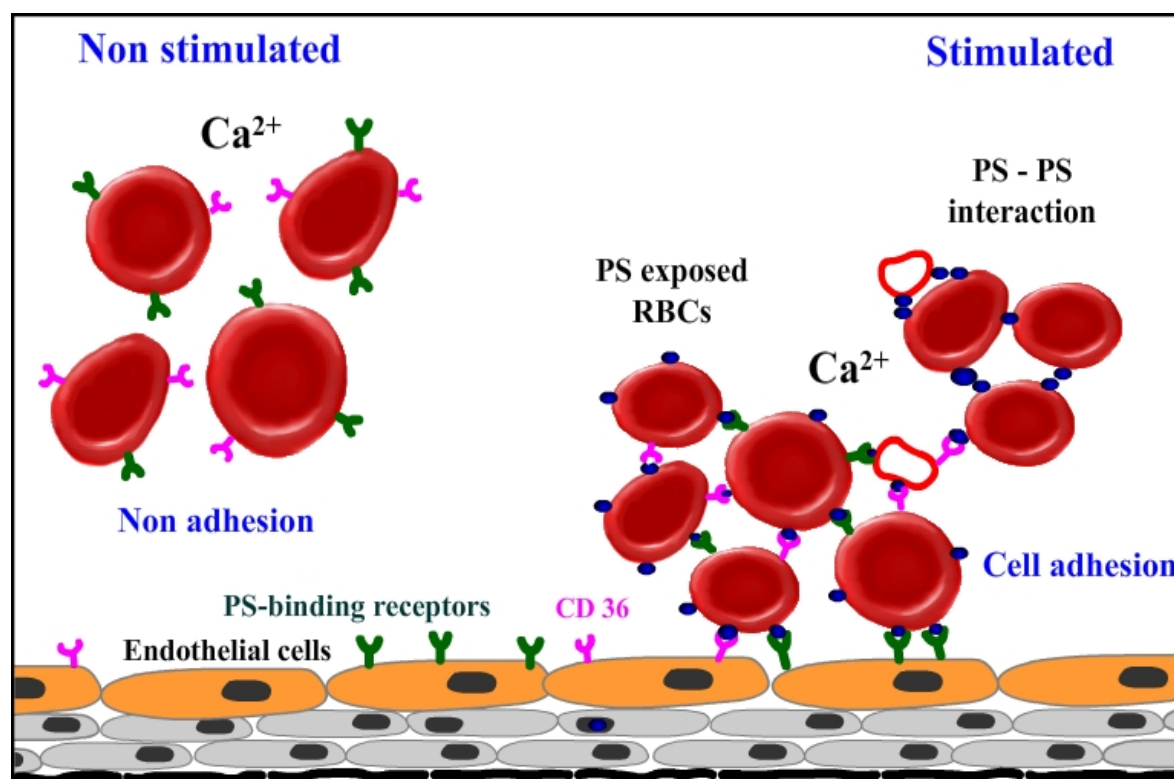


Fig. 81: Proposed model for the process of adhesion of PS exposed RBCs under stimulated condition. In the proposed model, the CD36, PS-binding receptors, and other receptors are present on the surface of RBCs or endothelial cells. Under normal conditions, RBCs do not show PS exposure on the outer leaflet of the membrane. Hence, they do not adhere to endothelial cells and to themselves as well. Under certain conditions when RBCs or microvesicles show PS on the outer leaflet of the membrane, the existing receptors such as CD36 and PS-binding receptors bind with PS. Therefore, RBCs and microvesicles carrying PS exposure can adhere to together and to the endothelial cells. The RBCs showing PS exposure also can be adhered together by the interaction of PS-PS in the presence of Ca^{2+} . These interactions forms a so called “bridge structure” that can facilitate the adhesion of RBCs.

5.6. Role of red blood cells in the process of thrombosis

As mentioned before, according to the traditional opinion, coagulation and thrombosis are primarily a function of endothelial cells, platelets, and soluble coagulation factors, in which platelets take a central role. RBCs in contrast, are generally regarded as innocent bystanders, passively entrapped in a developing thrombus as they flow through the

vasculature. However, some findings and the results of this work show the active role of RBCs in the process of thrombosis.

It should be noticed that under normal conditions the concentration of PGE₂ in human plasma is extremely low. In 1983, Smith et al. [224] reported that the concentration in healthy volunteers is 2.8 ± 2.0 pg/ml by using capillary gas chromatography negative ion chemical ionization mass spectrometry. Araujo et al [225] noted the concentration of PGE₂ is 1.057 ± 0.758 ng/ml. Wu et al. [226] showed that the concentration of PGE₂ in human plasma varies from 7.8 to 500 pg/ml. The concentration of LPA in human plasma is about 0.41 μ M under normal conditions [227]. When platelets are activated, the concentration of LPA elevated to be about 20 μ M in plasma [205] or even higher up to 200 μ M in plasma and malignant ascites fluid of ovarian and cervical cancer patients [124, 228, 229].

As mentioned before, Kaestner and Bernhardt proposed a cascade for the aggregation of RBCs under stimulated conditions (Fig. 6). It suggests that when platelets are activated, they release LPA. Subsequently, LPA activates the non-selective voltage dependent cation (NSVDC) channel leading to an increase of intracellular Ca²⁺ by the induction of an influx of Ca²⁺ through the channel. Some events involving Ca²⁺ such as the activation of the Gardos channel, scramblase, and inhibition of aminophospholipid translocase (APTL) lead to cell shrinkage and PS exposure. The consequences are the aggregation and adhesion of RBCs. In this model, the adhesion of RBCs can be explained based on the combining action of the PS exposed RBCs, and the microvesicles carrying exposed PS with the receptors existing on the cell membrane surface.

There are some evidences supporting this opinion. In principle, the adhesion of cells is based on cell-cell interaction. In resting state, there is no or very less PS exposure on the outer leaflet of the RBC membrane. Under stimulated conditions, cells and microvesicles carrying exposed PS provide a catalytic surface promoting the assembly of the characteristic enzyme complexes of the coagulation cascade. Microvesicles shed from activated platelets constitute the main circulating population. They harbour major membrane glycoproteins, including functional adhesive receptors, and consequently disseminate a procoagulant potential that can be targeted according to the nature of counter ligands [118]. Likewise, the microvesicle containing exposed PS can bind to soluble or immobilized fibrinogen and aggregate with platelets [119]. Jimenez et al. [120] noted that the procoagulant potential of cells or microvesicles carrying PS is not restricted only to

platelet microvesicles. However, microvesicles from monocytes, lymphocytes, RBCs or endothelial cells also show PS at their outer surface. Other factors were also detected at the surface of circulating endothelial microvesicles, for instance the von Willebrand factor and E-selectin.

According to Kawakami [230], the RBC was identified as the most active membrane surface among blood cells and endothelial cells in catalyzing the coagulation process. The exposure of PS may be necessary for assembly of contact coagulation factors because of the interaction of anionic phospholipids with coagulators. Exposed PS provides a procoagulant surface that facilitates the conversion of prothrombin into thrombin [231-233]. Other evidences about the role of membrane phospholipids in the activation of the conversion of pro-thrombin into thrombin were given by Zwaal et al. [72]. Membrane phospholipids propagate the proteolytic reactions that result in thrombin formation by promoting the assembly of coagulation factors on their surface. The most important pathway of coagulation is initiated by tissue factor (TF), an integral membrane protein expressed on the surface of activated or disrupted cells. According to Ruf et al [232], the anionic phospholipids are indispensable to promote membrane binding and catalytic activity of the two subsequent coagulation factor complexes in the cascade that leads to thrombin formation.

Treatment of 0.1 % haematocrit RBC suspension with 100 IU of thrombin at 37°C for 30 min leads to more than 50 % of cells showing PS exposure (own result, data now shown). Therefore, it seems that the RBCs showing PS exposure on the outer leaflet can mediate the conversion of prothrombin to thrombin (in the presence of other factors, see Fig. 82). If thrombin by itself can stimulate the exposure of PS on the outer leaflet of the RBC membrane, RBCs are not merely bystanders but can act as mediating cells in a signal propagation cascade of the thrombus formation. In other words, RBCs take part in a cycle of signal amplification. It should be mentioned that the number of RBCs is much larger than the number of platelets. Therefore, when RBCs are stimulated they will play an important role in blood clot formation. Details of the proposed coagulation cascade are presented in Fig. 82.

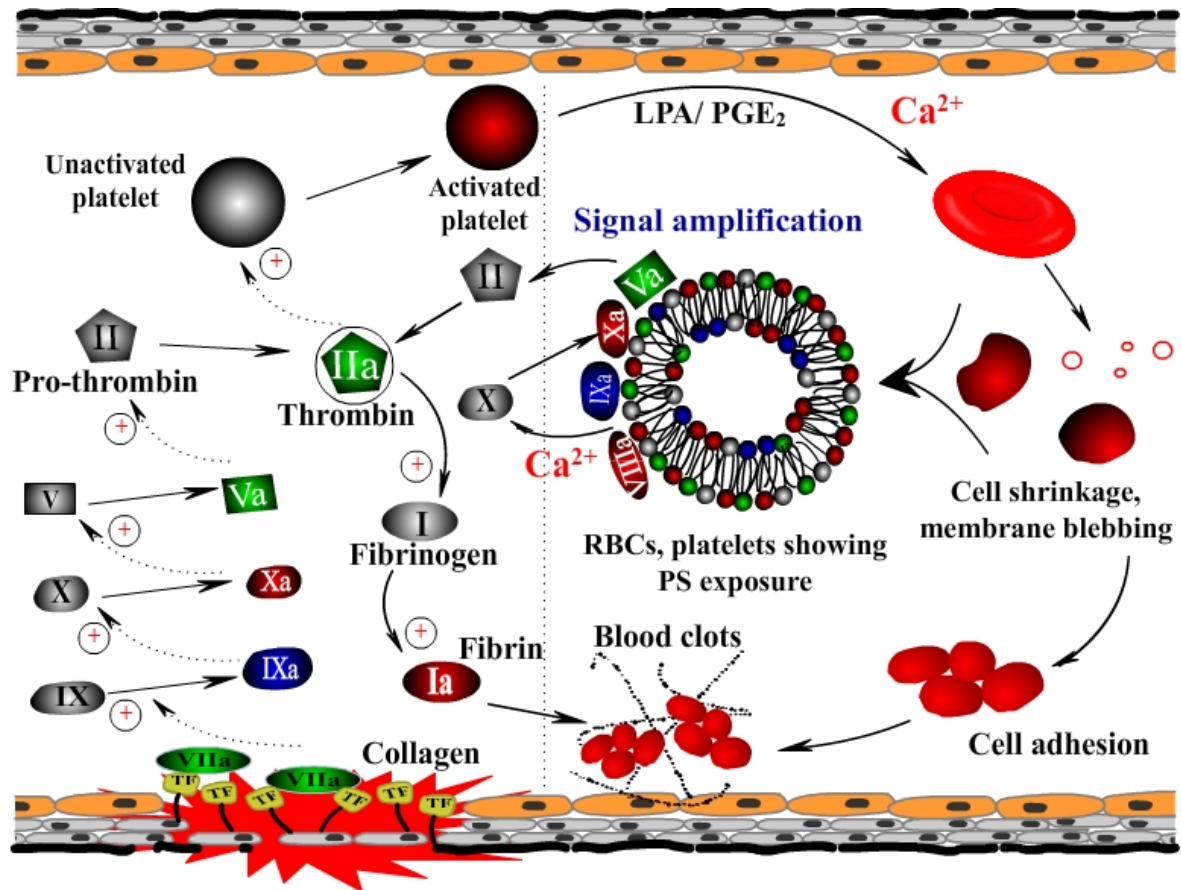


Fig. 82: Role of RBCs in signal amplification in the thrombus formation. Under normal conditions, the tissue factors (TF) do not expose to the bloodstream. When an injury or stimulation occurs, the collagen and tissue factors are released from the endothelial cells. This leads to the activation of factor VII (from VII into VIIa). In a cascade, the factor VIIa activates factor IX to IXa. Subsequently, factor IXa activates the conversion of factor X (pro-thrombinase) to Xa (thrombinase). A cofactor (also called factor V) is activated, it helps for the conversion of factor II (pro-thrombin) to IIa (thrombin) leads to the activation of platelet and fibrinogen (factor I). LPA or PGE₂ are released from the activated platelets, they act as the second messengers leading to the activation of the non-selective voltage dependent cation channel. The increase of the intracellular Ca²⁺ content in RBCs leads to membrane shrinkage, membrane blebbing, PS exposure, and vesicle formation. The RBCs showing PS exposure on the outer leaflet of their membrane can propagate the cascade signal by the assembly of factors VIIIa, IXa, Xa, and Va. These factors activate the conversion of pro-thrombin to thrombin and the cycle is continued. In addition, the RBCs showing PS exposure also can adhere together. This adhesion facilitates the formation of the blood clots in the presence of fibrin network.

6. Summary

In the presented work the question about the role of Ca^{2+} in PS exposure process in RBCs has been clarified. Treatment of RBCs with LPA, A23187 and PMA in the presence of extracellular Ca^{2+} leads to an increase of the intracellular Ca^{2+} level, PS on the outer leaflet of the membrane, membrane blebbing, and microvesicle formation. These effects are influenced by the function of the phospholipid scramblase, flippase, protein kinase C and Gardos channel. It is also demonstrated that the exposure of PS does not only depend on the increase of the intracellular Ca^{2+} content but also on the function of protein kinase C. A model has been developed to contribute to our understanding of the mechanisms of this process.

The RBCs showing PS exposure can adhere together. This may explain why RBCs adhere together during blood clot formation. It seems likely that the interaction of PS with its receptors and PS-PS in the presence of Ca^{2+} play a substantial role. A model to explain the process of cell-cell adhesion is presented.

The hypothesis of the blood clot formation cascade developed by Kaestner and Bernhardt is also supported by experiments. The PS exposure on the outer leaflet of RBCs is an important factor for propagation the signal in clot formation process. A model in which the RBCs play an active role in blood clot formation is developed.

The question about the Ca^{2+} content in RBCs is also answered. There is no significant difference of the free Ca^{2+} content in young and old RBCs.

Zusammenfassung

In der vorliegenden Arbeit wurde die Rolle, die Ca^{2+} bei der PS-Exposition spielt, geklärt. Die Behandlung roter Blutzellen mit LPA, A23187 und PMA in Gegenwart von extrazellulärem Ca^{2+} führt zu einem Anstieg des intrazellulären Ca^{2+} , PS-Exposition, „Membrane Blebbing“ und der Bildung von Mikrovesikeln. Diese Effekte werden beeinflusst durch die Funktion der Phospholipid Scramblase, der Flippase, der Proteinkinase C und des Gardos Kanal. Auch wurde gezeigt, dass die PS-Exposition nicht nur vom Anstieg des intrazellulären Ca^{2+} abhängig ist sondern auch von der Funktion der Proteinkinase C.

Rote Blutzellen mit PS-Exposition können aneinander haften. Dies kann eine Erklärung dafür sein, weshalb rote Blutzellen bei der Bildung eines Gerinnsels adhären. Die Interaktion von PS mit seinen Rezeptoren und eine PS-PS-Interaktion in Gegenwart von Ca^{2+} übernehmen hierbei wahrscheinlich eine wichtige Rolle.

Die vorgeschlagene Kaskade von Kaestner und Bernhardt, die eine aktive Beteiligung roter Blutzellen an der Thrombusentstehung beschreibt, wird durch Experimente gestützt. Die Exposition von PS an die Außenseite der Membran ist hierbei ein wichtiger Faktor, welcher der Signalweiterleitung während der Thrombusentstehung dient.

Die Frage bezüglich des intrazellulären Ca^{2+} -Gehalts in roten Blutzellen wurde beantwortet. Es gibt keinen signifikanten Unterschied im Gehalt an freiem intrazellulärem Ca^{2+} zwischen jungen und alten roten Blutzellen.

7. References

1. Haest, C.W.M., *Distribution and movement of membrane lipids. In: Red cell membrane transport in health and disease (eds. Bernhardt, I., Elorry, J.C.)*. Springer-Verlag, Berlin, Heidelberg, New York, 2003, pp. 1-25.
2. Dodge J.T., Mitchell C., Hanahan D.J., *The preparation and chemical characteristics of hemoglobin-free ghosts of human erythrocytes*. Arch Biochem Biophys, 1963, **100**: 119-130.
3. Nelson, G.J., *Lipid composition and metabolism of erythrocytes. In: Blood lipids and lipoproteins: Quantitation, composition, and metabolism (eds. Nelson, G.J.)*. Wiley Interscience, New York, 1972, pp. 317-386.
4. Nelson, G.J., *Composition of neutral lipids from erythrocytes of common mammals*. J Lipid Res, 1967, **8**: 374-379.
5. Broekhuysse, R.M., *Improved lipid extraction of erythrocytes*. Clin Chim Acta, 1974, **51**: 341-343.
6. Broekhuysse, R.M., *Quantitative two-dimensional thin-layer chromatography of blood phospholipids*. Clin Chim Acta, 1969, **23**: 457-461.
7. Zwaal, R.F., Fluckiger, R., Moser, S., Zahler, P., *Lecithinase activities at the external surface of ruminant erythrocyte membranes*. Biochim Biophys Acta, 1974, **373**: 416-424.
8. Florin Christensen, J., Suarez, C.E., Florin Christensen, M., Wainszelbaum, M., Brown, W.C., McElwain, T.F., Palmer, G.H., *A unique phospholipid organization in bovine erythrocyte membranes*. Proc Natl Acad Sci USA, 2001, **98**: 7736-7741.
9. Farquhar, J.W., Ahrens, E.H., *Effects of dietary fats on human erythrocyte fatty acid patterns*. J Clin Invest, 1963, **42**: 675-685.
10. Rao, G.A., Siler, K., Larkin, E.C., *Diet-induced alterations in the discoid shape and phospholipid fatty acid compositions of rat erythrocytes*. Lipids, 1979, **14**: 30-38.
11. Shohet, S.B., *Hemolysis and changes in erythrocyte membrane lipids*. N Engl J Med, 1972, **286**: 577-583.
12. Renooij, W., Van Golde, L.M., Zwaal, R.F., Roelofsen, B., Van Deenen, L.L., *Preferential incorporation of fatty acids at the inside of human erythrocyte membranes*. Biochim Biophys Acta, 1974, **363**: 287-292.
13. Mandal, D., Mazumder, A., Das., P, Kundu, M., Basu, J., *Fas-, caspase 8-, and caspase 3-dependent signaling regulates the activity of the aminophospholipid translocase and phosphatidylserine externalization in human erythrocytes*. J Biol Chem, 2005, **280**: 39460-39467.
14. Woon, L.A., Holland, J.W., Kable, E.P., Roufogalis, B.D., *Ca²⁺ sensitivity of phospholipid scrambling in human red cell ghosts*. Cell Calcium, 1999, **25**: 313-320.

15. Verkleij, A.J., Zwaal, R.F., Roelofsen, B., Comfurius, P., Kastelijn, D., van Deenen, L.L., *The asymmetric distribution of phospholipids in the human red cell membrane. A combined study using phospholipases and freeze-etch electron microscopy*. Biochim Biophys Acta, 1973, **323**: 178-193.
16. Renooij, W., Van Golde, L.M., Zwaal, R.F., Van Deenen, L.L., *Topological asymmetry of phospholipid metabolism in rat erythrocyte membranes. Evidence for flip-flop of lecithin*. Eur J Biochem, 1976, **61**: 53-58.
17. Rawlyer, A., Van der Schaft, P.H., Roelofsen, B., Op den Kamp, J.A., *Phospholipid localization in the plasma membrane of friend erythroleukemic cells and mouse erythrocytes*. Biochemistry, 1985, **24**: 1777-1783.
18. Van der Schaft, P.H., Beaumelle, B., Vial, H., Roelofsen, B., Op den Kamp, J.A., Van Deenen, L.L., *Phospholipid organization in monkey erythrocytes upon Plasmodium knowlesi infection*. Biochim Biophys Acta, 1987, **901**: 1-14.
19. Bevers, E.M., Comfurius, P., Dekkers, D.W., Zwaal, R.F., *Lipid translocation across the plasma membrane of mammalian cells*. Biochim Biophys Acta, 1999, **1439**: 317-330.
20. Hugel, B., Martinez, M.C., Kunzelmann, C., Freyssinet, J.M., *Membrane microparticles: two sides of the coin*. Physiology (Bethesda), 2005, **20**: 22-27.
21. Yawata, Y., *Cell membrane: the red blood cell as a model*. WILEY-VCH Verlag, 2003, pp. 1-46.
22. Fairbanks, G., Steck, T.L., Wallach, D.F., *Electrophoretic analysis of the major polypeptides of the human erythrocyte membrane*. Biochemistry, 1971, **10**: 2606-2617.
23. Cohen, C.M., Gascard, P., *Regulation and post-translational modification of erythrocyte membrane and membrane-skeletal proteins*. Semin Hematol, 1992, **29**: 244-292.
24. Bernhardt, I., *Biomembranen - Wächter des zellulären Grenzverkehrs. Von Pumpen, Carriern und Kanälen*. Biologie in unserer Zeit, 2007, **37**: 310-319.
25. Skou, J.C., *The influence of some cations on an adenosine triphosphatase from peripheral nerves. 1957*, Biochim Biophys Acta, 1989, **1000**: 439-446.
26. Jorgensen, P.L., *Mechanism of the Na⁺,K⁺ pump. Protein structure and conformations of the pure (Na⁺,K⁺)-ATPase*. Biochim Biophys Acta, 1982, **694**: 27-68.
27. Mohraz, M., Smith, P.R., *Three-dimensional structure of Na,K-ATPase and a model for the oligomeric form and the mechanism of the Na,K pump*. Prog Clin Biol Res, 1988, **268A**: 99-106.
28. Parker, J.C., *Volume-activated cation transport in dog red cells: detection and transduction of the volume stimulus*. Comp Biochem Physiol Comp Physiol, 1992, **102**: 615-618.
29. Olesen, C., Picard, M., Winther, A.M., Gyruup, C., Morth, J.P., Oxvig, C., Moller, J.V., Nissen, P., *The structural basis of calcium transport by the calcium pump*. Nature, 2007, **450**: 1036-1042.

30. Kibak, H., Taiz, L., Starke, T., Bernasconi, P., Gogarten, J.P., *Evolution of structure and function of V-ATPases*. J Bioenerg Biomembr, 1992, **24**: 415-424.
31. Nelson, N., Perzov, N., Cohen, A., Hagai, K., Padler, V., Nelson, H., *The cellular biology of proton-motive force generation by V-ATPases*. J Exp Biol, 2000, **203**: 89-95.
32. Diepholz, M., Borsch, M., Bottcher, B., *Structural organization of the V-ATPase and its implications for regulatory assembly and disassembly*. Biochem Soc Trans, 2008, **36**: 1027-1031.
33. Gaballo, A., Zanotti, F., Papa, S., *Structures and interactions of proteins involved in the coupling function of the proton motive F_0F_1 -ATP synthase*. Curr Protein Pept Sci, 2002, **3**: 451-460.
34. Zanotti, F., Gnoni, A., Mangiullo, R., Papa, S., *Effect of the ATPase inhibitor protein IF1 on H^+ translocation in the mitochondrial ATP synthase complex*. Biochem Biophys Res Commun, 2009, **384**: 43-48.
35. Jones, P.M., George, A.M., *The ABC transporter structure and mechanism: perspectives on recent research*. Cell Mol Life Sci, 2004, **61**: 682-699.
36. Bennekou P., C.P., *Ion channels*. In: *Red cell membrane transport in health and disease* (eds. Bernhardt, I., Elorry, J.C.). Springer-Verlag, Berlin, Heidelberg, New York, 2003, pp. 139-152.
37. Hille, B., *Ion Channels of excitable membranes (3rd Edition)*. Sinauer Associates, 2001, pp. 61-168.
38. Miller, C., *An overview of the potassium channel family*. Genome Biol, 2000, **1**: 0004.1-0004.5.
39. Agre, P., *The aquaporin water channels*. Proc Am Thorac Soc, 2006, **3**: 5-13.
40. Bernhardt, I., Weiss, E., *Passive membrane permeability for ions and the membrane potential*. In: *Red cell membrane transport in health and disease* (eds. Bernhardt, I., Elorry, J.C.). Springer-Verlag, Berlin, Heidelberg, New York, 2003, pp. 83-109.
41. Devaux, P.F., Herrmann, A., Ohlwein, N., Kozlov, M.M., *How lipid flippases can modulate membrane structure*. Biochim Biophys Acta, 2008, **1778**: 1591-1600.
42. Daleke, D.L., *Regulation of transbilayer plasma membrane phospholipid asymmetry*. J Lipid Res, 2003, **44**: 233-242.
43. Daleke, D.L., *Regulation of phospholipid asymmetry in the erythrocyte membrane*. Curr Opin Hematol, 2008, **15**: 191-195.
44. Seigneuret, M., Devaux, P.F., *ATP-dependent asymmetric distribution of spin-labeled phospholipids in the erythrocyte membrane: relation to shape changes*. Proc Natl Acad Sci USA, 1984, **81**: 3751-3755.
45. Sleight, R.G., Pagano, R.E., *Transbilayer movement of a fluorescent phosphatidylethanolamine analogue across the plasma membranes of cultured mammalian cells*. J Biol Chem, 1985, **260**: 1146-1154.
46. Colleau, M., Herve, P., Fellmann, P., Devaux, P.F., *Transmembrane diffusion of fluorescent phospholipids in human erythrocytes*. Chem Phys Lipids, 1991, **57**: 29-37.

47. Bitbol, M., Fellmann, P., Zachowski, A., Devaux, P.F., *Ion regulation of phosphatidylserine and phosphatidylethanolamine outside-inside translocation in human erythrocytes*. *Biochim Biophys Acta*, 1987, **904**: 268-282.
48. Daleke, D.L., Huestis, W.H., *Incorporation and translocation of aminophospholipids in human erythrocytes*. *Biochemistry*, 1985, **24**: 5406-5416.
49. Contreras, F.X., Basanez, G., Alonso, A., Herrmann, A., Goni, F.M., *Asymmetric addition of ceramides but not dihydroceramides promotes transbilayer (flip-flop) lipid motion in membranes*. *Biophys J*, 2005, **88**: 348-359.
50. Schrier, S.L., Zachowski, A., Herve, P., Kader, J.C., Devaux, P.F., *Transmembrane redistribution of phospholipids of the human red cell membrane during hypotonic hemolysis*. *Biochim Biophys Acta*, 1992, **1105**: 170-176.
51. Sheetz, M.P., Dai, J., *Modulation of membrane dynamics and cell motility by membrane tension*. *Trends Cell Biol*, 1996, **6**: 85-89.
52. Rauch, C., Farge, E., *Endocytosis switch controlled by transmembrane osmotic pressure and phospholipid number asymmetry*. *Biophys J*, 2000, **78**: 3036-3047.
53. Dai, J., Sheetz, M.P., *Membrane tether formation from blebbing cells*. *Biophys J*, 1999, **77**: 3363-3370.
54. Zachowski, A., *Phospholipids in animal eukaryotic membranes: transverse asymmetry and movement*. *Biochem J*, 1993, **294**: 1-14.
55. Devaux, P.F., *Static and dynamic lipid asymmetry in cell membranes*. *Biochemistry*, 1991, **30**: 1163-1173.
56. Daleke, D.L., *Purification and substrate specificity of the human erythrocyte aminophospholipid transporter*. *NATO ASI Ser*, 1995, **91**: 49-59.
57. Morrot, G., Herve, P., Zachowski, A., Fellmann, P., Devaux, P.F., *Aminophospholipid translocase of human erythrocytes: phospholipid substrate specificity and effect of cholesterol*. *Biochemistry*, 1989, **28**: 3456-3462.
58. Stevens, H.C., Malone, L., Nichols, J.W., *The putative aminophospholipid translocases, DNF1 and DNF2, are not required for 7-nitrobenz-2-oxa-1,3-diazol-4-yl-phosphatidylserine flip across the plasma membrane of *Saccharomyces cerevisiae**. *J Biol Chem*, 2008, **283**: 35060-35069.
59. Pomorski, T., Holthuis, J.C., Herrmann, A., Van Meer, G., *Tracking down lipid flippases and their biological functions*. *J Cell Sci*, 2004, **117**: 805-813.
60. Zachowski, A., Favre, E., Cribier, S., Herve, P., Devaux, P.F., *Outside-inside translocation of aminophospholipids in the human erythrocyte membrane is mediated by a specific enzyme*. *Biochemistry*, 1986, **25**: 2585-2590.
61. Johnson, J.E., Zimmerman, M.L., Daleke, D.L., Newton, A.C., *Lipid structure and not membrane structure is the major determinant in the regulation of protein kinase C by phosphatidylserine*. *Biochemistry*, 1998, **37**: 12020-12025.
62. Hoffmann, P.R., de Cathelineau, A.M., Ogden, C.A., Leverrier, Y., Bratton, D.L., Daleke, D.L., Ridley, A.J., Fadok, V.A., Henson, P.M., *Phosphatidylserine (PS) induces PS receptor-mediated macropinocytosis and promotes clearance of apoptotic cells*. *J Cell Biol*, 2001, **155**: 649-660.

63. Fadok, V.A., de Cathelineau, A., Daleke, D.L., Henson, P.M., Bratton, D.L., *Loss of phospholipid asymmetry and surface exposure of phosphatidylserine is required for phagocytosis of apoptotic cells by macrophages and fibroblasts*. J Biol Chem, 2001, **276**: 1071-1077.
64. Hall, M.P., Huestis, W.H., *Phosphatidylserine headgroup diastereomers translocate equivalently across human erythrocyte membranes*. Biochim Biophys Acta, 1994, **1190**: 243-247.
65. Kuypers, F.A., Yuan, J., Lewis, R.A., Snyder, L.M., Kiefer, C.R., Bunyaratvej, A., Fucharoen, S., Ma, L., Styles, L., De Jong, K., Schrier, S.L., *Membrane phospholipid asymmetry in human thalassemia*. Blood, 1998, **91**: 3044-3051.
66. Dekkers, D.W., Comfurius, P., Schroit, A.J., Bevers, E.M., Zwaal, R.F., *Transbilayer movement of NBD-labeled phospholipids in red blood cell membranes: outward-directed transport by the multidrug resistance protein 1 (MRP1)*. Biochemistry, 1998, **37**: 14833-14837.
67. Connor, J., Pak, C.H., Zwaal, R.F., Schroit, A.J., *Bidirectional transbilayer movement of phospholipid analogs in human red blood cells. Evidence for an ATP-dependent and protein-mediated process*. J Biol Chem, 1992, **267**: 19412-19417.
68. Bitbol, M., Devaux, P.F., *Measurement of outward translocation of phospholipids across human erythrocyte membrane*. Proc Natl Acad Sci USA, 1988, **85**: 6783-6787.
69. Borst, P., Zelcer, N., Van Helvoort, A., *ABC transporters in lipid transport*. Biochim Biophys Acta, 2000, **1486**: 128-144.
70. Borst, P., Elferink, R.O., *Mammalian ABC transporters in health and disease*. Annu Rev Biochem, 2002, **71**: 537-592.
71. Williamson, P., Kulick, A., Zachowski, A., Schlegel, R.A., Devaux, P.F., *Ca²⁺ induces transbilayer redistribution of all major phospholipids in human erythrocytes*. Biochemistry, 1992, **31**: 6355-6360.
72. Zwaal, R.F., Schroit, A.J., *Pathophysiologic implications of membrane phospholipid asymmetry in blood cells*. Blood, 1997, **89**: 1121-1132.
73. Toti, F., Satta, N., Fressinaud, E., Meyer, D., Freyssinet, J.M., *Scott syndrome, characterized by impaired transmembrane migration of procoagulant phosphatidylserine and hemorrhagic complications, is an inherited disorder*. Blood, 1996, **87**: 1409-1415.
74. Wiedmer, T., Zhou, Q., Kwoh, D.Y., Sims, P.J., *Identification of three new members of the phospholipid scramblase gene family*. Biochim Biophys Acta, 2000, **1467**: 244-253.
75. Strausberg, R.L., Feingold, E.A., Grouse, L.H., Derge, J.G., Klausner, R.D., Collins, F.S., Wagner, L., Shenmen, C.M., Schuler, G.D., Altschul, S.F., Zeeberg, B., Buetow, K.H., Schaefer, C.F., Bhat, N.K., Hopkins, R.F., Jordan, H., Moore, T., Max, S.I., Wang, J., Hsieh, F., Diatchenko, L., Marusina, K., Farmer, A. A., Rubin, G.M., Hong, L., Stapleton, M., Soares, M.B., Bonaldo, M.F., Casavant, T.L., Scheetz, T.E., Brownstein, M.J., Usdin, T.B., Toshiyuki, S., Carninci, P., Prange, C., Raha, S.S., Loquellano, N.A., Peters, G.J., Abramson, R.D., Mullahy, S.J., Bosak, S.A., McEwan, P.J., McKernan, K.J., Malek, J.A., Gunaratne, P.H., Richards, S., Worley, K.C., Hale, S., Garcia, A.M., Gay, L.J., Hulyk, S.W.,

- Villalon, D.K., Muzny, D.M., Sodergren, E.J., Lu, X., Gibbs, R.A., Fahey, J., Helton, E., Kettman, M., Madan, A., Rodrigues, S., Sanchez, A., Whiting, M., Young, A.C., Shevchenko, Y., Bouffard, G.G., Blakesley, R.W., Touchman, J.W., Green, E.D., Dickson, M.C., Rodriguez, A.C., Grimwood, J., Schmutz, J., Myers, R.M., Butterfield, Y.S., Krzywinski, M.I., Skalska, U., Smailus, D.E., Schnerch, A., Schein, J.E., Jones, S.J., Marra, M.A., *Generation and initial analysis of more than 15,000 full-length human and mouse cDNA sequences*. Proc Natl Acad Sci USA, 2002, **99**: 16899-16903.
76. Sahu, S.K., Gopala Krishna, A., Gummadi, S.N., *Over-expression of recombinant human phospholipid scramblase 1 in E. coli and its purification from inclusion bodies*. Biotechnol Lett, 2008, **30**: 2131-2137.
77. Lopez-Montero, I., Velez, M., Devaux, P.F., *Surface tension induced by sphingomyelin to ceramide conversion in lipid membranes*. Biochim Biophys Acta, 2007, **1768**: 553-561.
78. Frasnch, S.C., Henson, P.M., Kailey, J.M., Richter, D.A., Janes, M.S., Fadok, V.A., Bratton, D.L., *Regulation of phospholipid scramblase activity during apoptosis and cell activation by protein kinase Cdelta*. J Biol Chem, 2000, **275**: 23065-23073.
79. Schroit, A.J., Zwaal, R.F., *Transbilayer movement of phospholipids in red cell and platelet membranes*. Biochim Biophys Acta, 1991, **1071**: 313-329.
80. Manodori, A.B., Barabino, G.A., Lubin, B.H., Kuypers, F.A., *Adherence of phosphatidylserine-exposing erythrocytes to endothelial matrix thrombospondin*. Blood, 2000, **95**: 1293-1300.
81. Blumenfeld, N., Zachowski, A., Galacteros, F., Beuzard, Y., Devaux, P.F., *Transmembrane mobility of phospholipids in sickle erythrocytes: Effect of deoxygenation on diffusion and asymmetry*. Blood, 1991, **77**: 849-854.
82. De Jong, K., Larkin, S.K., Styles, L.A., Bookchin, R.M., Kuypers, F.A., *Characterization of the phosphatidylserine-exposing subpopulation of sickle cells*. Blood, 2001, **98**: 860-867.
83. Muller, P., Zachowski, A., Beuzard, Y., Devaux, P.F., *Transmembrane mobility and distribution of phospholipids in the membrane of mouse beta-thalassaemic red blood cells*. Biochim Biophys Acta, 1993, **1151**: 7-12.
84. Cines, D.B., Pollak, E.S., Buck, C.A., Loscalzo, J., Zimmerman, G.A., McEver, R.P., Pober, J.S., Wick, T.M., Konkle, B.A., Schwartz, B.S., Barnathan, E.S., McCrae, R., Hug, B.A., Schmidt, A.M., Stern, D.M., *Endothelial cells in physiology and in the pathophysiology of vascular disorders*. Blood, 1998, **91**: 3527-3561.
85. Fadok, V.A., Bratton, D.L., Frasnch, S.C., Warner, M.L., Henson, P.M., *The role of phosphatidylserine in recognition of apoptotic cells by phagocytes*. Cell Death Differ, 1998, **5**: 551-562.
86. Andrews, D.A., Low, P.S., *Role of red blood cells in thrombosis*. Curr Opin Hematol, 1999, **6**: 76-82.
87. Turitto, V.T., Weiss, H.J., *Red blood cells: their dual role in thrombus formation*. Science, 1980, **207**: 541-543.

88. Solum, N.O., *Procoagulant expression in platelets and defects leading to clinical disorders*. *Arterioscler Thromb Vasc Biol*, 1999, **19**: 2841-2846.
89. Weiss, H.J., Lages, B., *Platelet prothrombinase activity and intracellular calcium responses in patients with storage pool deficiency, glycoprotein IIb-IIIa deficiency, or impaired platelet coagulant activity a comparison with Scott syndrome*. *Blood*, 1997, **89**: 1599-1611.
90. Wu, Y., Tibrewal, N., Birge, R.B., *Phosphatidylserine recognition by phagocytes: a view to a kill*. *Trends Cell Biol*, 2006, **16**: 189-197.
91. Verhoven, B., Schlegel, R.A., Williamson, P., *Mechanisms of phosphatidylserine exposure, a phagocyte recognition signal, on apoptotic T lymphocytes*. *J Exp Med*, 1995, **182**: 1597-1601.
92. Uchida, K., *Induction of apoptosis by phosphatidylserine*. *J Biochem*, 1998, **123**: 1073-1078.
93. Schlegel, R.A., Williamson, P., *Phosphatidylserine, a death knell*. *Cell Death Differ*, 2001, **8**: 551-563.
94. Ravichandran, K.S., Lorenz, U., *Engulfment of apoptotic cells: signals for a good meal*. *Nat Rev Immunol*, 2007, **7**: 964-974.
95. Kuypers, F.A., De Jong, K., *The role of phosphatidylserine in recognition and removal of erythrocytes*. *Cell Mol Biol*, 2004, **50**: 147-158.
96. Lang, P.A., Kaiser, S., Myssina, S., Wider, T., Lang, F., Huber, S.M., *Role of Ca^{2+} -activated K^+ channels in human erythrocyte apoptosis*. *Am J Physiol Cell Physiol*, 2003, **285**: C1553-C1560.
97. Lang, F., Shumilina, E., Ritter, M., Gulbins, E., Vereninov, A., Huber, S.M., *Ion channels and cell volume in regulation of cell proliferation and apoptotic cell death*. In: *Mechanisms and significance of cell volume regulation. Contributions to nephrology (ed. Lang, F.)*. Karger, Basel Freiburg Paris London New York, 2006, pp. 142-160.
98. Lang, F., *Mechanisms and significance of cell volume regulation*. *J Am Coll Nutr*, 2007, **26**: 613S-623S.
99. Kaestner, L., Tabellion, W., Lipp, P., Bernhardt, I., *Prostaglandin E_2 activates channel-mediated calcium entry in human erythrocytes: an indication for a blood clot formation supporting process*. *Thromb Haemost*, 2004, **92**: 1269-1272.
100. Lang, F., Lang, K.S., Lang, P.A., Huber, S.M., Wieder, T., *Osmotic shock-induced suicidal death of erythrocytes*. *Acta Physiol (Oxford)*, 2006, **187**: 191-198.
101. Akel, A., Hermle, T., Niemoeller, O.M., Kempe, D.S., Lang, P.A., Attanasio, P., Podolski, M., Wieder, T., Lang, F., *Stimulation of erythrocyte phosphatidylserine exposure by chlorpromazine*. *Eur J Pharmacol*, 2006, **532**: 11-17.
102. Sopjani, M., Foller, M., Lang, F., *Gold stimulates Ca^{2+} entry into and subsequent suicidal death of erythrocytes*. *Toxicology*, 2008, **244**: 271-279.
103. Sopjani, M., Föller, M., Dreischer, P., Lang, F., *Stimulation of eryptosis by cadmium ions*. *Cell Physiol Biochem*, 2008, **22**: 245-252.
104. Föller, M., Sopjani, M., Mahmud, H., Lang, F., *Vanadate-induced suicidal erythrocyte death*. *Kidney Blood Press Res*, 2008, **31**: 87-93.

105. Braun, M., Foller, M., Gulbins, E., Lang, F., *Eryptosis triggered by bismuth*. *Biomaterials*, 2009, **22**: 453-460.
106. Lang, K.S., Durantou, C., Poehlmann, H., Myssina, S., Bauer, C., Lang, F., Wieder, T., Huber, S.M., *Cation channels trigger apoptotic death of erythrocytes*. *Cell Death Differ*, 2003, **10**: 249-256.
107. Klarl, B.A., Lang, P.A., Kempe, D.S., Niemoeller, O.M., Akel, A., Sobiesiak, M., Eisele, K., Podolski, M., Huber, S.M., Wieder, T., Lang, F., *Protein kinase C mediates erythrocyte "programmed cell death" following glucose depletion*. *Am J Physiol Cell Physiol*, 2006, **290**: C244-C253.
108. Quan, G.B., Han, Y., Yang, C., Hu, W.B., Liu, M.X., Liu, A., Wang, Y., Wang, J.X., *Mechanism of erythrocyte phosphatidylserine exposure induced by high concentrated glucose*. *Zhongguo Shi Yan Xue Ye Xue Za Zhi*, 2008, **16**: 1181-1184.
109. Kiedaisch, V., Akel, A., Niemoeller, O.M., Wieder, T., Lang, F., *Zinc-induced suicidal erythrocyte death*. *Am J Clin Nutr*, 2008, **87**: 1530-1534.
110. Kempe, D.S., Lang, P.A., Eisele, K., Klarl, B.A., Wieder, T., Huber, S.M., Durantou, C., Lang, F., *Stimulation of erythrocyte phosphatidylserine exposure by lead ions*. *Am J Physiol Cell Physiol*, 2005, **288**: C396-C402.
111. Berg, C.P., Engels, I.H., Rothbart, A., Lauber, K., Renz, A., Schlosser, S.F., Schulze-Osthoff, K., Wesselborg, S., *Human mature red blood cells express caspase-3 and caspase-8, but are devoid of mitochondrial regulators of apoptosis*. *Cell Death Differ*, 2001, **8**: 1197-1206.
112. Sutton, D.J., Tchounwou, P.B., *Mercury-induced externalization of phosphatidylserine and caspase 3 activation in human liver carcinoma (HepG2) cells*. *Int J Environ Res Public Health*, 2006, **3**: 38-42.
113. Mandal, D., Moitra, P.K., Saha, S., Basu, J., *Caspase 3 regulates phosphatidylserine externalization and phagocytosis of oxidatively stressed erythrocytes*. *FEBS Lett*, 2002, **513**: 184-188.
114. Diamant, M., Tushuizen, M.E., Sturk, A., Nieuwland, R., *Cellular microparticles: new players in the field of vascular disease?* *Eur J Clin Invest*, 2004, **34**: 392-401.
115. Setty, B.N., Kulkarni, S., Stuart, M.J., *Role of erythrocyte phosphatidylserine in sickle red cell-endothelial adhesion*. *Blood*, 2002, **99**: 1564-1571.
116. Telen, M.J., *Red blood cell surface adhesion molecules: their possible roles in normal human physiology and disease*. *Semin Hematol*, 2000, **37**: 130-142.
117. Closse, C., Dachary-Prigent, J., Boisseau, M.R., *Phosphatidylserine-related adhesion of human erythrocytes to vascular endothelium*. *Br J Haematol*, 1999, **107**: 300-302.
118. Fox, J.E., *Shedding of adhesion receptors from the surface of activated platelets*. *Blood Coagul Fibrinolysis*, 1994, **5**: 291-304.
119. Holme, P.A., Solum, N.O., Brosstad, F., Pedersen, T., Kveine, M., *Microvesicles bind soluble fibrinogen, adhere to immobilized fibrinogen and coaggregate with platelets*. *Thromb Haemost*, 1998, **79**: 389-394.

120. Jimenez, J.J., Jy, W., Mauro, L.M., Horstman, L.L., Soderland, C., Ahn, Y.S., *Endothelial microparticles released in thrombotic thrombocytopenic purpura express von Willebrand factor and markers of endothelial activation*. Br J Haematol, 2003, **123**: 896-902.
121. Duke, W.W., *The relation of blood platelets to hemorrhagic disease*. JAMA, 1983, **250**: 1201-1209.
122. Hellem, A.J., Borchgrevink, C.F., Ames, S.B., *The role of red cells in haemostasis: the relation between haematocrit, bleeding time and platelet adhesiveness*. Br J Haematol, 1961, **7**: 42-50.
123. Blajchman, M.A., Bordin, J.O., Bardossy, L., Heddle, N.M., *The contribution of the haematocrit to thrombocytopenic bleeding in experimental animals*. Br J Haematol, 1994, **86**: 347-350.
124. Chung, S.M., Bae, O.N., Lim, K.M., Noh, J.Y., Lee, M.Y., Jung, Y.S., Chung, J.H., *Lysophosphatidic acid induces thrombogenic activity through phosphatidylserine exposure and procoagulant microvesicle generation in human erythrocytes*. Arterioscler Thromb Vasc Biol, 2007, **27**: 414-421.
125. Tiffert, T., Bookchin, R.M., Lew, V.L., *Calcium homeostasis in normal and abnormal human red cells*. In: *Red cell membrane transport in health and disease* (eds. Bernhardt, I., Elorry, J.C.). Springer-Verlag, Berlin, Heidelberg, New York, 2003, pp. 373-405.
126. Lew, V.L., Tsien, R.Y., Miner, C., Bookchin, R.M., *Physiological $[Ca^{2+}]_i$ level and pump-leak turnover in intact red cells measured using an incorporated Ca chelator*. Nature, 1982, **298**: 478-481.
127. Desai, S.A., Schlesinger, P.H., Krogstad, D.J., *Physiologic rate of carrier-mediated Ca^{2+} entry matches active extrusion in human erythrocytes*. J Gen Physiol, 1991, **98**: 349-364.
128. Ferreira, H.G., Lew, V.L., *Passive Ca transport and cytoplasmic Ca buffering in intact red cells*. In: *Membrane transport in red cells*, (eds. Ellory, J. C., Lew, V. L.) Academic Press, London., 1977, pp. 53-91.
129. Carafoli, E., *Plasma membrane calcium pump: structure, function and relationships*. Basic Res Cardiol, 1997, **92**: 59-61.
130. Kaestner, L., Tabellion, W., Weiss, E., Bernhardt, I., Lipp, P., *Calcium imaging of individual erythrocytes: problems and approaches*. Cell Calcium, 2006, **39**: 13-19.
131. Tiffert, T., Lew, V.L., *Apparent Ca^{2+} dissociation constant of Ca^{2+} chelators incorporated non-disruptively into intact human red cells*. J Physiol, 1997, **505**: 403-410.
132. Tiffert, T., Etzion, Z., Bookchin, R.M., Lew, V.L., *Effects of deoxygenation on active and passive Ca^{2+} transport and cytoplasmic Ca^{2+} buffering in normal human red cells*. J Physiol, 1993, **464**: 529-544.
133. Williamson, P., Bevers, E.M., Smeets, E.F., Comfurius, P., Schlegel, R.A., Zwaal, R.F., *Continuous analysis of the mechanism of activated transbilayer lipid movement in platelets*. Biochemistry, 1995, **34**: 10448-10455.

134. Martin, D.W., Jesty, J., *Calcium stimulation of procoagulant activity in human erythrocytes. ATP dependence and the effects of modifiers of stimulation and recovery.* J Biol Chem, 1995, **270**: 10468-10474.
135. Romero, P.J., Romero, E.A., *The role of calcium metabolism in human red blood cell ageing: a proposal.* Blood Cells Mol Dis, 1999, **25**: 9-19.
136. Yang, L., Andrews, D.A., Low, P.S., *Lysophosphatidic acid opens a Ca²⁺ channel in human erythrocytes.* Blood, 2000, **95**: 2420-2425.
137. Itagaki, K., Kannan, K.B., Hauser, C.J., *Lysophosphatidic acid triggers calcium entry through a non-store-operated pathway in human neutrophils.* J Leukoc Biol, 2005, **77**: 181-189.
138. Orrenius, S., Zhivotovsky, B., Nicotera, P., *Regulation of cell death: the calcium-apoptosis link.* Nat Rev Mol Cell Biol, 2003, **4**: 552-565.
139. Saito, N., Kikkawa, U., Nishizuka, Y., *The family of protein kinase C and membrane lipid mediators.* J Diabetes Complications, 2002, **16**: 4-8.
140. Andrews, D.A., Yang, L., Low, P. S., *Phorbol ester stimulates a protein kinase C-mediated agatoxin-TK-sensitive calcium permeability pathway in human red blood cells.* Blood, 2002, **100**: 3392-3399.
141. Murphy, H.S., Maroughi, M., Till, G.O., Ward, P.A., *Phorbol-stimulated influx of extracellular calcium in rat pulmonary artery endothelial cells.* Am J Physiol, 1994, **267**: L145-L151.
142. Romero, P.J., Romero, E.A., Mateu, D., Hernandez, C., Fernandez, I., *Voltage-dependent calcium channels in young and old human red cells.* Cell Biochem Biophys, 2006, **46**: 265-276.
143. De Jong, K., Rettig, M.P., Low, P.S., Kuypers, F.A., *Protein kinase C activation induces phosphatidylserine exposure on red blood cells.* Biochemistry, 2002, **41**: 12562-12567.
144. Nishizuka, Y., Nakamura, S., *Lipid mediators and protein kinase C for intracellular signalling.* Clin Exp Pharmacol Physiol Suppl, 1995, **22**: S202-S203.
145. Nakamura, S., *Phosphatidylcholine hydrolysis and protein kinase C activation for intracellular signaling network.* J. Lipid Mediat Cell Signal, 1996, **14**: 197-202.
146. Tanaka, C., Nishizuka, Y., *The protein kinase C family for neuronal signaling.* Annu Rev Neurosci, 1994, **17**: 551-567.
147. Bessis, M., *Living blood cells and their ultrastructure.* Springer-Verlag, Berlin, Heidelberg, New York, 1973, pp. 85-261.
148. Kemp, P., Ellory, J.C., Munn, E.A., *Changes in the phospholipid composition of sheep reticulocytes on maturation.* Biochem Soc Trans, 1975, **3**: 749-751.
149. Lutz, H.U., Stammeler, P., Fasler, S., Ingold, M., Fehr, J., *Density separation of human red blood cells on self forming Percoll gradients: correlation with cell age.* Biochim Biophys Acta, 1992, **1116**: 1-10.
150. Canham, P.B., *Difference in geometry of young and old human erythrocytes explained by a filtering mechanism.* Circ Res, 1969, **25**: 39-45.

151. Tiffert, T., Daw, N., Etzion, Z., Bookchin, R.M., Lew, V.L., *Age decline in the activity of the Ca²⁺-sensitive K⁺ channel of human red blood cells*. J Gen Physiol, 2007, **129**: 429-436.
152. McLellan, A.C., Thornalley, P.J., *Glyoxalase activity in human red blood cells fractionated by age*. Mech Ageing Dev, 1989, **48**: 63-71.
153. Burton, G.W., Cheng, S.C., Webb, A., Ingold, K.U., *Vitamin E in young and old human red blood cells*. Biochim Biophys Acta, 1986, **860**: 84-90.
154. Magnani, M., Cucchiaroni, L., Stocchi, V., Dacha, M., Fornaini, G., *Adult and fetal galactokinases in human red blood cells*. Mech Ageing Dev, 1982, **18**: 215-223.
155. Shimizu, Y., Suzuki, M., *The relationship between red cell aging and enzyme activities in experimental animals*. Comp Biochem Physiol B, 1991, **99**: 313-316.
156. Rizvi, S.I., Jha, R., Maurya, P.K., *Erythrocyte plasma membrane redox system in human aging*. Rejuvenation Res, 2006, **9**: 470-474.
157. Hyun, D.H., Hernandez, J.O., Mattson, M.P., de Cabo, R., *The plasma membrane redox system in aging*. Ageing Res Rev, 2006, **5**: 209-220.
158. Romero, P.J., Romero, E.A., Winkler, M.D., *Ionic calcium content of light dense human red cells separated by Percoll density gradients*. Biochim Biophys Acta, 1997, **1323**: 23-28.
159. Kirkpatrick, F.H., Muhs, A.G., Kostuk, R.K., Gabel, C.W., *Dense (aged) circulating red cells contain normal concentrations of adenosine triphosphate (ATP)*. Blood, 1979, **54**: 946-950.
160. Siems, W.G., Sommerburg, O., Grune, T., *Erythrocyte free radical and energy metabolism*. Clin Nephrol, 2000, **53**: S9-S17.
161. Matteucci, E., Giampietro, O., *Electron pathways through erythrocyte plasma membrane in human physiology and pathology: potential redox biomarker?* Biomarker Insights, 2007, **2**: 321-329.
162. Arese, P., Turrini, F., Schwarzer, E., *Band 3/complement-mediated recognition and removal of normally senescent and pathological human erythrocytes*. Cell Physiol Biochem, 2005, **16**: 133-146.
163. Grey, A.D.N.J.d., *The plasma membrane redox system: a candidate source of aging-related oxidative stress*. AGE, 2005, **27**: 129-138.
164. Medina, M.A., Del Castillo-Olivares, A., Nunez de Castro, I., *Multifunctional plasma membrane redox systems*. Bioessays, 1997, **19**: 977-984.
165. Del Principe, D., Frega, G., Savini, I., Catani, M.V., Rossi, A., Avigliano, L., *The plasma membrane redox system in human platelet functions and platelet-leukocyte interactions*. Thromb Haemost, 2009, **101**: 284-289.
166. Bosman, G.J., Willekens, F.L., Werre, J.M., *Erythrocyte aging: a More than superficial resemblance to apoptosis?* Cell Physiol Biochem, 2005, **16**: 1-8.
167. Franco, R.S., Yasin, Z., Lohmann, J.M., Palascak, M.B., Nemeth, T.A., Weiner, M., Joiner, C.H., Rucknagel, D.L., *The survival characteristics of dense sickle cells*. Blood, 2000, **96**: 3610-3617.

168. Chiu, D., Lubin, B., Roelofsen, B., van Deenen, L.L., *Sickled erythrocytes accelerate clotting in vitro: an effect of abnormal membrane lipid asymmetry*. Blood, 1981, **58**: 398-401.
169. Gee, K.R., Brown, K.A., Chen, W.N., Bishop Stewart, J., Gray, D., Johnson, I., *Chemical and physiological characterization of fluo-4 Ca²⁺-indicator dyes*. Cell Calcium, 2000, **27**: 97-106.
170. Tiffert, T., Spivak, J.L., Lew, V.L., *Magnitude of calcium influx required to induce dehydration of normal human red cells*. Biochim Biophys Acta, 1988, **943**: 157-165.
171. Morris, M.J., Dufilho, M.D., Devynck, M.A., *In vivo and in vitro effects of isradipine on cytosolic Ca²⁺ concentration in erythrocytes from spontaneously hypertensive rats*. Am J Hypertens, 1992, **5**: 887-891.
172. Williams, D.A., Fay, F.S., *Intracellular calibration of the fluorescence calcium indicator fura-2*. Cell Calcium, 1990, **11**: 75-83.
173. Blackwood, A.M., Sagnella, G. A., Markandu, N. D., MacGregor, G. A., *Problems associated with using Fura-2 to measure free intracellular calcium concentrations in human red blood cells*. J Hum Hypertens, 1997, **11**: 601-604.
174. Tsien, R.Y., *Fluorescent indicators of ion concentrations*. Methods Cell Biol, 1989, **30**: 127-156.
175. Thomas, J.A., Buchsbaum, R.N., Zimniak, A., Racker, E., *Intracellular pH measurements in Ehrlich ascites tumor cells utilizing spectroscopic probes generated in situ*. Biochemistry, 1979, **18**: 2210-2218.
176. Dunham, P.B., Ellory, J.C., *Passive potassium transport in low potassium sheep red cells: dependence upon cell volume and chloride*. J Physiol, 1981, **318**: 511-530.
177. Ellory, J.C., Flatman, P.W., Stewart, G.W., *Inhibition of human red cell sodium and potassium transport by divalent cations*. J Physiol, 1983, **340**: 1-17.
178. Avron, M., Shavit, N., *A sensitive and simple method for determination of ferrocyanide*. Anal Biochem, 1963, **6**: 549-554.
179. Inada, Y., Okamoto, H., Kanai, S., Tamaura, Y., *Faster determination of clottable fibrinogen in human plasma: an improved method and kinetic study*. Clin Chem, 1978, **24**: 351-353.
180. Laemmli, U.K., *Cleavage of structural proteins during the assembly of the head of bacteriophage T4*. Nature, 1970, **227**: 680-685.
181. Veeco Metrology Group., *Scanning probe microscopy training notebook*. Digital instruments, 2000, (version 3), pp. 1-56.
182. Howland, R., Benatar, L., *A practical guide to scanning probe*. Park Scientific Instruments, 1997, pp. 1-79.
183. Saitou, N., Nei, M., *The neighbor-joining method: a new method for reconstructing phylogenetic trees*. Mol Biol Evol, 1987, **4**: 406-425.
184. King, W.G., Rittenhouse, S.E., *Inhibition of protein kinase C by staurosporine promotes elevated accumulations of inositol trisphosphates and tetrakisphosphate in human platelets exposed to thrombin*. J Biol Chem, 1989, **264**: 6070-6074.

185. Kucherenko, Y.V., Weiss, E., Bernhardt, I., *Effect of the ionic strength and prostaglandin E₂ on the free Ca²⁺ concentration and the Ca²⁺ influx in human red blood cells*. Bioelectrochemistry, 2004, **62**: 127-133.
186. Altschul, S.F., Gish, W., Miller, W., Myers, E.W., Lipman, D.J., *Basic local alignment search tool*. J Mol Biol, 1990, **215**: 403-410.
187. Altschul, S.F., Madden, T.L., Schaffer, A.A., Zhang, J., Zhang, Z., Miller, W., Lipman, D.J., *Gapped BLAST and PSI-BLAST: a new generation of protein database search programs*. Nucleic Acids Res, 1997, **25**: 3389-3402.
188. Lutz, H.U., Stammeler, P., Fasler, S., Ingold, M., Fehr, J., *Density separation of human red blood cells on self forming Percoll gradients: correlation with cell age*. Biochim Biophys Acta, 1992, **1116**: 1-10.
189. Inaba, M., Maede, Y., *Correlation between protein 4.1a/4.1b ratio and erythrocyte life span*. Biochim Biophys Acta, 1988, **944**: 256-264.
190. Romero, P.I., Romero, E.A., *The role of calcium metabolism in human red blood cell ageing: a proposal*. Blood Cells, Molecules, and Diseases, 1999, **25**: 9-19.
191. Ringer, S., *A further contribution regarding the influence of the different constituents of the blood on the contraction of the heart*. J Physiol, 1883, **4**: 29-42.
192. Murphy, E., Berkowitz, L.R., Orringer, E., Levy, L., Gabel, S.A., London, R.E., *Cytosolic free calcium levels in sickle red blood cells*. Blood, 1987, **69**: 1469-1474.
193. Gazarini, M.L., Thomas, A.P., Pozzan, T., Garcia, C.R., *Calcium signaling in a low calcium environment: how the intracellular malaria parasite solves the problem*. J Cell Biol, 2003, **161**: 103-110.
194. Stout, J.G., Zhou, Q., Wiedmer, T., Sims, P.J., *Change in conformation of plasma membrane phospholipid scramblase induced by occupancy of its Ca²⁺ binding site*. Biochemistry, 1998, **37**: 14860-14866.
195. Basse, F., Stout, J.G., Sims, P.J., Wiedmer, T., *Isolation of an erythrocyte membrane protein that mediates Ca²⁺-dependent transbilayer movement of phospholipid*. J Biol Chem, 1996, **271**: 17205-17210.
196. Govekar, R.B., Zingde, S.M., *Protein kinase C isoforms in human erythrocytes*. Ann Hematol, 2001, **80**: 531-534.
197. Verhoven, B., Schlegel, R.A., Williamson, P., *Mechanisms of phosphatidylserine exposure, a phagocyte recognition signal, on apoptotic T lymphocytes*. J Exp Med, 1995, **182**: 1597-1601.
198. Schlegel, R.A., Callahan, M.K., Williamson, P., *The central role of phosphatidylserine in the phagocytosis of apoptotic thymocytes*. Ann N Y Acad Sci, 2000, **926**: 217-225.
199. Krieser, R.J., White, K., *Engulfment mechanism of apoptotic cells*. Curr Opin Cell Biol, 2002, **14**: 734-738.
200. Wolfs, J.L., Comfurius, P., Rasmussen, J.T., Keuren, J.F., Lindhout, T., Zwaal, R.F., Bevers, E.M., *Activated scramblase and inhibited aminophospholipid translocase cause phosphatidylserine exposure in a distinct platelet fraction*. Cell Mol Life Sci, 2005, **62**: 1514-1525.

201. Schoenwaelder, S.M., Yuan, Y., Josefsson, E.C., White, M.J., Yao, Y., Mason, K.D., O'Reilly, L.A., Henley, K.J., Ono, A., Hsiao, S., Willcox, A., Roberts, A.W., Huang, D., Salem, H.H., Kile, B.T., Jackson, S.P., *Two distinct pathways regulate platelet phosphatidylserine exposure and procoagulant function*. *Blood*, 2009, **114**: 663-666.
202. Eichholtz, T., Jalink, K., Fahrenfort, I., Moolenaar, W.H., *The bioactive phospholipid lysophosphatidic acid is released from activated platelets*. *Biochem J*, 1993, **291**: 677-680.
203. Pages, C., Simon, M.F., Valet, P., Saulnier-Blache, J. S., *Lysophosphatidic acid synthesis and release*. *Prostaglandins Other Lipid Mediat*, 2001, **64**: 1-10.
204. Moolenaar, W.H., *Lysophosphatidic acid signalling*. *Curr Opin Cell Biol*, 1995, **7**: 203-210.
205. Gaits, F., Fourcade, O., Le Balle, F., Gueguen, G., Gaige, B., Gassama-Diagne, A., Fauvel, J., Salles, J.P., Mauco, G., Simon, M.F., Chap, H., *Lysophosphatidic acid as a phospholipid mediator: pathways of synthesis*. *FEBS Lett*, 1997, **410**: 54-58.
206. Kaestner, L., Bollensdorff, C., Bernhardt, I., *Non-selective voltage-activated cation channel in the human red blood cell membrane*. *Biochim Biophys Acta*, 1999, **1417**: 9-15.
207. Kaestner, L., Christophersen, P., Bernhardt, I., Bennekou, P., *The non-selective voltage-activated cation channel in the human red blood cell membrane: reconciliation between two conflicting reports and further characterisation*. *Bioelectrochemistry*, 2000, **52**: 117-125.
208. Kaestner, L., Bernhardt, I., *Ion channels in the human red blood cell membrane: their further investigation and physiological relevance*. *Bioelectrochemistry*, 2002, **55**: 71-74.
209. Tiffert, T., Lew, V.L., *Kinetics of inhibition of the plasma membrane calcium pump by vanadate in intact human red cells*. *Cell Calcium*, 2001, **30**: 337-342.
210. Sahu, S.K., Gummadi, S.N., Manoj, N., Aradhyam, G.K., *Phospholipid scramblases: an overview*. *Arch Biochem Biophys*, 2007, **462**: 103-114.
211. Verhoven, B., Schlegel, R.A., Williamson, P., *Rapid loss and restoration of lipid asymmetry by different pathways in resealed erythrocyte ghosts*. *Biochim Biophys Acta*, 1992, **1104**: 15-23.
212. Williamson, P., Algarin, L., Bateman, J., Choe, H.R., Schlegel, R.A., *Phospholipid asymmetry in human erythrocyte ghosts*. *J Cell Physiol*, 1985, **123**: 209-214.
213. Govekar, R.B., Zingde, S.M., *Protein kinase C isoforms in human erythrocytes*. *Ann Hematol*, 2001, **80**: 531-534.
214. Bucki, R., Pastore, J.J., Giraud, F., Janmey, P.A., Sulpice, J.C., *Involvement of the Na⁺/H⁺ exchanger in membrane phosphatidylserine exposure during human platelet activation*. *Biochim Biophys Acta*, 2006, **1761**: 195-204.
215. Zsembery, A., Strazzabosco, M., Graf, J., *Ca²⁺-activated Cl⁻ channels can substitute for CFTR in stimulation of pancreatic duct bicarbonate secretion*. *FASEB J*, 2000, **14**: 2345-2356.

216. Wagner, J.A., Cozens, A.L., Schulman, H., Gruenert, D.C., Stryer, L., Gardner, P., *Activation of chloride channels in normal and cystic fibrosis airway epithelial cells by multifunctional calcium/calmodulin-dependent protein kinase*. *Nature*, 1991, **349**: 793-796.
217. Kummerow, D., Hamann, J., Browning, J.A., Wilkins, R., Ellory, J.C., Bernhardt, I., *Variations of intracellular pH in human erythrocytes via (K⁺, Na⁺)/H⁺ exchange under low ionic strength conditions*. *J Membr Biol*, 2000, **176**: 207-216.
218. Ohki, S., Duzgunes, N., Leonards, K., *Phospholipid vesicle aggregation: effect of monovalent and divalent ions*. *Biochemistry*, 1982, **21**: 2127-2133.
219. Nir, S., Duzgunes, N., Bentz, J., *Binding of monovalent cations to phosphatidylserine and modulation of Ca²⁺ and Mg²⁺ induced vesicle fusion*. *Biochim Biophys Acta*, 1983, **735**: 160-172.
220. Bentz, J., Duzgune, N., Nir, S., *Kinetics of divalent cation induced fusion of phosphatidylserine vesicles: correlation between fusogenic capacities and binding affinities*. *Biochemistry*, 1983, **22**: 3320-3330.
221. Papahadjopoulos, D., Nir, S., Duzgunes, N., *Molecular mechanisms of calcium-induced membrane fusion*. *J Bioenerg Biomembr*, 1990, **22**: 157-179.
222. Van Schravendijk, M.R., Handunnetti, S.M., Barnwell, J.W., Howard, R.J., *Normal human erythrocytes express CD36, an adhesion molecule of monocytes, platelets, and endothelial cells*. *Blood*, 1992, **80**: 2105-2014.
223. Tait, J.F., Smith, C., *Phosphatidylserine receptors: role of CD36 in binding of anionic phospholipid vesicles to monocytic cells*. *J Biol Chem*, 1999, **274**: 3048-3054.
224. Smith, B.J., Herold, D.A., Ross, R.M., Marquis, F.G., Bertholf, R.L., Ayers, C.R., Wills, M.R., Savory, J., *Measurement of plasma prostaglandin E₂ using capillary gas chromatography negative ion chemical ionization mass spectrometry*. *Res Commun Chem Pathol Pharmacol*, 1983, **40**: 73-86.
225. Araujo, P., Bjorkkjaer, T., Berstad, A., Froyland, L., *Improved quantification of prostaglandins in biological samples by optimizing simultaneously the relationship eicosanoid/internal standard and using liquid chromatography tandem mass spectrometry*. *Prostaglandins Leukot Essent Fatty Acids*, 2007, **77**: 9-13.
226. Wu, C., Irie, S., Yamamoto, S., Ohmiya, Y., *A bioluminescent enzyme immunoassay for prostaglandin E₂ using Cypridina luciferase*. *Luminescence*, 2009, **24**: 131-133.
227. Kishimoto, T., Matsuoka, T., Imamura, S., Mizuno, K., *A novel colorimetric assay for the determination of lysophosphatidic acid in plasma using an enzymatic cycling method*. *Clin Chim Acta*, 2003, **333**: 59-67.
228. Xu, Y., Shen, Z., Wiper, D.W., Wu, M., Morton, R.E., Elson, P., Kennedy, A.W., Belinson, J., Markman, M., Casey, G., *Lysophosphatidic acid as a potential biomarker for ovarian and other gynecologic cancers*. *JAMA*, 1998, **280**: 719-723.
229. Westermann, A.M., Havik, E., Postma, F.R., Beijnen, J.H., Dalesio, O., Moolenaar, W.H., Rodenhuis, S., *Malignant effusions contain lysophosphatidic acid (LPA)-like activity*. *Ann Oncol*, 1998, **9**: 437-442.

230. Kawakami, S., Kaibara, M., Kawamoto, Y., Yamanaka, K., *Rheological approach to the analysis of blood coagulation in endothelial cell-coated tubes: activation of the intrinsic reaction on the erythrocyte surface*. *Biorheology*, 1995, **32**: 521-536.
231. Qu, J., Conroy, L.A., Walker, J.H., Wooding, F.B., Lucy, J.A., *Phosphatidylserine-mediated adhesion of T-cells to endothelial cells*. *Biochem J*, 1996, **317**: 343-346.
232. Ruf, W., Rehemtulla, A., Morrissey, J.H., Edgington, T.S., *Phospholipid-independent and -dependent interactions required for tissue factor receptor and cofactor function*. *J Biol Chem*, 1991, **266**: 2158-2566.
233. Comfurius, P., Smeets, E.F., Willems, G.M., Bevers, E.M., Zwaal, R.F., *Assembly of the prothrombinase complex on lipid vesicles depends on the stereochemical configuration of the polar headgroup of phosphatidylserine*. *Biochemistry*, 1994, **33**: 10319-10324.

Statement / Erklärung

I hereby declare that I have independently done this dissertation. I did not use any unauthorized assistance and unmentioned materials.

Hiermit erkläre ich an Eides statt, die vorliegende Dissertation selbstständig angefertigt zu haben. Ich habe keine unerlaubten sowie unerwähnten Hilfen benutzt.

Saarbrücken,

13.03.2010

Acknowledgment

I would like to express my special gratitude to my supervisor Professor Dr. Ingolf Bernhardt for introducing me to this project and for providing excellent scientific facilities and friendly working conditions. He kindly supported me, and always had time for questions and discussions.

I am grateful to Professor Dr. Claus-Michael Lehr for his interest in this work and for acting as the co-supervisor.

I am also thankful to Leon Muis and Daniel Mörsdorf for their help in using atomic force microscope, flow cytometry, laser scanning confocal microscope and solving technical problems at any time.

My thanks also go to my colleagues in our laboratory: Lyubomira Ivanova, Aravind Pasula, Daniel Mörsdorf, and Lisa Wagner. A special thank is sent to Jorge Riedel for his kindness and stimulation environment in the laboratory.

I am thankful to Dr. med. Harald Reinhard in Department of Pediatric Hematology and Oncology, Saarland University Hospital for supporting sickle cell anaemia bloods.

Special thanks go to all staff members of the Department of Biochemistry, and Department of Plant genetics of our University for a friendly and synergistic cooperation.

I am grateful for DAAD (Deutscher Akademischer Austausch Dienst) for granting me a PhD scholarship.

Especially, I would like to give my deep thanks to my wife for her understanding.

My sincere thanks are to my parents for educating, for unconditional support and for encouragement me to finish my PhD work, and to my brother for his care towards me throughout.